



Universidad de Valladolid

**REMOVAL OF ODOR EMISSIONS FROM FOOD
FERMENTATION AND PETROCHEMICAL PRODUCTION
PROCESSES USING BIOLOGICAL TREATMENT METHODS**

itü



PhD Thesis: İLKER AKMIRZA



Universidad de Valladolid



**PROGRAMA DE DOCTORADO EN INGENIERÍA QUÍMICA
Y
AMBIENTAL**

TESIS DOCTORAL:

**Removal of odor emissions from food fermentation and
petrochemical production processes using biological treatment
methods**

Presentada por İlker AKMIRZA para optar

al grado de

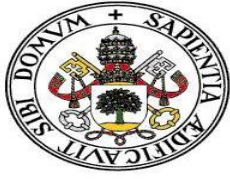
Doctor/a por la Universidad de Valladolid

Dirigida por:

Dra. Raquel Lebrero Fernández

Dr. Raúl Muñoz Torre

Dr. Kadir Alp



Universidad de Valladolid



**Memoria para optar al grado de Doctor,
con Mención Doctor Internacional,
presentada por el Ingeniero Ambiental:
İlker AKMIRZA**

Siendo los tutores en la Universidad de Valladolid:

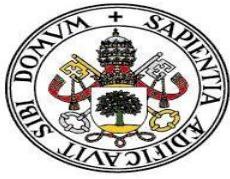
Dra. Raquel Lebrero Fernández

Dr. Raúl Muñoz Torre

Y en la Technical University of Istanbul (Turquia):

Dr. Kadir Alp

Valladolid, Enero de 2019



Universidad de Valladolid



UNIVERSIDAD DE VALLADOLID
ESCUELA DE INGENIERÍAS INDUSTRIALES

Secretaría

**La presente tesis doctoral queda registrada en el
folio número _____ del correspondiente libro de
registro número _____**

Valladolid, a _____ de _____ de 2019

Fdo. El encargado del registro

Raquel Lebrero Fernández
Profesora Ayudante Doctor
Departamento de Ingeniería Química y Tecnología del Medio Ambiente
Universidad de Valladolid

y

Raúl Muñoz Torre
Profesor Titular
Departamento de Ingeniería Química y Tecnología del Medio Ambiente
Universidad de Valladolid

Certifican que:

Ílker AKMIRZA ha realizado bajo su dirección el trabajo *“Removal of odor emissions from food fermentation and petrochemical production processes using biological treatment methods”*, en el Departamento de Ingeniería Química y Tecnología del Medio Ambiente de la Escuela de Ingenierías Industriales de la Universidad de Valladolid. Considerando que dicho trabajo reúne los requisitos para ser presentado como Tesis Doctoral expresan su conformidad con dicha presentación.

Valladolid, a _____ de _____ de 2019

Raquel Lebrero Fernández

Raúl Muñoz Torre



Universidad de Valladolid



Reunido el tribunal que ha juzgado la Tesis Doctoral titulada *“Removal of odor emissions from food fermentation and petrochemical production processes with using biological treatment methods”* presentada por İlker AKMIRZA y encumplimiento con lo establecido por el Real Decreto 99/2011 de 28 de enero de 2011 acuerda conceder por _____ la calificación de _____.

Valladolid, a _____ de _____ de 2019

PRESIDENTE

SECRETARIO

VOCAL

Table of Content

Abstract	i
Resumen	v
List of publications	ix
Contribution to the papers included in the thesis	xi
1 Introduction	1
1.1 Air Pollution.....	3
1.2 Volatile Organic Compounds.....	4
1.3 Odor.....	5
1.4 Kinetic Parameter Estimation and Modelling.....	6
1.5 Industrial Air Pollution Control.....	8
1.6 Air Pollution Control Technologies (VOC and Odor Emissions).....	8
1.6.1 Biofilters.....	10
1.6.2 Bioscrubber.....	12
1.6.3 Biotrickling Filter.....	13
1.6.4 Bubble Column Bioreactor.....	14
1.7 Model Sectors: Bakery yeast production and Petroleum industry.....	15
1.8 References.....	16
2 Aim and Scope of the Thesis	21
2.1 Justification of the thesis.....	23
2.2 Main objectives.....	23
2.3 Development of the thesis.....	25
3 Characterization and Treatment of Yeast Production Process Emissions in a Biofilter	27
4 Ethanethiol Gas Removal in an Anoxic Bio-scrubber	39
5 Anoxic Denitrification of BTEX: Biodegradation Kinetics and Pollutant Interactions	67
6 Anoxic Biodegradation of BTEX in a Biotrickling Filter	87
7 Trimethylamine Abatement in Algal-Bacterial Photobioreactors Coupled with Nitrogen Recovery 103	
8 Conclusion	119
9 About the Author	125

Abstract

Up to date, air pollution, which includes contamination of both indoor and outdoor air, has received less attention compared with other forms of pollution such as water or soil pollution. However, the increasing public concern on environmental challenges and human wellbeing has driven the attention of the public administration to air pollution management. Although some air pollutants are emitted naturally from volcanoes or forest fires, most sources are originated from human activities (transportation, industrial activity, waste management, etc.). Thus, abatement and minimization of anthropogenic air pollution have become one of the main challenges in air pollution management in this XXI century.

Nowadays malodorous emissions are considered a part of the main components of air pollution. Although odor threshold levels are tightly dependent on human sensation, and in some cases malodours can not be detected even at trace concentrations, malodorous emissions can contain toxic materials for humans and the environment even if concentrations remain below their odour thresholds.

Food and petrochemical industries are major sources of pollutant emissions to atmosphere. Most of these emissions can cause odor nuisance in the surrounding residential areas of industries, while long-term exposure to these emissions result on symptoms such as emotional stresses. At this point, an accurate characterization of malodorous emissions is crucial for a proper and effective odor abatement in the industrial sector. However, there is a lack of comparative data assessing the proper characterization of volatile organic compounds (VOCs) and malodorous compounds in literature. As a result of the sensorial impact of malodorous VOC, the characterization of emissions by instrumental techniques such as gas chromatography coupled mass spectrometry does not typically provide a sufficient understanding of the direct impact of air pollution on humans. In this context, sensorial techniques such as dynamic olfactometry, based on the use of the human nose as a sensor, allow to determine the odor threshold and the concentration/intensity of odor emissions, which ultimately characterize the direct impact of malodorous VOCs on people.

The first study of this thesis consisted of a case study carried out for bakery yeast fermentation process. The emissions of this process were analyzed with instrumental and dynamic olfactometry methods to characterize malodorous VOCs. The emissions were treated in a pilot scale biofilter. Instrumental analyses were performed to determine the chemical composition of

waste gas emissions for a gas flowrate of $6500 \text{ m}^3 \text{ h}^{-1}$. Ethanol represented the main VOC of the process with a peak hour concentration of 764 mg m^{-3} , followed by acetaldehyde and acetone as 331 and 65 mg m^{-3} , respectively. Moreover, only trace propanol levels were recorded only at peak hours in a 17-hour fermentation cycle. Dynamic olfactometry analyses were also performed to quantify the sensory impact of malodorous VOC emissions. The odor concentration was recorded in terms of European Odor Unit (OUE) as 39725 OUE m^{-3} , which was almost 40 times higher than the regulatory limits in Turkey. At this point, a biofilter was selected as a suitable alternative for the abatement of dilute VOC emissions ($< 2000 \text{ mg VOC m}^{-3}$) at waste gas treatment capacities of the process. Thus, malodorous emissions from the fermentation process were treated in a 46 L biofilter packed with raschig rings with a surface area $400 \text{ m}^2 \text{ m}^{-3}$ at an empty bed residence time (EBRT) of 80 s with ethanol concentrations 200, 400 and 700 mg m^{-3} with an almost complete biodegradation regardless of the ethanol concentration. On the other hand, ternary waste gas streams containing acetaldehyde ($\sim 300 \text{ mg m}^{-3}$), acetone (70 mg m^{-3}) and ethanol (700 mg m^{-3}) were treated with removal efficiencies higher than 90 % for ethanol and acetaldehyde at EBRT of 53-80 seconds, while only a partial acetone removal which reached to its maximum with 70 % of RE was observed. An improvement in the abatement of acetone and in the VOC mass transfer in order to decrease the operational EBRT will be required to achieve a proper process optimization.

Petrochemical industry was also analysed as a model sector as a result of its major contribution to the emissions of various sulfur based organic compounds such as ethanethiol (ET) and also human and environmental toxic compounds such as benzene, toluene, ethylbenzene, xylene (BTEX), which are used as reagents for the synthesis of multiple C-based products.

To date, petrochemical emissions are well characterized but there is a lack of studies in literature assessing the abatement of O_2 -free petrochemical industry emissions. A new generation of O_2 -free biological abatement alternatives capable of coping with the potential explosion risks of petrochemical emissions is required. At this point of concept, ET emissions which are commonly present in petrochemical industry, were investigated due to its low odor threshold level as $0.7 \mu\text{g L}^{-1}$ and its flammable character at extremely low concentrations. The use of an anoxic bio-scrubber for ET biotreatment enables the integration of waste gas treatment and wastewater treatment. The nitrification step uses NO_3^- as an electron acceptor source to oxidize ET under a specific ET/ NO_3^- ratio (0.74 in theory) to the main end product of S^0 , while during denitrification NO_3^- is converted to N_2 gas. In order to optimize process design and operation for ET emissions removal, anoxic bioscrubber operation was examined as a function of inlet

concentration (150, 350, 850, 1450 mg m⁻³), EBRT (30, 60, 90, 120 s) and spray density of irrigation (0.12, 0.18, 0.23, 0.30, 0.45 m³ m⁻² h⁻¹). According to the results, the best operation conditions were achieved at an inlet concentration of 150 mg m⁻³, a spray density of 0.23 m³ m⁻² h⁻¹ and an EBRT of 90 s. Under these conditions, an average RE of 91% and an elimination capacity (EC) of 24.74 g m⁻³ h⁻¹ were recorded, while S⁰ was obtained as end product rather than SO₄²⁻. Average experimental yield values close to the Y_{ET/NO₃⁻} theoretical value of 0.74 were observed.

Apart from ET emissions in petrochemical industry, BTEX emissions widely used in the sector present a major impact due to their carcinogenic effects. Nevertheless, presence of multiple BTEX compounds and their interactions during the biodegradation process are still poorly understood. Similarly, kinetic parameter estimation is of key relevance for a correct dimensioning of O₂ free VOC abatement bioreactors.

Anoxic mineralization of BTEX represents a promising alternative for the abatement of these VOCs from O₂-deprived emissions. However, the kinetics of anoxic BTEX biodegradation and the interactions underlying the treatment of BTEX mixtures are still unknown. An activated sludge inoculum was used for the anoxic abatement of single, dual and quaternary BTEX mixtures, being acclimated prior performing the biodegradation kinetic tests. The Monod model and a Modified Gompertz model were then used for the estimation of the biodegradation kinetic parameters. Results showed that both toluene and ethylbenzene are readily biodegradable under anoxic conditions, whereas the accumulation of toxic metabolites resulted in partial xylene and benzene degradation when present either as single components or in mixtures. Moreover, the supplementation of an additional pollutant always resulted in an inhibitory competition, with xylene inducing the highest degree of inhibition. The Modified Gompertz model provided an accurate fitting for the experimental data for single and dual substrate experiments, satisfactorily representing the antagonistic pollutant interactions. Finally, microbial analysis suggested that the degradation of the most biodegradable compounds required a lower microbial specialization and diversity, while the presence of the recalcitrant compounds resulted in the selection of a specific group of microorganisms.

The continuous biodegradation of BTEX (benzene, toluene, ethylbenzene and xylene) using nitrate as the electron acceptor is of key interest to reuse the residual gas for inertization purposes. However, the biological mineralization of BTEX is often limited by their recalcitrant nature and the toxicity of the secondary metabolites produced. The potential of an anoxic biotrickling filter for the treatment of a model O₂-free BTEX-laden emission at inlet individual

concentrations of $\sim 700 \text{ mg m}^{-3}$ was here evaluated. A UV oxidation step was also tested both in the recycling liquid and in the inlet gas emission prior to biofiltration. Removal efficiencies $> 90\%$ were achieved for both toluene and ethylbenzene, corresponding to ECs of $1.4 \pm 0.2 \text{ g m}^{-3} \text{ h}^{-1}$ and $1.5 \pm 0.3 \text{ g m}^{-3} \text{ h}^{-1}$, respectively, while $\sim 45\%$ of xylene ($\text{EC} = 0.6 \pm 0.1 \text{ g m}^{-3} \text{ h}^{-1}$) was removed at a liquid recycling rate of 2 m h^{-1} . Benzene biodegradation was however limited by the accumulation of toxic metabolites in the liquid phase. The oxidation of these intermediates in the recycling liquid by UV photolysis boosted benzene abatement, achieving an average EC of $0.5 \pm 0.2 \text{ g m}^{-3} \text{ h}^{-1}$ and removals of $\sim 40\%$. However, the implementation of UV oxidation as a pretreatment step in the inlet gas emission resulted in the deterioration of the BTEX biodegradation capacity of the biotrickling filter. Finally, a high bacterial diversity was observed throughout the entire experiment, the predominant phyla being *Proteobacteria* and *Deinococcus-thermus*.

Another case study was carried out to remove trimethylamine emissions from a chemical production facility. For this purpose, the performance of a bacterial bioreactor and an algal-bacterial photobioreactor was comparatively evaluated. Thus, a bacterial Bubble Column Photobioreactor (BCB) was operated with a synthetic TMA laden emission at $\sim 500 \text{ mg m}^{-3}$ at an EBRT of 2 min, which resulted in 78 % of TMA oxidation. The operation of the BCB with an algal-bacterial consortium increased TMA removal by 10 % at an EBRT of 2 min, and supported a decrease in the EBRT down to 1.5 min and 1 min without a detrimental effect on TMA biodegradation (REs of $98 \pm 2\%$ and $94 \pm 6\%$, respectively).

Resumen

Tradicionalmente, la contaminación atmosférica (incluyendo la contaminación de aire de interior y de exterior), ha recibido una menor atención en comparación con la contaminación del agua o del suelo. Sin embargo, la mayor concienciación pública en lo relativo a cambios medioambientales y bienestar social ha dirigido la atención de la administración pública hacia el control de la contaminación atmosférica. Si bien algunos contaminantes gaseosos son emitidos de forma natural (p. ej. emisiones de volcanes o incendios forestales), la mayoría de las fuentes son de origen antropogénico (transporte, actividad industrial, gestión de residuos, etc.). Por lo tanto, la minimización y tratamiento de la contaminación gaseosa de origen antropogénico se ha convertido en uno de los principales retos del siglo XXI.

Hoy en día, las emisiones olorosas son consideradas una parte importante de la contaminación atmosférica. Aunque los niveles de detección de olor están estrechamente vinculados con la sensación humana, y en algunos casos los malos olores pueden no ser detectados a concentraciones traza, estas emisiones pueden contener componentes tóxicos para el ser humano y el medio ambiente incluso si sus concentraciones permanecen por debajo de su umbral de detección.

Las industrias alimentaria y petroquímica representan una de las mayores fuentes de emisiones gaseosas a la atmósfera. La mayoría de estas emisiones pueden causar molestias debido a malos olores en las áreas residenciales cercanas a las industrias, y la exposición a largo plazo a estas emisiones resulta en síntomas como el estrés emocional. La caracterización precisa de estas emisiones olorosas es crucial para una gestión eficaz. Sin embargo, existe en la literatura una falta de datos comparativos que evalúen la caracterización de compuestos orgánicos volátiles (COVs) y otros compuestos malolientes. Como resultado del impacto sensorial de los COVs olorosos, la caracterización de las emisiones mediante técnicas instrumentales como cromatografía gaseosa acoplada a espectrometría de masas no proporciona, por lo general, suficiente conocimiento acerca del impacto directo de la contaminación del aire en humanos. En este sentido, técnicas sensoriales como la olfactometría dinámica, basada en el uso de la nariz humana como sensor, permite determinar el límite de olor y la concentración/intensidad de la emisión olorosa, lo que en última instancia caracteriza el impacto directo de los COVs malolientes en la población.

El primer estudio presentado en esta tesis se centró en las emisiones de un proceso de fermentación de levadura de panadería. Las emisiones de este proceso fueron analizadas con métodos de olfactometría instrumental y dinámica para caracterizar los COVs olorosos y tratadas

posteriormente en un biofiltro a escala piloto. Análisis instrumentales fueron desarrollados para determinar la composición química de la emisión gaseosa residual para un caudal de gas de $6500 \text{ m}^3 \text{ h}^{-1}$. El etanol representó el principal COV emitido del proceso, con una concentración máxima de 764 mg m^{-3} , seguido del acetaldehído y de la acetona con concentraciones de 331 y 65 mg m^{-3} , respectivamente. Además, se detectaron trazas de propanol sólo durante las horas punta en un ciclo de fermentación de 17 horas. Se realizaron además análisis de olfactometría dinámica para cuantificar el impacto sensorial de la emisión de COVs. La concentración de olor se determinó en Unidades Europeas de Olor (OUE), con un valor de 39725 OUE m^{-3} , casi 40 veces superior a los límites normativos en Turquía. En este punto, se seleccionó un biofiltro como la alternativa más adecuada para el tratamiento de la emisión diluida de COVs ($<2000 \text{ mg m}^{-3}$) a las capacidades de tratamiento del proceso. La emisión se trató en un biofiltro de 46 L empacado con anillos raschig y un área superficial de $\text{m}^2 \text{ m}^{-3}$ a un tiempo de retención del gas (EBRT) de 80 s y concentraciones de etanol de 200, 400 y 700 mg m^{-3} , obteniendo una eliminación prácticamente completa independientemente de la concentración de etanol. Por otro lado, durante el tratamiento de una corriente de gas residual que contenía acetaldehído ($\sim 300 \text{ mg m}^{-3}$), acetona (70 mg m^{-3}) y etanol (700 mg m^{-3}) se obtuvieron eliminaciones superiores al 90% para etanol y acetaldehído a EBRT de 53-80 s, mientras que las eliminaciones máximas alcanzadas para la acetona fueron del 70%. Aumentar la eficacia de eliminación de la acetona y favorecer la transferencia de masa de los COVs para reducir el EBRT de operación son necesarios para una adecuada optimización del proceso de tratamiento.

La industria petroquímica fue también analizada como sector modelo debido a su importante contribución a las emisiones gaseosas de varios compuestos orgánicos sulfurados como el etanotiol (ET), así como de otros compuestos tóxicos para el ser humano y el medio ambiente como el benceno, tolueno, etilbenceno y xileno (BTEX), que son empleados como reactivos para la síntesis de numerosos productos.

Hoy en día, las emisiones de la industria petroquímica están bien caracterizadas, si bien existe una falta de estudios en literatura centrados en el tratamiento de estas emisiones que se caracterizan por la ausencia de oxígeno. En este sentido, se necesita una nueva generación de biotecnologías alternativas capaces de tratar estas corrientes libres de O_2 y así hacer frente a los riesgos potenciales de explosión asociados a los tratamientos aerobios de estas emisiones. En esta tesis se estudiaron las emisiones de ET frecuentemente presentes en la industria petroquímica, debido a su bajo límite de detección de olor ($0.7 \mu\text{g L}^{-1}$) y su carácter inflamable a concentraciones extremadamente reducidas. La implementación de un biolavador anóxico

para el tratamiento biológico de ET permite integrar el tratamiento de la corriente residual de gas con el de la corriente de aguas residuales. La etapa de nitrificación utiliza NO_3^- como fuente aceptora de electrones para oxidar ET hasta S^0 a un ratio específico de ET/NO_3^- (0.74 teórico), mientras que durante la desnitrificación el NO_3^- es transformado en N_2 gaseoso. Para optimizar el diseño y operación del proceso de eliminación de ET, se operó un biolavador anóxico a distintas concentraciones de entrada de ET (150, 350, 850, 1450 mg m^{-3}), EBRT (30, 60, 90, 120 s) y tasas de irrigación (0.12, 0.18, 0.23, 0.30, 0.45 $\text{m}^3 \text{m}^{-2} \text{h}^{-1}$). Los resultados obtenidos muestran que las mayores eficacias de eliminación se alcanzan a concentraciones de entrada de 150 mg m^{-3} , una irrigación de 0.23 $\text{m}^3 \text{m}^{-2} \text{h}^{-1}$ y un EBRT de 90 s. En estas condiciones se obtienen una eficacia de eliminación promedio de ET de 90% y una capacidad de eliminación (CE) de 24.74 $\text{g m}^{-3} \text{h}^{-1}$, siendo oxidado principalmente a S^0 en lugar de SO_4^{2-} .

Además de las emisiones de ET en la industria petroquímica, la liberación de BTEX a la atmósfera tiene un gran impacto debido a sus efectos carcinógenos en el ser humano. Sin embargo, la presencia de múltiples contaminantes y sus interacciones durante el proceso de biodegradación son todavía poco entendidos. Además, la estimación de los parámetros cinéticos es de especial relevancia para un correcto dimensionado y operación de los biorreactores de tratamiento de emisiones de COVs libres de O_2 .

La mineralización anóxica de BTEX representa una alternativa prometedora para la eliminación de estos COVs en corrientes anaerobias. Sin embargo, las cinéticas de biodegradación anóxica de BTEX y las interacciones entre ellos aún se desconocen. En esta tesis se ha evaluado la capacidad de un fango activo para la eliminación anóxica de BTEX y mezclas binarias y cuaternarias de estos compuestos, empleando los modelos de Monod y el Modificado de Gompertz para la estimación de los parámetros cinéticos de biodegradación. Los resultados mostraron que tanto el tolueno como el etilbenceno son fácilmente biodegradables en condiciones anóxicas, mientras que la acumulación de metabolitos tóxicos resultó en la degradación parcial del xileno y del benceno cuando estaban presentes tanto como compuestos individuales como en mezclas. Además, la presencia de un contaminante adicional resultó en cualquier caso en una competición inhibitoria, siendo el xileno el compuesto con mayor efecto inhibitorio. El modelo Modificado de Gompertz proporcionó un ajuste de gran precisión de los datos experimentales para los experimentos con sustratos individuales y mezclas binarias, representando de forma satisfactoria las interacciones antagónicas entre los contaminantes. Finalmente, el análisis de la comunidad microbiana sugiere que la degradación de los compuestos más biodegradables requiere menor especialización y diversidad microbiológica,

mientras que la presencia de compuestos recalcitrantes deriva en la selección de grupos específicos de microorganismos.

La degradación de BTEX en continuo y en condiciones anóxicas utilizando nitrato como aceptor de electrones es de especial interés para poder reutilizar el gas residual como inertizante. Sin embargo, la mineralización biológica de estos compuestos está generalmente limitada por su naturaleza recalcitrante y los metabolitos secundarios producidos. En la presente tesis, se evaluó el potencial de un biofiltro percolador anóxico para el tratamiento de una emisión modelo de BTEX sin oxígeno y con concentraciones de entrada individuales de $\sim 700 \text{ mg m}^{-3}$. Se estudió también la eficacia de una etapa de oxidación UV tanto en el líquido de recirculación como en la entrada de la corriente gaseosa antes del biofiltro. Se obtuvieron eficacias de eliminación $> 90\%$ para tolueno y etilbenceno, que correspondían a capacidades de eliminación de $1.4 \pm 0.2 \text{ g m}^{-3} \text{ h}^{-1}$ y $1.5 \pm 0.3 \text{ g m}^{-3} \text{ h}^{-1}$, respectivamente, mientras que $\sim 45\%$ del xileno ($\text{CE} = 0.6 \pm 0.1 \text{ g m}^{-3} \text{ h}^{-1}$) fue eliminado a una velocidad de recirculación del líquido de 2 m h^{-1} . La degradación del benceno estuvo por el contrario limitada por la acumulación de metabolitos tóxicos en la fase líquida. La oxidación de estos compuestos intermediarios en el líquido de recirculación por fotólisis UV potenció la eliminación del benceno, alcanzando CE promedio de $0.5 \pm 0.2 \text{ g m}^{-3} \text{ h}^{-1}$ y eficacias de eliminación de $\sim 40\%$. Sin embargo, la implementación de la oxidación UV como etapa de pretratamiento en la corriente gaseosa de entrada resultó en el deterioro de la capacidad de biodegradación del biofiltro percolador. Finalmente, se observó durante todo el periodo experimental una alta diversidad bacteriana, siendo los filos predominantes *Proteobacteria* y *Deinococcus-thermus*.

Por último, se realizó un estudio orientado a la eliminación de las emisiones de una planta de producción química. En este caso, se evaluaron y compararon dos sistemas biológicos para el tratamiento de la emisión contaminada con TMA: un biorreactor de bacterias y un fotobiorreactor de algas-bacterias de columna de burbujeo. Se operó con una concentración de entrada de TMA de $\sim 500 \text{ mg m}^{-3}$ a un EBRT de 2 min, lo que resultó en la oxidación de un 78% de la TMA. En el caso del fotobiorreactor, la eficacia de eliminación aumentó en un 10% al mismo EBRT, manteniendo altas eficacias de eliminación a EBRT inferiores de 1.5 y 1 min (eliminaciones de $98 \pm 2\%$ y $94 \pm 6\%$, respectivamente).

List of publications

The following publications are presented as part of the present thesis. Three of them are published in international journals indexed in ISI web of knowledge (Papers I to IV). Paper V has been submitted for publication.

Paper I. **Akmirza, I.**, Turker, M., Alp, K. (2018). *Characterization and treatment of yeast production process emissions in a biofilter*. Fresen. Environ. Bull 27, 7099-7107

Paper II. Mhemid, R.K.S., **Akmirza, I.**, Shihab, M.S., Turker, M., Alp, K., (2019). *Ethanethiol gas removal in an anoxic bio-scrubber*. J. Environ. Manage. 233, 612–625.

Paper III. Carvajal, A., **Akmirza, I.**, Navia, D., Pérez, R., Muñoz, R., Lebrero, R., (2018). *Anoxic denitrification of BTEX: Biodegradation kinetics and pollutant interactions*. J. Environ. Manage. 214, 125–136.

Paper IV. **Akmirza, I.**, Pascual, C., Carvajal, A., Perez, R., Munoz, R., Lebrero, R. (2017). *Anoxic Biodegradation of BTEX in a biotrickling filter*. Sci. Total Environ. 587-588 :457-465.

Paper V. Pascual, C., **Akmirza, I.**, R. Munoz., Lebrero, R. *Trimethylamine abatement in algal-bacterial photobioreactors coupled with nitrogen recovery*, Unpublished manuscript.

Contribution to the papers included in the thesis

Paper I. In this work, I was responsible for the waste gas characterization with instrumental techniques and design, start-up and operation of the experimental set-up in collaboration with Dr. Mustafa Türker and under the supervision of Dr. Kadir ALP. Additionally, I was responsible for data analysis. I was in charge also of the manuscript writing under the supervision of Dr. Kadir ALP.

Paper II. In this work, I was responsible for experimental design and start-up of the experimental setup and collaborated with Rasha Mmemid and Mohammed Shihab for operation of the experimental set-up. I was also in charge for manuscript writing with the collaboration of Rasha Mmemid and Mohammed Shihab under the supervision of Dr. Mustafa Türker and Dr. Kadir Alp

Paper III. During the implementation of this thesis study, I was responsible for the operation of the experimental set-up and results evaluation, besides collaborating with Dr. Daniel Navia during data analysis. I was also responsible for manuscript writing with the collaboration of Dr. Andrea Carvajal under the supervision of Dr. Raquel Lebrero and Dr. Raúl Muñoz Torre. Dr. Rebeca Perez was responsible for the microbiological characterization, where I contributed in the data analysis and discussion.

Paper IV. In this work, I was responsible for the design, start-up and operation of the experimental set-up and results evaluation in collaboration with the student Celia Pascual. I was also in charge of manuscript writing under the supervision of Dr. Raúl Muñoz and Dr. Raquel Lebrero. Dr. Rebeca Perez was responsible for the microbiological characterization, where I contributed in the data analysis and discussion.

Paper V. In this work, I was responsible for the design and start-up of the experimental setup, and the operation of the system in collaboration with Master student Celia Pascual. I also worked in manuscript writing under the supervision of Dr. Raúl Muñoz and Dr. Raquel Lebrero.



Universidad de Valladolid

CHAPTER 1

Introduction

1.1 Air Pollution

Air pollution is defined as the presence of one or more substances in the air for a duration or at a concentration above their natural levels, with the potential to produce an adverse effect on humans and/or the environment [1]. It is considered nowadays one of the greatest threats for the environment and human health [2,3], not only due to the advances in science and technology in the last century that have led to incredible improvements in the quality of life, but also to the increased awareness of the society on the real impact of anthropogenic atmospheric pollution. One of the major environmental air pollution disasters occurred in London on December 1952 when a thick layer of smog covered the city area during four days and resulted in more than 4000 deaths. [4]. This episode is considered a turning point in the way air pollution was handled all over the world. After this big tragedy, many scientists focused on highlighting the detrimental effects of air pollution on human and as well as on environment in their various researches [5,6]. In addition, many health organizations took into prominent the health effects of air pollution. Indeed, The World Health Organisation (WHO) has classified air pollution as the greatest environmental risk to human health in the present century (note that this is based on current risk, while longer-term environmental threats such as climate change, may exceed this in the future). Additionally, air pollution is considered as the primary responsible for many diseases such as stroke, heart disease, chronic obstructive lung diseases like lung cancer, asthma and pulmonary disease, diabetes and dementia, and acute respiratory infections in children [7–10]. In recent years, more than 90% of the world's population is living in areas where air quality levels failed to meet the targets of WHO [11]. Apart from the adverse health effects of air pollutants, increased wellbeing standards and public awareness on the exposure to unpleasant air pollutants are leading to an intensification of complaints in residential areas.

In this sense, human activities that are major sources of outdoor air pollution include (Figure 1)[12]:

- Fuel combustion from motor vehicles (e.g. cars and heavy-duty vehicles)
- Heat and power generation (e.g. oil and coal power plants and boilers)
- Industrial facilities (e.g. manufacturing factories, mines, and oil refineries)
- Municipal and agricultural waste sites and waste incineration/burning
- Residential cooking, heating, and lighting with polluting fuels

Poor urban planning, which leads to sprawl and over-dependence on private vehicle transport, is also a key factor in the accelerated increase in pollution emissions.

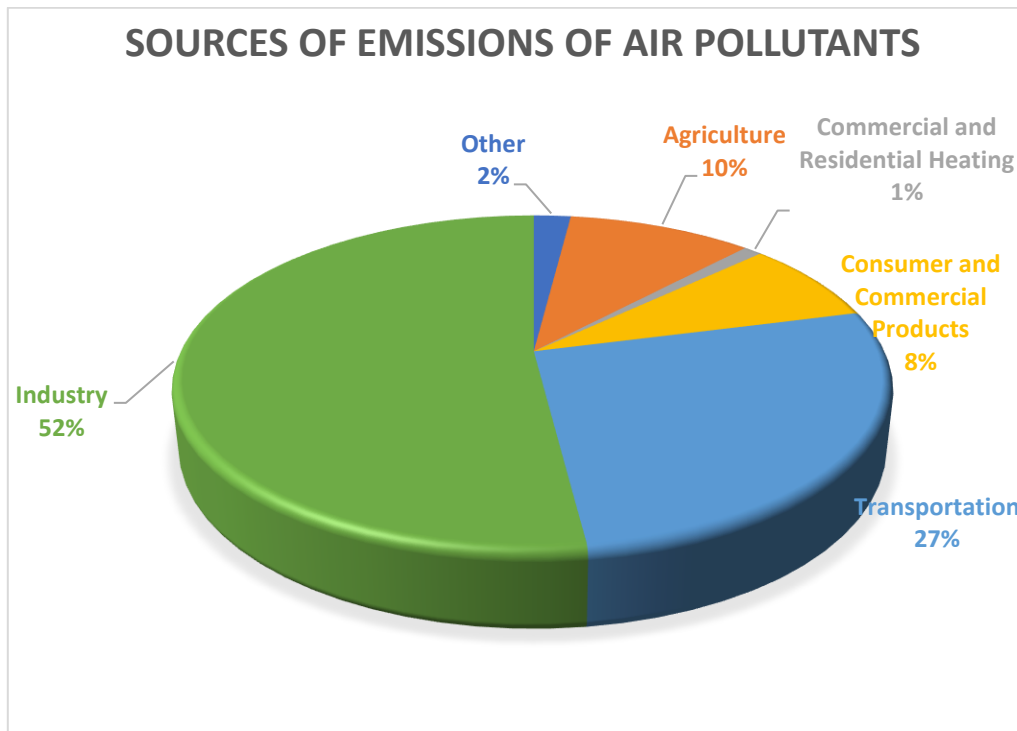


Figure 1 Main anthropogenic sources of air pollution emissions[12]

All the above-mentioned issues make atmospheric pollution control a key concern, especially in the fast-developing urban areas driven by globalization and exponential economic growth.

1.2 Volatile Organic Compounds

Volatile organic compounds (VOCs) are considered one of the main types of air pollutants due to their adverse effects on human health. VOCs are organic chemicals with a boiling point below or equal to 250 °C measured at a standard atmospheric pressure of 101.3 kPa, and include a wide range of chemical families such as aromatics, alcohols, alkanes, esters, aromatics, halocarbons, esters, ketones etc. VOCs are emitted to the atmosphere either in gas or liquid form from different sources: storage and transfer operations, waste disposal processes, and many industries such as paper, paint, solvents or fuel/petroleum industries [13,14]. VOCs have become an important topic of research due to their complexity and important negative effects

on human health (headaches, irritation, insomnia, loss of appetite, respiratory problems, damage to liver, kidney and central nervous system, etc.) and the environment (for instance in ozone formation) [15,16]. Apart from the detrimental health effects of VOCs, most of them are malodorous and can be perceived by the sense of smell despite being present at trace level concentration, potentially resulting in odor nuisance on the nearby populations [17,18].

1.3 Odor

Odor nuisance is considered nowadays one of the most important environmental pollution problems due to its direct impact on the community's quality of life. Among all the senses, the sense of smell is considered the most complex due to a series of chemical and neurological interactions that take place in the human olfactory system, which hinders the proper understanding of odorous pollution and its impact on the population. Moreover, the subjective nature of odorous nuisance depends on the age, natural sensitivity, sex, personal experience, health problems, education, etc. [19,20]. Odor nuisance is also determined by odor characterisation parameters such as intensity, frequency and hedonic tone. Despite not being a direct cause of disease, long-term exposure to odorant emissions has a detrimental effect on human health and results in social and physical problems.

Odorous emissions are complex mixtures of multiple chemicals present at trace level concentrations (ppb-ppm range). Nevertheless, despite their low concentrations, the olfactory detection thresholds of these odorants determine the high impact associated to the odorous emission (Table 1). The wide range of odorants include organic and inorganic compounds that are released to the atmosphere from various industrial activities in gaseous or particulate (dissolved in liquid drops) forms. Because of their structures, these compounds rapidly disperse in the surrounding environment leading to important disturbances. Furthermore, organic compounds might trigger ozone synthesis in the atmosphere and contribute to the formation of greenhouse gases with their oxidation products. Therefore, odor causing VOC emissions do not just threaten human health and welfare (long-term exposure to such odorants cause nausea, headaches, insomnia, loss of appetite, respiratory problems, etc.), but also to air quality, as they contribute to photochemical smog formation and the emission of particulate secondary contaminants.

In recent days, attention to odorous VOCs has been growing because of the encroachment of residential areas on industrial activities (resulting in an increase in the number and severity of public complaints), and the awareness of people's need for a cleaner environment [21]. This has triggered governmental authorities to enforce stricter environmental regulations on odor emissions management, which has turned odorants abatement into a key issue for industrial operators [22–24]. Basic legal requirements of European Union for ambient air quality control are specified in the Directive 2008/50/EC (2008) and Directive 2010/75/EU (2010). Also, Turkey enforced in 2013 the "Regulation on Control of Emissions that Contribute to Odor (KOEKHY)" to establish the legal requirements.

Table 1 Olfactory detection threshold of the most important malodorous compounds (Adapted from [15])

COMPOUND	DETECTION THRESHOLD (ppmv)
H₂S	0.0005
Dimethyl Sulphide	0.001
Dimethyl Disulphide	0.000026
Ammonia	0.038
Indole	0.0001
Trimethylamine	0.004
Propionic Acid	0.028
Butyric Acid	0.0003
Butanone	0.25
Acetadehyde	0.0001
Toluene	2.1
Phenol	46

1.4 Kinetic Parameter Estimation and Modelling

The estimation of the kinetic parameters is essential in the field of biodegradation [25]. Up to date, the biodegradation pathways for individual VOCs are well known and have been applied in the modelling field. However only few studies have focused on the assessment of substrate interactions such as inhibition, cometabolism and competition in VOCs mixtures [26–28]. Particularly in the petroleum industry, the presence of several VOCs in gas emissions (i.e. mixtures of benzene, toluene, ethyl-benzene and xylene, BTEX) might result in positive or

negative interactions during the biodegradation process, thus identifying and predicting this behavior is of key importance [29]. The identification of the unpredictable behavior of multiple compound interactions during their biodegradation is possible with the estimation of kinetic parameters, which are playing a fundamental role for the optimization of planning, modelling, design management and upgrading of the biological systems and also usually a cheaper and faster tool to evaluate the impacts of changes in the operating conditions on system performance. Furthermore, none of the studies available in literature have investigated up to date the kinetics of VOC biodegradation under O₂-free biodegradation processes for model sector emissions. [28]. At this point, the determination of kinetic parameters under anoxic conditions will help to overcome the limitations to understand the biodegradation pathways and promote further studies to properly design and model biodegradation processes in petrochemical industry [30][31].

Up to date, many different mathematical models have been used to estimate kinetic parameters, which were further used in optimizing bioreactor designs. Among the existing models, Monod model is widely accepted and applied as the most suitable model for kinetic parameter estimation under non-inhibitory conditions. Monod model offers a suitable estimation when describing the biodegradation of a single substrate, and parameters such as μ_{max} (the maximum specific growth rate), S (the concentration of the limiting growth substrate) and K_S (the half-velocity constant) can be determined with high accuracy (Eq 1). On the contrary, Monod Model presents important shortcomings when estimating kinetic parameters for multiple substrates due to substrate interactions [32].

$$\mu = \frac{\mu_{max}S}{K_S+S} \quad (\text{Eq 1})$$

To overcome this uncertainty, non linear regression models such as the Modified Gompertz kinetic model have been proposed for multiple compounds, where the kinetic parameters such as the maximum rate of production (R_m), the maximum production (P_{max}), the elapsed time (t) and the lag-phase (l), can be estimated with high certainty [28].

$$P(t) = P_{max} \exp\left(-\exp\left(\frac{R_m}{D_{max}}(\lambda - t) + 1\right)\right) \quad (\text{Eq2})$$

Nevertheless, further research is required for the optimization of such models for BTEX biodegradation under anoxic conditions.

1.5 Industrial Air Pollution Control

The proximity of residential areas to industrial facilities has increased the demand for VOC and odor characterization and control systems to provide a clean and nuisance-free air [33]. Industrial activities release gas pollutants into the atmosphere directly from their production processes or from failures or inadequacies on their installations. Meeting legal requirements on odor-causing VOC emissions and increasing quality of life makes the management of these emissions a mandatory and complex issue [34]. For an effective and proper odor nuisance abatement to be implemented, the problem must be first quantified, and the characteristics of the waste gas stream should be identified prior selection of optimum VOC treatment technology [35].

Due to the challenging character of odorous VOC emissions, both instrumental and sensorial analyses are recommended for a complete chemical characterization of the emission together with the evaluation of odor annoyance [36]. In this sense, instrumental techniques can only assess the quantitative composition of a gas mixture, while sensorial analysis is mandatory to determine the intensity of odor emissions and its impact on the receptor [17,23].

In waste gas streams, odorants and VOCs are usually present at very low concentrations, thus preliminary adsorption (concentration) on sorbent tubes followed by gas chromatography coupled with mass spectrometry is typically for characterization. Method EPA TO-17 is officially announced by the US-EPA as the preferred analytical method. On the other hand, dynamic olfactometry, which allows to characterize the direct effect of the odorous VOC emission on people and eliminates the lack of subjectivity of the instrumental analyses, is the most common sensorial technique [37].

1.6 Air Pollution Control Technologies (VOC and Odor Emissions)

Due to negative impact of malodorous VOC emissions on human and environment, there is an urgent need to develop cost-effective VOC and odor control systems to ensure a proper air quality [33]. Also governmental authorities urge polluting industries to adopt proper treatment

processes to overcome population complaints and impose penalties when industrial facilities exceed regulatory limits.

The selection of proper treatment processes mainly depends on the composition and flow rate of the waste gas stream, odor emission characterization being one of the key challenges during technology selection. A proper odor emission characterization helped the authorities to select the most suitable odor treatment process to tackle the odor problem. In addition, other parameters such as moisture, temperature and particulate content have to be taken into account to properly select, design and operate gas treatment technologies. Furthermore, the local conditions, availability of land area, and limitations in investment and operating cost are considered critical parameters to be considered. In this way, selection and design of proper odorous VOC removal processes must aim at finding an optimum where the required treatment efficiency is achieved as cost-effectively as possible, while offering environmentally friendly alternatives that can be adapted to the specific conditions [38].

Nowadays, a large variety of alternatives used for off-gas treatment is based on pollutant transfer from the waste gas stream towards a solid (adsorption) or a liquid (absorption) phase, commonly followed by a biological or chemical oxidation of the pollutant [4]. During the past decades, physical/chemical treatment processes such as condensation, incineration, adsorption, thermal oxidation, chemical scrubbers, ozonation and catalytic oxidation have been widely used due to their advantages: rapid start-up, low footprint and widescale experience in design and operation. Among these technologies, chemical scrubbers and incineration processes represent nowadays a highly costly alternative for the treatment of odorous emissions both in terms of operation, due to their high chemical and heat demand [39]. Other well-known technologies such as activated carbon adsorption or UV / ozone-based treatments do not often provide satisfactory levels of treatment because of the high moisture content typically present in odorous emissions. Apart from these drawbacks, their non-environmental friendly nature associated to the generation of secondary waste streams often limits their implementation in nuisance sensitive scenarios [40]. In this context, the development of environmentally friendly and economically viable alternative treatment technologies has received increasing attention worldwide. Nowadays, biological air treatment has emerged as a cost-efficient and environmentally friendly alternative to physical/chemical odor treatment technologies. It relies on the activity of microorganisms able to biodegrade organic contaminants for cell growth and maintenance, with a conversion into non-odorous and less harmful by-products (mainly CO₂ and H₂O) [38,41,42]. Additionally, the low pollutants concentration found in odorous waste gas

streams and the relatively high flow rates constitutes the ideal framework for the application of biotechnologies (Figure 2). As a result of these advantages, within the last decades biological techniques have been applied more frequently as promising alternatives to control odorous VOC emissions [43,44]. Though a number of different bioreactor configurations have been used up to date, the main types of conventional air-phase bioreactors include biofilter (BF), bioscrubber (BS), biotrickling filter (BTF), and bubble column bioreactors (BCB). The main differences between these reactor configurations are related with the type of liquid (continuous flow or stationary) and the microbial community (suspended in the liquid broth or fix forming a biofilm) [45].

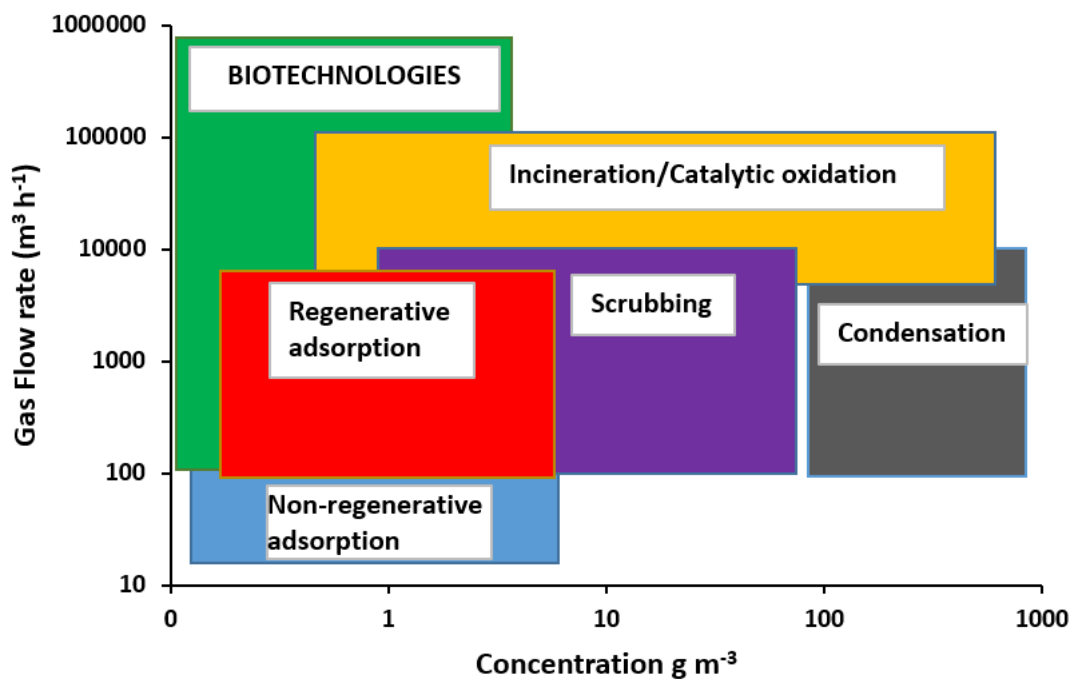


Figure 2 Comparative chart for the selection of air pollution control techniques traditionally employed since the 90s. [4]

1.6.1 Biofilters

Biofilters are most popular bioreactor type capable of removing a wide range of organic and inorganic pollutants at high removal efficiencies (>90%). In general, biofilters are defined as bioreactors in which a waste gas stream is passed through a porous packed bed material on which a mixed culture of pollutant-degrading microorganisms are immobilized. Compost, peat, root wood, bark, wood chips and their different kind of combinations are typically used as packed material in the biofilter columns and also responsible to supply essential nutrient for microbial growth [46]. BFs possess a wide-range of application and up to now have been used in Europe more than 600 chemical processing industries to treat VOC and odor exhaust streams

[47]. Although BFs first application was devoted to the treatment of odorous emissions from sewage treatment plants and composting facilities, BFs now find wide application in the treatment of several VOCs and odors such as ammonia, hydrogen sulphide, mercaptan, disulphides, etc., and VOCs like propane, butane, styrene, phenols, ethylene chloride, methanol, etc.

Overall, BFs have advantages over other biological treatment systems due to their easy start-up procedure, cost effectiveness in both capital and operation cost, low-pressure drops and no generation of secondary waste gas streams. Additionally BFs are used for the treatment of large volumes of air streams containing low concentration of VOCs or odorants, and recent studies have shown that 60 out of 189 hazardous air pollutants (HAPs) can be successfully treated with biofilters [48]. Biofilters have high removal efficiency up to 99 % for hydrophilic odorous VOCs (Henry's Law constant lower than 0.07 M atm^{-1}), while are moderately efficient (removal efficiencies of up to 75 %) for hydrophobic compounds (up to 75%) (Henry's Law constant higher than 20 M atm^{-1}) [21].

Despite the above cited advantages of biofilter systems, they have some drawbacks during operation such as the difficulty to control moisture and pH in the biofilm, clogging of the medium due to particulate matter and biomass overgrowth, problem of packing media deterioration and lower removal efficiencies at high VOC concentrations [33]. Schematic presentation of biofilter setup has been illustrated in Figure 3.

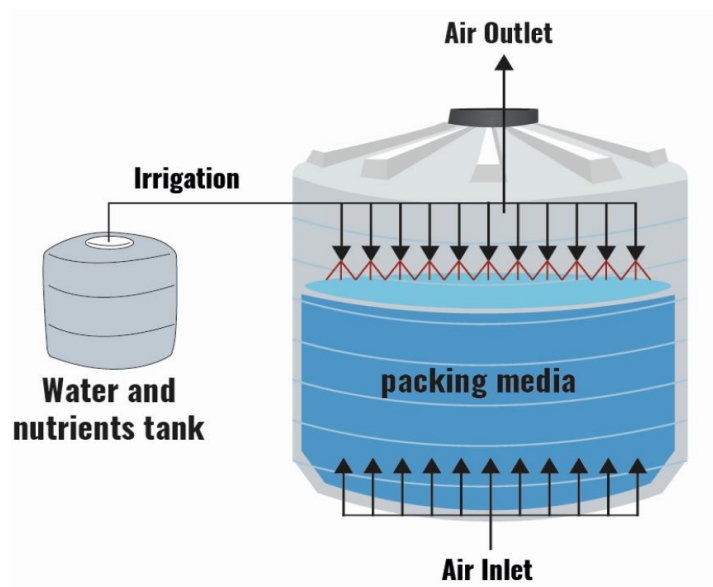


Figure 3 Schematic view of biofilter. [4]

1.6.2 Bioscrubber

Bioscrubbers consist of two subunits, a packed tower (absorption column) and a bioreactor, where pollutant absorption and biodegradation takes place, respectively (Figure 4). In bioscrubbers, the waste gas enters the absorption unit where the pollutants are transferred from the gas phase to an aqueous solution (flowing either co-currently or counter-currently) [49,50]. The liquid scrubbing solution containing the dissolved gas contaminants is subsequently drawn off and transferred to a biological tank that contains the microorganisms, generally suspended in the cultivation broth, responsible for the biodegradation of the absorbed gas. Bioscrubbers are the preferred technique to treat hydrophilic VOCs (alcohols, ketones), with low Henry coefficients (<0.01), since they must be transfer to the aqueous phase prior degradation.

The main advantages of bioscrubbers are [33] :

- Operational stability and better control over operating parameters such as pH, moisture and nutrient content.
- Relatively lower pressure drop and less area requirement apart biotreatment alternatives

Disadvantages of bioscrubbers include:

- Low removal efficiency for hydrophobic compounds.
- Provides low specific surface area for gas–liquid mass transfer (generally $<300\text{ m}^{-1}$)
- Excess sludge generation
- Generation of secondary liquid waste stream

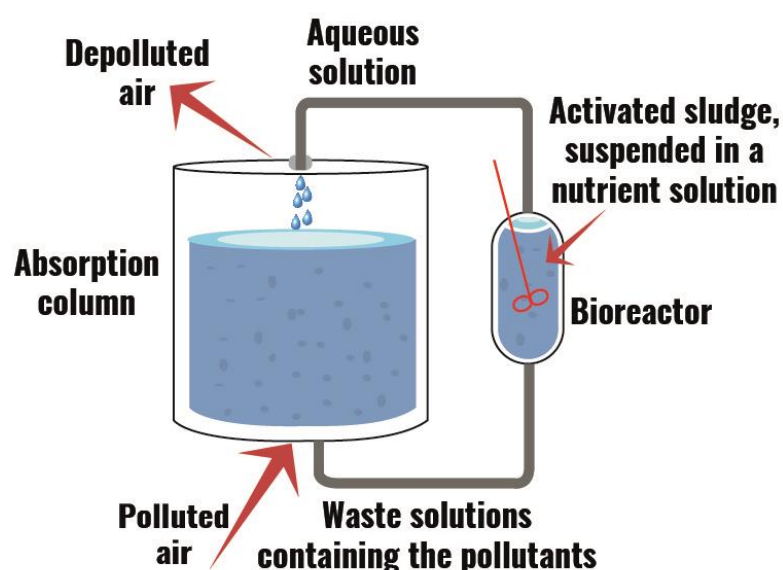


Figure 4 Schematic representation of a bioscrubber. [33]

1.6.3 Biotrickling Filter

A biotrickling filter (BTF) consists of a cylindrical column packed with inert material that promotes the growth of microorganisms as a biofilm [4]. The polluted gas stream passes through the packed bed, which is continuously irrigated with a recirculating aqueous solution containing essential nutrients required by the microbial community, washing away the excess biomass and secondary products [33,51]. In BTFs, the microorganisms grow forming biofilms on the surface of the packing material, and pollutants are initially absorbed in the aqueous film trickling over the biofilm and degraded afterwards by the microbial community (

Figure 5). BTFs present multiple advantages over other biological alternatives, such as lower pressure drops across the packed bed due to the high porosity of the inert packing material, less operating costs, easier control of the operating parameters (pH, nutrient feed), capability to treat by-products from VOCs degradation, lower area requirements, less dead zones, and higher removal efficiencies (REs) for aromatics, chlorinated hydrocarbons and organic sulfur compounds [33,52]. Despite these advantages, the accumulation of excess biomass in the filter bed and the production of a secondary waste stream are considered the major drawbacks of BTFs.

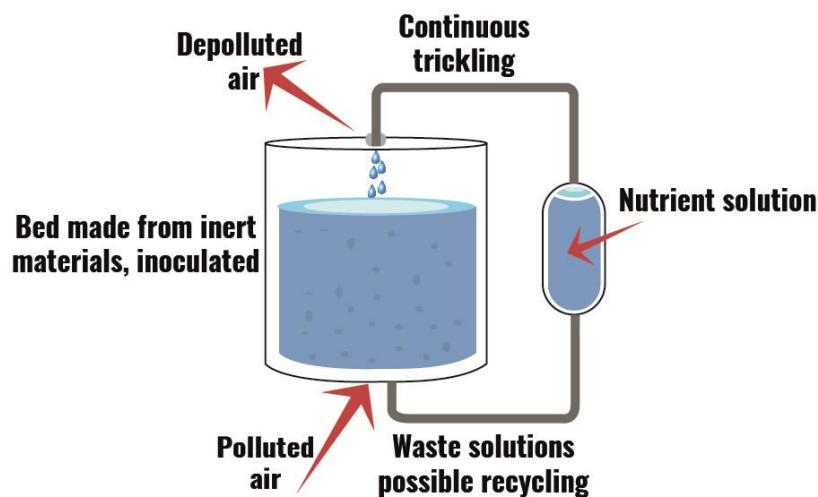


Figure 5 Schematic representation of a biotrickling filter. [33]

1.6.4 Bubble Column Bioreactor

The VOCs removal performance in the aboved-revised biotechnologies is usually limited by mass transfer of the compound from the gas to the liquid phase or biofilm, thus resulting in low removal efficiencies for poorly water-soluble (hydrophobic) compounds. In this context, bubble column bioreactors (BCBs) present high mass transfer capacities compared with other biotreatment alternatives due to the supplementation of the gas stream through ultrafine bubble diffusers with micropores <math> < 0.5 \mu\text{m}</math>, which allow increasing the contact between the gas and liquid phase, and results in an enhanced mass transfer. Generally, BCBs consist of cylindrical vessels with a gas distributor at the bottom. The gas stream is sparged in the form of fine bubbles into the biomass suspension. In addition, the performance of BCBs can be further boosted via internal gas recycling, which allows the decoupling of the actual gas residence time and turbulence in the microbial broth from the overall empty bed residence time [53–55]. Additionally, BCBs require little maintenance, present low footprint and have low operating costs compared to other reactor configurations. Due to these advantages, BCBs are widely employed in chemical, biochemical and petrochemical industries.

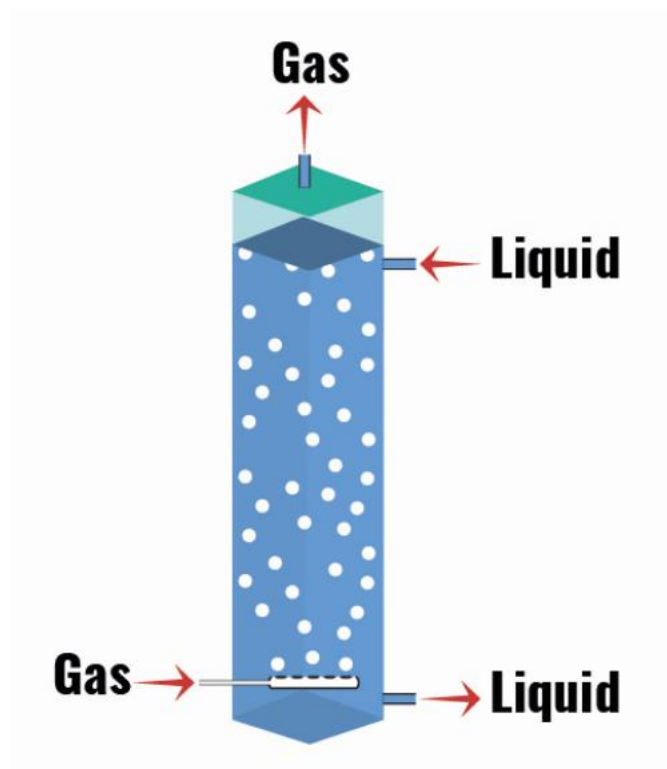


Figure 6 Schematic representation of a bubble column bioreactor[56]

BCBs can easily adapted to photobioreactors, which are bioreactors that utilize a light source to promote the phototrophic growth of algae and cyanobacteria in symbiosis with bacteria.

Photobioreactors are typically described as an enclosed, illuminated culture vessel designed for controlled biomass production [57]. Photobioreactor support the symbiotic growth of microalgae and bacterial, a consortium that provides mutual benefits to remove malodorous compounds such as amines due to their superior NH_3 fixation and enhanced O_2 supply.

1.7 Model Sectors: Bakery yeast production and Petroleum industry

From the beginning of the industrial revolution in the mid-1900s, industries started to release air emissions to atmosphere without considering protection to the environment or human health. More recently, many different types of industries and related sectors have been required to meet higher social expectations in the form of new laws and regulations. Because of these new air quality standards, especially focused on odorous VOCs, industries started to control their gas emission via improving process efficiency and implementing end-of-the-pipe treatment processes. Among them, bakery yeast production represents one of the main industrial sources of odors due to its huge VOC release from its fermentation cycle. Ethanol and acetaldehyde, which are VOCs with low odor threshold levels (5-500 ppb_v and 10-120 ppb_v for ethanol and acetaldehyde, respectively), are released into the ambient air from the bakery yeast production process, resulting in important odor nuisance in the surrounding neighbourhoods [58]. Besides the main air emissions of acetaldehyde and ethanol, many different types of VOCs are released to the atmosphere via yeast fermentation process. However, the detailed waste gas characterization is still unknown.

Chemical industry was also selected in this thesis as a model sector due to the large variety of chemical compound manufacture. Among malodorous compounds, trimethylamine (TMA, $\text{C}_3\text{H}_9\text{N}$) has been identified as one of the main pollutants emitted. TMA is a potentially toxic and likely carcinogenic VOC with a low odor threshold level of $0.2 \mu\text{g m}^{-3}$ [59–61]. Proper management of TMA emissions according to legislation limits is crucial to not only avoid health hazards and ensure occupational safety, but also to reduce impacts on the environment. [59,62]. Petrochemical industry is also an important source of VOCs emission. Apart sulphric volatile organic compounds Ethanethiol came into forward due to its low odor threshold level and highly flammable character. Apart from that Benzene, Toluene, and Ethylbenzene and Xylene (BTEX) being key pollutants due to their widespread use in the sector. In this sense, BTEX emissions accounts nowadays for up to 59% (w/w) of gasoline pollutants and represent 80% of the total

VOC emissions in petrochemical plants [47,63]. In addition, BTEX have genotoxic properties and are included in the Hazardous Air Pollutants List of the United State Environmental Protection Agency (USEPA) and rank 78 in the CERCLA List out of the 275 substances identified to pose a significant potential threat to human health [52,64].

1.8 References

- [1] Seinfeld JH, Pandis S, *Atmospheric Chemistry and Physics: From Air Pollution to Climate Change. 2nd Edition*. John Wiley & Sons, New York, 2006.
- [2] IARC Monographs, *To Humans Outdoor Air Pollution*, Vol. 109, 2015.
- [3] E.R. Rene, M. Estefanía López, M.C. Veiga and C. Kennes, *Neural network models for biological waste-gas treatment systems*, N. Biotechnol. 29 (2011), pp. 56–73.
- [4] J.M. Estrada, *Biotechnologies for Air Pollution Control : Overcoming Design and Operational Limitations*, (2014), .
- [5] E. Sanidas, D.P. Papadopoulos, H. Grassos, M. Velliou, K. Tsioufis, J. Barbetseas et al., *Air pollution and arterial hypertension. A new risk factor is in the air*, J. Am. Soc. Hypertens. 11 (2017), pp. 709–715.
- [6] C.J. Nobles, E.F. Schisterman, S. Ha, K. Kim, S.L. Mumford, G.M. Buck Louis et al., *Ambient air pollution and semen quality*, Environ. Res. 163 (2018), pp. 228–236.
- [7] C.A. Garcia, P.S. Yap, H.Y. Park and B.L. Weller, *Association of long-term PM2.5 exposure with mortality using different air pollution exposure models: Impacts in rural and urban California*, Int. J. Environ. Health Res. 26 (2016), pp. 145–157.
- [8] A.G. Barnett, G.M. Williams, J. Schwartz, A.H. Neller, T.L. Best, A.L. Petroschevsky et al., *Air pollution and child respiratory health: A case-crossover study in Australia and New Zealand*, Am. J. Respir. Crit. Care Med. 171 (2005), pp. 1272–1278.
- [9] S. Li, K. Feng and M. Li, *Identifying the main contributors of air pollution in Beijing*, J. Clean. Prod. 163 (2017), pp. S359–S365.
- [10] J. Huang, X. Pan, X. Guo and G. Li, *Impacts of air pollution wave on years of life lost: A crucial way to communicate the health risks of air pollution to the public*, Environ. Int. 113 (2018), pp. 42–49.
- [11] R. Brugha, C. Edmondson and J.C. Davies, *Outdoor air pollution and cystic fibrosis*, Paediatr. Respir. Rev. (2018), .
- [12] H. Singh, *Experimental Comparative Study of Performance and Emission Characteristics of a CI Engine using Diesel Oil and Rice Bran-Ethanol Blends*, (2017),
- [13] C. Yang, H. Qian, X. Li, Y. Cheng, H. He, G. Zeng et al., *Simultaneous Removal of Multicomponent VOCs in Biofilters*, Trends Biotechnol. 36 (2018), pp. 673–685.
- [14] P. Balasubramanian, L. Philip and S. Murty Bhallamudi, *Biotrickling filtration of complex pharmaceutical VOC emissions along with chloroform*, Bioresour. Technol. 114 (2012), pp. 149–159.

- [15] Q. Wang, S. Li, M. Dong, W. Li, X. Gao, R. Ye et al., *VOCs emission characteristics and priority control analysis based on VOCs emission inventories and ozone formation potentials in Zhoushan*, *Atmos. Environ.* 182 (2018), pp. 234–241.
- [16] S. Malakar, P. Das Saha, D. Baskaran and R. Rajamanickam, *Comparative study of biofiltration process for treatment of VOCs emission from petroleum refinery wastewater—A review*, *Environ. Technol. Innov.* 8 (2017), pp. 441–461.
- [17] R. Muñoz, E.C. Sivret, G. Parcsi, R. Lebrero, X. Wang, I.H. Suffet et al., *Monitoring techniques for odour abatement assessment*, *Water Res.* 44 (2010), pp. 5129–5149.
- [18] M. Schiavon, L.M. Martini, C. Corrà, M. Scapinello, G. Coller, P. Tosi et al., *Characterisation of volatile organic compounds (VOCs) released by the composting of different waste matrices*, *Environ. Pollut.* 231 (2017), pp. 845–853.
- [19] S. Sironi, L. Capelli, P. Céntola, R. Del Rosso and S. Pierucci, *Odour impact assessment by means of dynamic olfactometry, dispersion modelling and social participation*, *Atmos. Environ.* 44 (2010), pp. 354–360.
- [20] G. Bianchi, M. Palmiotto, M. Giavini and E. Davoli, *Environmental odor pollution: A complex GC-MS, olfactometry and diffusion modeling approach to define air quality*, *Compr. Anal. Chem.* 61 (2013), pp. 97–114.
- [21] J.M. Estrada, N.J.R.B. Kraakman, R. Muñoz and R. Lebrero, *A comparative analysis of odour treatment technologies in wastewater treatment plants.*, *Environ. Sci. Technol.* 45 (2011), pp. 1100–1106.
- [22] J. Badach, P. Kolasińska, M. Paciorek, W. Wojnowski, T. Dymerski, J. Gębicki et al., *A case study of odour nuisance evaluation in the context of integrated urban planning*, *J. Environ. Manage.* 213 (2018), pp. 417–424.
- [23] L. Capelli, S. Sironi, R. Del Rosso, P. Céntola and M. Il Grande, *A comparative and critical evaluation of odour assessment methods on a landfill site*, *Atmos. Environ.* 42 (2008), pp. 7050–7058.
- [24] J.E. Hayes, R.M. Fisher, R.J. Stevenson, C. Mannebeck and R.M. Stuetz, *Unrepresented community odour impact: Improving engagement strategies*, *Sci. Total Environ.* 609 (2017), pp. 1650–1658.
- [25] D.E.G. Trigueros, A.N. Módenes, A.D. Kroumov and F.R. Espinoza-Quiñones, *Modeling of biodegradation process of BTEX compounds: Kinetic parameters estimation by using Particle Swarm Global Optimizer*, *Process Biochem.* 45 (2010), pp. 1355–1361.
- [26] R.A. Deeb and L. Alvarez-Cohen, *Temperature effects and substrate interactions during the aerobic biotransformation of BTEX mixtures by toluene-enriched consortia and Rhodococcus rhodochrous*, *Biotechnol. Bioeng.* 62 (1999), pp. 526–536.
- [27] M.J. Horn and D.B. Jones, *Communication to the editor*, *J. Am. Chem. Soc.* 62 (1940), pp. 234.
- [28] I. Akmirza, A. Carvajal, R. Muñoz and R. Lebrero, *Interactions between BTEX compounds during their anoxic degradation*, *Chem. Eng. Trans.* 54 (2016), pp. 115–120.
- [29] J.A. Morlett-Chávez, J.Á. Ascacio-Martínez, A.M. Rivas-Estilla, J.F. Velázquez-

- Vadillo, W.E. Haskins, H.A. Barrera-Saldaña et al., *Kinetics of BTEX biodegradation by a microbial consortium acclimatized to unleaded gasoline and bacterial strains isolated from it*, *Int. Biodeterior. Biodegrad.* 64 (2010), pp. 581–587.
- [30] M.C. Annesini, V. Piemonte, M.C. Tomei and A.J. Daugulis, *Analysis of the performance and criteria for rational design of a sequencing batch reactor for xenobiotic removal*, *Chem. Eng. J.* 235 (2014), pp. 167–175.
- [31] L. da R. Novaes, N.S. de Resende, V.M.M. Salim and A.R. Secchi, *Modeling, simulation and kinetic parameter estimation for diesel hydrotreating*, *Fuel* 209 (2017), pp. 184–193.
- [32] H. Dette, V.B. Melas and N. Strigul, *Design of Experiments for Microbiological Models*, *Appl. Optim. Des.* (2005), pp. 137–180.
- [33] S. Mudliar, B. Giri, K. Padoley, D. Satpute, R. Dixit, P. Bhatt et al., *Bioreactors for treatment of VOCs and odours - A review*, *J. Environ. Manage.* 91 (2010), pp. 1039–1054.
- [34] K. Barbusinski, K. Kalemba, D. Kasperczyk, K. Urbaniec and V. Kozik, *Biological methods for odor treatment – A review*, *J. Clean. Prod.* 152 (2017), pp. 223–241.
- [35] A.C. Romain, J. Delva and J. Nicolas, *Complementary approaches to measure environmental odours emitted by landfill areas*, *Sensors Actuators, B Chem.* 131 (2008), pp. 18–23.
- [36] L. Wenjing, D. Zhenhan, L. Dong, L.M.C. Jimenez, L. Yanjun, G. Hanwen et al., *Characterization of odor emission on the working face of landfill and establishing of odorous compounds index*, *Waste Manag.* 42 (2015), pp. 74–81.
- [37] L. Capelli, S. Sironi and R. del Rosso, *Odor sampling: Techniques and strategies for the estimation of odor emission rates from different source types*, *Sensors (Switzerland)* 13 (2013), pp. 938–955.
- [38] M. Schlegelmilch, J. Streese and R. Stegmann, *Odour management and treatment technologies: An overview*, *Waste Manag.* 25 (2005), pp. 928–939.
- [39] D. Gabriel and M. a Deshusses, *Retrofitting existing chemical scrubbers to biotrickling filters for H₂S emission control.*, *Proc. Natl. Acad. Sci. U. S. A.* 100 (2003), pp. 6308–6312.
- [40] R. Lebrero, E. Rodríguez, M. Martín, P.A. García-Encina and R. Muñoz, *H₂S and VOCs abatement robustness in biofilters and air diffusion bioreactors: A comparative study*, *Water Res.* 44 (2010), pp. 3905–3914.
- [41] J.C. López, L. Merchán, R. Lebrero and R. Muñoz, *Feast-famine biofilter operation for methane mitigation*, *J. Clean. Prod.* 170 (2018), pp. 108–118.
- [42] S. Malakar, P. Das Saha, D. Baskaran and R. Rajamanickam, *Comparative study of biofiltration process for treatment of VOCs emission from petroleum refinery wastewater—A review*, *Environ. Technol. Innov.* 8 (2017), pp. 441–461.
- [43] P. Balasubramanian, L. Philip and S. Murty Bhallamudi, *Biotrickling filtration of VOC emissions from pharmaceutical industries*, *Chem. Eng. J.* 209 (2012), pp. 102–112.
- [44] J.W. Van Groenestijn and N.J.R. Kraakman, *Recent developments in biological waste gas purification in Europe*, *Chem. Eng. J.* 113 (2005), pp. 85–91.

- [45] H. Wu, H. Yan, Y. Quan, H. Zhao, N. Jiang and C. Yin, *Recent progress and perspectives in biotrickling filters for VOCs and odorous gases treatment*, J. Environ. Manage. 222 (2018), pp. 409–419.
- [46] K. Barbusinski, K. Kalemba, D. Kasperczyk, K. Urbaniec and V. Kozik, *Biological methods for odor treatment – A review*, J. Clean. Prod. 152 (2017), pp. 223–241.
- [47] G. Gallastegui, A. Ávalos Ramirez, A. Elías, J.P. Jones and M. Heitz, *Performance and macrokinetic analysis of biofiltration of toluene and p-xylene mixtures in a conventional biofilter packed with inert material*, Bioresour. Technol. 102 (2011), pp. 7657–7665.
- [48] Z. Shareefdeen, B. Herner and A. Singh, *1 Biotechnology for Air Pollution Control – an Overview*, (2005), .
- [49] S. Potivichayanon, P. Pokethitiyook and M. Kruatrachue, *Hydrogen sulfide removal by a novel fixed-film bioscrubber system*, Process Biochem. 41 (2006), pp. 708–715.
- [50] G.M. Nisola, E. Cho, J.D. Orata, M.C.F.R. Redillas, D.M.C. Farnazo, E. Tuuguu et al., *NH₃ gas absorption and bio-oxidation in a single bioscrubber system*, Process Biochem. 44 (2009), pp. 161–167.
- [51] M. Schiavon, M. Ragazzi, E.C. Rada and V. Torretta, *Air pollution control through biotrickling filters: a review considering operational aspects and expected performance*, Crit. Rev. Biotechnol. 36 (2016), pp. 1143–1155.
- [52] I. Akmirza, C. Pascual, A. Carvajal, R. Pérez, R. Muñoz and R. Lebrero, *Science of the Total Environment Anoxic biodegradation of BTEX in a biotrickling filter*, 588 (2017), pp. 457–465.
- [53] Z. Ahmed, S.J. Hwang, S.K. Shin and J. Song, *Enhanced toluene removal using granular activated carbon and a yeast strain Candida tropicalis in bubble-column bioreactors*, J. Hazard. Mater. 176 (2010), pp. 849–855.
- [54] T. García-Pérez, J.C. López, F. Passos, R. Lebrero, S. Revah and R. Muñoz, *Simultaneous methane abatement and PHB production by Methylocystis hirsuta in a novel gas-recycling bubble column bioreactor*, Chem. Eng. J. 334 (2018), pp. 691–697.
- [55] N. Kantarci, F. Borak and K.O. Ulgen, *Bubble column reactors*, Process Biochem. 40 (2005), pp. 2263–2283.
- [56] M. Sui and E. Sakarinen, *Design of a bubble column reactor*, (2017), .
- [57] R.N. Singh and S. Sharma, *Development of suitable photobioreactor for algae production - A review*, Renew. Sustain. Energy Rev. 16 (2012), pp. 2347–2353.
- [58] F.A. Fazzalari, I.B. Machines and H. Junction, *Compilation of Odor and Taste*, .
- [59] C.T. Chang, B.Y. Chen, I.S. Shiu and F.T. Jeng, *Biofiltration of trimethylamine-containing waste gas by entrapped mixed microbial cells*, Chemosphere 55 (2004), pp. 751–756.
- [60] S. Wan, G. Li, L. Zu and T. An, *Bioresource Technology Purification of waste gas containing high concentration trimethylamine in biotrickling filter inoculated with B350 mixed microorganisms*, Bioresour. Technol. 102 (2011), pp. 6757–6760.
- [61] A. Aguirre, P. Bernal, D. Maureira, N. Ramos, J. Vásquez, H. Urrutia et al.,

- Biofiltration of trimethylamine in biotrickling filter inoculated with Aminobacter aminovorans*, Electron. J. Biotechnol. 33 (2018), pp. 63–67.
- [62] P.M. Perillo and D.F. Rodríguez, *Low temperature trimethylamine flexible gas sensor based on TiO₂ membrane nanotubes*, J. Alloys Compd. 657 (2016), pp. 765–769.
- [63] M.H. El-Naas, J.A. Acio and A.E. El Telib, *Aerobic biodegradation of BTEX: Progresses and Prospects*, J. Environ. Chem. Eng. 2 (2014), pp. 1104–1122.
- [64] A. Carvajal, I. Akmirza, D. Navia, R. Pérez, R. Muñoz and R. Lebrero, *Anoxic denitrification of BTEX: Biodegradation kinetics and pollutant interactions*, J. Environ. Manage. 214 (2018), pp. 125–136.



Universidad de Valladolid

CHAPTER 2

Aim and Scope of the Thesis

2.1 Justification of the thesis

Odor is typically defined as the “perception of smell” or in scientific terms as “a perception resulting from the reception of stimulus by the olfactory sensory system”. Unlike conventional air pollutants, odorous pollutants have different characteristics and its impact is tightly determine by human perception. Due to the subjective nature of odorous pollutant perception, odor pollution has become nowadays a topic of increasing importance within the global quest to improve air quality standards and increase well-being level of people. The increasing industrialization and encroachment of residencial areas in industrial sectors have resulted in an increase in the number of public complaints related to odor nuisance. Many studies have consistently pointed out the serious adserve effects of odorous emissions on human health and the environment, which has arised a increasing public concern to reduce the impact of odour pollution in cities. In order to find the proper strategy to prevent and to reduce the adverse effects of odor emissions, the identification of the problem via a proper characterization methodology followed by a selection of cost-effective and environmental friendly solutions to abate odor emissions should be investigated in the industrial sector. Among the industrial processes, food fermentation, and chemistry/petrochemical industries represent key pollution sectors due to their large volumes of odor emissions release to atmosphere. This is central in many developing countries, where a major part of these industrial processes release their off-gases without any treatment. Apart from the above mentioned odour nuisance, waste gas streams released to atmosphere by chemical/petrochemical industries containg toxic volatile organic compounds such as ethanethiol, benzene, toluene, ethlybenzene and xylene (BTEX), which are responsible for health problems such as central nervous system depression, negative effects on the respiratory system and leukemia cancer. In this context, odor emissions abatement has become a priority that requires simultaneously a proper emission characterization and the development of cost-competitive and environmentally friendly abatement technologies.

2.2 Main objectives

It is generally accepted that for an effective and proper odor abatement to be implemented, the problem must first be quantified. Up to date, many studies didn't take into account the characteristics of the emission, which resulted in a poor abatement performance. Within the primary aim of this thesis work, malodourous gas emissions in model industrial sectors such as

food fermentation and chemical/petrochemical were investigated to obtain a proper characterization of the odorous waste gas. The second major goal of thesis work involved the development of cost-effective and green treatment technologies in the model industrial sectors. Until now many physical/chemical odor treatment techniques have been widely used due to their low footprint, high efficiency and rapid start-up, and extensive experience in design and operation, but these techniques are not environmental friendly and entail high investment costs. In this context, the specific aims of this thesis can be summarized as follows:

1. Determination of bakery yeast fermentation emissions characteristic in real scale case study via both subjective and objective methodologies such as “dynamic olfactometer” and “instrumental analyses”, respectively to help the selection of proper treatment process to overcome the odor nuisance in surrounding residential areas.
2. Semi-pilot scale biofilter operation for the treatment of well-characterized bakery yeast fermentation emissions, and investigation the influence of operation parameters such as EBRT, IL for both single and ternary VOC feeding regimes.
3. Anoxic bioscrubber operation for ethanethiol containing waste gas emission removal was carried out under specific S/NO_3^- to enable less hazardous form of S as S_0 production rather than SO_4^- and investigation the influence of operation parameters for ET removal.
4. Microbial kinetic parameters estimation of communities anoxically treating BTEX under O_2 -free conditions for single, dual and quaternary BTEX mixtures and the effect of substrate interactions over biodegradation.
5. Lab scale anoxic biotrickling filter operation for biotreatment of BTEX mixture and study of the influence of dilution rate, pH and UV treatment over biodegradation.
6. Comparative evaluation of a bacterial bubble column reactor and algal-bacteria bubble column photobioreactor for TMA biodegradation.

2.3 Development of the thesis

Instrumental and olfactometric analyses are recommended as methods for odor nuisance assessment. Within instrumental techniques, gas chromatography coupled with mass-spectrometry (GC–MS) allows a qualitative and quantitative determination of the composition of a gas mixture, while sensorial techniques such as dynamic olfactometry uses human nose as a sensor to determine both the odor threshold and concentration/intensity of odor emissions. This thesis was carried out in two universities. Thus, studies dealing with fermentation process emissions were carried out at Istanbul Technical University, where the characterization of odor emissions in bakery yeast fermentation process was conducted using instrumental and olfactometric techniques (Chapter 3). The performance of a semi-pilot scale biofilter for the treatment of single and tertiary mixtures of gas pollutants from fermentation processes was also evaluated (Chapter 3). In addition, the anoxic removal of ethanethiol, a model pollutant from petroleum refineries and food industry with a low odor threshold, was assessed in a bioscrubber (Chapter 4) at Istanbul Technical University. On the other hand, studies at Valladolid University were focused on the chemical/petrochemical industry as a model sector. Kinetic parameter estimation for microbial communities degrading O₂-free BTEX emissions under anoxic conditions were done for single, dual and quaternary mixtures (Chapter 5). In addition, the continuous biotreatment of BTEX emissions was carried out in an anoxic biotrickling filter (Chapter 6). Finally, based on the preliminary characterization of TMA-laden emission conducted at Istanbul Technical University, a comparative evaluation of a bacterial and an algal-bacterial bubble column photobioreactor for TMA abatement was carried at Valladolid University (Chapter 7). These works that were conducted within this thesis study were pertained to the specific aims of main objectives and summarized in Figure 7.

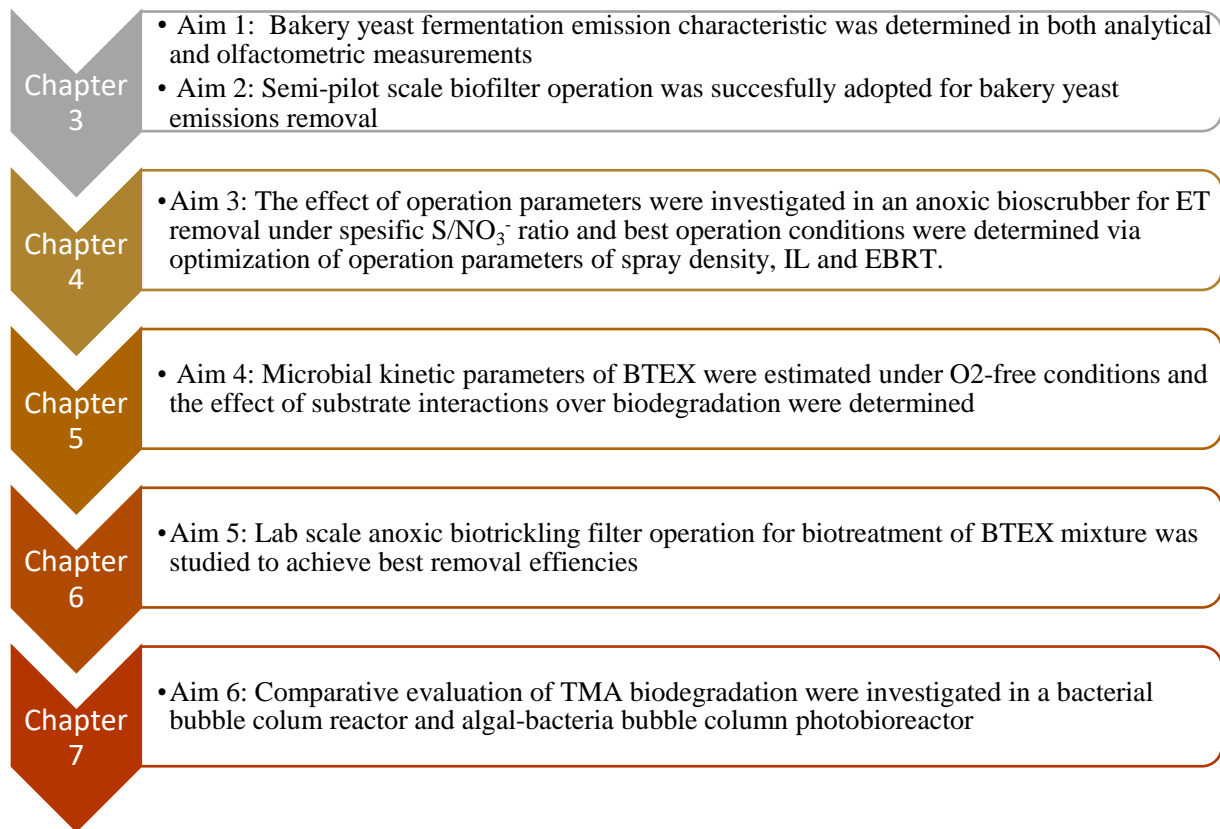


Figure 7 Correlation of specific aims within the works conducted



Universidad de Valladolid

CHAPTER 3

**Characterization and Treatment of Yeast
Production Process Emissions in a Biofilter**

CHARACTERIZATION AND TREATMENT OF YEAST PRODUCTION PROCESS EMISSIONS IN A BIOFILTER

Ilker Akmirza^{1,2,*}, Mustafa Turker³, Kadir Alp¹

¹Department of Environmental Engineering, Technical University of Istanbul, 34469 Istanbul, Turkey

²Department of Chemical Engineering and Environmental Technology, University of Valladolid, Dr. Mergelina s/n. 47011, Valladolid, Spain

³Pakmaya, PO Box 149, 41310, Kocaeli, Turkey

ABSTRACT

Characterization of odorous VOC emissions in waste gas stream and removal of characterized pollutants with a proper technique become prominent. Within this study, bakery yeast fermentation emissions were analyzed with both instrumental and olfactometric methods to illustrate emission characterization in terms of both objective and subjective views and were biodegraded in a pilot scale biofilter. Instrumental analyses determined the chemical composition of emissions where ethanol emission was reached to 764 mg m^{-3} at peak hour, which were followed by acetaldehyde (331 mg m^{-3}) and acetone (65 mg m^{-3}). Olfactometric analyses were carried out to quantify the sensory impact of odors and the odor concentration was measured at peak hour as 39725 OU m^{-3} , which resulted 40 times higher concentration than legal limits. Process emissions were treated in a pilot scale biofilter primarily for single ethanol load and achieved to maximum removal of $97 \pm 1 \%$ with an elimination of $31.7 \pm 1.2 \text{ g m}^{-3} \text{ h}^{-1}$ while ternary waste gas stream simulation within addition of acetaldehyde and acetone to synthetic stream resulted to removal of $92 \pm 1 \%$, $86 \pm 2 \%$, $62 \pm 1 \%$ with elimination of $38.5 \pm 1.9 \text{ mg m}^{-3}$, $12.4 \pm 1.1 \text{ mg m}^{-3}$, $2.5 \pm 0.3 \text{ mg m}^{-3}$ for ethanol, acetaldehyde and acetone, respectively. In brief the superior performance of biofilter operation were achieved for both single and ternary gas streams from process emissions while still process improvement on VOC mass transfer enhancement for high waste gas flow will be required.

KEYWORDS:

Odor, emission, yeast fermentation, characterization, biofilter

INTRODUCTION

Air pollution has become a topic of significant importance and its adverse effect on human as well as on environment have been recorded in various case studies [1]. Wide variety of air pollutants cause many environmental problems at global, regional and local scale and threat air quality that lowered life standards [2]. Nowadays anthropogenic sources like

agricultural and industrial activities are considered primary air pollution sources and causing very serious environmental problems especially in many developing countries [3]. Additionally, important part of the gaseous emissions and chemical compounds from industrial processes are being released to atmosphere without any control mechanism and most of the emissions are responsible for odor nuisance. Long term exposure to odor emissions can cause on people to symptoms prevalence of emotional stresses such as states of headache, unease or depression to physical symptoms such as, eye irritation, nausea, respiratory problems or vomiting depending on nature and compositions of odor emissions [4, 5]. Numerous studies have pointed out the associations between high concentration of air pollutants and increased mortality [6, 7]. Apart from the health effect of odor emissions, increased wellbeing level of people and the evolution of public awareness to exposure to unpleasant odors are becoming one of the most frequent causes of air quality complaints in both industrial and urban areas [8–11]. To develop effective odor emission abatement, governmental authorities enacted strict legislations and have led industries to adopt proper air pollution treatment alternatives to comply with the legislations. Basic legal requirements of European union are specified in the Directive 2008/50/EC (2008) and Directive 2010/75/EU (2010). Also, Turkey enacted in 2013 "Regulation on Control of Emissions that Contribute to Odor (KOEKHY)" to specify the legal requirements.

It is generally accepted that for effective and proper odor abatement to be implemented, the problem must first be quantified, and odor characterization should be defined. For odor nuisance assessment, instrumental and olfactometric analyses are recommended as methods in many cases to determine odorous waste gas emission [12]. Within instrumental techniques e.g. gas chromatography coupled with mass-spectrometry (GC–MS) the qualitative and quantitative composition of a gas mixture can be determined while sensorial technique of olfactometry uses human nose as a sensor and allows to determine the threshold of odor and concentration/intensity of odor emissions [13, 14]. Selection of proper odor abatement techniques tightly depend on both

instrumental and olfactometric odor characterization. Until now many physical and chemical odor emission treatment techniques such as adsorption, condensation, ozonation catalytic oxidation, thermal oxidation have been widely used due to their advantages of compact equipment requirement and rapid operation start-up, widescale experience in design and operation [15, 16]. Although these advantages of physical and chemical odor emission treatment techniques, their non-environmental friendly nature and, their high capital and operating costs have required the development of new treatment techniques. Biological treatment alternatives eliminate many drawbacks of physical and chemical techniques and represent environmental friendly and low-cost alternatives to these technologies for treatment of odorous volatile organic compounds [17–20]. In this context, main types of conventional air phase bioreactors include biofilters, bio scrubbers and bio trickling filters. Among these bioreactor configurations, biofilters are used efficiently in wide variety of many hazardous industrial air pollutants [21, 22]. Biofilters are packed bed reactors in which microorganisms are attached on the surface of packing materials (e.g. plastic, compost, peat) and air stream passed through packing bed material where gas pollutants are transferred to the microbial film [23]. Also biofilters offer advantages over other biological air treatment alternatives due to their high flowrate waste gas elimination capacities especially for the abatement of dilute volatile organic compound (VOC) emission streams (<2000 mg m⁻³) [24–26].

Through industrial processes, bakery yeast production is a branch of food industry with a high frequency of odor emissions that resulted odor nuisance at surrounding settlements. As a result of yeast production process alcohol group members of VOCs such as ethanol (E) and acetaldehyde (AD) and acetone (A), which have relatively low odor threshold levels with wide ranges due to their subjective perception between 20-1000 ppbV, 10-210 ppbV and, 40-10000 ppbV respectively, are released to atmosphere from the process and lead to odor problem [27, 28]. Although it is difficult to standardize the emission perception, reduction of emission disposal to atmosphere within the help of treatment technologies will affect to reduce odor nuisance at surrounding neighborhoods.

This study aims to reveal the odor emission characteristic of food fermentation process and to determine proper biofilter operation conditions on behalf of odor nuisance abatement for determined odor emissions.

At this concept both instrumental and olfactometric odor pollution characterization analyses were performed and odor level and characteristics in yeast production process were determined and pilot scale biofilter operation carried

out to check its performance for fermentation emissions abatement.

MATERIALS AND METHODS

Yeast Factory Description and Gas Sampling. Field studies were conducted from a fermentation process of yeast factory in-Turkey. The waste gas from fermentation process are released to atmosphere and lead to odor problem at sources also often causes odor pollution to surrounding communities.

To understand characteristics of process waste gas emissions, instrumental and olfactometric analyses were carried out directly from the discharge point of waste gas at the stack. For instrumental analyses; sampling campaigns were conducted hourly as duplicate directly from the stack onto multisorbent tubes (to catch both hydrophobic and hydrophilic compounds onto surface of sorbent tubes) that contained the sorbent materials 20:35 Tenax-TA™, 60:80 Carboxen™ 1000, and 60:80 Carbosieve™ SIII. All samples were brought to the laboratory and analyzed within 24 h, following ASTM 2009 standards. For dynamic olfactometry measurements, pick hour emissions according to instrumental analyses results were selected and measurements were carried out according to EN 13725:2003 standards in parallel with second instrumental measurements. Samples for dynamic olfactometry analyses were collected into tedlar bags with a volume of 1 Liter and were analyzed by accredited laboratories.

Instrumental Analyses. The chemical characterization of each waste gas sample from fermentation process were analyzed by gas chromatograph (GC, Agilent 7890A, USA) equipped with a mass selective detector (Agilent 5975C, USA) according to EPA TO17 US-EPA, 1999a, Compendium Method TO17 (ASTM,2009). Thermal Desorber (TD, CDS 9300) was used as preconcentration equipment and waste gas samples onto sorbent tubes were first injected to TD and get concentrated for 10 minutes at 250°C then the concentrated gas stream passed through the a HP5MS (30 m × 0.25 mm × 0.25 μm) GC column. Oven temperature initially maintained at 40°C for 3 min, increased at 20 °C min⁻¹ up to final temperature of 140 °C and hold for 3 min at 140°C. Process waste gas emissions in the air sample were identified by comparing their retention times with the standards.

In pilot scale biofilter operation, gas samples from the inlet and outlet of column were collected via using 250 μl gas-tight syringe (Hamilton, USA) and direct injection to GC/MS were done by using same instrumental method for chemical component characterization within discarding preconcentration unit of TD.

Dynamic Olfactometric Analyses.

Olfactometry is sensorial technique directly related to the perception of human nose and allows to characterize odor concentration (c_{od}), that defined by Sironi et al. as the number of dilutions of odor sample with neutral air that are necessary to bring the odorous sample to its odor detection threshold concentration. It is expressed as European odor unit per cubic meter ($ouE\ m^{-3}$) [4]. Dynamic olfactometric analyses are based on dilution of an odor sample to the its odor threshold level, at which the odor can just barely be perceived by 50 % of the test panelists. With this aim of concept gas samples for olfactometric analyses were send to accredited laboratory and analyses were carried out in 24 hours after sampling with olfactometer ECOMA TO8 GmbH, based on the “yes/no” method according to EN 13725 (2003). Panelists sniffed odor samples with an increasing concentration until start to sense an odor that is different from the neutral reference air. Odor concentration (c_{od}) was then calculated as the geometric mean of the odor threshold values of each panelist. Detailed analysis method for dynamic olfactometry was described by the authors elsewhere [4, 5].

Biofilter Experimental Setup and Operation Procedure. Biofilter operation carried out in cylindrical jacketed PVC column with 0.2 m inner diameter and height of 2.7 m. Raschig rings (specific

surface area $>400\ m^2/m^3$) were used as packing material and reactor operation took place in a working volume of 47 Liter. Biofilter was inoculated with the activated sludge of recycling line from wastewater treatment plant of Ambarli, Istanbul (Turkey) and schematic view of experimental setup illustrated in Figure 1. 8 L of the activated sludge with a volatile suspended solids (VSS) concentration of $12500\ mg\ L^{-1}$ were used as inoculum and were resuspended in 2000 mL of MSM and added to the biofilter column and homogenised before the start-up. The system was operated for 144 days within 6 different steady-state conditions (Table 1).

Biofilter operation was started primarily for single component biodegradation experiments and the synthetic inlet gas stream was prepared by injecting of E with a syringe pump as a liquid for single component stages from the bottom of the reactor column in a counter mode with the humidification liquid flow. The biofilter system was operated with a waste gas flowrate of $2\ m^3\ h^{-1}$ and resulted gas loading rate of $63.7\ m^3\ m^{-2}\ h^{-1}$ consisting E emissions of $237 \pm 55\ mg\ m^{-3}$, $387 \pm 37\ mg\ m^{-3}$, $667 \pm 131\ mg\ m^{-3}$, respectively during the first 92 days of operation. AD and A were added to feed gas stream at the 93rd day of operation, purpose of proper waste gas characterization of industrial process, containing emission concentrations at inlet gas stream as $647 \pm 97\ mg\ m^{-3}$ for E, $255 \pm 48\ mg\ m^{-3}$ for AD and $68 \pm 16\ mg\ m^{-3}$ for A.

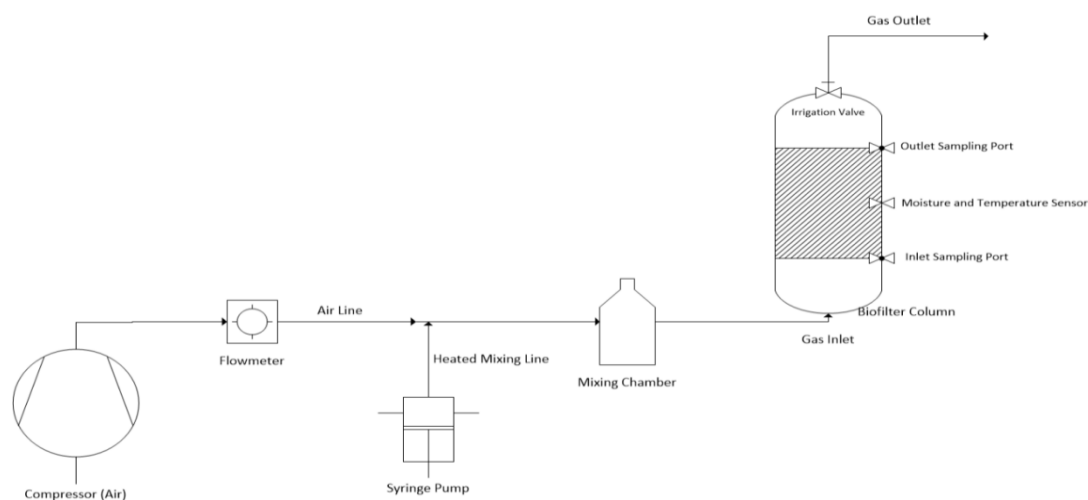


FIGURE 1
Schematic representation of experimental setup

TABLE 1
Experimental conditions established during the operational stages

Stage	Days of Operation	Compound	Organic Load
1	1-15	Ethanol	$10.1 \pm 2.3\ g\ m^{-3}\ h^{-1}$
2	15-30	Ethanol	$16.5 \pm 1.6\ g\ m^{-3}\ h^{-1}$
3	30-92	Ethanol	$28.4 \pm 5.5\ g\ m^{-3}\ h^{-1}$
4	92-122	Ethanol, Acetaldehyde and Acetone	$41.27 \pm 6.8\ g\ m^{-3}\ h^{-1}$
5	122-129	Ethanol, Acetaldehyde and Acetone	$61.92 \pm 8.8\ g\ m^{-3}\ h^{-1}$
6	129-144	Ethanol, Acetaldehyde and Acetone	$41.27 \pm 6.8\ g\ m^{-3}\ h^{-1}$

Gas empty bed residence time (EBRT) maintained as 80 seconds until the 5th stage of operation where gas flow was increased to 3 m³ h⁻¹ which is resulted a decrease in EBRT to 53 seconds while gas loading rate increased to 95.5 m³ m⁻² h⁻¹. Irrigation liquid kept main moisture in biofilter column at 50 % and includes all nutrients and was composed of (g L⁻¹): Na₂HPO₄·12H₂O, 6.15; KH₂PO₄, 1.52; MgSO₄·7H₂O, 0.2; CaCl₂, 0.038; and 10 mL L⁻¹ of a trace element solution containing (g L⁻¹): EDTA, 0.5; FeSO₄·7H₂O, 0.2; ZnSO₄·7H₂O, 0.01; MnCl₂·4H₂O, 0.003; H₃BO₃, 0.03; CoCl₂·6H₂O, 0.02; CuCl₂·2H₂O, 0.001; NiCl₂·6H₂O, 0.002; NaMoO₄·2H₂O, 0.003 [24].

Inlet and outlet E, AD and A concentrations in the gas phase were daily analysed via using a gas-tight syringe (Hamilton, USA) by GC-MS. Liquid samples were also daily collected to determine the pH level on the irrigation liquid. Moisture content in the biofilter coloumn was monitored continously via moisture meter and temperature in the column was monitored continusly via temperature probe.

The performance of the studied biofilter was generally evaluated in terms of the removal efficiency (RE) and elimination capacity (EC) which were calculated by following equations Eq 1 and Eq 2:

$$\text{Removal Efficiency (\%)} = \frac{C_{in} - C_{out}}{C_{out}} * 100 \quad (\text{Eq 1})$$

C_{in}: Inlet Concentration (mg m⁻³)

C_{out}: Outlet Concentration(mg m⁻³)

$$\text{Elimination Capacity (g m}^{-3}\text{h}^{-1}\text{)} = \frac{(C_{in} - C_{out}) * Q_{gas}}{V} \quad (\text{Eq 2})$$

Q_{gas}: Gas flowrate (m³ h⁻¹)

V: Volume of biofilter (m³)

RESULTS AND DISCUSSION

Determiration of Emission Characteristic by TD-GC-MS. The instrumental analyses in TD-GC-MS allowed to determine the emission concentrations of one complete fermentation cycle from process. In order to understand chemical composition and sensorial effects on human at the same time, intrumental analyses were done twice. At the first test assay peak hour emissions were selected for following olfactometric analyses and at the second test, sample were collected hourly as duplicate, simultaneous to olfactometric analyses and results were illustrated in Table 2 and Figure 2. Results showed clearly E and AD were primary pollutants that were consisting of higher than 95% of total emissions with the maximum concentration of 764 and 331 mg m⁻³, respectively while only less than 5% of total emissions were relased to atmosphere via A with the maximum concentration of 65 mg m⁻³ and trace propanol concentration was recorded during the cycle. Process emissions reached to their maximum values during the first hour of fermentation cycle for all characterized pollutants and peak emissions continued until the 7th hour of cycle and emissions were started to decrease sharply after the 8th hour of process and no emissions were observed at the 16th and 17th hours.

TABLE 2
Time course of average food fermentation cycle emissions

<i>Fermentation Cycle (h)</i>	<i>Ethanol (mg/m³)</i>	<i>Acetone (mg/m³)</i>	<i>Propanol (mg/m³)</i>	<i>Acetaldehyde (mg/m³)</i>	<i>Total Emission(mg/m³)</i>
1	764	65	21	331	1181
2	711	55	18	285	1069
3	704	54	20	275	1053
4	720	58	21	290	1089
5	634	44	18	215	911
6	629	38	18	197	882
7	720	47	20	224	1011
8	612	39	17	197	865
9	663	34	15	172	884
10	396	23	11	110	540
11	359	31	6	145	541
12	210	20	1	88	321
13	109	10	1	43	163
14	15	3	0	7	25
15	1	2	0	5	8
16	0	0	0	1	1
17	0	0	0	0	0

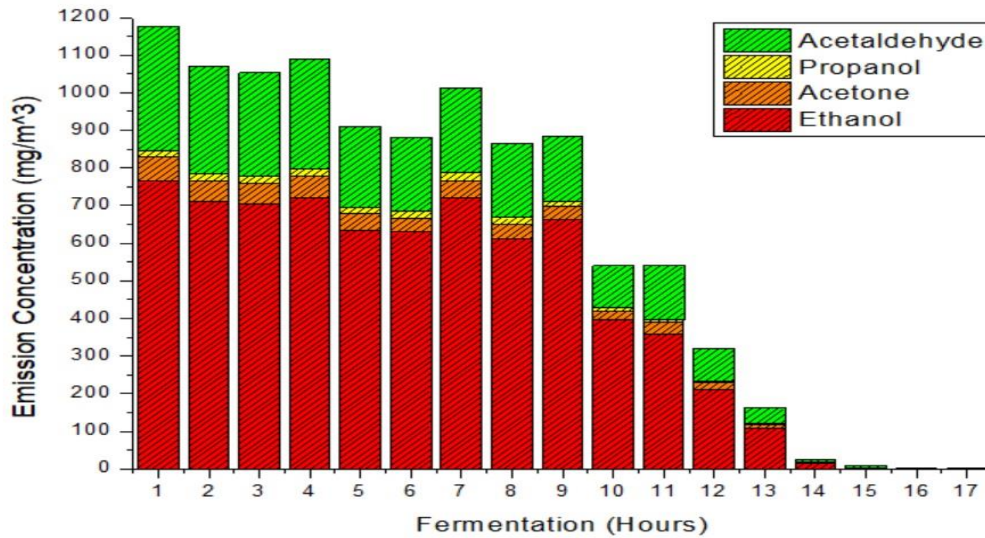


FIGURE 2
Change of food fermentation process emissions versus time

TABLE 3
Dynamic Olfactometry Odour Concentration

Fermentation Cycle (h)	Sampling Point	Odour	Odour	Odour	Odour
		Concentration	Concentration	Concentration	Concentration
		1. Measurement	2. Measurement	3. Measurement	Geometrical Mean
1	Fermentor Chimney	36781	41285	41285	39725
4	Fermentor Chimney	36781	21870	27554	28090

Determination of Odor Concentration via Dynamic Olfactometry Analyses. According to the results of first instrumental measurements, peak emission hours were selected for dynamic olfactometry measurements and on the second sampling procedure, the samples at the 1st and 4th hour of process cycle were collected for dynamic olfactometry analyses while the second instrumental measurement were repeated for entire cycle. Odor emissions for olfactometric analyses were determined by sniffing the odorous gas emissions by panelists and odor threshold level were perceived by panel members as 39725 OU m⁻³ and 28090 OU m⁻³ respectively, the first of which almost 40 times higher than legal limits. Additionally dynamic field olfactometry measurements were found in the range of previous odor threshold levels from literature [27, 28] and Table 3 illustrates results for dynamic olfactometric measurement.

Biofilter Operation Results. Since E was the dominant form of pollutant in the exhaust emission, biofilter operation was started primarily with single E feed with an EBRT of 80 seconds for 237 ± 55 mg m⁻³ E concentration and with an air flowrate of 2 m³ h⁻¹. After a startup period, the RE gradually increased to 90± 5% at the 3rd day, corresponding to EC of 8.5 ± 0.7 g m⁻³ h⁻¹ **Figure 3**. At the first steady state, the system reached to the RE up to 98±1% with an E.C. of 9.5 ± 0.7 g m⁻³ h⁻¹ on the 12th day of the

operation. At the 15th day, the inlet E concentration was increased to 387 ± 37 mg m⁻³ where no notable change on both RE and EC were observed during second steady state conditions while biofilter was able to remove higher than 95% of organic load input. After the 30th days of operation, the E concentration at the inlet increased to 667 ± 131 mg m⁻³ which presented peak E emissions during fermentation cycle. A step change in E concentration was resulted in only slight reduction in RE as 90±1 % with an EC of 28.3 ± 1.1 g m⁻³ h⁻¹ by day 33 while on the following days system reached again RE of 97±1% with an E.C of 31.7 ± 1.2 g m⁻³ h⁻¹ by the day 54. Accidentally stopping irrigation at the day 62 resulted in a sharp decrease in RE to 81±2% corresponding to E.C of 23.3 ± 1.0 g m⁻³ h⁻¹ in consequence of decelerating the microbial activity under limiting moisture content below % 25. At this point of concept, it is important to highlight that also previous authors were pointed out the detrimental effect of moisture content reduction on microbial activity and studies reported a sharp decrease by RE for target component when the moisture content remained below % 35 [29, 30]. Noticeable increase was recorded after returning previous irrigation cycle to supply % 50 of moisture content and system reached to maximum removal by the day 77 with RE of 98±1 % and resulted in E.C. of 32.7 ± 0.9 g m⁻³ h⁻¹.

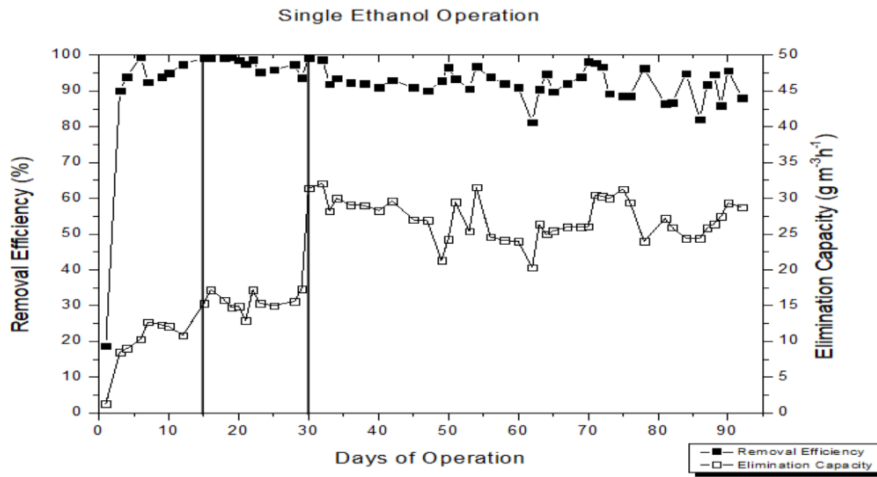


FIGURE 3

Time course of ethanol removal efficiency (—■—) and elimination capacity (—□—). Vertical lines represent different operating stages as indicated in the upper part of the figure.

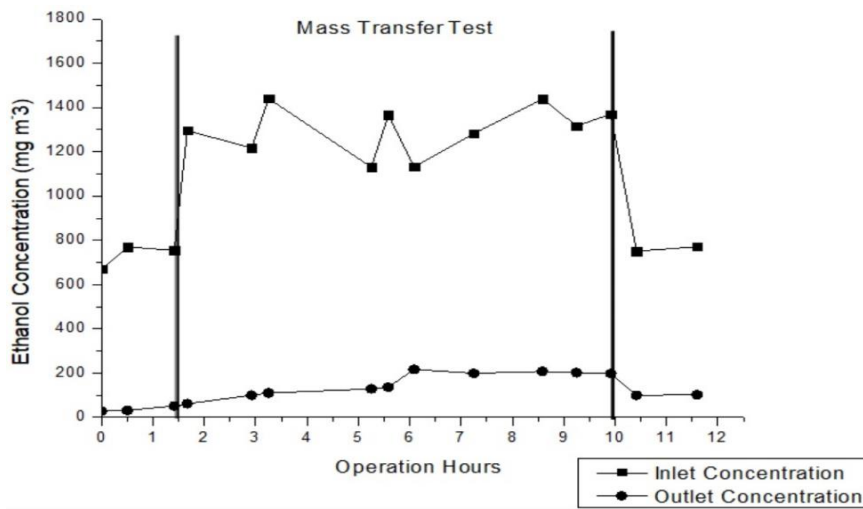


FIGURE 4

Inlet and outlet concentrations of ethanol during the mass transfer test

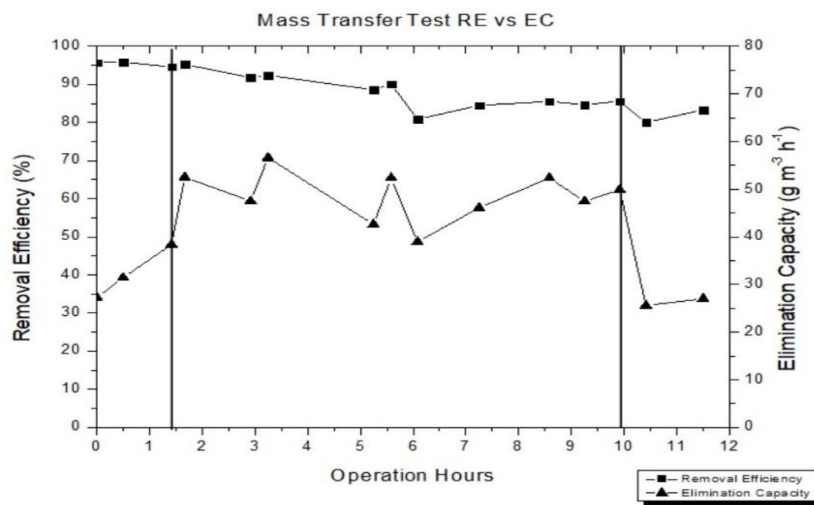


FIGURE 5

Ethanol removal efficiency and elimination capacity during the mass transfer test

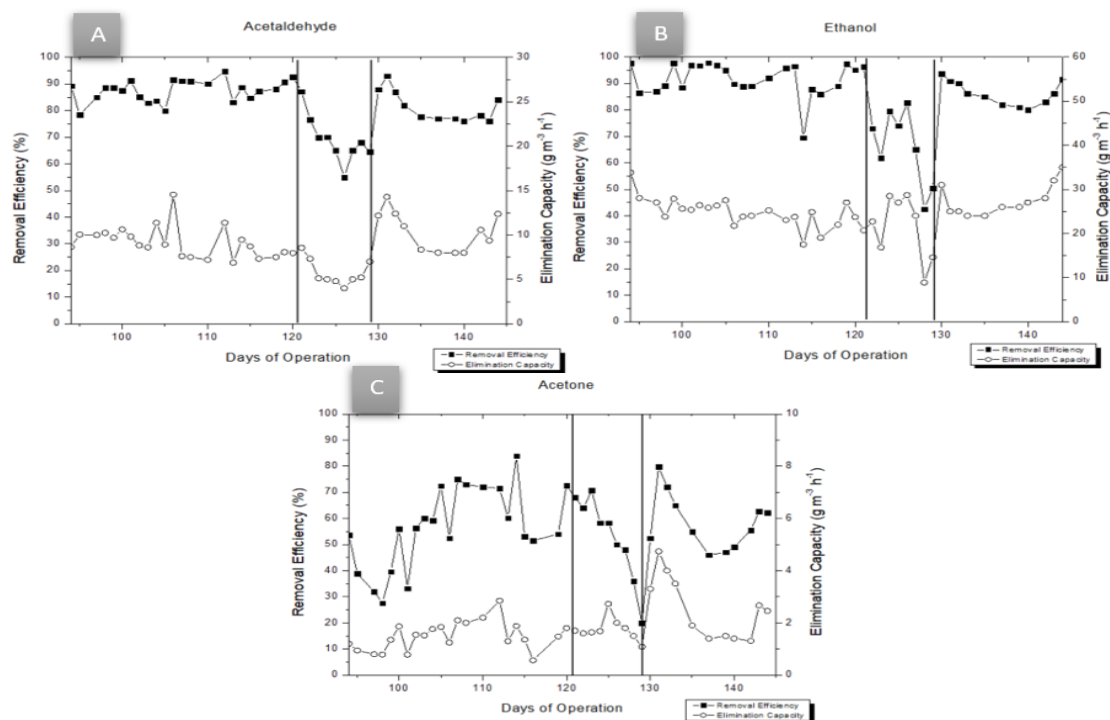


FIGURE 6

Time course of acetaldehyde(A), ethanol(B) and acetone(C) removal efficiency (—■—) and elimination capacity (—○—). Vertical lines represent different operating stages as indicated in the upper part of the figure.

After successfully elimination of E as a single component in the system by day 93, a mass transfer test was performed via increasing E inlet concentration two times in order to identify if the system was limited either by biological activity or by mass transfer for further step (mixture emissions). Samples from inlet and outlet were taken hourly during the test and illustrated in Figure 4 and the effect of increase by mass transfer to EC and RE was shown in Figure 5.

An increase in EC upon step change at inlet E concentration, showed that biodegradation capacity of microbial community on biofilter almost doubled with only slight decrease on RE. These results indicate the contribution of mass transfer limitation on the performance of the biofilter. Increasing the mass transfer capacity of the system may result in further use of mineralization capacity of microorganisms present in the biofilter. At day 93, AD and A were added to synthetic gas stream together with E to simulate complete pick hour waste gas characterization of the yeast fermentation process cycle. Therefore, inlet gas stream to biofilter contained $647 \pm 97 \text{ mg m}^{-3}$ of E, $255 \pm 48 \text{ mg m}^{-3}$ of AD and $68 \pm 16 \text{ mg m}^{-3}$ for A to simulate peak process conditions in Figure 6.

During the early steps of ternary gas mixture feeding to the biofilter, E removal was not affected by other compounds. Similar characteristics were observed for AD removal with RE of $89 \pm 1 \%$ and an

E.C of $9.7 \pm 1.2 \text{ g m}^{-3} \text{ h}^{-1}$ by the day 99 while only partly removal was observed for A corresponding to R.E of $28 \pm 1 \%$ and an E.C of $1 \pm 0.2 \text{ g m}^{-3}$ (Figure 6). After 10 days of adaptation period, A removal doubled and E.C reached to $1.9 \pm 0.2 \text{ g m}^{-3}$, while same elimination levels were observed for E and AC. By the day 122 after reaching stable elimination for both three compounds synthetic waste gas flow increased 50 % and reached to $3 \text{ m}^3 \text{ h}^{-1}$ that corresponded EBRT of 53 seconds. Increase by in organic loading by 50 % resulted in a sharp decrease by removal for all compounds and recorded by day 128 R.E. of $50 \pm 1 \%$, $64 \pm 1 \%$, $20 \pm 1 \%$ for E, AD and A respectively corresponding lowest E.C. at day 128 with $14.6 \pm 1.2 \text{ g m}^{-3}$, $9 \pm 1.2 \text{ g m}^{-3}$, $1.1 \pm 0.3 \text{ g m}^{-3}$ for E, AD and A. Also other studies pointed possible antagonistic reactions during simultaneous biodegradation of multicomponent under high organic loads and could led to production of possible inhibiting by-products [31, 32]. This might be explain the detrimental effect of organic load increase on biodegradation, to avoid the detrimental effect after increasing the organic load, system returned to previous conditions by the day 129 and recovered itself in a day and system operation stopped by day 144 after reaching R.E. of $92 \pm 1 \%$, $86 \pm 2 \%$, $62 \pm 1 \%$ with E.C. $38.5 \pm 1.9 \text{ g m}^{-3}$, $12.4 \pm 1.1 \text{ g m}^{-3}$, $2.5 \pm 0.3 \text{ g m}^{-3}$ for E, AC and A, respectively due to problems on the air line compressors.

CONCLUSION

To the best of our knowledge, the present work constitutes the first field study for odor causing emission characterization simultaneously by both objective (instrumental) and subjective (olfactometric) views in yeast industry. Results were recorded as quite higher than legal limits and it was compulsory to eliminate the emissions with high RE to reach legal limits. Pilot scale biofilter was selected in this study due to its low capital cost and environmental friendly nature for characterized yeast fermentation emissions to reach legal limits and this study demonstrated the feasibility of using biofilter as an alternative treatment for directly simulate VOC emissions from the bakery yeast industry. Although the features of this process make biofilter application suitable as end-of-pipe technology in this process, but more research on VOC mass transfer enhancement should be developed and still process optimization by operation parameters should be investigated to improve degradation.

ACKNOWLEDGEMENTS

This research was supported by The Scientific and Technological Research Council of Turkey within the project number TUBITAK 112Y273 and the name "Removal of odor emissions from food fermentation and Petrochemical Production Processes with using Biofilter and Bioscrubber.

REFERENCES

- [1] Rene, E.R., Estefanía López, M., Veiga, M.C., Kennes, C. (2011) Neural network models for biological waste-gas treatment systems. *N. Biotechnol.* 29, 56–73.
- [2] Kahya, C., Bekta Balçık, F., Oztaner, Y.B., Ozcomak, D., Seker, D.Z. (2017) Spatio-Temporal Analysis of Pm_{2.5} Over Marmara Region, Turkey. *Fresen. Environ. Bull.* 26, 310–317.
- [3] Kanada, M., Dong, L., Fujita, T., Fujii, M., Inoue, T., Hirano, Y., Togawa, T., Geng, Y. (2013) Regional disparity and cost-effective SO₂ pollution control in China: A case study in 5 mega-cities. *Energy Policy.* 61, 1322–1331.
- [4] Sironi, S., Capelli, L., Céntola, P., Del Rosso, R., Pierucci, S. (2010) Odour impact assessment by means of dynamic olfactometry, dispersion modelling and social participation. *Atmos. Environ.* 44, 354–360.
- [5] Wenjing, L., Zhenhan, D., Dong, L., Jimenez, L.M.C., Yanjun, L., Hanwen, G., Hongtao, W. (2015) Characterization of odor emission on the working face of landfill and establishing of odorous compounds index. *Waste Manag.* 42, 74–81.
- [6] Nobles, C.J., Schisterman, E.F., Ha, S., Kim, K., Mumford, S.L., Buck Louis, G.M., Chen, Z., Liu, D., Sherman, S., Mendola, P. (2018) Ambient air pollution and semen quality. *Environ. Res.* 163, 228–236.
- [7] Huang, J., Pan, X., Guo, X., Li, G.: Impacts of air pollution wave on years of life lost (2018) A crucial way to communicate the health risks of air pollution to the public. *Environ. Int.* 113, 42–49.
- [8] Pettarin, N., Campolo, M., Soldati, A. (2015) Urban air pollution by odor sources: Short time prediction. *Atmos. Environ.* 122, 74–82.
- [9] Franssen, E.A.M., Staatsen, B.A.M., Lebre, E. (2002) Assessing health consequences in an environmental impact assessment: The case of Amsterdam Airport Schiphol. *Environ. Impact Assess. Rev.* 22, 633–653.
- [10] Baltrenas, P., Andrulevičius, L., Zuokaite, E. (2013) Application of dynamic olfactometry to determine odor concentrations in ambient air. *Polish J. Environ. Stud.* 22, 331–336.
- [11] Badach, J., Kolasińska, P., Paciorek, M., Wojnowski, W., Dymerski, T., Gębicki, J., Dymnicka, M., Namieśnik, J. (2018) A case study of odour nuisance evaluation in the context of integrated urban planning. *J. Environ. Manage.* 213, 417–424.
- [12] Romain, A.C., Delva, J., Nicolas, J. (2008) Complementary approaches to measure environmental odours emitted by landfill areas. *Sensors Actuators, B Chem.* 131, 18–23.
- [13] Capelli, L., Sironi, S., Del Rosso, R., Céntola, P., Il Grande, M. (2008) A comparative and critical evaluation of odour assessment methods on a landfill site. *Atmos. Environ.* 42, 7050–7058.
- [14] Gostelow, P., Parsons, S. a, Stuetz, R.M. (2001) Review Paper Odour Measurements for Sewage Treatment. *Wat. Res. Vol.* 35, 579–597.
- [15] Lebrero, R., Rodríguez, E., Martín, M., García-Encina, P.A., Muñoz, R. (2010) H₂S and VOCs abatement robustness in biofilters and air diffusion bioreactors: A comparative study. *Water Res.* 44, 3905–3914.
- [16] Barbusinski, K., Kalemba, K., Kasperczyk, D., Urbaniec, K., Kozik, V. (2017) Biological methods for odor treatment – A review. *J. Clean. Prod.* 152, 223–241.
- [17] Van Groenestijn, J.W., Kraakman, N.J.R. (2005) Recent developments in biological waste gas purification in Europe. *Chem. Eng. J.* 113, 85–91.
- [18] Akmirza, I., Pascual, C., Carvajal, A., Pérez, R., Muñoz, R., Lebrero, R. (2017) Anoxic biodegradation of BTEX in a biotrickling filter. *Sci. Total Environ.* 587–588, 457–465.
- [19] Malakar, S., Saha, P. Das, Baskaran, D., Rajamanickam, R. (2017) Comparative study of

- biofiltration process for treatment of VOCs emission from petroleum refinery wastewater— A review. *Environ. Technol. Innov.* 8, 441–461.
- [20] Lebrero, R., Gondim, A.C., Pérez, R., García-Encina, P.A., Muñoz, R. (2014) Comparative assessment of a biofilter, a biotrickling filter and a hollow fiber membrane bioreactor for odor treatment in wastewater treatment plants. *Water Res.* 49, 339–350.
- [21] Alfonsín, C., Hernández, J., Omil, F., Prado, Ó.J., Gabriel, D., Feijoo, G., Moreira, M.T. (2013) Environmental assessment of different biofilters for the treatment of gaseous streams. *J. Environ. Manage.* 129, 463–470.
- [22] López, J.C., Merchán, L., Lebrero, R., Muñoz, R. (2018) Feast-famine biofilter operation for methane mitigation. *J. Clean. Prod.* 170, 108–118.
- [23] Yaman, C., Karaca, F., Korkut, E.N., Paul Martin, J., Çinar, Ö. (2010) Selection of optimum operational conditions for the treatment performance of geotextile biofilters using artificial neural networks. *Fresen. Environ. Bull.* 19, 2587–2596
- [24] Muñoz, R., Souza, T.S.O., Glittmann, L., Pérez, R., Quijano, G. (2013) Biological anoxic treatment of O₂-free VOC emissions from the petrochemical industry: A proof of concept study. *J. Hazard. Mater.* 260, 442–450.
- [25] Estrada, J.M., Kraakman, N.J.R.B., Muñoz, R., Lebrero, R. (2011) A comparative analysis of odour treatment technologies in wastewater treatment plants. *Environ. Sci. Technol.* 45, 1100–1106.
- [26] Mudliar, S., Giri, B., Padoley, K., Satpute, D., Dixit, R., Bhatt, P., Pandey, R., Juwarkar, A., Vaidya, A. (2010) Bioreactors for treatment of VOCs and odours - A review. *J. Environ. Manage.* 91, 1039–1054.
- [27] Leonardos, G., Kendall, D., Barnard, N. (1969) Odor threshold determinations of 53 odorant chemicals. *J. Air Pollut. Control Assoc.* 19, 91–95.
- [28] Murnane, S.S., Lehocky, A.H., Owens, P.D. (2013) Odor Thresholds for Chemicals with Established Health Standards. *Odor Threshold. Chem. with Establ. Heal. Stand.* 182.
- [29] Xue, S., Chen, W., Deng, M., Luo, H., Huang, W., Han, Y., Li, L. (2018) Effects of moisture content on the performance of a two-stage thermophilic biofilter and choice of irrigation rate. *Process Saf. Environ. Prot.* 113, 164–173.
- [30] Yang, L., Kent, A.D., Wang, X., Funk, T.L., Gates, R.S., Zhang, Y. (2014) Moisture effects on gas-phase biofilter ammonia removal efficiency, nitrous oxide generation, and microbial communities. *J. Hazard. Mater.* 271, 292–301.
- [31] Jiang, L., Zhu, R., Mao, Y., Chen, J., Zhang, L. (2015) Conversion characteristics and production evaluation of styrene/o-Xylene mixtures removed by DBD pretreatment. *Int. J. Environ. Res. Public Health.* 12, 1334–1350.
- [32] Yang, C., Qian, H., Li, X., Cheng, Y., He, H., Zeng, G., Xi, J. (2018) Simultaneous Removal of Multicomponent VOCs in Biofilters. *Trends Biotechnol.* 36, 673–685.

Received: 25.06.2018

Accepted: 26.07.2018

CORRESPONDING AUTHOR

Ilker Akmirza

Department of Environmental Engineering,
Technical University of Istanbul,
34469 Istanbul – Turkey

e-mail: akmirzailker@itu.edu.tr

ilker.akmirza@alumnos.uva.es



Universidad de Valladolid

CHAPTER 4

Ethanethiol Gas Removal in an Anoxic Bio-scrubber

Ethanethiol Gas Removal in an Anoxic Bio-scrubber

Rasha Khalid Sabri MHEMID^{a,b}, Ilker AKMIRZA^{a,c}, Mustafa TURKER^d, Mohammed Salim SHIHAB^{a,e}, Kadir ALP^a.

^a Department of Environmental Engineering, Istanbul Technical University, 34469 Istanbul (Turkey)

^b College of Environmental Science and Technology, Mosul University, 41002 (Iraq).

Tel. +90 534 785 99 31, Email: mhemid@itu.edu.tr

^c Department of Chemical Engineering and Environmental Technology, University of Valladolid, Dr. Mergelina s/n. 47011, Valladolid, Spain.

^d Pakmaya P.O. Box 149, 41001, Izmit, Kocaeli, Turkey.

^e Environmental Engineering Dept, Mosul University, 41002 (Iraq).

ARTICLE INFO

ABSTRACT

Keywords:

Lab-scale bio-scrubber, Ethanethiol, Bio-degradation, Volatile organic sulphur compounds, Kinetics and stoichiometric characterization.

The performance of ethanethiol removal in an anoxic lab-scale bio-scrubber was investigated under different operating parameters and conditions for 300 days. The removal efficiency (RE) of ethanethiol was examined as a function of inlet concentration, empty bed residence time (EBRT) and spray density of irrigation. The results showed the best operation conditions and operation characteristics of the bio-scrubber for this study were at an inlet concentration of 150 mg/m³, a spray density of 0.23 m³/m² h and an EBRT of 90 s. An average RE of 91% and elimination capacity (EC) of 24.74 g/m³ h was found for all inlet ethanethiol concentrations. Variations in spray density higher than 0.23 m³/m² h had no effect on ethanethiol RE at different ethanethiol concentrations. The average experimental yield values were closer to the Y_{ET/NO_3^-} theoretical value of 0.74 when the main product was elemental sulphur (S⁰). This indicates that S⁰ and other forms of sulphur were formed rather than sulphate (SO₄²⁻) as the end product. Furthermore, growth kinetics for bio-degradation were evaluated in batch culture experiments using the Monod model, and bio-kinetic parameters of μ_{max} , K_s , Y_{xs} and q_{max} were obtained as 0.14 1/h, 1.17 mg/L, 0.52 g_s/g_s and 0.26 g_s/g_s h, respectively.

1. INTRODUCTION

Ethanethiol (ET) is a volatile organic sulphur compound (VOSC). It has a gas density that is heavier than air, and is a colourless malodorous sulphide, with a minimal odour threshold value of 0.7 µg/L. It has a flammable vapor that is detectable by humans at extremely low concentrations. Its maximal allowable concentration in the environment should not exceed 10.0 mg/L in a liquid phase, and its maximal acute exposure guideline level should not exceed 1.3 mg/m³ in a gas phase [1,2]. ET is usually released by both natural and anthropogenic sources, such as biogenic processes, industrial processes (food industries, papermaking industry, pharmaceutical plants, and petroleum refineries), wastewater treatment, and disposal in landfills. ET is used as an intermediate in the manufacture of plastics, insecticides, and antioxidants and is used as an odorant to serve as a warning property for natural gas [3]. Compared with other VOCs or mercaptans (ethyl mercaptan, methyl mercaptan, propyl mercaptan, and butyl mercaptan), it is determined as being a major odorous pollutant species, and it is known as an important air contaminant. Moreover, ET is

significantly toxic to human health, can cause poisoning, headaches, nausea, and can even lead to death from respiratory paralysis. In addition, it has potential corrosive effects, even at low concentrations [4]. Furthermore, this compound contributes to toxic environmental effects and global environmental problems (such as acid rain formation and ocean acidification) and poisons aquatic organisms [4,5]. Therefore, its removal from waste gas stream emissions is highly desirable in the field of environmental engineering.

Up to date several physico-chemical treatment technologies (such as incineration, catalytic oxidation and adsorption) have been used for the abatement of waste gases. However, the high capital and operating costs associated with these technologies, along with their high-energy requirements and non-environmentally friendly natures, have encouraged the development of new treatment technologies [6]. Rafson et al. [7] treated sulphur compounds by studying physical and chemical air pollution control technologies including incineration, regenerative thermal oxidation, and wet scrubbers. They found that thermal elimination and incineration methods have high operating costs and are not environmentally friendly, due

to the production of a greenhouse gas (CO₂), and requirement to SO₂ scrubbing. In addition, Kastner and Das [8] investigated the use of a chemical wet scrubber for volatile organic compound removal and found that this system requires expensive large amounts of water and oxidizing chemicals such as ClO₂ or NaOCl and could produce chlorinated hydrocarbons if not properly controlled. The mercaptans groups from gas emissions of refinery combustion sources can be removed by their absorption into amines and caustics as described by Jones and Weiland [9].

To improve the system with respect to the environment, to date, most biological treatment studies have focused on the aerobic oxidation of ET into the end products of SO₄²⁻ (Fig. 1) [13]. Several authors have proposed the possibility of aerobically degrading these pollutant VOSCs in

different biological reactor configurations, including bio-filters, bio-scrubbers, and bio-trickling filters. Wang et al. [14] used microorganisms fixed on iron oxide-based porous ceramsite in a bio-trickling filter for removal of waste gas containing ET under aerobic conditions. Sedighi et al. [1] investigated the degradability of ET via phenol utilizing cells of *Ralstonia eutropha* in both suspended and immobilized culture systems in a gas trickle-bed reactor packed with kissiris particles. ET can be degraded biologically as a sole source of carbon and energy or as mixture with dimethyl disulphide (DMDS) and methyl phenyl sulphide (MPS) by immobilized microorganisms of the B350 group in a bio-trickling filter [15].

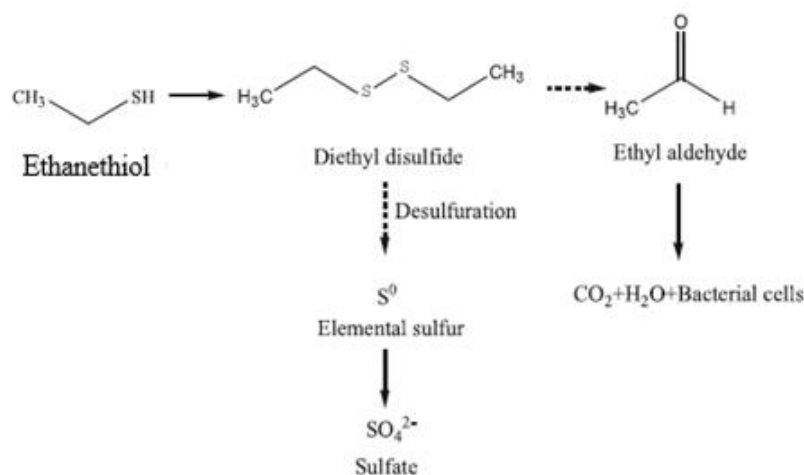


Fig. 1 Aerobic pathways of ethanethiol degradation by *Pseudomonas* sp. strain WL2. Solid-arrow: identified intermediate (products); dashed-arrow: possible intermediate.

However, although their environmentally friendly nature, the use of aerobic biological processes have high capital costs with respect to the aeration equipment, high operating costs (particularly relating to energy for pumps or aerators), and high maintenance requirements [10,11–12]. Moreover, despite the multiple advantages of aerobically biological treatment of sulphur compounds possible undesirable by-product production due to their rapid conversion to H₂S in the absence of oxygen is considered as one of the drawbacks of the aerobic systems [13,16]. To overcome these problems, it is necessary to develop alternative bio-technologies that use an electron acceptor other than O₂ within the bio-degradation process. In this context, anoxic conditions offer a promising alternative solution for the removal

of ET from waste gas emissions. Furthermore, they can assist in nitrogen removal and decrease the amount of SO₄²⁻ produced under the specific ET/NO₃⁻ ratio, which thus enables S⁰ production as the end product (rather SO₄²⁻). In anoxic systems, the addition of air is unnecessary, and there is no gas–liquid mass transfer limitation because oxygen is already dissolved in the liquid medium [16]. The use of nitrate (NO₃⁻) as an electron acceptor in sulphur compounds oxidation has been studied by several researchers. Yavuz et al. [17] studied the removal of sulphide from industrial wastewater using oxygen and NO₃⁻ as electron acceptors in lab-scale batch experiments, and found that 80% sulphide removal occurred when oxygen was used as an electron acceptor with activated sludge, and 100% sulphide removal was

achieved when NO_3^- was used. Turker et al. [18] investigated the removal of hydrogen sulphide (H_2S) in biogas to S^0 or SO_4^{2-} using NO_3^- and nitrite present in feed wastewater within a pilot-scale bio-scrubber system under denitrifying conditions. The results showed that biogas desulphurization was combined with nitrogen removal, which is normally required in most industrial wastewater treatment plants, but more than 90% of the H_2S in the biogas was removed with simultaneous nitrogen removal at wastewater/biogas ratios between 2 and 3. Through the biological treatment alternatives, bio-scrubbers offer considerable advantages over others for treating odorous waste gas, as they result in low pressure drops during operation, the possibility of avoiding accumulation of products, and enable better control of reaction conditions (pH, nutrients) with water-soluble compounds, which avoids high spray columns and large water flows. In addition, use of an anoxic bio-scrubber enables the integration of waste gas treatment and wastewater treatment when the nitrification step uses NO_3^- as an electron acceptor source to oxidize ET to the main end product of S^0 . In this respect, denitrification occurs and NO_3^- is converted to N_2 gas [4]. However, bio-scrubber studies are limited, and no report has been published on an anoxic bio-scrubber being used with the main aim of bio-degrading ET. It would thus be important to investigate the conditions involved in the anoxic removal of ET.

In this study, a gas stream contaminated with ET was treated in a lab-scale bio-scrubber under anoxic conditions. The batch experiments were conducted to study the kinetics of the mixed culture of the lab-scale bio-scrubber, and to determine the bio-degradation capability of ET by the acclimated mixed culture under anoxic conditions. In addition, the kinetic parameters of ET were estimated for the first time using the Monod model under anoxic conditions. Experimental investigations were then conducted to remove the target gas, ET, in a lab-scale bio-scrubber under anoxic conditions. ET was absorbed by microorganisms and then degraded and transformed into inorganic sulphur using a limited NO_3^- source to obtain S^0 for recovery and use. This study also aimed to examination of the effects of inlet concentration, EBRT, and spray density on the performance of the lab-scale bio-scrubber system. Furthermore, a stoichiometry of ET

degradation was developed for different end products of sulphur and tested under anoxic conditions.

2. MATERIALS AND METHODS

2.1. Kinetic assay in batch system

Batch experiments were conducted to evaluate the bio-degradation of ET by acclimated microbial communities when ET was present as single substrate, and the kinetics of the mixed microbial population of the bio-scrubber under anoxic conditions were studied. ET degradation was also evaluated at two concentrations of sludge, 300 and 3000 mg of volatile suspended solid (VSS)/L, to study the effect of sludge concentration on the ET degradation process.

2.1.1. Experimental setup and acclimation procedure

Four 1-L air-sealed bottles (batch mode), two of which contained 100 mL of MSM, were inoculated with activated sludge from the MBR of Kemerburgaz Leachate Treatment Plant (Istanbul, Turkey) under anoxic denitrifying conditions, and a final concentration of ~300 mg of VSS/L was attained. Another two bottles were inoculated with anoxic activated sludge that reached a final concentration of ~3000 mg of VSS/L. The bottles were closed with rubber stoppers and sealed with aluminium caps. The gas headspace of the bottles was washed with N_2 (purity > 99.999%) for at least 15 min to remove any molecular oxygen. The ET compound was injected into the bottles at an initial concentration $840 \pm 10 \text{ mg/m}^3$. The bottles were continuously stirred at 320 rpm by magnetic stirring at room temperature, samples were then extracted hourly from the headspace using a gas-tight syringe (Hamilton, USA) and ET concentrations were analysed by GC-MS. During the acclimation period, 30% of the MSM was periodically exchanged with a fresh medium to provide required nutrients for microbial growth and to avoid the possibility of producing microbial inhibition from toxic metabolites excreted during the bio-degradation process. In addition, an amount of NO_3^- was periodically added according to the theoretical $Y_{\text{ET}/\text{NO}_3^-}$ value of 0.54, and this was monitored during the test using ion chromatography (IC) to maintain the batch mode under anoxic conditions. Five complete bio-degradation

cycles were conducted for the acclimation of microorganisms to ET as a single source. Each cycle was considered to be complete when the ET concentration in the headspace was totally degraded. At the end of each bio-degradation cycle, the ET content was replenished by adding it to the bottles to restore the content to its initial concentration.

2.1.2. Kinetic test

A kinetic test was conducted in batch mode to determine the kinetic parameters of aqueous ET, such as the half saturation point (K_s), maximal growth rate (μ) and yield coefficient (Y_{xs}) under anoxic conditions. After completing five bio-degradation cycles of the acclimation period, 30% of the media was exchanged with new MSM, and NaNO_3 was added to ensure sufficient nutrients and NO_3^- during the test. The compound ET was then added to the headspace, and gas samples were then taken over time until ET was completely degraded, or until the end of bio-degradation. The liquid samples were taken before and after the kinetic test to determine the amount of NO_3^- consumed through the test and amounts of total suspended solids (TSS) and VSS.

2.2. Experimental setup and technological process

The lab-scale bio-scrubber setup is shown in Fig. 2. The bio-scrubber column was made from cylindrical jacketed PVC (0.10 m inner diameter, 0.5 m height) packed with Kaldness rings (polyethylene measuring $14 \times 9.8 \text{ mm}^2$, specific surface area of $> 800 \text{ m}^2/\text{m}^3$, porosity $> 85\%$, and packing density of $0.98 \text{ g}/\text{cm}^3$) to provide a working volume of 2 L (0.25 m height). The column was supported by perforated sieves at the bottom and top. The scrubbing column was interconnected with a 3 L working volume stirring tank (biological

reactor) and magnetically agitated at 400 rpm (bio-reactor, manufactured with PVC with an inner diameter of 0.15 m, and a height of 0.2 m). The pollutant gas was absorbed into the liquid phase in the scrubbing column and then transferred to the biological reactor to reduce the pollutant (bio-transformation step) biologically to either S^0 or SO_4^{2-} under anoxic conditions (depending on the availability of NO_3^-). The activated sludge with concentration of 3000 mg VSS/L in the bio-reactor was obtained from the membrane biological reactor (MBR) at Kemerburgaz Leachate Treatment Plant (Istanbul, Turkey), and it adapted to the substrate over 36 days (Section 3.1). It was then connected to a 3 L working volume sedimentation tank (manufactured with PVC, the first part cylindrical with 0.15 m inner diameter x 0.15 m height, and second part conical with 0.15 m inner diameter x 0.15 m height). The clean solution from the sedimentation tank was recycled into the scrubbing column. A peristaltic pump was fitted at each connection to control the flowrate of the sludge and supernatant. Certain concentrations of ET were prepared by injecting liquid ET via a syringe pump (MODEL LSP02-1B Dual Channels Syringe Pump) into a container connected with nitrogen gas (N_2) (Linde Turkey, purity $> 99.999\%$). In other words, a small amount of nitrogen was bubbled into the container to evaporate and produce the pure ET gas, and the gas then entered the mixing gas tank and was mixed with nitrogen gas to adjust the concentration to the desired level.

Exhaust gas is detrimental to the environment, and the exhaust gas compound that passed through the bio-scrubber was thus finally absorbed with 32% NaOH to convert the unhandled gas into water-soluble thiolate salts, as shown in Eq. (1) [19],



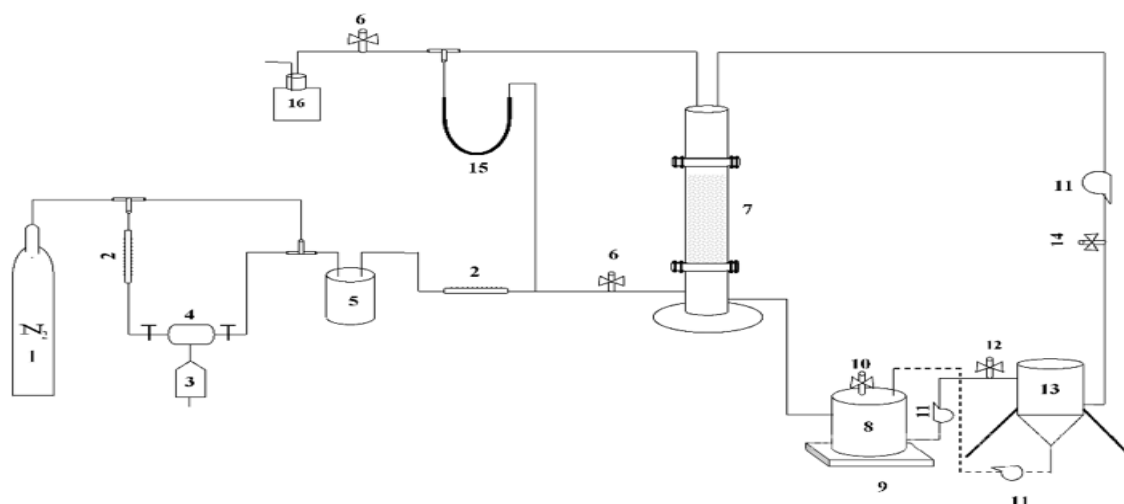


Fig.2. Schematic diagram of lab-scale bio-scrubber: (1) N₂ gas bottle; (2) gas-flow meter; (3) syringe pump; (4) evaporation container; (5) mixing gas tank; (6) ET gas sampling port for inlet and outlet gas; (7) scrubbing column; (8) biological tank; (9) magnetic stirrer; (10) CO₂ sampling port; (11) peristaltic pump; (12) liquid sampling port for VSS and TSS test; (13) sedimentation tank; (14) liquid sampling port for COD, SO₄²⁻, and NO₃⁻ tests; (15) manometer; and (16) NaOH absorption bottle.

The synthetic inlet gas stream was controlled by the gas-flow meter (AALBORG, NY 10962, USA), and it entered the media from the bottom of the scrubbing column and then exited from the top. In contrast, the supernatant from the sedimentation tank was circulated in a counter-current mode; it was sprayed from top to bottom and was lifted to the biological reactor and then to the settling tank by the water pump (PR1 peristaltic

pump, SEKO Italia S.P.A). Furthermore, a manometer was used to measure the pressure drop (head-loss) between the input and output of the scrubbing column.

The experiments were conducted to study three factors in the lab-scale bio-scrubber: ET inlet concentration, spray density and EBRT, as shown in Table 1, and they were designed to determine the optimal conditions of the lab-scale bio-scrubber required to achieve the highest RE.

Table 1. Experimental conditions of lab-scale bio-scrubber.

Experiments	ET inlet concentrations (mg/m ³)	EBRT (s)	Spray density (m ³ /m ² h)	Irrigation flowrate (mL/min)	Hydraulic retention time HRT (h) of biological tank	Total operation days of all inlet concentrations	Gas/Liquid ratio	Target
E1	150 350 850 1450	60	0.12	14	3.5	0–36	150	start-up (acclimation)
E2	150 350 850 1450	60	0.12	14	3.5	36–66	150	(Best) Spray density m ³ /m ² h
			0.18	21	2.4	67–95	100	
			0.23	26	2.0	96–121	80	
			0.3	35	1.4	122–153	60	
			0.45	52	1.0	154–180	40	
E3	150 350 850 1450	30	Best spray density from E2	Best Irrigation flowrate	Best HRT (h)	181–207	Best Gas/Liquid ratio	EBRT (s)
		60				208–239		
		90				240–272		
		120				273–300		

2.3. Chemical and mineral salt medium

The chemical ethanethiol (99.0% purity) was purchased from Sigma Aldrich. All nutrient mineral salt media (MSM) were composed of (g/L) $\text{Na}_2\text{HPO}_4 \cdot 12\text{H}_2\text{O}$, 6.15; KH_2PO_4 , 1.52; $\text{MgSO}_4 \cdot 7\text{H}_2\text{O}$, 0.2; CaCl_2 , 0.038; and 10 mL/L of a trace element solution containing: (g/L) EDTA, 0.5; $\text{FeSO}_4 \cdot 7\text{H}_2\text{O}$, 0.2; $\text{ZnSO}_4 \cdot 7\text{H}_2\text{O}$, 0.01; $\text{MnCl}_2 \cdot 4\text{H}_2\text{O}$, 0.003; H_3BO_3 , $\text{CoCl}_2 \cdot 6\text{H}_2\text{O}$, 0.02; $\text{CuCl}_2 \cdot 2\text{H}_2\text{O}$, 0.001; $\text{NiCl}_2 \cdot 6\text{H}_2\text{O}$, 0.002 and $\text{NaMoO}_4 \cdot 2\text{H}_2\text{O}$, 0.003 [20] was used as a nutrient for the microorganisms. Ethylenediaminetetraacetic acid (EDTA) was used at a low level of concentration as a chelating agent, and it was mixed with the trace element solution to remove free metal ions. Every week, 30% of the liquid media was exchanged with new MSM to provide sufficient nutrients for microbial growth, and pH was kept neutral between 7.2 and 7.6 for all experiments by daily renewal of the MSM with pH 7.0.

NaNO_3 ranging between 5 g/L and 10 g/L was prepared in a biological tank to supplement the electron acceptor as NO_3^- for gas oxidation and as a nitrogen source for microbial growth [20]. In addition, NO_3^- was added in accordance with the ET/NO_3^- molar ratio calculated from stoichiometric equations (A.4 and A.5 in the appendix). Prior to beginning each experiment, $Y_{\text{ET}/\text{NO}_3^-}$ was fixed at a 0.54 average value between two stoichiometric ratios of 0.34 or 0.74 when the end product was SO_4^{2-} or S^0 , respectively. An ET/NO_3^- ratio of 0.54 was selected to ensure sufficient available nitrate at the beginning of the operation. Nitrate consumption increased as the operating time progressed, and thus the ratio of ET/NO_3^- may have approached 0.74 and complete ET oxidation to S^0 only was achieved under NO_3^- limitation. Furthermore, the consumption of NO_3^- was monitored via ion chromatograph during the experiment to maintain anoxic conditions.

2.4. Analytical methods

Measurements of inlet and outlet ET concentrations in the gaseous phase were obtained from the scrubbing column, and CO_2 concentrations were obtained from the biological tank, and both were analysed daily (duplicate analysis) using an alignment gas chromatograph (GC-7890A, USA) equipped

with a mass spectrometry detector (MSD 5795C, USA) and an HP-5MS 5% phenyl methyl silox (30 m \times 0.25 mm \times 0.25 μm) capillary column. Gas samples measuring 100 μL were taken at regular intervals from the inlet and outlet using a gas-tight syringe (Hamilton, USA), and they were then injected into the column to determine the concentration in split mode (using a split ratio of 20). The oven temperature was programmed from 40 $^\circ\text{C}$ (held 3 min) to 130 $^\circ\text{C}$ at 10 $^\circ\text{C}/\text{min}$ (held 10 min), and helium was used as a carrier gas at a flowrate of 1.3 mL/min. The ET concentrations in the liquid phase were estimated using the partition coefficient Henry's constant at equilibrium between two phases, gas and liquid, within 60 min (as described in [6]). Liquid samples were taken daily (triplicate) and measured with a pH-meter (Orion 720 A⁺, USA) to control the pH of the sludge in the biological reactor. Concentrations of NO_3^- and SO_4^{2-} in the irrigation liquid samples were measured at the beginning and end of each experimental (duplicate analysis) using an ion chromatograph (DIONEX ICS-3000, USA) equipped with an AG11-HC P/N 052963 precolumn, an AS11-HC P/N 052961 analytical column, and a Dionex conductivity detector. The eluent of the anion and cation was 0.2 mM Na_2CO_3 and 26 mM $\text{CH}_3\text{SO}_3\text{H}$, respectively, the temperature of column was controlled at 30 $^\circ\text{C}$, and the flowrate was 0.38 mL/min. Twice a week, the chemical oxygen demand (COD) of irrigation liquid samples was measured according to the standard method, (1998) (5220-B) open reflexed [21]. In addition, samples from the activated sludge at the end of the operating period were drawn and measured for the VSS and TSS according to standard methods [22]. The performance of the studied bio-scrubber was evaluated using the following: RE (%) is the fraction of pollutant removed from the bio-treatment (expressed as a percentage) and is defined as Eq. 2,

$$RE(\%) = \frac{C_{ET}^{in} - C_{ET}^{out}}{C_{ET}^{in}} \times 100, \quad (2)$$

where C_{ET}^{in} (g/m^3) is the inlet concentration and C_{ET}^{out} (g/m^3) is the outlet concentration of the gas compounds. In addition, the inlet loads IL ($\text{g}/\text{m}^3 \text{ h}$), another significant parameter of bio-scrubber performance, were calculated by Eq. (3) as

$$IL = \frac{C_{in} \times Q_g}{V}, \quad (3)$$

where Q_g (m^3/h) is the gas flowrate, and V (m^3) is the volume of the scrubbing column.

In addition, $EBRT(s)$ and spray density ρ ($m^3/m^2 h$), two necessary parameters, were calculated as

$$EBRT(s) = \frac{V}{Q_g} \times 3600, \quad (4)$$

$$\rho = \frac{4Q_l}{\pi D^2}, \quad (5)$$

where $EBRT$ is (s), and Q_g and V in (4) are identically defined in (3); and Q_l (m^3/h) and D (m) in (5) are the liquid spray flow and the inner diameter of the filter, respectively.

Furthermore, Volumetric NO_3^- removal rate (NRR) and Volumetric ET removal rate (ETRR) ($Kg/m^3 day$) could be defined as,

$$NRR = \frac{(C_N^{in} - C_N^{out})}{V} Q_l, \quad (6)$$

$$ETRR = \frac{(C_{ET}^{in} - C_{ET}^{out})}{V} Q_g, \quad (7)$$

Finally, the elimination capacity, EC ($g/m^3 hr$) was determined as

$$EC = \frac{(C_{ET}^{in} - C_{ET}^{out})}{V} Q_g, \quad (8)$$

where Q_g , Q_l , C_{ET}^{in} , C_{ET}^{out} and V in (6), (7) and (8) are as defined in (2), (3), (4) and (5), whereas C_N^{in} and C_N^{out} are the concentrations of NO_3^- from the liquid irrigation flow at the beginning and end of the experiment.

3. RESULTS AND DISCUSSION

3.1. Kinetic assay results

3.1.1. Acclimation and bio-degradability of ET in a batch system

Prior to conducting kinetic experiments, five bio-degradation cycles were completed in each bottle to adapt the microorganisms to the ET compound as the sole carbon source of energy metabolism and cell synthesis. During the acclimation period, 30% of the MSM was periodically exchanged with fresh medium, to avoid the possibility of producing microbial inhibition in relation to toxic metabolites excreted during the bio-degradation process. Fig. 3 a and b show the trends of the five cycles of ET degradation in a gas phase during the batch experiments using two different sludge concentrations of 300 mg of VSS/L (525 mg of TSS/L) and 3000 mg of VSS/L (5190 mg of TSS/L). The compound was completely removed in a shorter time (0.5 days) at VSS 3000 mg/L compared to VSS 300 mg/L (5 days), which shows that the ET degradation time when using the mixed culture of 3000 VSS mg/L was approximately ten times higher than that using the sludge concentration of 300 VSS mg/L, because of the increased competition between microorganisms to survive, which thus led to a higher compound removal efficiency over a shorter time. Based on this result, the kinetic constants for ET bio-degradation (kinetic parameters) were studied at 3000 mg VSS/L. Furthermore, results showed that ET removal rate increased by approximately 90% with an increase in the sludge concentration. A previous study found that ET was completely metabolized by *R. eutropha* at various initial concentrations ranging from 115 to 320 mg/m^3 under aerobic conditions within 120 to 168 h, and no clear increase in the biomass concentration of 2000 mg of VSS/L was obtained [6]. In addition, An et al. [3] found that a new *Lysinibacillus sphaericus* strain, RG-1, totally aerobically bio-degraded 2000 to 4000 mg/m^3 of ET within 96 h. Furthermore, Yavuz et al. [17] used laboratory batch-scale experiments for removing sulphide under anoxic condition and found that the sulphide removal rate increased by approximately 88% with an increase in the activated sludge concentration, and sulphide was completely removed within 6 min.

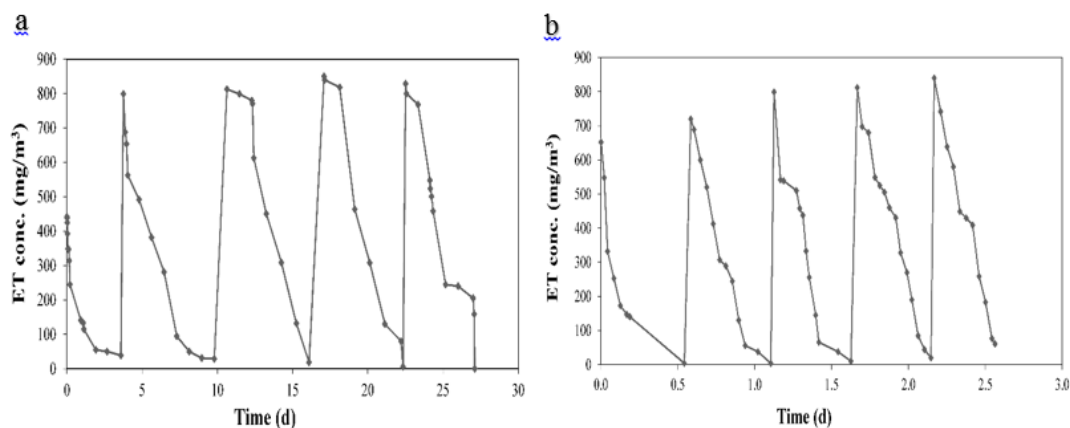


Fig.3. Time course of ET-gas concentration during adaptation period at: (a) 300 mg of VSS/L (525 mg of TSS/L) and (b) 3000 mg of VSS /L (5190 mg of TSS/L).

Although sulphate appeared in small quantities (data not shown) from the ET oxidation reaction in the present study, which directed the focus towards enzymatic reactions involved in energy production. That resulted an increase in the biomass growth rate of 47 mg TSS/L which was considered that ET was the source of energy and biomass growth. As previously reported, oxidation of inorganic/organic sulphur compounds to sulphate leads to energy production during the reaction [23]. The acclimation period of VOSCs, such as ET, was also reported by [13], in which *Pseudomonas sp. WL2* bacteria were used to mineralize ET in aerobic batch reactors, and ET was found to spontaneously convert to DEDS during the acclimation period, the concentrations from 1107 to 4963.5 mg/m³ of initial DEDS were then inoculated and bio-degraded within 14–32 h, and a growth rate of 9.7 to 31.1 mg of TSS/L, respectively, was found. The results obtained from batch mode experiments compared with those reported in previous literature provide a better understanding of the behaviour of ET degradation under anoxic conditions, and also indicate that ET bio-degradation occurs in a short time period and achieves a high biomass production when NO₃⁻ is used as the electron acceptor and ET as the electron donor. This result can thus be applied to an anoxic lab-scale bio-scrubber.

3.1.2. Evaluation of kinetics constants for ET bio-degradation

Microbial cells are considered as catalysts in the degradation of a substrate. In this respect, theoretical models, including the Monod model, have been developed to understand the saturation kinetics during bio-degradation

processes in a batch mode. The Monod model is believed to be the best model for describing bio-degradation of a single substrate through batch growth mode, and it provides the opportunity to compare different bio-degradation kinetic behaviours [24]. The specific growth rate of bacterial cultures is often described using the Monod kinetics test [25].

Jennings et al. [26] developed theoretical models that adopt Monod-type rate equations to describe the removal of solo pollutants. Furthermore, Ottengraf and Oever [27] derived design equations based on two extreme Monod equation conditions, zero-order and first-order, to predict partial removal. However, the Monod equation has limitations when used in two cases. The first case is at low substrate concentrations (relative to the half-saturation constant) $S \ll K_s$, at which the growth rate becomes a function of the substrate concentration (first-order equation); and the second case is at high substrate concentrations where $S \gg K_s$, at which the degradation rate is independent of the substrate concentration (zero-order equation) [26-28].

In this study, a mixed microbial population (suspended growth) was first studied in batch mode under anoxic conditions to determine the ET degradation ability in relation to kinetic parameters, prior using it in an anoxic bio-scrubber system. Models such as the Monod model are useful because they can assist in estimating growth constants, such as K_s , that are difficult to determine experimentally, and they quickly describe how changes in any of the experimental parameters affect growth without the need to conduct long and tedious sets of experiments. The batch experiments were conducted to determine the maximal specific

growth rate (μ_{\max} , 1/h), half-saturation coefficient (K_s , mg/L), biomass yield coefficient (Y_{XS} , g_x/g_s) and maximal specific degradation rate (q_{\max} , g_s/g_x h) for the biodegradation of 5.6 mg/L ET in an aqueous phase by mixed culture under anoxic conditions, using the Monod expression described as [24]

$$\mu = \frac{\mu_{\max} \times S}{K_s + S}, \quad (9)$$

where μ is the specific growth rate (1/h) and S is the substrate concentration in a liquid phase (mg/L).

In addition, the biomass growth rate of any organism can be expressed using

$$\frac{dx}{dt} = \mu X, \quad (10)$$

where X is the total biomass concentration of microorganisms.

It is also necessary to relate biomass growth (X) to substrate concentration (S) and time (t). By using mass balances and biological kinetics, it is possible to obtain one equation for the variation in substrate concentration versus time, and depletion of growth associated with substrates in a batch degradation can be described by

$$\frac{-ds}{dt} = \frac{\mu x}{Y_{XS}}, \quad (11)$$

where is the biomass yield coefficient equal to 0.52 g of biomass produced per gram of substrate consumed, where the substrate ET consumed by microorganisms is 5.45 mg per 2.84 mg of biomass production. It is of note that the value of Y_{XS} calculated in the batch experiment in this study approached the theoretical value of Y_{XS} in stoichiometry equations (Appendix).

Furthermore, the maximal specific degradation rate (q_{\max}) was calculated according to the following equation,

$$q_{\max} = \frac{1}{Y_{XS}} \times \mu_{\max}, \quad (12)$$

In this respect, a plot of $1/\mu$ against $1/S$ should produce a straight line with the intercept on the y-axis at $1/\mu_{\max}$ and a gradient equal to K_s/μ_{\max} . And when the values of K_s , μ_{\max} , Y_{XS} and q_{\max} are known, a complete quantitative description of the growth events occurring during a batch culture can be obtained. The linear regression plots used to determine the coefficient were created using Microsoft Excel 2010. As shown in Fig. 4, the experimental data were fitted to the model, and the value for the correlation coefficient (R^2) was calculated as 0.97, which indicates a good correlation, and values of μ_{\max} , K_s , Y_{XS} and q_{\max} were 0.14 1/h, 1.17 mg/L, 0.52 g_x/g_s and 0.26 g_s/g_x h, respectively. Results confirm that when ET is present as the sole carbon and energy source, it is readily biodegradable during the ET bio-degradation process under anoxic condition., and its biodegradation is consistent with the Monod model.

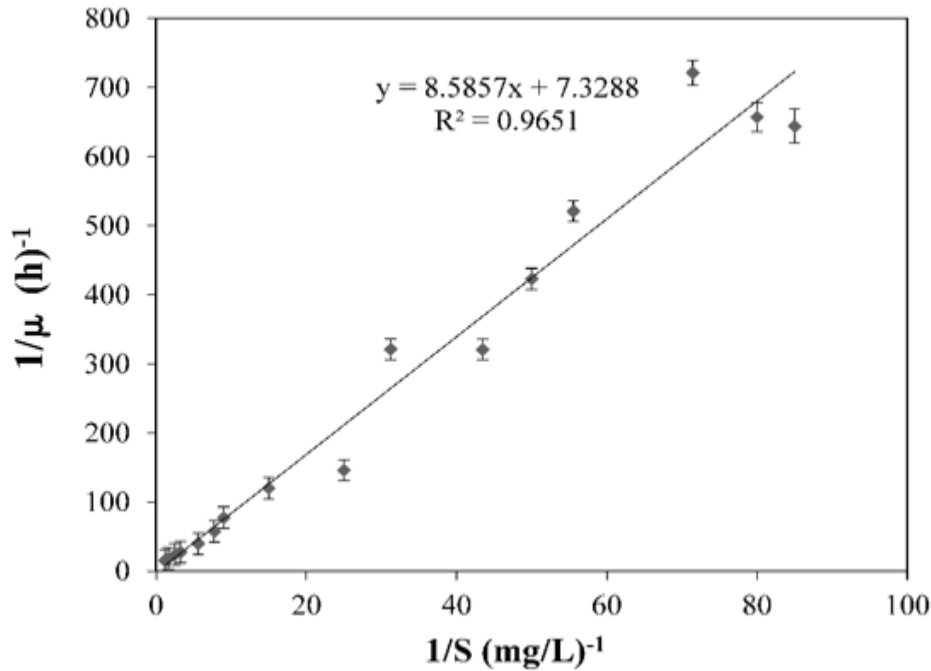


Fig.4. Representation of ET degradation kinetics in batch experiment under anoxic conditions.

The Monod equation has previously been fitted to bio-degradation kinetic parameter data for ET compounds (at initial ET concentrations of 1-4 mg/L) under aerobic conditions using *R. eutropha* in batch mode by employing Graph Pad Prism 5 software, where q_{max} and K_s were 0.00023 g_s/g_x h and 1.379 mg/L, respectively [6]. Comparatively, in this study, ET degraded by a mixed culture under anoxic conditions at a maximal specific degradation rate that is 1.130×10^3 times higher than that for ET aerobic degradation by *R. eutropha*, whereas, the values of K_s were closer of each other. Furthermore, μ_{max} of 0.0308 1/h for ET degradation by *L. sphaericus* strain RG-1 in batch mode [29] was achieved using the pseudo-first-order model, which was 0.22 times lower than that by the mixed culture under anoxic conditions (0.14 1/h). The results show that anoxic ET degradation by the mixed culture was more efficient than by other aerobic pure cultures obtained in previous studies. In addition, the Monod model predicted that the mixed microorganisms applied degraded higher concentrations of ET in accordance with the kinetic parameter ($S \ll K_s$). Furthermore, the biomass-to-substrate yield coefficient, Y_{XS} , was used in bio-scrubber modelling to avoid further adjustments and assumptions for X and Y_{XS} .

3.2. Bio-scrubber start-up and running performance

The bio-scrubber was started and ran for 36 days (E1 in Table 1) to adapt microorganisms on the ET and until steady-state conditions were attained (i.e., RE and output gas concentrations attained a regular pattern). The process was operated under conditions in which the experimental temperature was 20–25 °C, the inlet concentration of the ET was approximately 50–1500 mg/m³, the spray density was 0.12 m³/m² h with a flowrate of 0.12 m³/h and the EBRT was 60 s. Outlet gas samples were determined when the bio-system was stabilized for 24 h at a certain inlet ET concentration. Fig. 5 shows the performance of the bio-scrubber during the acclimation period for ET gas removal over 36 days. The ET REs were 53.90%, 64.40% and 85.80% on the 1st, 10th and 18th days, respectively, with ET concentrations of less than 486.23 mg/m³. The REs stabilized at an average of 86% between the 19th and 28th days of steady running of the bio-scrubber with increased ET inlet concentrations from 469 to 875 mg/m³. Afterwards, the inoculation of microorganisms to ET was achieved after 28 d. To understand interruptions in the system operation (such as weekend shutdown, higher loading rates, and excessive biomass growth) that often lead to a temporary lack of feed of waste gas, nutrient medium, NO₃⁻ and low gas diffusion through the microbial community in the bio-tank, the system was fed with high

concentrations of ET from 900 to 1500 mg/m³ in a non-permanent irrigation liquid during the final eight days. By day 29, the RE began to decrease slightly, and it reached 79.20% on the 36th day. It thus appears that re-acclimation of the pollutant plays an important role in preventing lower pollutant elimination in the system.

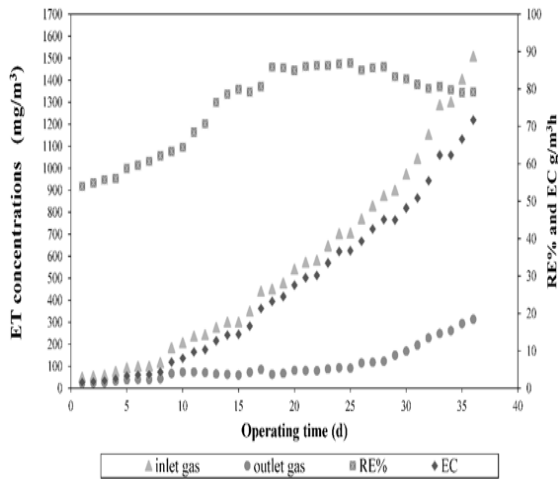


Fig.5. Performance of bio-scrubber at ET inlet, outlet concentration, and removal efficiency during start-up period (36 days).

The results also showed that the ECs of ET were increased from 1.6 to 71.7 g/m³ h with increasing inlet concentrations from 50 mg/m³ (IL= 3 g/m³h) to 1500 mg/m³ (IL = 90.51 g/m³h), which caused the COD values to increase from 30 to 820 mg/L and indicated that ET was bio-degraded to its end products in the bio-reactor.

3.3. Effect of inlet concentration and spray density on RE % and EC.

In all biological desulphurization processes, the initial concentration and spray density are

significant parameters for RE [30]. In this study, different concentrations of 150 mg/m³, 350 mg/m³, 850 mg/m³ and 1450 mg/m³ were supplied in a lab-scale bio-scrubber under the following experimental operating conditions: spray densities of 0.12, 0.18, 0.23, 0.3 and 0.45 m³/m² h; flowrate of 0.124 m³/h and EBRT of 60 s (E2 in Table 1).

Fig. 6 a-d shows the effects of inlet ET concentrations and spray densities on RE and EC. There was a decrease in the REs of ET with an increase in the inlet concentration in all cases, and vice versa for EC. When the spray density ranged from 0.12 to 0.45 m³/m² h at a low inlet concentration of 150 mg/m³ (Fig. 6 a), the RE rose from 85% (EC = 7.68 g/m³ h) to 91.29% (EC = 8.25 g/m³ h); at a high inlet concentration of 1450 mg/m³ (Fig. 6 d), RE ranged from 71% (EC = 62 g/m³ h) to 76.61% (EC = 65.22 g/m³ h); and at inlet concentrations of 350 mg/m³ and 850 mg/m³ (Fig. 6 b and c), the average REs were approximately 84.54% (EC = 17.82 g/m³ h) and 77.32% (EC = 39.59 g/m³ h), respectively. Furthermore, the RE and EC decreased at a higher spray density of 0.45 m³/m² h when the spray density was reduced to 0.12 m³/m² h; this occurred because the decrease in the liquid flowrate helped to reduce the mass transfer rate between the gas and liquid [31] and hence decrease the ET RE and EC, and vice versa. The reason for the reduction of RE with increasing inlet concentrations is summarized as follows. While the increase by IL resulted in an increase in ET absorption in the scrubber column (due to enhancement by mass transfer), the possible substance inhibition in the liquid bioreactor tank at high IL decelerated the biological activity and resulted in a decrease of RE [32].

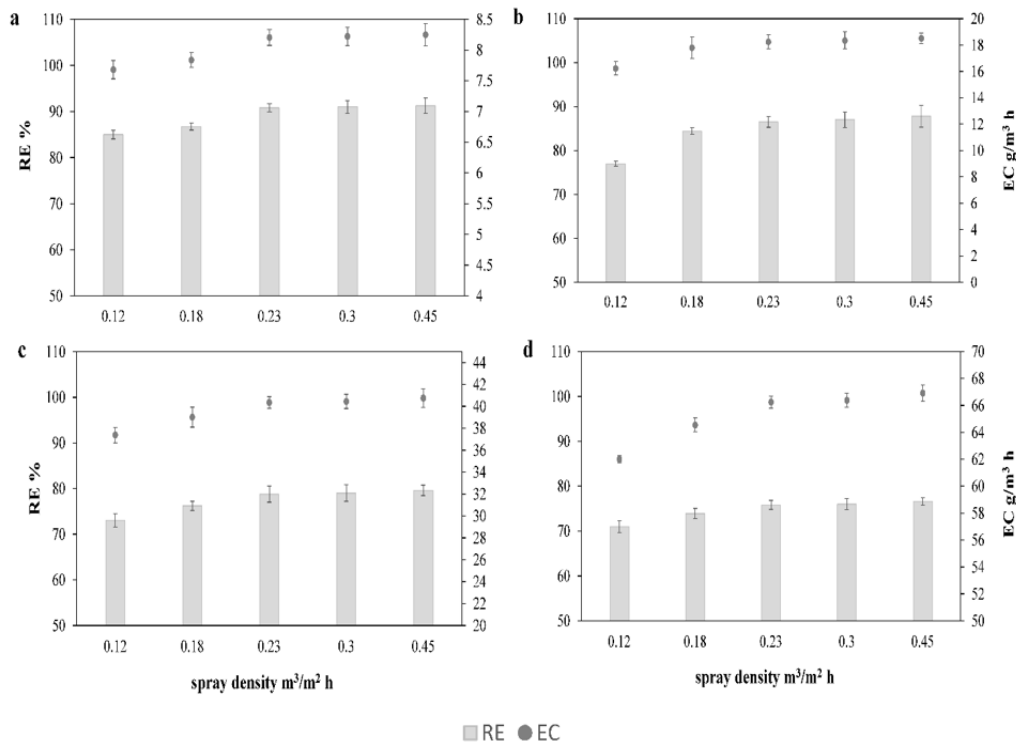


Fig.6. Effect of spray density on ET RE% and EC of bio-scrubber at different ET inlet concentrations and fixed EBRT of 60 s: (a) 150 mg/m³, (b) 350 mg/m³, (c) 850 mg/m³, and (d) 1450 mg/m³. Error bars indicate standard deviation (SD) of duplicate samples.

However, it is possible that biomass accumulations may have been enhanced in the biological reactor owing to an increase in the ET inlet concentrations with various ILs ranging from 9.32 to 87.10 g/m³ h during the process. An increase of approximately 30% in the biomass concentration (in terms of VSS mg/L) in the biological reactor was observed every six consecutive days. Fig. 6 a–d shows that the ET REs and EC of four inlet concentration groups were unstable when the spray density was less than 0.23 m³/m² h. Correspondingly, stability of the REs and EC was accomplished at a spray density greater than 0.23 m³/m² h. Thereafter, there was hardly any increase in the REs, even when the spray density was increased, for the following reasons: the ET reached a saturation point, there were moderately soluble properties in the water (Henry's coefficient: 0.15–0.21) [14] and it is considered that the excessive biomass thickness in the bio-tank could have affected inside diffusion of the ET gas molecules. Therefore, the microorganisms were unable to adequately decompose ET and were probably returned in the irrigation liquid. Otherwise, the increasing spray density caused decreasing HRT from 2 h at 0.23 m³/m² h to 1.4 h at 0.3 m³/m² h and 1 h at 0.45 m³/m² h. Thus, if the ET bio-degradation time is reduced in a

biological tank, quantities of incomplete ET decomposition are likely to be returned in the irrigation water. Our results conclude that the best spray density was 0.23 m³/m² h (HRT = 2 h), and this achieved an average 83% removal of all ET concentrations (EC = 33.26 g/m³ h). A previous study determined the effect of spray density on ET removal from an aerobic bio-trickling filter, and reported that the REs of three ET concentration groups (110, 200 and 300 mg/m³) greatly improved when the spray density was increased to 0.24 m³/m² h, and RE values of approximately 60% were attained. In addition, when the spray density was greater than 0.24 m³/m² h, a stable RE trend was obtained in the three groups, because the increase in the moisture content of the packing material surface led to an excessive increase in the thickness of the biomass, thus the inside diffusion within the microorganisms for the ET molecule obstructed ET degradation [14]. In contrast, the anoxic bio-scrubber studied here is more able to effectively eliminate ET (RE > 83%, EC > 33 g/m³ h) with a lower irrigation flowrate of 26 mL/min (spray density = 0.23 m³/m² h).

3.4. Influence of inlet concentration and EBRT on RE % and EC

EBRT is also a significant parameter in any bio-treatment desulphurization process, and it can be evaluated as the time needed to reach the concentration limit [33]. The influence of EBRT on the RE and EC of ET is presented in Fig. 7 a-d; these results were obtained under experimental conditions in which the temperature was approximately 20–25 °C and the best spray density was 0.23 m³/m² h. Various inlet concentrations were used in the bio-treatment system. The results of ET RE indicated that a longer residence time is a benefit to ET removal when EBRT is too short to obtain biological oxidization of ET into the by-product before release. A comparison of four different inlet concentrations with respect to the influence of EBRT on RE and EC showed that

high RE values were similar (at approximately 99%) at ET concentrations of 150 and 350 mg/m³ and at ET concentrations of 850 and 1450 mg/m³ (at approximately 98%) with EBRT of 120 s. Maximum EC values were 14.40, 33.10, 76.50 and 125.28 g/m³ h for 150, 350, 850 and 1450 mg/m³ at a lower EBRT of 30 s, respectively. In addition, better RE values were found with comparative values of the four inlet ET concentrations: 150 > 350 > 850 > 1450 mg/m³, and vice versa for EC. It is of note that the high REs for the four inlet concentrations (Fig. 7 a-d) were approximately 91% and 99%, which corresponds to average ECs of 24.74 and 20.60 g/m³ h at an EBRT of 90 s and 120 s, respectively.

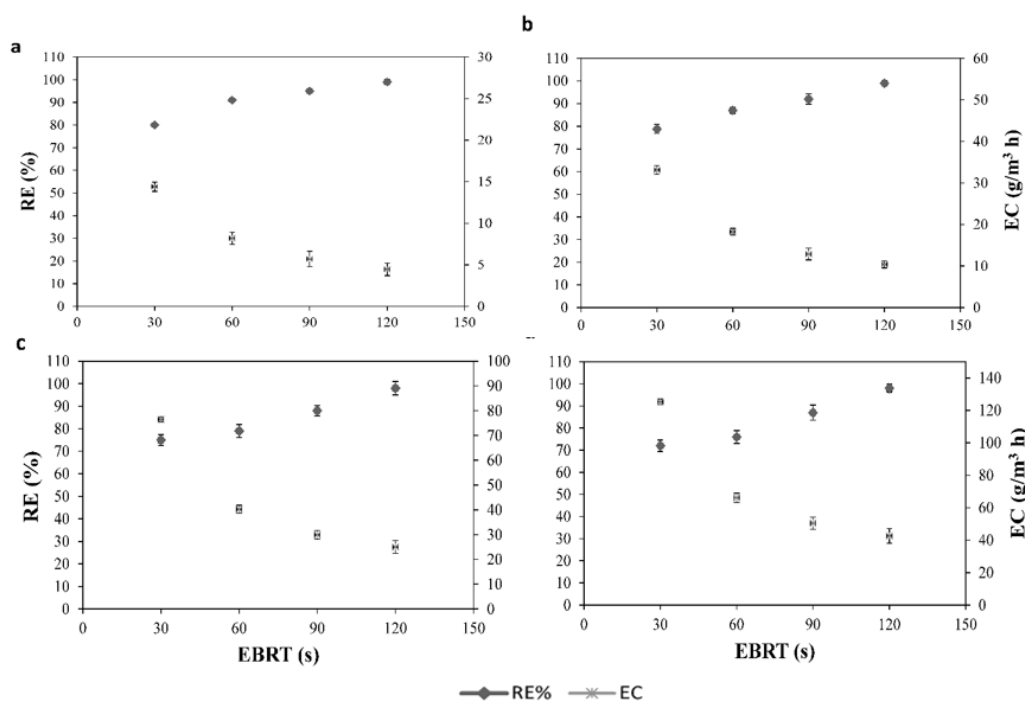


Fig.7. Influence of EBRT on ET RE% and EC of bio-scrubber at different ET inlet concentrations and fixed spray density of 0.23 m³/m² h: (a) 150 mg/m³, (b) 350 mg/m³, (c) 850 mg/m³ and (d) 1450 mg/m³. Error bars indicate SD of duplicate samples.

Therefore, according to REs and ECs, the best EBRT is 90 s of ET treatment in the anoxic bio-scrubber system at a fixed spray density 0.23 m³/m² h. Furthermore, the best gas-to-liquid ratio is 53, according to an EBRT of 90 s and spray density of 0.23 m³/m² h. In comparison with other studies, all the results in this work showed a much higher ET RE and EC with a lower EBRT under anoxic conduction and a mixed culture, and without the use of a specific type of bacteria. For example, the study of An et al. [3] seeded mixed microorganisms with strains RG-1 and B350 in twin bio-trickling filter columns to purify ET under aerobic conditions, and the maximal ECs for

RG-1 and B350 were 38.36 g/m³ h with 89.20% RE and 25.82 g/m³ h with 57.10% RE, respectively, at EBRT of 83 s. In another study, the maximum EC was only 3.70 g/m³ h with a RE of 50% for ET at EBRT of 40 s in an aerobic bio-trickling filter inoculated with alkaliphilic sulpho-oxidizing bacteria under alkaline conditions [34]. A comparison of bio-scrubber performances with various bioreactors for removing sulphur compounds under anoxic conditions is provided in Table 2. Most practical experiments have used lab-scale and pilot-scale traditional bioreactors for sulphur compound removal.

Table 2. Bio-reactors for sulphur-containing compound removal under anoxic conditions.

Bio-reactor type	Target pollutants	Scale	C _{in} /loading	RE/EC	EBRT (s)	Irrigation flowrate (mL/min)	References
Bio-trickling filter	H ₂ S	Lab-scale	78 g/m ³ h	99%	144	180	[35]
Bio-trickling filter + Bubble column	H ₂ S	Lab-scale	2164–2225 mg/m ³	100% / 54.5 gH ₂ S/m ³ h	300	5	[36]
Bio-trickling filter	Methyl mercaptan (MM)	Lab-scale	160–192 mg/ m ³	82% / 1.8 g S–MM/ m ³ h	180	100	[37]
Bio-trickling filter	H ₂ S	Pilot-scale	400–800 gH ₂ S/ m ³ h	100% / 270–300 gH ₂ S/ m ³ h	1080	500	[38]
Bio-filter	H ₂ S	Pilot-scale	1527 mg/ m ³	100% / 30.3 gH ₂ S/ m ³ h	300	1.33	[39]
			1249 mg/ m ³	100% / 25.2 gH ₂ S/ m ³ h	240		
Bio-scrubber	ET	Lab-scale	150 mg/ m ³ 6 g/ m ³ h 1450 mg/ m ³ 58 g/ m ³ h	95% / 5.7 g/ m ³ h 87% / 50.46 g/ m ³ h	90	26	This study

Table 2 shows results of calculated RE%, EC, EBRT and irrigation flowrates obtained from this study and other studies. As reported, the RE%, EC, EBRT and irrigation flowrate values are all different between studies because of the different types of bio-reactors, pollutants, scales, inlet concentrations, loading rates, liquid flowrates and another experimental condition employed. Moreover, in this study, the best RE% and EC ranged from 95–87% and 5.70–50.46 g/ m³ h at an EBRT of 90 s, irrigation flowrate of 26 mL/min (spray density = 0.23 m³/m² h) and an inlet ET concentration ranging from 150 to 1450 mg/m³.

3.5. Metabolic product analysis and mass balance of carbon, sulphur and nitrogen

To ensure that ET was not only removed into the irrigation liquid by physical absorption, but also biologically oxidized, the SO₄²⁻

concentrations, biomass growth of the liquid samples and CO₂ of the gas samples from the bio-reactor at an EBRT of 90 s and spray density of 0.23 m³/m² h were monitored daily during 32 days of observation under steady-state conditions (E3 in Table 1). An initial gas ET injection amount of 150 to 1450 mg/m³ was eventually converted in terms of mass (g/d) into an aqueous phase (expressed as ET-aqueous: the ET transferred from gas to liquid after the scrubbing ET gas phase by the irrigation liquid), and the aqueous ET was calculated according to Henry's coefficient constant of 0.15 [14]. In Fig. 8, aqueous ET is utilized as the sole carbon source by a mixed culture and is biologically oxidized to either CO₂, SO₄²⁻ or another intermediate, which are then utilized by the cells to produce biomass. Stoichiometrically, 1 g/d of ET converts to 0.516 g/d of S⁰, 0.31 g/d of CO₂ and 0.565 g/d of bacterial growth (according to Equation A.4), and according to A.5 in the

appendix, 1 g/d of ET converts to 1.548 g/d of sulphate, 0.57 g/d of CO₂ and 0.44 g/d of bacterial growth.

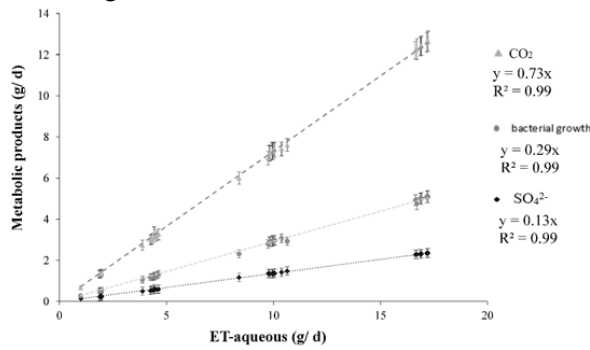


Fig.8. Relationship between by-products (bacterial growth, CO₂ production and SO₄²⁻) with mass of initial ET-dissolved. Error bars indicate the SD of duplicate samples.

The results show that the CO₂ production from converting 1.91 to 17.22 g/d dissolved ET increased from 1.345 to 12.59 g/d, and the bacterial growth ranged from 0.56 to 5.09 g/d. Furthermore, SO₄²⁻ values biologically produced from ET degradation were 0.26 to 2.36 g/d. These results prove that the main end products fluctuated between S⁰ and SO₄²⁻, because the empirical results of production biomass, CO₂ and SO₄²⁻ lay between two stoichiometric equations (A.4) and (A.5). Previous research confirmed mineralization during ET aerobic degradation by *pseudomonas sp.* WL2 to CO₂, in addition to bacterial yield and SO₄²⁻ production in a batch reactor, where it was shown that for 4.2–25.2 mg of initial ET degradation, 8.9–29.0 mg of CO₂ and 1.2–3.5 mg TSS were produced after the substrate was completely consumed within 24 h. In addition, the SO₄²⁻ production from oxidation of initial ET values of 6.7, 15.1 and 23.5 mg was 100.3, 32.5 and 15.2 mg/L, respectively [13]. Comparatively, the results obtained in this study were more efficient in terms of ET removal at a low energy consumption, in addition to the reduced production of SO₄²⁻, which indicates that the system operates under a limited NO₃⁻ source.

The carbon mass balance was conducted with respect to the carbon molecules in ET used by microorganisms for energy metabolism and cell synthesis. The carbon balance for the lab-scale bio-scrubber system can be defined by

$$C_I = C_o + C_{biom} + C_G, \quad (13)$$

where C_I represents the influent ET amount as a carbon source (suffix as ET-C) in g/d within

the bio-tank, C_{biom} represents the carbon assimilated for bacterial growth, C_G is the amount of carbon converted to produce gas and C_o represents the outlet ET-C calculated from the COD measurement divided by a factor of 1.43 (which represents the COD of ET).

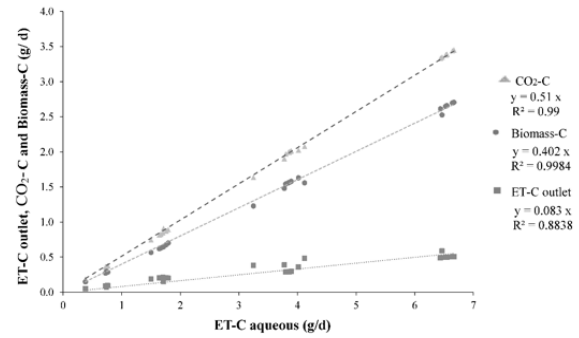


Fig.9. Carbon mass balance.

According to the calculated mass balance, 0.38 to 6.67 g/d of incoming ET-C was consumed by the cells for biomass growth and CO₂ production, which equalled approximately 40% and 52% of the total ET, respectively. The remaining part of ET-C was approximately 8%, as reported in Fig. 9. In addition, there were no intermediate compounds containing carbon molecules.

Furthermore, the bio-degradation of the ET was mainly oxidized to either S⁰ or SO₄²⁻ according to Equations (A.4) and (A.5), and it was thus assumed that the solo end products were S⁰ and SO₄²⁻, in accordance with stoichiometric equations. In this respect, a sulphur mass balance was conducted using subtraction [37] to estimate the quantity of sulphur produced in the system. As studied previously, the pathway of ET degradation under aerobic conditions by strain WL2: diethyl disulphide (DEDS) was formed and then converted to SO₄²⁻ at complete mineralization of ET, while S⁰ occurs inside the bacterial cells by the transformation of DEDS to S⁰ prior to being further oxidized to SO₄²⁻. Therefore, the only final products were S⁰ and SO₄²⁻ [13]. In this study, the relationship between ET removed and NO₃⁻ consumed is presented as $ET_{rem} / NO_{3-}^{cons}$, and the mass balance of sulphur, SO₄²⁻ production is expressed as SO₄²⁻-S. The S⁰ formation in the lab-scale bio-scrubber system from oxidation of aqueous ET (expressed as ET-S) was calculated and is depicted in Fig. 10 a and b. Initially, different amounts of ET were input with time (from 0.288 to 2.86 g/d) and NO₃⁻ feeding was

maintained at a molar ratio of 0.54 at each ET inlet renewal rate. The empirical molar ratio data fall between two limits of stoichiometric equations 0.74 and 0.34, where the $ET_{rem}/NO_3^-_{cons}$ molar ratio was approximately 0.58 between the 1st and 25th days. However, after the 26th day, the ratio decreased to approximately 0.48 mol/mol during the operation period, which may be due to accumulation of remaining NO_3^- with time and variations in the amount of ET removed to NO_3^- consumed. The accumulated SO_4^{2-} -S increased markedly from 0.09 g/d (at day 1) to 12.21 g/d (by day 32); an increasing

amount of sulphur was obtained as time progressed, and the molar ratio $ET_{rem}/NO_3^-_{cons}$ decreased from 0.60 to 0.47, respectively. The results obtained from calculated S^0 range between 1.37 and 127.13 g/d. It is clear that most ET oxidation was converted to S^0 rather than SO_4^{2-} . This was also confirmed by the estimated percentage of S^0/ET -S from the sulphur mass balance, which was approximately 90% of ET -S biologically converted to S^0 . The percentage of SO_4^{2-}/ET -S was approximately only 9% of the ET -S transferred to SO_4^{2-} Fig. 10 b.

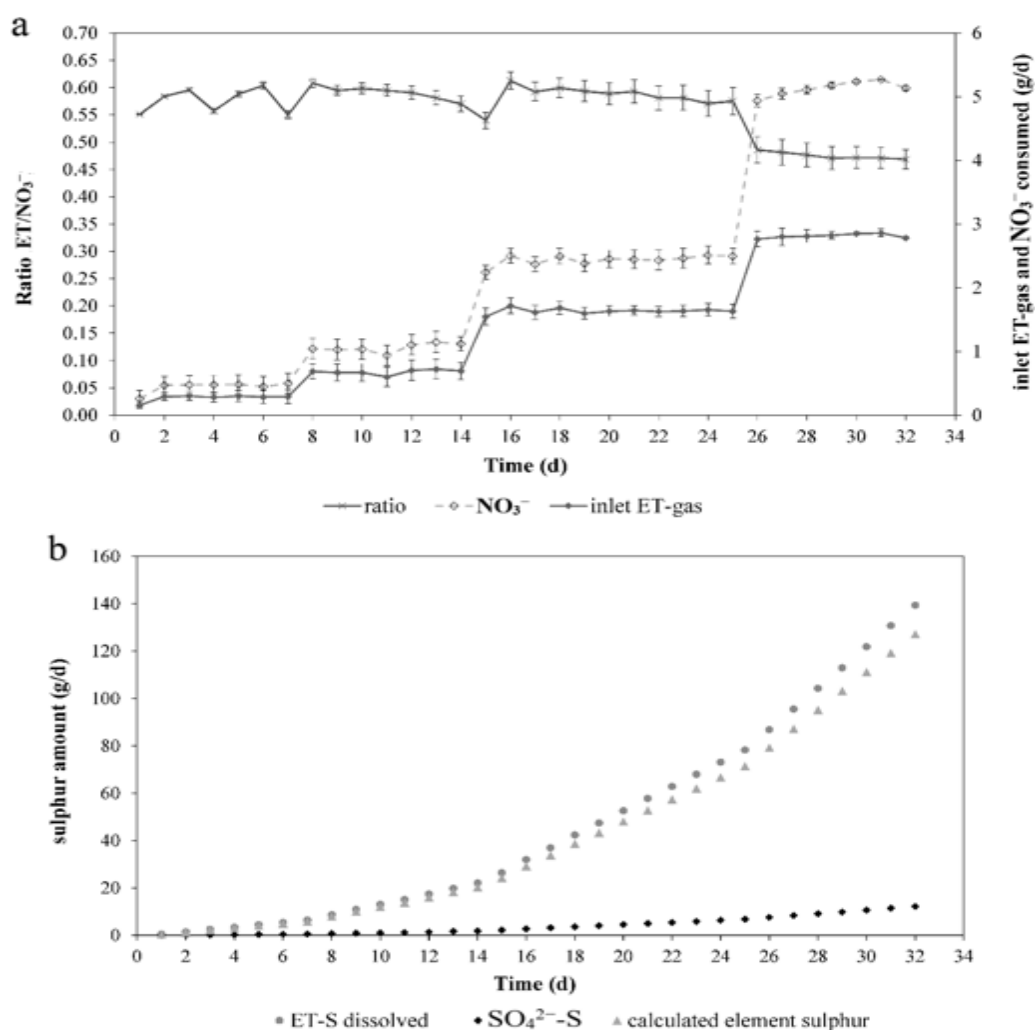


Fig.10. Time course of (a) ratio of ET/NO_3^- , ET inlet loading nitrate and consumption rate and (b) sulphur mass balance (i.e., SO_4^{2-} -S and calculated sulphur formation in the bio-scrubber system from ET -S dissolved loading rate). Error bars indicate the SD of duplicate samples.

However, there was a certain pale-yellow substance (that had some S^0 material characteristics) within the biomass of the reactor. This indicated that the desulphurization process had occurred in the bio-reactor for the ET remaining in an aqueous phase, and it confirmed that the remaining ET had been

converted into S^0 and other forms of sulphur, rather than SO_4^{2-} , via the desulphurization process [1]. A previous study found that degradation of the H_2S -S loading rate fluctuated during anoxic bio-trickling filtering to S^0 or SO_4^{2-} because of variations in the molar ratio of $N_{supplied}/S_{removed}$ and H_2S ILs [40]. Through the

sulphur mass balance, the study also found that the ratio of $\text{SO}_4^{2-}\text{S}/\text{S}^0$ was increased from 5% to 70% when $\text{H}_2\text{S}\text{-S}$ was converted to SO_4^{2-} . In addition, S^0 was noticed in the polyurethane foam. Several studies have reported the important role of the $N_{\text{sup}}/N_{\text{remo}}$ molar ratio in controlling desulphurization products, and this has been adjusted while the IL has been fixed [36, 38]. However, controlling the amount of nitrate supplied for the complete oxidation of sulphide to sulphate in real operating conditions is inflexible owing to rapid variations in ILs, which results in the partial oxidation of sulphide to S^0 [41]. Janssen et al. [42] mentioned that the production of S^0 is related to the amount of dissolved oxygen, where S^0 is the major end product of sulphide oxidation under oxygen-limiting conditions. However, in current study, the correlation between the $\text{ET}_{\text{rem}}/\text{NO}_3^-$ molar ratio and forms of S^0 production were evident in the end products, and this result is consistent with those in the studies mentioned above.

A nitrogen mass balance (expressed as NO_3^- -N) was conducted according to the actual inputs of feeding nitrogen and the concentrations of measured nitrogen in the system. The nitrogen balance for the whole system was calculated by

$$N_I = N_o + N_{\text{biom}} + N_G, \quad (14)$$

where N_I represents the amount of nitrogen input to the system, N_o represents the amount of nitrogen output from the biological tank, N_{biom} represents the amount of nitrogen consumed for biomass growth and N_G is nitrogen gas produced during the denitrification process, which is assumed by taking the average from the stoichiometric equations (A.4) and (A.5); however, as it was the same as the carrier gas contaminant, it was difficult to measure. To calculate the mass balance, a mass flow diagram was prepared (in Fig. 11) for one case under certain system operation conditions (ET inlet 150 mg/m^3 , spray density of $0.23 \text{ m}^3/\text{m}^2 \text{ h}$ and EBRT of 90 s) for 7 days. The initial nitrogen load into the bio-reactor was a rate of 121.90 mg N/day , and approximately 13% of this was

found to be outgoing (with a value of 15.73 mg N/d).

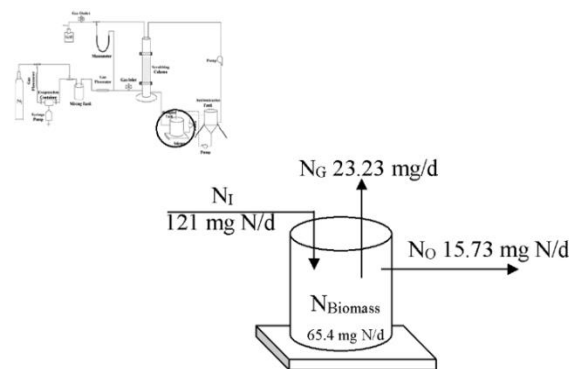


Fig.11. Nitrogen mass balance

The net growth of biomass in the denitrification reactor accounted for 54% ($65.4 \text{ mg N}_{\text{biomass}}/\text{day}$) of the inlet nitrogen load. A total of 23.23 mg N/d of inlet N was converted to nitrogen gas through the denitrification process, which was approximately 19% of total incoming N. The difference between inlet and outgoing N was approximately 14%.

3.6. Biological ET oxidation stoichiometry and energetic reactions

Microorganisms oxidize inorganic and organic materials from oxidation reduction reactions to obtain energy for growth and maintenance [43]. Oxidation reduction reactions always involve an electron exchange (food substrate for the organism), and the electron acceptor is oxygen (under aerobic conditions). Whether under anaerobic or anoxic conditions, some microorganisms can use other electron acceptors in energy metabolism, including NO_3^- , SO_4^{2-} and carbon dioxide. Stoichiometry expresses quantitative relationships between reactants and products in a chemical equation. In this study, the reaction stoichiometry and the biomass yield ($Y_{X/D}$) for biological ET oxidation were calculated by taking a thermodynamic approach [44]. The following stoichiometric equations were derived from the thermodynamic analysis presented in the appendix. When NO_3^- was used as an electron acceptor and the nitrogen source for biomass was NO_3^- , the end product was sulphur



or sulphate,



Table 3. Thermodynamic calculated yield values (Y_{ET/NO_3^-}) and free energies of ET oxidation when NO_3^- was used as the electron acceptor.

Thermodynamically calculated yield values and Gibbs free energies	Nitrogen source for biomass	Main product SO_4^{2-}	Main product S^0
Y_{ET/NO_3^-} (mol/mol)		0.34	0.74
Gibbs free energy kJ/e-mole	NO_3^-	-1398.88	-675.73

Table 3 shows the theoretical yield molar ratios (Y_{ET/NO_3^-}) calculated from Eq. (15) and (16) and the Gibbs free energy at different end products when NO_3^- was used as the biomass source. As seen in Table 3, S^0 is formed as a by-product when NO_3^- is limited. NO_3^- consumption and biomass production are lower when electron acceptors are used, and S^0 is formed as the main product than in systems where SO_4^{2-} is formed as the main product. Energies of -1398.88 kJ/e-mole and -675.73 kJ/e-mole were obtained from the anoxic oxidation of ET to SO_4^{2-} and S^0 , respectively; the negative signal refers to the reaction being exothermic and spontaneous (and product-favoured). Fig. 12 shows the theoretical upper and lower limits of the yield molar ratios (Y_{ET/NO_3^-}) given in Table 3 and presents the experimental data for optimized operating conditions using a spray density of $0.23 \text{ m}^3/\text{m}^2 \text{ h}$ and EBRT at 90 s under different ET concentrations.

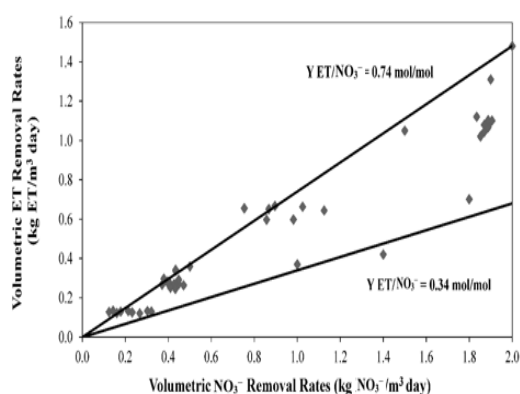


Fig.12. Volumetric ET removal versus volumetric NO_3^- removal

In a previous study, NO_3^- and NO_2^- were both present in the wastewater to de-sulphurate biogas (H_2S) in a continuous bio-scrubber, and as they were used as electron acceptors, the

stoichiometric molar ratios ($S^{-2}/(NO_3^- + NO_2^-)$) at different end products were 0.44–0.72 and 1.75–2.89 for SO_4^{2-} and S^0 , respectively. Most of the experimental molar ratios were scattered within these limits, owing to the mixture of nitrate and nitrite and the variance of H_2S oxidation end products [45]. In addition, Li et al. [36] investigated the effect of the S/N ratio on the removal of H_2S from biogas in a bio-trickling filter (BTF) and a bubble column (BC). They found that the BTF was more stable in terms of H_2S removal performance than the BBC, which was attributed to their different gas–liquid mass transfers. For S/N ratios of 1–2.5, H_2S was almost completely removed by the bio-trickling filters, and the maximum EC of H_2S was $54.5 \text{ g } H_2S/\text{m}^3 \text{ h}$. The S/N ratios did not significantly influence the biogas desulphurization efficiency, but the desulphurization products were obviously affected. With increasing S/N ratios from 1.0 to 2.5, the percentages of SO_4^{2-} decreased, and the denitrification performance clearly improved. In this study, the experimental data are distributed between two limits, and most data are scattered near the upper value of Y_{ET/NO_3^-} (0.74) when the end product is sulphur, as shown in Fig. 12. This result refers to the presence of S^0 . In addition, Table 4 summarizes an average Y_{ET/NO_3^-} ratios obtained with different spraying densities and ET loading rates; according to the table, the average experimental yield values are closer to the Y_{ET/NO_3^-} theoretical value of 0.74 when the main product is S^0 . This indicates that the partial formation of S^0 and other forms of sulphur were produced rather than SO_4^{2-} and proves that S^0 was produced in the bio-reactor tank. Therefore, to produce less biomass and consume less energy in biological ET oxidation systems, S^0 needs to be the desired end product. It is known

that a lower NO_3^- consumption can considerably reduce costs. Furthermore, S^0 is non-toxic, stable and insoluble in water, and it can thus be recovered easily [45]. The formation of S^0 is preferred for the following reasons; first, S^0 is non-soluble and thus can be removed easily; second, S^0 can be recovered and used as a valuable raw material (e.g., in bioleaching processes in sulphuric acid production factories after purification from the water stream by gravity sedimentation, such as in a titled plate settler); and finally, as more oxygen is required to form SO_4^{2-} , a higher energy consumption is thus required for aeration [42,46].

Methods used to separate S^0 from the water stream include settlers, filter presses and

sulphur melters, depending on the quality of elemental sulphur required [46,47]. Accordingly, in our practical system, S^0 can be recovered from the bio-scrubber system by transferring the settled sludge from the sedimentation tank to the vacuum filter press.

The concentrations of NO_3^- consumed are shown in Table 4. They gradually and significantly increased with an increase in the ET loading rate, which occurred in relation to the need for more NO_3^- (electron acceptor) by microorganisms to oxidize the ET, and this subsequently promoted the denitrification process.

Table 4. Comparison of thermodynamically and empirically calculated $Y_{\text{ET}/\text{NO}_3^-}$ values when NO_3^- is used as the electron acceptor.

Loading rate g/m ³ h	Spray density m ³ /m ² h	Average ET removal g/day	Average NO_3^- consumption g/day	Experimental $Y_{\text{ET}/\text{NO}_3^-}$ mol/mol	Thermodynamically calculated $Y_{\text{ET}/\text{NO}_3^-}$ (mol/mol)	
					Main product S^0	Main product SO_4^{2-}
6±1.5	0.45	0.27	0.73	0.37	0.74	0.34
	0.3	0.28	0.43	0.65		
	0.23	0.27	0.44	0.61		
	0.18	0.26	0.37	0.7		
	0.12	0.25	0.31	0.8		
Average ± S.D.		0.2760.01	0.4660.16	0.6360.16		
14±0.6	0.45	0.64	1.93	0.33		
	0.3	0.61	1.18	0.52		
	0.23	0.59	0.90	0.66		
	0.18	0.60	0.80	0.75		
	0.12	0.54	0.75	0.72		
Average ± S.D.		0.6060.04	1.1160.49	0.660.17		
34±1.5	0.45	1.38	2.4	0.58		
	0.3	1.36	1.87	0.72		
	0.23	1.34	1.94	0.69		
	0.18	1.33	1.91	0.70		
	0.12	1.27	1.9	0.67		
Average ± S.D.		1.3460.04	260.22	0.6760.05		
58±1.35	0.45	2.22	5.22	0.43		
	0.3	2.2	4.75	0.46		
	0.23	2.19	3.9	0.56		
	0.18	2.14	3.54	0.60		
	0.12	2.1	3.4	0.62		
Average ± S.D.		2.1760.05	4.1660.79	0.5360.08		

4. CONCLUSIONS

This paper reveals that a lab-scale bio-scrubber under anoxic conditions offers a promising alternative to remove the sulphurous odour of ET from waste gas. The results showed that the best running conditions for ET degradation were at an inlet concentration of 150 mg/m³, spray density of 0.23 m³/m² h and EBRT of 90s (with an average RE of 91% at four sets of inlet concentrations). The results of batch experiments made it clear that ET was considered a readily biodegradable compound under anoxic conditions. The Monod model was

used to indicate the values for μ_{max} , K_s , Y_{XS} and q_{max} , which were obtained as 0.14 1/h, 1.17 mg/L, 0.52 g_x/g_s and 0.26 g_s/g_x h, respectively. The average experimental yield value was closer to the theoretical value (Y_{ET/NO_3^-}) of 0.74 when the main product was S⁰, which indicates that S⁰ and other sulphur forms were produced as the end product, rather than SO₄²⁻.

Appendix

Calculation of total reaction stoichiometry, biomass yield and free energy for ET oxidation systems.

The reaction stoichiometry of biological ET oxidation can be mathematically calculated from the biomass yield, ($Y_{X/D}$), which is calculated using the following equation [44],

$$Y_{X/D} = \frac{\gamma_D}{\gamma_X} = \frac{\Delta G_{eD} - \Delta G_{eA}}{(\Delta G_{eD} - \Delta G_{eA}) + \left[\frac{Y_{G/X}}{\gamma_X} + (\Delta G_{eX} - \Delta G_{eD}) \right]} \quad (\text{A. 1})$$

- where
- $Y_{X/D}$: Biomass yield (C-mole biomass/C-mole electron donor)
 - $\Delta G_{eD}, \Delta G_{eA}$: Gibbs free energy for electron donor and acceptor, respectively (kJ/e-mole)
 - ΔG_{eX} : Gibbs free energy for biomass (kJ/e-mole)
 - γ_D, γ_X : Degree of reduction of electron donor and biomass (e-mole/C-mole)
 - $Y_{G/X}$: Gibbs free energy released per C-mole of biomass (kJ/C-mole)

The values of $Y_{G/X}$ for electron donors are equal to 434 and 1176 kJ/C-mole of S⁰ and SO₄²⁻ respectively, based on Heijnen (1999) [48]. When the biomass yield is known, the reaction stoichiometry can be obtained using the half-reactions (see Table, App. 1) as given in Eq. (A. 2) [49],

$$R = R_d - Y_{X/D} R_c - (1 - Y_{X/D}) R_a, \quad (\text{A. 2})$$

where

- R : The total reaction
- R_d : The half-reaction for the electron donor
- R_a : The half-reaction for the electron acceptor
- R_c : The half-reaction for biomass synthesis

Table App.1. Reactions for ET oxidation and Gibbs standard free energies at pH 7 [50,51]

Reduced–oxidized Compounds	Half-reaction	ΔG° (kJ/e-mol)
S ⁰ /CH ₃ CH ₂ SH*	$\frac{1}{7} CO_2 + H^+ + \frac{1}{14} S^0 + e^- \rightarrow \frac{1}{14} CH_3CH_2SH + \frac{2}{7} H_2O$	+28.097**
SO ₄ ²⁻ /CH ₃ CH ₂ SH*	$\frac{1}{10} CO_2 + \frac{11}{10} H^+ + \frac{1}{20} SO_4 + e^- \rightarrow \frac{1}{20} CH_3CH_2SH + \frac{2}{5} H_2O$	+25.39**
NO ₃ ⁻ /N ₂	$\frac{1}{5} NO_3 + \frac{6}{5} H^+ + e^- \rightarrow \frac{1}{10} N_2 + \frac{3}{5} H_2O$	-72.2
NO ₃ ⁻ (Biomass)	$\frac{5}{28} CO_2 + \frac{1}{28} NO_3 + \frac{29}{28} H^+ + e^- \rightarrow \frac{1}{28} C_5H_7NO_2 + \frac{11}{28} H_2O$	+10.36***

* Half-reactions of ET were written according to the steps mentioned by Rittman and McCarty [50];
 Calculated using table App.2; *Calculated based on Heijnen (1999) [48].

The standard free energies of half-reactions (S^0/CH_3CH_2SH) and (SO_4^{2-}/CH_3CH_2SH) can be calculated using values of free energy of formation for individual constituents, as listed in Table App. 2 and Eq. A.3).

Table App. 2. Free energies of formation for various chemical species, 25°C [50,52,17]

Compounds	Gibbs free energy kJ/e-mole
CH ₃ CH ₂ SH	-4.8
H ₂ O	-237.2
CO ₂	-394.359
H ⁺	-39.87
S ⁰	ZERO
SO ₄ ²⁻	-744.63
NO ₃ ⁻	-111.34
N ₂	0
C ₅ H ₇ NO ₂ (Biomass)	-340.28

The free energy of the reaction (ΔG_r^0) is equal to the sum of the free energies of formation of the products minus the sum of the free energies of the reactants at standard state [53],

$$\Delta G_r^0 = \sum \Delta G_f^0 (products) - \sum \Delta G_f^0 (reactants) \quad (A.3)$$

$$= (S^0/CH_3CH_2SH) = +28.097 \text{ kJ/e-mole,}$$

$$\Delta G_r^0 = (SO_4^{2-}/CH_3CH_2SH) = +25.39 \text{ kJ/e-mole.}$$

The biomass yield and reaction stoichiometry were determined for the system where NO₃⁻ was used as the electron acceptor and a nitrogen source of biomass, while ET was used as the electron donor. To calculate the reaction stoichiometry of the system where the main product was sulphur, the degree of reduction S⁰ to ET was $\gamma_D = +4.7$, and the Gibbs free energy for biomass (C₅H₇NO₂) production was $\Delta G_{eX} = +10.36 \text{ kJ/e-mol}$. The degree of reduction of 1 C mol (CH_{1.4} N_{0.2} O_{0.4}) of biomass, $\gamma_X = 28/5 = 5.6$. Gibbs free energy, was taken for 1 C mol of biomass, $Y_{GX} = 434 \text{ kJ/C-mole}$.

$$Y_{X/D} = \frac{4.7}{5.6} \frac{(28.09 - (-72.2))}{(28.09 - (-72.2)) + \left[\frac{434}{5.6} + (10.36 - 28.09) \right]}$$

$$Y_{X/D} = 0.52 \frac{C - molbiomass}{molET}$$

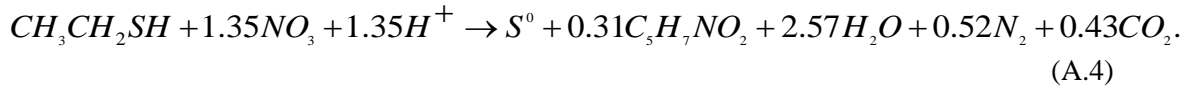
$$Y_{X/D} = 0.52 \frac{C - molbiomass}{molET} \cdot \frac{1molET}{4.7e - mol} \cdot \frac{5.6e - molbiomass}{1C - molbiomass}$$

and was found to be

$$Y_{X/D} = 0.63 \frac{e - molbiomass}{e - mol}$$

The Rd, Rc and Ra values were as follows for the ET oxidation systems using NO₃⁻ as the electron acceptor. By using Eq. A. 2, the total reaction stoichiometry where the main product was sulphur was

found to be R:



For the reaction stoichiometry of the system where the main product was SO_4^{2-} , the biomass yield was calculated according to Eq. A. 1.

The degree SO_4^{2-} reduced to ET was $\gamma_D = +6.7$, and the Gibbs free energy for biomass ($C_5H_7NO_2$) production was $\Delta G_{eX} = +10.36$ kJ/e-mol. The degree of reduction of 1 C mol ($CH_{1.4}N_{0.2}O_{0.4}$) of biomass was $\gamma_X = 28/5 = 5.6$, and the Gibbs free energy was taken for 1 C mol of biomass, $Y_{G/X} = 1176$ kJ/C-mole.

$$Y_{X/D} = \frac{6.7}{5.6} \frac{(25.39 - (-72.2))}{(25.39 - (-72.2)) + \left[\frac{1176}{5.6} + (10.36 - 25.39) \right]}$$

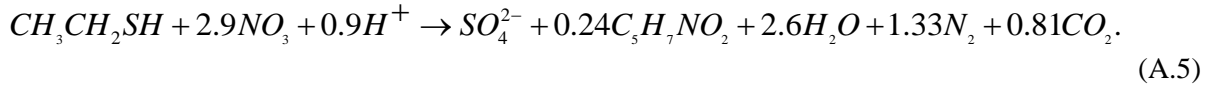
$$Y_{X/D} = 0.4 \frac{C - molbiomass}{molET}$$

$$Y_{X/D} = 0.4 \frac{C - molbiomass}{molET} \cdot \frac{1molET}{6.7e - mol} \cdot \frac{5.6e - molbiomass}{1C - molbiomass}$$

and was found to be

$$Y_{X/D} = 0.33 \frac{e - molbiomass}{e - mol}$$

In the systems where the main product was SO_4^{2-} , only the electron donor reaction changes. Therefore, new R_d , R_c and R_a values were as follows, and the total reaction stoichiometry was found to be as follows, using Eq. A. 2,



To obtain the free energies for the full-reaction stoichiometry for ET oxidation for each of Eq. A. 4 and A. 5, the free energy of the reaction (ΔG_r^0) was found to be as shown in Table App. 3 using Eq. A.3, and the values of Gibbs free energy is shown in Table App. 2.

Table App. 3. Free energies of total-reaction stoichiometry for ET oxidation (A.4) when the main product was S^0 , and (A.5) when the main product was SO_4^{2-} .

Free energy of reaction (ΔG_r^0)	Main product S^0	Main product SO_4^{2-}
kJ/e-mole	-675.73	-1398.88

References.

1. Sedighi, M., S.M. Zamir and F. Vahabzadeh (2016) Cometabolic degradation of ethyl mercaptan by phenol-utilizing *Ralstonia eutropha* in suspended growth and gas-recycling trickle-bed reactor. *Journal of Environmental Management*, 165: 53-61.
2. Patnaik, P. (2007) *A comprehensive guide to the hazardous properties of chemical substances*. 3rd ed., pp.877-878. John Wiley & Sons, Inc., Hoboken, New Jersey, Canada.
3. An, T., S. Wan, G. Li, L. Suna and B. Guoc (2010) Comparison of the removal of ethanethiol in twin-biotrickling filters inoculated with strain RG-1 and B350 mixed microorganisms. *Journal of Hazardous Materials*, 183: 372–380.
4. Li, L., J. Zhang, J. Lin and J. Liu (2015) Biological technologies for the removal of sulphur containing compounds from waste streams: bioreactors and microbial characteristics, *World J. Microbiol. Biotechnol.*, 31: 1501–1515.
5. Kachina, A., S. Preis and J. Kallas (2006) Catalytic TiO₂ oxidation of ethanethiol for environmentally benign air pollution control of sulphur compounds, *Environ Chem Lett* ., 4: 107–110.
6. Sedighi, M., F. Vahabzadeh, S. M. Zamir and A. Naderifar (2013) Ethanethiol degradation by *Ralstonia eutropha*. *Biotechnology and Bioprocess Engineering*, 18: 827-833.
7. Rafson, H.J. (1998) *Odor and VOC control handbook*. Pp.101-102. The McGraw-Hill, New York.
8. Kastner, J.R. and Das, K.C. (2002) Wet scrubber analysis of volatile organic compounds removal in the rendering industry. *J. Air Waste Manage. Assoc.*, 52:459–469.
9. Jones, C. E., N. A. Hatcher and R. H. Weiland (2014) Mercaptans Removal from Gases by Absorption into Amines and Caustic, <http://www.digitalrefining.com/article/1000903>, [Mercaptans removal from gases by absorption into amines and caustic.html](http://www.digitalrefining.com/article/1000903), *Optimized Gas Treating*, Inc., Buda.
10. Fernández, M., M. Ramírez, R. M. Pérez, J. M. Gómez, D. Cantero (2013) Hydrogen sulphide removal from biogas by an anoxic biotrickling filter packed with Pall rings, *Chemical Engineering Journal*, 225: 456–463.
11. Kennes, C. and F. Thalasso (1998) Waste gas biotreatment technology. *J. Chem. Technol. Biotechnol.*, 72: 303-319
12. Qaisar, M., Z. Ping ., C. Jing., H. Yousaf, H. M. Jaffar, W. Dong-lei and H. Bao-lan (2007) Sources of sulfide in waste streams and current biotechnologies for its removal. *Journal of Zhejiang University Science*. 8:1126-1140
13. Wang, X., C. Wu, N. Liu, S. Li, W. Li, J. Chen and D. Chen (2015) Degradation of ethyl mercaptan and its major intermediate diethyl disulfide by *Pseudomonas* sp. strain WL2. *Appl Microbiol Biotechnol*, 99: 3211–3220.
14. Wang, P., S. Peng, C. Zhu, X. Zhang and F. Teng (2015) Removal of ethanethiol gas by iron oxide porous ceramsite biotrickling filter, *Journal of Chemistry*, 2015: 1-9.
15. Wan, S., G. Li and T. An. (2011) Treatment performance of volatile organic sulfide compounds by the immobilized microorganisms of B350 group in a biotrickling filter, *J Chem. Technol Biotechnol.*, 86: 1166–1176.
16. Dumont, E. (2015) H₂S removal from biogas using bioreactors: a review. *International journal of energy and environment*. 6:479-498
17. Yavuz, B., M. Türker, and G.Ö. Engin (2007) Autotrophic removal of sulphide from industrial wastewaters using oxygen and nitrate as electron acceptors. *Environmental engineering science*, 24: 457-470.
18. Türker, M., A.B. Baspinar and A. Hocalar (2012) Monitoring and control of biogas desulphurization using oxidation-reduction potential under denitrifying conditions. *Journal of Chemical Technology & Biotechnology*, 87: 682-688.
19. Frederick, A., W.H. Brown, M.K. Campbell and S.O. Farrel (2013) *Introduction to organic and biochemistry*.

- 7th ed., pp. 106-107. Brooks/ Cole, Cengage learning, USA.
20. Muñoz R., Souza T.S., Glittmann L., Pérez R. and Guillermo G. (2013) Biological anoxic treatment of O₂-free VOC emissions from the petrochemical industry: A proof of concept study. *Journal of Hazardous Materials*. 260: 442–450
 21. Lenore S. Clescerl, Arnold E., Greenberg (1998) *Standard Methods for the Examination of Water and Wastewater* 20th ed., pp. 14-16. APHA American Public Health Association, USA
 22. P. Aarne V., Susan M.M. and Lauren G.H. (2010) *Introduction to environmental engineering* 3rd ed., pp. 260-261. Cengage learning, USA.
 23. Tang, K., V. Baskaran, and M. Nemati (2009) Bacteria of sulphur cycle: An overview of microbiology, biokinetics and their role in petroleum and mining industries. *Biochem. Eng. J.* 44: 73-94.
 24. Carvajal, A., I. Akmirza, D. Navia, R. Perez, R. Muñoz, R. Lebrero (2018) Anoxic denitrification of BTEX: Biodegradation kinetics and pollutant interactions. *Journal of Environmental Management*. 214:125-136.
 25. Giri, B. S., M. Goswamia, R.A Pandey and K.H Kimb (2015) Kinetics and biofiltration of dimethyl sulfide emitted from P&P industry. *Biochemical Engineering Journal*, 102: 108–114.
 26. Jennings, P.A., V.L. Snoeyink and E.S.K. Chian (1976) Theoretical model for a submerged biological filter, *Biotechnol. Bioeng.* 18: 1249-1273.
 27. Ottengraf, S.P.P. and A.H.C. Van den Oever. 1983. Kinetics of organic compound removal from waste gases with a biological filter. *Biotechnol. Bioeng.* 25: 3089-102.
 28. Okpokwasili, G.C. and C.O. Nweke (2005) Microbial growth and substrate utilization kinetics. *Journal of Biotechnology*, 5: 305-317.
 29. Wan, S., G. Li, T. An, B. Guo, L. Sun, L. Zu, A. Ren (2010) Biodegradation of ethanethiol in aqueous medium by a new *Lysinibacillus sphaericus* strain RG-1 isolated from activated sludge. *Biodegradation*, 21: 1057–1066.
 30. [Fortuny, M.](#), [X. Gamisans](#), [M. A. Deshusses](#), [J. Lafuente](#), [C. Casas](#) and [D. Gabriel](#) (2011) Operational aspects of the desulphurization process of energy gases mimics in biotrickling filters. *Water Research*, 45: 5665-5674.
 31. Potivichayanon, S., P. Pokethitiyook and M. Kruatrachue (2006) Hydrogen sulfide removal by a novel fixed-film bioscrubber system. *Process Biochemistry*, 41: 708-715.
 32. Rappert, S. and R. Müller (2005) Odor compounds in waste gas emissions from agricultural operations and food industries, *Waste Management*, 25: 887–907.
 33. Pokorna D., J. M. Carceller, L. Paclik and J. Zabranska (2015) Biogas cleaning by hydrogen sulfide scrubbing and bio-oxidation of captured sulfides, *Energy & Fuels*, 29: 4058-4065
 34. Garcia, L. A., A. G. Sanchez, G. Baquerizo, S. H. Jimenez and S. Revah (2010) Treatment of carbon disulfide and ethanethiol vapors in alkaline biotrickling filters using an alkaliphilic sulfo-oxidizing bacterial consortium. *J Chem. Technol. Biotechnol.* 85: 328–335.
 35. Fernandez, M., M. Ramirez, R. M. Perez, J. M. Gomez and D. Cantero (2013) Hydrogen sulphide removal from biogas by an anoxic biotrickling filter packed with Pall rings. *Chemical Engineering Journal*, 225:456–463.
 36. Li, X., X. Jiang, Q. Zhou and W. Jiang (2016) Effect of S/N Ratio on the Removal of Hydrogen Sulfide from Biogas in Anoxic Bioreactors. *Appl. Biochem. Biotechnol.* 180:930–944.
 37. Montebello, A. M., M. Fernandez, F. Almenglo, M. Ramirez, D. Cantero, M. Baeza and D. Gabriel (2012) Simultaneous methylmercaptan and hydrogen sulfide removal in the desulfurization of biogas in aerobic and anoxic biotrickling filters, *Chemical Engineering Journal*, 200–202:237–246.

38. Soreanu, G., M. Beland, P. Falletta, K. Edmonson, and P. Seto (2008) Laboratory pilot scale study for H₂S removal from biogas in an anoxic biotrickling filter. *Water Sci Technol.*, 57:201-207.
39. Jaber, M. B., A. Couverta, A. Amrane, P. L. Cloireca and E. Dumontb (2017) Hydrogen sulfide removal from a biogas mimic by biofiltration under anoxic conditions. *Journal of Environmental Chemical Engineering*, 5:5617–5623.
40. Lebrero, R., L., A. T. Cervantes, R. Muñoz, V. Nery, and E. Forestib (2015) Biogas upgrading from vinasse digesters: a comparison between an anoxic biotrickling filter and an algal-bacterial photobioreactor. *J. Chem. Technol. Biotechnol.* 91:2488–2495.
41. Fernandez, M., M. Ramirez, J. M. Gomez and D. Cantero (2014) Biogas biodesulfurization in an anoxic biotrickling filter packed with open-pore polyurethane foam. *Journal of Hazardous Materials*, 264: 529–535.
42. Janssen, A. J. H., S. C. Ma, P. Lens and G. Lettinga (1997) Performance of a Sulfide-Oxidizing Expanded-Bed Reactor Supplied with Dissolved Oxygen. *Biotechnology and Bioengineering*, 53: 32–40.
43. Sawyer, C.N, P.L. McCarty and G.F. Parkin (2003) *Chemistry for Environmental Engineering and Science*. 5th ed., pp. 336-338. McGraw-Hill, New York, USA.
44. Dogan, E.C., M. Türker, L. Dağışan and A. Arslan (2012) Simultaneous sulfide and nitrite removal from industrial wastewaters under denitrifying conditions, *Biotechnology and Bioprocess Engineering*. 17: 661-668.
45. Baspiner, A.B., M. Türker, A. Hocalar and I. Ozturk (2011) Biogas desulphurization at technical scale by lithotrophic denitrification: Integration of sulphide and nitrogen removal, *Process Biochemistry*. 46: 916-922.
46. Tichy, R., A. Janssen, J.T.C. Grotenhuis, G. Lettinga, W.H. Rulkens (1994) Possibilities for using biologically-produced sulfur particles for cultivation of Thiobacilli with respect to bioleaching processes. *Biores.Technol.*, 48: 221–227.
47. Pagella, C., P. Silvestri and [D. F. D. Marco](#) (1996) H₂S treatment with Thiobacillus ferrooxidans: overall process performance and chemical step. *Chemical Engineering Technology*, 19: 79-88.
48. Heijnen J.J. (1999). *Bioenergetics of microbial growth*. pp. 267-290. In M.C. Flickinger and S.W. Drew, Eds., *Bioprocess Technology; Fermentation Biocatalysis and Bioseparation*. New York: Wiley
49. Orhon, D., and N. Artan (1994). *Modeling of Activated Sludge Systems*. pp. 101-110. Lancaster, PA, Technomic.
50. Rittmann, B.E., and P.L. McCarty (2001) *Environmental Biotechnology: Principles and Applications*. pp. 130-172. McGraw-Hill, New York, USA.
51. Tchobanoglous, G., F. L. Burton, and H. D. Stensel (2003) *Wastewater Engineering, Treatment and Reuse*. 4th ed. pp. 571-579. Metcalf & Eddy, Inc. Mc Graw-Hill Companies, NY, USA.
52. Joback, K.G. and R.C. Reid (1987) *Estimation of Pure-Component Properties from Group-Contributions*, *Chem. Eng. Common*, 57:233–243.
53. Anderson, G.M. (2005). *Thermodynamics of Natural Systems*. 2nd ed., pp. 91-100. Cambridge University Press, New York, USA.



Universidad de Valladolid

CHAPTER 5

**Anoxic Denitrification of BTEX: Biodegradation
Kinetics and Pollutant Interactions**

Anoxic denitrification of BTEX: Biodegradation kinetics and pollutant interactions

Andrea Carvajal ^{a,b}, Ilker Akmirza ^{a,c}, Daniel Navia ^b, Rebeca Pérez ^a, Raúl Muñoz ^a, Raquel Lebrero ^{a,*}

^a Department of Chemical Engineering and Environmental Technology, University of Valladolid, Dr. Mergelina s/n, 47011, Valladolid, Spain

^b Departamento de Ingeniería Química y Ambiental, Universidad Técnica Federico Santa María, Av. España, 1680, Valparaíso, Chile

^c Department of Environmental Engineering, Technical University of Istanbul, 34469 Istanbul, Turkey

JOURNAL OF ENVIRONMENTAL MANAGEMENT

ARTICLE INFO

Article history:

Received 8 November 2017

Received in revised form

2 February 2018

Accepted 5 February 2018

Keywords:

Anoxic denitrification

Biodegradation kinetics

BTEX biodegradation

Mathematical modelling

ABSTRACT

Anoxic mineralization of BTEX represents a promising alternative for their abatement from O₂-deprived emissions. However, the kinetics of anoxic BTEX biodegradation and the interactions underlying the treatment of BTEX mixtures are still unknown. An activated sludge inoculum was used for the anoxic abatement of single, dual and quaternary BTEX mixtures, being acclimated prior performing the biodegradation kinetic tests. The Monod model and a Modified Gompertz model were then used for the estimation of the biodegradation kinetic parameters. Results showed that both toluene and ethylbenzene are readily biodegradable under anoxic conditions, whereas the accumulation of toxic metabolites resulted in partial xylene and benzene degradation when present both as single components or in mixtures. Moreover, the supplementation of an additional pollutant always resulted in an inhibitory competition, with xylene inducing the highest degree of inhibition. The Modified Gompertz model provided an accurate fitting for the experimental data for single and dual substrate experiments, satisfactorily representing the antagonistic pollutant interactions. Finally, microbial analysis suggested that the degradation of the most biodegradable compounds required a lower microbial specialization and diversity, while the presence of the recalcitrant compounds resulted in the selection of a specific group of microorganisms.

© 2018 Elsevier Ltd. All rights reserved.

1. Introduction

Benzene, toluene, ethylbenzene and xylene (BTEX) are volatile organic compounds (VOCs) commonly used in petrochemical industry and in many industrial sectors as reagents for the synthesis of multiple C-based products (e.g. plastics, synthetic fibers, pesticides) (El-Naas et al., 2014; Mazzeo et al., 2010). The extensive use of BTEX is often criticized due to their hazardous effects on the environment and to human health (Morlett-Chávez et al., 2010): they have genotoxic properties, human exposure to BTEX-laden emissions can cause central nervous system depression and negative effects on the respiratory system (Rahul and Balomajumder, 2013), and benzene has been classified within Group A-known human carcinogens of medium carcinogenic hazard by US EPA (United States Environmental Protection Agency).

Due to the detrimental effects of BTEX on both the environment and human health, there is an urgent need to develop cost-efficient treatment technologies able to minimize or abate the emissions of these gas pollutants (El-Naas et al., 2014). In this sense, biological techniques are preferred over traditional physicochemical processes such as absorption, adsorption or combustion, due to their lower operating costs and their environmentally-friendly nature (Estrada et al., 2011; Trigueros et al., 2010). Aerobic BTEX biodegradation has been successfully achieved in different bioreactor configurations such as biofilters (Leili et al., 2017; Singh et al., 2010), biotrickling filters (Chen et al., 2010) or airlifts (Lebrero et al., 2016). However, most VOC emissions from the petrochemical industry are characterized by their O₂-free nature, BTEX accounting for up to 59% (w/w) of gasoline pollutants and representing ≈80% of the total VOC emissions in petrochemical plants (Barona et al., 2007; El-Naas et al., 2014). The absence of oxygen in these off-gas streams limits the implementation of conventional biotechnologies as end-of-pipe abatement methods (Muñoz et al., 2013).

* Corresponding author.

E-mail address: raquel.lebrero@iq.uva.es (R. Lebrero).

Notation list	
<i>Abbreviation</i>	
BTEX	Benzene-toluene-ethylbenzene-xylene (-)
C_0	Initial pollutant concentration (mg m^{-3})
C_i	Pollutant concentration at time i (mg m^{-3})
D	Cumulative degradation (-)
D_{max}	Maximum degradation potential (mg mg^{-1})
DGGE	Denaturing gradient gel electrophoresis (-)
GC-TCD	Gas Chromatography with Thermal Conductivity Detector (-)
GC-FID	Gas Chromatography with Flame Ionization Detector (-)
H	Shannon-Wiener diversity index (-)
HPLC-IC	High performance liquid chromatography-Ion Chromatography (-)
K_i	Inhibition parameter (mg m^{-3})
K_S	Half-velocity parameter (mg m^{-3})
MSM	Mineral salt medium (-)
P	Cumulative production (mg m^{-3})
P_{max}	Maximum cumulative production (mg m^{-3})
PCR	Polymerase chain reaction (-)
R_m	Maximum rate of production ($\text{mg mg}^{-1} \text{s}^{-1}$)
S	Concentration of the limiting growth substrate (mg m^{-3})
T	Time (s)
t_{∞}	End time (negligible variation of pollutant concentration) (s)
VOC	Volatile organic compounds (-)
VSS	Volatile suspended solids (kg m^{-3})
X	Total biomass concentration (mg m^{-3})
Y_{XS}	Biomass yield coefficient (mg mg^{-1})
μ_{max}	Maximum specific growth rate (s^{-1})
λ	Lag-phase (s)

This requires the engineering of alternative biotechnologies able to use an electron acceptor other than O_2 during pollutant oxidation. In this sense, anoxic BTEX mineralization via $\text{NO}_3^-/\text{NO}_2^-$ denitrification represents a promising platform for the removal of these pollutants from O_2^- deprived emissions. However, the number of studies devoted to anoxic BTEX removal is still scarce and little is known about the kinetics underlying BTEX biodegradation, which is central for an optimum bioreactor design (Annesini et al., 2014). Moreover, whereas most previous studies have focused on the aerobic biodegradation of individual BTEX compounds (either benzene, toluene or xylene alone), and their metabolic pathways for aerobic degradation have been fully elucidated (El-Naas et al., 2014; Oh et al., 1994), substrate interactions such as competition, inhibition and co-metabolism during BTEX mixture treatment can modify the biodegradation kinetics, thus resulting in the enhancement or inhibition of BTEX biodegradation (Deeb and Alvarez-Cohen, 1999; Littlejohns and Daugulis, 2008). Culture enrichment aiming at isolating and identifying specific degrading species is usually performed before kinetic assays. However, the experimental conditions selected for the enrichment process commonly differ from those used in real treatment systems, thus the results obtained in the kinetic assays are not an accurate representation of the treatment process (Dou et al., 2008; Jiang et al., 2015). Therefore, it is important to set similar conditions for both acclimation and kinetic tests in terms of pollutant concentration in the headspace, temperature and source of inoculum.

This work aimed at evaluating the biodegradation of BTEX by acclimated microbial communities under anoxic conditions

when BTEX were present as single substrates and as dual/quaternary mixtures. Moreover, the biodegradation kinetic parameters of single, dual and quaternary BTEX mixtures are estimated for the first time using two mathematical models: Monod model and a Modified Gompertz model. In addition, the influence of the type of BTEX compound or BTEX mixture on the structure of the microbial community was also assessed.

2. Materials and methods

2.1. Inoculum

Activated sludge from the anoxic denitrification tank of the urban wastewater treatment plant (WWTP) of Valladolid (Spain) was used as inoculum. One sample of the fresh sludge was stored at 253 K for microbial characterization.

2.2. Chemicals and mineral salt medium

All chemicals for mineral salt medium (MSM) preparation were purchased from PANREAC (Barcelona, Spain) with at least 99% purity. Benzene, toluene, ethylbenzene and o-xylene (99.0% purity) were obtained from SigmaAldrich (Madrid, Spain). The MSM was composed of (kg m^{-3}): $\text{Na}_2\text{HPO}_4 \cdot 12\text{H}_2\text{O}$, 6.15; KH_2PO_4 , 1.52; $\text{MgSO}_4 \cdot 7\text{H}_2\text{O}$, 0.2; CaCl_2 , 0.038; and 10 mL L^{-1} of a trace element solution containing (kg m^{-3}): EDTA, 0.5; $\text{FeSO}_4 \cdot 7\text{H}_2\text{O}$, 0.2; $\text{ZnSO}_4 \cdot 7\text{H}_2\text{O}$, 0.01; $\text{MnCl}_2 \cdot 4\text{H}_2\text{O}$, 0.003; H_3BO_3 , 0.03; $\text{CoCl}_2 \cdot 6\text{H}_2\text{O}$, 0.02; $\text{CuCl}_2 \cdot 2\text{H}_2\text{O}$, 0.001; $\text{NiCl}_2 \cdot 6\text{H}_2\text{O}$, 0.002; $\text{NaMoO}_4 \cdot 2\text{H}_2\text{O}$, 0.003 (Muñoz et al., 2013). The final pH of the MSM was 7. Nitrate (NO_3^-) (supplemented as NaNO_3) was used as the electron acceptor for BTEX oxidation and as the nitrogen source for microbial growth.

2.3. Experimental procedure

Air-tight bottles of 1.1 L with 100mL of MSM were inoculated with 5mL of the inoculum to a final concentration of $\sim 200\text{mg L}^{-1}$ of volatile suspended solids (VSS). Two additional bottles containing acidified MSM (pH = 2) to prevent any biological activity and without inoculum were used as controls to rule out any potential abiotic BTEX loss. The assays were performed under continuous agitation at 320 rpm by magnetic stirring and at constant ambient temperature of 298 K in a thermostatic room. After inoculation, the bottles were closed with rubber stoppers and sealed with plastic caps. The headspace of the bottles was purged with N_2 (Abello Linde, Spain, purity $>99.999\%$) for at least 10 min, in order to remove all the oxygen present in the initial air atmosphere (the time required to reach anoxic conditions was previously set by GCTCD analysis of the headspace composition). Single, dual and quaternary BTEX combinations were prepared in duplicate in order to study the degradation of these pollutants individually (4 experimental conditions), as dual mixtures (6 experimental conditions) and in the presence of the four BTEX simultaneously (1 experimental condition) (Littlejohns and Daugulis, 2008). The quaternary mixture was also added to the control bottles containing the acidified MSM. Each BTEX was supplemented individually to the corresponding bottle in liquid form with a precision syringe. The syringe was kept during 3 min after injection in the bottle headspace in order to ensure complete volatilization. The dosing procedure was always performed in a laboratory fume hood. The BTEX concentration achieved in the headspace (Table 1) corresponded to the typical VOC concentrations found in biological waste gas treatment (ranging between 300 and 700 mg m^{-3}) and in passive emissions from gasoline ($\sim 200 \mu\text{g m}^{-3}$) (Barona et al., 2007; Khan et al., 2018).

2.4. Culture enrichment assays

At the beginning of the acclimation period, the corresponding BTEX were added to the bottles headspace to the initial concentration of each assay (Table 1). Afterwards, samples were daily taken from the headspace using a gas-tight syringe (Hamilton, USA) and BTEX concentration was analysed by GC-FID. One cycle was considered completed when BTEX

concentration in the headspace was completely depleted. In those bottles where the degradation stopped before complete pollutant depletion (presumably due to the accumulation of toxic intermediate metabolites), 30% of the cultivation broth was renewed by biomass centrifugation and resuspension in fresh MSM, in order to promote the biodegradation of the remaining pollutant. At the end of each degradation cycle, the BTEX content was replenished by adding to the bottles the pertaining quantity of each compound to restore the initial concentration (Fig. 1).

Additionally, 30% of the cultivation broth was weekly exchanged with fresh MSM to provide sufficient nutrients for microbial growth. The biomass in the cultivation broth extracted was returned to the system by centrifugation and resuspension in the fresh MSM. Therefore, during the acclimation period, the bottles operated as fed-batch reactors with a hydraulic retention time of ~ 23 d and 100% of biomass retention.

Finally, NO_3^- was supplemented to the bottles from a 10 g L^{-1} NaNO_3 stock solution every two weeks to prevent NO_3^- limitation. The amount of the stock solution supplied was always twice the theoretical value required for total pollutant degradation. Prior NO_3^- supplementation, liquid samples were taken for nitrate analysis by HPLC-IC.

Five biodegradation cycles were completed under each experimental condition using BTEX as a single carbon and energy source before the comparative kinetic assays were performed.

2.5. Kinetic assays

After the fifth biodegradation cycle of the acclimation period, kinetic assays were carried out for each experimental condition studied. Before pollutant injection, 30% of the cultivation broth was exchanged with fresh sterile MSM and supplemented with NaNO_3 to guarantee sufficient nutrients and nitrate during the test, the biomass being recovered and returned to the bottle. Then, the specific compound or mixture were added to the bottle headspace (Fig. 1). The BTEX concentration in the headspace was measured every 40 min until complete BTEX depletion or until BTEX biodegradation stopped. After the kinetic assays, liquid samples were taken for VSS and NO_3^- quantification and for molecular analyses.

Samples for molecular analyses were immediately stored at 253 K.

2.6. Analytical and microbiological procedure

BTEX concentration in the bottles headspace was analysed by using a Bruker 3900 gas chromatograph (Palo Alto, USA) equipped with a flame ionization detector (GC-FID) and a Supelco Wax (15m × 0.25mm × 0.25 μm) capillary column. Samples of 100 μL were taken using a gas-tight syringe (Hamilton, USA). The oven temperature was initially maintained at 323 K for 60 s, increased at 0.83 K s⁻¹ up to 343 K and then at 1.1 K s⁻¹ to a final temperature of 413 K (Akmirza et al., 2017).

The concentration of total and volatile suspended solids (TSS and VSS) was quantified according to the Standard Methods Guideline for the Examination of Water and Wastewater (AWWA, 2012). Nitrite and nitrate concentrations in the liquid phase were analysed via HPLC-IC using a Waters 515 pump coupled with a conductivity detector (Waters 432) and equipped with an IC-Pak Anion HC column (4.6 × 150 mm) and an IC-Pak Anion Guard-Pak (Waters). Samples were eluted isocratically at 2mL min⁻¹ (at room temperature) with a mobile phase composed of distilled water/acetonitrile/n-butanol/buffer at 84/12/2/2% v/v (the buffer solution consisted of (kg m⁻³): C₆H₁₁NaO₇, 16; Na₂B₄O₇.10H₂O, 25; H₃BO₃, 18; and 250 mL L⁻¹ of glycerol) (Muñoz et al., 2013).

The bacterial community established in the samples was characterized by denaturing gradient gel electrophoresis (DGGE) analysis. Samples were stored at 253 K. The V6-V8 regions of the bacterial 16SrRNA genes were amplified by Polymerase Chain Reaction (PCR) using the universal bacterial primers 968-F-GC and 1401-R (SigmaAldrich, St. Louis, MO, USA). The analysis was carried out according to Lebrero et al. (2012). The DGGE analysis of the amplicons was performed with a D-Code Universal Mutation Detection System (Bio Rad Laboratories) using 8% (w/v) polyacrylamide gels with a urea/formamide denaturing gradient of 45-65%. DGGE running conditions were applied according to Roest et al. (2005). The desired DGGE bands were excised from the DGGE gel in order to elucidate the bacterial composition of each sample. The procedure was previously described in Lebrero et al. (2012).

The DGGE profiles were processed by GelCompar IITM software (Applied Maths BVBA, Sint-Martens-Latem, Belgium). The Shannon-Wiener diversity index (H) was determined according to the expression:

$H = -\sum [P_i \ln(P_i)]$, where P_i is the importance probability of the bands in a lane, and is calculated as n_i/n , where n_i is the height of an individual peak, and n the sum of all peak heights in the densitometric curves of the DGGE profile. Therefore, this index reflects both the sample richness (relative number of DGGE bands) and evenness (relative intensity of every band). According to McDonald (2003), it ranges from 1.5 to 3.5 (low and high species evenness and richness, respectively).

Similarity indices of the compared profiles were calculated from the densitometric curves of the scanned DGGE profiles by using the Pearson product-moment correlation coefficient (H€ane et al., 1993). The taxonomic position of the sequenced DGGE bands was obtained by the RDP (Ribosomal Database Project) classifier tool at a confidence level of 50% (Wang et al., 2007). Moreover, the closest matches to every band were obtained from the Blast search tool at the National Centre for Biotechnology Information (McGinnis and Madden, 2004). The sequences were deposited in the GenBank database under accession numbers KU991963-KU991989.

2.7. Kinetic modelling

Among the mathematical models used to describe microbial growth and pollutant biodegradation kinetics under different environmental conditions, the Monod model offers a suitable approach of the batch growth mode, especially when describing the biodegradation of a single substrate (Equation (1)) (Blok, 1994; Dette et al., 2005):

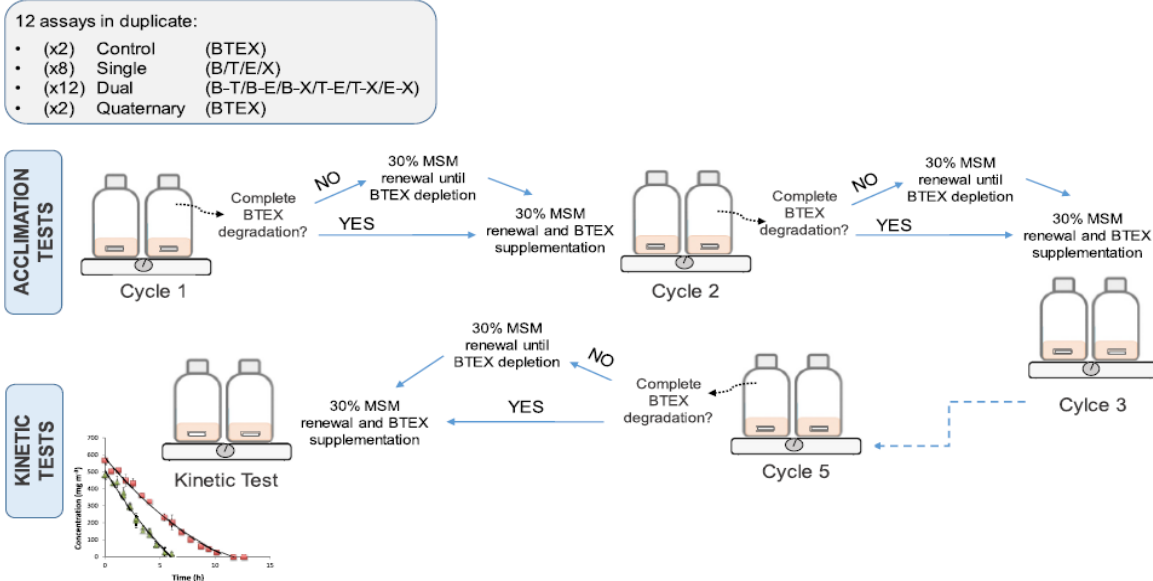
$$\mu = \frac{\mu_{max}S}{K_S+S} \quad (1)$$

where m stands for the specific growth rate, m_{max} for the maximum specific growth rate, S for the concentration of the limiting growth substrate and K_S represents the half-velocity constant. Moreover, this model is commonly

Table 1

Initial BTEX concentration in the batch tests and duration of the acclimation period for each experimental condition (T -toluene; E-ethylbenzene; X-xylene; B-benzene).

Experiment		Concentration (mg m ⁻³)				Acclimation period (d)
		Benzene	Toluene	Ethylbenzene	Xylene	
1	B	465 ± 33				76
2	T		564 ± 77			29
3	E			533 ± 40		27
4	X				564 ± 100	115
5	B-T	560 ± 50.2	557 ± 16.7			79
6	B-E	495 ± 57		584 ± 79		104
7	B-X	479 ± 128			511 ± 88	154
8	T-E		499 ± 33	505 ± 38		21
9	T-X		439 ± 36.7		440 ± 28	91
10	E-X			560 ± 56	552 ± 40	107
11	B-T-E-X	522 ± 50	541 ± 57	600 ± 115	553 ± 34	146
12	Control	466 ± 21	515 ± 10	543 ± 12	490 ± 30	–

**Fig 1.** Schematic flowchart of the experimental procedure

used to represent biomass growth rate according to the following mass balance (X standing for the total biomass concentration) (Equation (2)):

$$\frac{dX}{dt} = \mu X \quad (2)$$

In addition, it is also possible to describe the time course of the substrate concentration (S) during batch pollutant degradation (Equation (3)):

$$\frac{-dS}{dt} = \frac{\mu X}{Y_{XS}} \quad (3)$$

where Y_{XS} is the biomass yield coefficient. It should be noted that Y_{XS} accounts for the consumption of gas and dissolved pollutants in batch systems, assuming a non-limiting gas-liquid mass transfer due to the high volatility of BTEX.

In this context, the Monod model accurately estimates the kinetic parameters (μ_{max} and K_S)

for single substrate biodegradation processes where no lag phase exists. Nevertheless, the presence of multiple substrates can increase the uncertainty during the modelling of substrate degradation due to substrate interactions. Thus, a modified Monod model may provide a better fit to experimental data by including an inhibition constant (K_I) as in Andrews model (Equation (4)):

$$\mu = \frac{\mu_{max} S}{K_S + S + S^2/K_I} \quad (4)$$

Conversely, several non-linear regression models have been proposed to describe only microbial growth without including the consumption of the substrate (Zwietering et al., 1990; Whiting, 1995). For instance, the Modified Gompertz Kinetic model (Equation (5)) will provide the cumulative production (P) as a function of time, and may offer a better fit to experimental data in systems with more than one substrate:

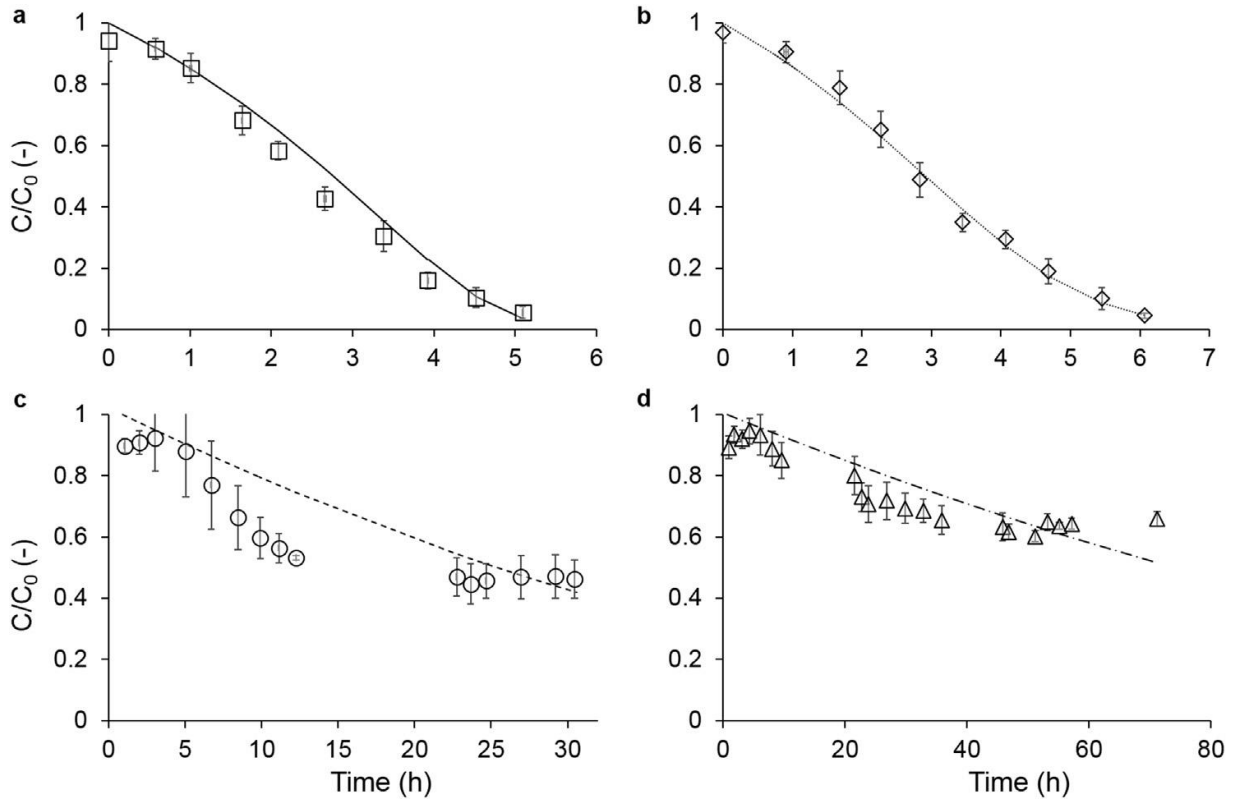


Fig. 2. Time course of the relative concentration (C/C_0) of (a) Toluene (\square), (b) Ethylbenzene (\diamond), (c) Xylene (\circ) and Benzene (\blacktriangle). Symbols represent experimental data, while the lines represent the Monod model fitting. Vertical lines represent the standard deviation between duplicates of the same experimental condition.

$$P(t) = P_{max} \exp\left(-\exp\left(\frac{R_m}{D_{max}}(\lambda - t) + 1\right)\right) \quad (5)$$

where P_{max} represents the maximum production, R_m the maximum rate of production, t the elapsed time and λ the lag-phase, which cannot be predicted with the Monod model. By using the Modified Gompertz Kinetic model, substrate consumption can be described as a degradation potential using Equation (6). In our particular context, the new variables used are the cumulative degradation (D) and the maximum degradation potential (D_{max}).

$$D(t) = D_{max} \exp\left(-\exp\left(\frac{R_m}{D_{max}}(\lambda - t) + 1\right)\right) \quad (6)$$

2.8. Data analysis

With the objective of estimating the kinetic parameters of the models used, a nonlinear curve fitting was performed for each data set. In the particular case of Monod model (Equation (1)), substrate concentration versus time was fitted using the numerically integrated substrate mass balance (Equation (3)). For the Modified Gompertz model (Equation (5)), the degradation (D) versus time data set was

directly fitted ($D(t)$ calculated as in Equation (7), with C_0 being the initial concentration of the pollutant and C_i the concentration as a function of time). In both cases the initial values of the parameters were estimated visually and constrained to values higher than 0.

$$D(t) = \frac{(c_0 - c_i)}{c_0} \quad (7)$$

The Solver tool of the Excel Software[®] was used for parameter determination using the GRG Nonlinear resolution method. The square of sum of residuals (RSS) between experimental and calculated data was minimized in the optimization process. The adequacy of the calculated parameters was confirmed by: 1) plotting residual vs. predicted data, and 2) calculating the R^2 value (Equation (8)).

$$R^2 = 1 - \frac{S^2(D_{exp})}{S^2(residuals)} \quad (8)$$

Finally, the estimated parameters using Andrews model (Equation (4)) did not improve the fitting obtained with the Monod and the Modified Gompertz models, thus the results are not presented in the manuscript.

For statistical comparison purposes, the 95% confidence bounds of each calculated parameter were determined using the `nlparci` function of Matlab Software[®].

3. Results and discussion

3.1. Kinetics of individual BTEX biodegradation

After the 5th pollutant amendment acclimation period (lasting 29, 27, 76 and 115 d for toluene, ethyl-benzene, benzene and xylene, respectively), kinetic assays were performed obtaining characteristic substrate degradation profiles for individual substrates (Fig. 2).

Table 2

Kinetic parameters for single compound degradation tests (T - toluene; E - ethylbenzene; X - xylene; B - benzene; K_S - half velocity parameter; μ_{max} - maximum specific growth rate; Y_{XS} - biomass yield coefficient; D_{max} - maximum degradation potential; R_m - maximum roduction rate; λ - lag-phase).

	T	E	B	X
Monod Model				
K_S (mg m ⁻³)	73	268	634	491
μ_{max} (h ⁻¹)	0.318	0.473	0.001	0.001
Y_{XS} (mg mg ⁻¹)	1.000	1.000	0.006	0.001
R^2	0.972	0.979	0.763	0.825
Gompertz Model				
D_{max} (mg mg ⁻¹)	1.000	1.000	0.329	0.496
R_m (mg mg ⁻¹ h ⁻¹)	0.812	0.697	0.035	0.187
λ (h)	0.907	0.949	7.021	4.313
R^2	0.984	0.983	0.908	0.910

E and T were rapidly and completely metabolized when present as single carbon and energy sources, their degradation being characterized by μ_{max} values of 0.473 h⁻¹ and 0.318 h⁻¹, respectively, and elapsed biodegradation periods (t_{∞} , corresponding to the time by which negligible variation in the contaminant concentration was detected) of 5 and 6 h for T and E, respectively (Fig. 2a and b and Tables 2 and S1). These results, also observed during the acclimation period, confirmed that those pollutants were the most readily biodegradable under anoxic conditions among the aromatic compounds tested. Toluene and ethyl-benzene have been also confirmed as readily biodegradable under aerobic conditions when present as the sole carbon and energy source, with μ_{max} values reported in literature within the same order of magnitude to those obtained in the present study (a summary of the μ_{max} values obtained in previous studies is presented in Table 3).

On the other hand, B and X were not totally metabolized by the consortium despite the long acclimation time provided; in fact, several MSM replacements were required for complete depletion during the acclimation period. In this context, the concentration of B decreased by 34 ± 9% within the first 11 h when fed as the sole carbon and energy source (B concentration stabilizing afterwards), while X reached a maximum removal of 49 ± 4% within the first 24 h (Fig. 1c and d). The inhibition of both X and B biodegradation was attributed to the accumulation of toxic intermediates in the liquid cultivation media, similar to the pattern observed during the acclimation cycles. This entailed low μ_{max} values and high t_{∞} , which accounted for 0.001 h⁻¹ and 30 h for X and 0.001 h⁻¹ and 70 h for B, respectively. The high recalcitrance of both X and B has been also reported under aerobic conditions, where X and B are typically the least biodegradable BTEX compounds or even non-biodegradable by indigenous microorganisms under oxygen-limited conditions (Shim and Yang, 1999; Trigueros et al., 2010). However, μ_{max} up to two orders of magnitude higher than those found in this study for B have been observed under aerobic conditions in both pure cultures and bacterial consortia. On the contrary, the μ_{max} values reported in literature for xylene degradation by pure cultures were similar or even lower, and some studies have described the inability of some bacterial consortia to metabolize X when present as the sole carbon and energy source (Littlejohns and Daugulis, 2008; El-Naas et al., 2014) (Table 3). All these findings are further supported by the K_S values predicted by the Monod model, which confirmed the higher affinity of the culture for T than for the other compounds (Table 2). It is worth noting that the half-saturations constants observed in this study are considerably lower than those typically observed under aerobic conditions, likely due to the low BTEX concentrations prevailing in the aqueous phase during culture enrichments. In accordance with the two different behaviours observed, further confirmed by the statistical comparison of the kinetic parameter confidence intervals (Table S1), a different accuracy of model fitting was obtained. In this context, the Monod model showed a good data description for T and E, with R^2 of ~0.97. On the contrary, the R^2 obtained for X and B was 0.825 and 0.763, respectively, which indicates that this model

was not able to describe the biodegradation kinetics of these single substrates. This lower accuracy was correlated with the duration of the lag phase (B and X presented lag phases of 7.0 and 4.3 h, respectively, while T and E exhibited a lag phase <1 h, as estimated by the Gompertz Model) (Table 2). In this context, some authors pointed out that the lag phase should be excluded during Monod model fitting (Littlejohns and Daugulis, 2008), while others fitted the model only to the post lag phase data (Strigul et al., 2009). Moreover, Ellis et al. (1996) demonstrated that the Monod model provides an accurate fit of the experimental data under anaerobic conditions when the S_0/K_S ratio is >1 . This finding is also valid in our particular study, as this ratio is clearly higher for T (>3) and E (~ 1.5), while S_0/K_S values near 1 were observed for X and B.

As previously mentioned, the fitting obtained for the biodegradation of B and X with Andrews model did not improve the results obtained with

the Monod model. This suggested that the degradation of single substrates was not inhibited by BTEX concentration over the range of initial substrate concentrations studied ($\sim 450\text{-}600\text{ mg m}^{-3}$), and confirmed the hypothesis of microbial inhibition derived from a build-up of intermediates. Other inhibition models could have been studied, but the identification and quantification of the specific inhibitory compound along with the understanding of the effect of the lag phase are necessary for a correct kinetic parameter determination, and these particular issues were out of the scope of this study. Unfortunately, the information available in literature on anoxic BTEX degradation does not provide enough data about the intermediate metabolites that could be responsible for the inhibition of the process, in contrast with the information available for BTEX degradation under aerobic or anaerobic conditions (Vogt et al., 2011; Weelink et al., 2010).

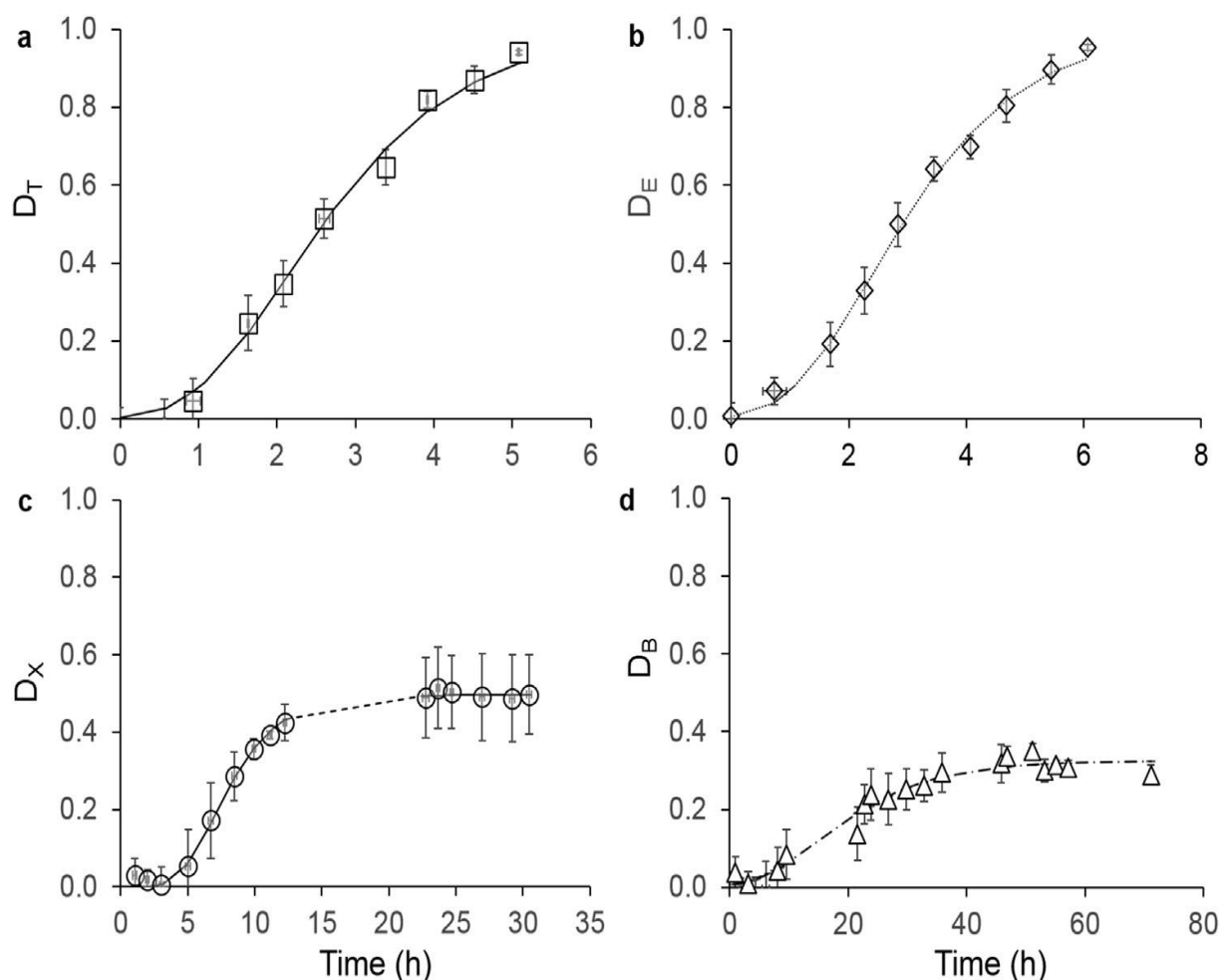


Fig. 3. Time course of the cumulative degradation of (a) Toluene (□), (b) Ethylbenzene (◇ ◊◊), (c) Xylene (○ ----) and Benzene (▲ ◦). Symbols represent experimental data, while the lines represent the Gompertz Model fitting. Vertical lines represent the standard deviation between duplicates of the same experimental condition.

Table 3

Summary of μ_{\max} values reported in previous literature studies (T - toluene; E - ethylbenzene; X - xylene; B- benzene; μ_{\max} - maximum specific growth rate).

μ_{\max} (h^{-1})				Inoculum source	Model	Experimental conditions	Reference
B	T	E	X				
0.3	0.33	0.27	0.24	<i>P. putida</i> F1	Monod	Aerobic	Trigueros et al., 2010
0.44	0.6	0.13	^a	7 species of <i>Pseudomonas</i>	Monod	Aerobic	Littlejohns and Daugulis, 2008
0.135	–	–	–	Aquifer Groundwater	Monod	Aerobic	Corseuil et al., 2015
0.05	–	–	–	Aquifer Groundwater	Monod	Sulfate Reducing	Corseuil et al., 2015
0.012	–	–	–	Aquifer Groundwater	Monod	Methanogenic	Corseuil et al., 2015
0.5	0.58	–	^a	<i>P. putida</i> F1	Monod	Aerobic	Robledo-Ortiz et al., 2011
0.161	0.172	–	–	<i>P. putida</i> F1	Monod	Aerobic	Mathur and Majumder, 2010
0.16	0.26	–	0.13	–	Monod	Aerobic	Goldsmith and Balderson, 1988
0.041	0.037	0.035	0.016	<i>P. putida</i> and <i>P. fluorescens</i>	Monod	Aerobic	Shim et al., 2005
0.22	0.46	0.26	0.19	<i>P. putida</i> F1	Andrews	Aerobic	Trigueros et al., 2010
0.62	0.61	–	–	<i>P. putida</i> F1	Andrews	Aerobic	Abuhamed et al., 2004
0.363	0.300	–	–	<i>P. putida</i> F1	Linearized-Haldane's	Aerobic	Mathur and Majumder, 2010
0.019	0.006	0.034	0.006	<i>P. aeruginosa</i>	Haldane model	Aerobic	Chi-Wen et al., 2007
0.41	0.42	0.45	0.05	<i>P. putida</i> F1	SKIP	Aerobic	Trigueros et al., 2010

^a Incomplete biodegradation.

In order to overcome the uncertainty observed using the Monod model, the Modified Gompertz model was used for the calculation of the anoxic biodegradation kinetic parameters with and without inhibition. This model allows describing the lag phase, thus providing an accurate fitting for all the BTEX (Fig. 3). The parameters obtained using the Modified Gompertz model confirmed the complete degradation of both T and E ($\mu_{\max} \approx 100\%$) with a limited lag phase (<1 h) at maximum specific degradation rates of 0.812 and 0.697 $\text{mgmg}^{-1} \text{h}^{-1}$ for T and E, respectively (Table 2, Table S1). On the other hand, X and B exhibited λ values of 4.31 and 7.02 h, respectively. Xylene was partially degraded at a specific rate of 0.187 $\text{mgmg}^{-1} \text{h}^{-1}$ (reaching a maximum degradation of ~50%), while the lowest specific degradation rate was estimated for B (0.035 $\text{mgmg}^{-1} \text{h}^{-1}$), with only 33% of this substrate being degraded by the microbial community. Despite the mean square regression ratios obtained for X and B were slightly lower than those calculated for T and E, the degradation kinetics of all BTEX fed as single substrates was satisfactorily described by the Modified Gompertz model ($R^2 > 0.9$), as also confirmed by the statistical analysis (Table S1). The analysis of NO_3^- concentration in the liquid phase confirmed that the assays were never limited by electron acceptor availability. However, NO_3^- consumption rates could not be calculated due to the low BTEX concentrations supplemented in this study, resulting in negligible variations of nitrate concentration in the liquid phase.

3.2. Kinetics of dual BTEX mixtures biodegradation

A detrimental effect on substrate biodegradation was observed regardless of the BTEX combination tested. The goodness of fit of the Monod model for the data recorded in the dual compounds biodegradation tests was similar to that obtained for single substrates. T and E combinations showed a good fitting, although lower R^2 values than those obtained during individual BTEX biodegradation were achieved for mixtures containing X and/or B (Fig. 4, Tables 4 and S2). On the contrary, the dual BTEX mixtures biodegradation assays were well described by the Modified Gompertz model (Fig. 5), except for the degradation of B, which presented a R^2 lower than 0.7 regardless of the mixture (Tables 5 and S3). This result could be explained by the limited biodegradation of this contaminant, with a reduction in its concentration always lower than 26%. On the other hand, Andrews model again failed to properly estimate the kinetic parameters of the dual BTEX mixtures biodegradation. In fact, the values obtained for the inhibition parameter (KI) were very high for the data sets that previously fitted the Monod model, reaching the maximum value allowed by the optimization (fixed as bound). On the contrary, the KI parameters for data sets that provided poor fittings were very low and again similar to the limit fixed as bound. However, it was not possible to improve the fitting of the curves either by increasing the R^2 , reducing the residues or by visual inspection. In this context, previous studies under aerobic conditions have also observed that conventional mathematical models accounting for competitive, non-competitive and uncompetitive inhibition between dual BTEX mixtures do not provide an accurate fit to the experimental data (Littlejohns and Daugulis, 2008).

The supplementation of an additional carbon and energy source always resulted in lower biodegradation rates and an increased biodegradation time compared to the biodegradation of BTEX as individual substrates. For instance, lag phase λ values of ~ 1.4 h were recorded for T and E, and ~ 12 h were required for their complete degradation. Similarly, specific biodegradation rates of 0.518 and 0.220 $\text{mg mg}^{-1} \text{h}^{-1}$ were estimated for T and E, respectively, when degraded together (Table 4). The presence of B decreased the specific T biodegradation rate by a factor of 4 (down to 0.139 $\text{mg mg}^{-1} \text{h}^{-1}$), while B showed a R_m of 0.088 $\text{mg mg}^{-1} \text{h}^{-1}$ and a partial degradation of 19%. The addition of X mediated a similar detrimental effect than that of B on T biodegradation, leading to lower specific degradation rates compared to their individual

degradation (0.102 $\text{mg mg}^{-1} \text{h}^{-1}$ and 0.090 $\text{mg mg}^{-1} \text{h}^{-1}$ for T and X, respectively). Moreover, the highest X degradation was recorded in the presence of T, with a X degradation potential of 41% and T depletion. Surprisingly, less than 0.4 h were necessary in these tests for the start-up of X and B degradation, which were firstly metabolized by the consortia in the presence of T, while T exhibited a lag phase > 2 h. The occurrence of this diauxic effect has been previously reported in BTEX mixtures, resulting in lag phases before the preferential substrate is consumed (El-Naas et al., 2014). Nevertheless, and despite the lower degradation rates recorded for T in the dual batch biodegradation assays due to antagonistic substrate interactions, a complete T degradation was always achieved regardless of the mixture.

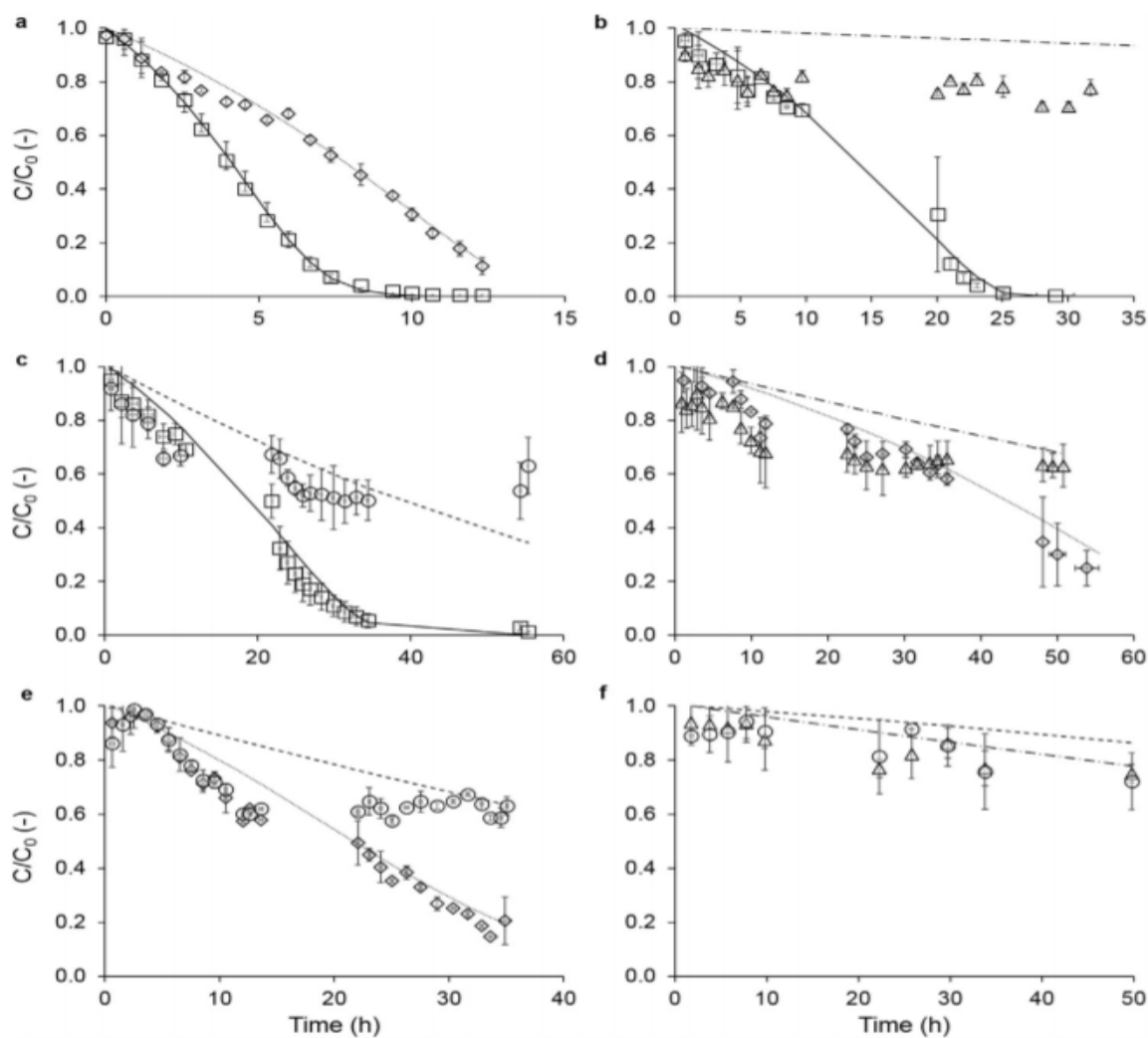


Fig. 4. Time course of the relative concentration (C/C_0) of the dual mixtures (a) T-E, (b) T-B, (c) T-X, (d) E-B, (e) E-X, (f) X-B. Toluene (\square), Ethylbenzene (\diamond \circ), Xylene (\circ $---$) and Benzene (\blacktriangle \circ). Symbols represent experimental data, while the lines represent the Monod model fitting. Vertical lines represent the standard deviation between duplicates of the same experimental condition.

Both X and B induced a detrimental effect on the biodegradation of E. However, while a complete E biodegradation was recorded in the presence of B (specific biodegradation rate of 0.034 mg mg⁻¹ h⁻¹ with a lag phase of 3.70 h), only 92% of E was biodegraded when X was fed as co-substrate at a specific degradation rate 0.079 mg mg⁻¹ h⁻¹ with ~2.3 h of lag phase. A partial degradation was recorded for B (26%) and X (34%) in dual substrate experiments supplemented with E. Finally, the presence of two hardly biodegradable compounds (i.e. B-X mixture) resulted in a negligible biodegradation of both pollutants, with only 15 and 18% of B and X degraded at specific rates of 0.367 and 0.442 mg mg⁻¹ h⁻¹, respectively. The highest lag phases (32.8 h for X and 9.3 h for B) were observed in this B-X assay. Previous studies under both aerobic and anaerobic (Dou et al., 2008) conditions revealed a range of substrate interaction patterns including no interaction, stimulation, competitive inhibition, noncompetitive inhibition (Lin et al., 2007), and cometabolism as a result of the concomitant presence of multiple BTEX compounds (Deeb and Alvarez-Cohen, 1999; Littlejohns and Daugulis, 2008).

Table 4. Kinetics parameters estimated with the Monod model for dual compounds degradation tests (T - toluene; E - ethylbenzene; X - xylene; B - benzene; K_S - half velocity parameter; μ_{max} e maximum specific growth rate; Y_{XS} - biomass yield coefficient)

Mixture	Compound	K _S (mg m ⁻³)	μ _{max} (h ⁻¹)	Y _{XS} (mg g ⁻¹)	R ²
T-E	T	175	0.297	1.000	0.994
	E	56	0.086	0.570	0.987
T-B	T	61	1.328	0.624	0.975
	B	515	0.001	0.004	0.770
T-X	T	79	0.037	0.563	0.977
	X	622	0.001	0.010	0.407
E-B	E	46	0.020	1.000	0.908
	B	451	0.001	0.030	0.578
E-X	E	459	0.079	0.915	0.957
	X	450	0.001	0.018	0.417
B-X	B	436	0.001	0.045	0.682
	X	62	0.008	1.000	0.550

However, the work here conducted showed that the dual combinations of these aromatic compounds under anoxic conditions always resulted in an inhibitory competition for the carbon and energy source, with xylene inducing the highest degree of inhibition among all BTEX. It is also worth-noting the fact that a noncompetitive inhibition model such as the Modified Gompertz model fitted accurately the experimental data for dual substrates experiments, which suggests that microbial inhibition is caused by the inhibitor binding to the enzyme at a site other than the enzyme's active site, as previously observed by Lin et al. (2007). These authors reported that this type of inhibition typically results in a change in the enzyme's active site structure and ultimately in reduced pollutant biodegradation rates, as here observed.

3.3. Kinetics for the quaternary BTEX mixture

When all BTEX were present in the headspace, the lowest specific degradation rates and highest lag phase values were obtained for all the compounds (Fig. 6, Tables 6 and S4). Thus, lag phases ~18 h were recorded for E and T, and more than 4 lower specific biodegradation rates were observed in comparison with single compound assays (0.179 and 0.151 mg mg⁻¹ h⁻¹, respectively). Moreover, and despite E and T reached a high goodness of fit (R² of 0.967 and 0.987, respectively), a poor fitting was obtained when applying the Modified Gompertz model to both B and X (R² as low as 0.154 and 0.468, respectively). The Monod model also failed in representing the biodegradation of these recalcitrant pollutants, as previously observed in the single and dual experiments.

Table 5

Kinetics parameters estimated with Gompertz model for dual compounds degradation tests (T - toluene; E - ethylbenzene; X - xylene; B - benzene; D_{max} - maximum degradation potential; R_m - maximum production rate; λ - lag-phase).

Mixture	Compound	D_{max}	R_m	λ	R^2
T-E	T	1.000	0.518	1.428	0.989
	E	1.000	0.220	1.403	0.957
T-B	T	1.000	0.139	2.287	0.936
	B	0.192	0.088	0.385	0.650
T-X	T	1.000	0.102	2.602	0.976
	X	0.411	0.090	0.352	0.855
E-B	E	1.000	0.034	3.704	0.857
	B	0.262	0.127	6.403	0.696
E-X	E	0.921	0.079	2.257	0.856
	X	0.336	0.170	4.598	0.927
B-X	B	0.156	0.367	9.282	0.570
	X	0.189	0.442	32.761	0.522

* D_{max} mg mg⁻¹ R_m mg g⁻¹h⁻¹ λ h⁻¹

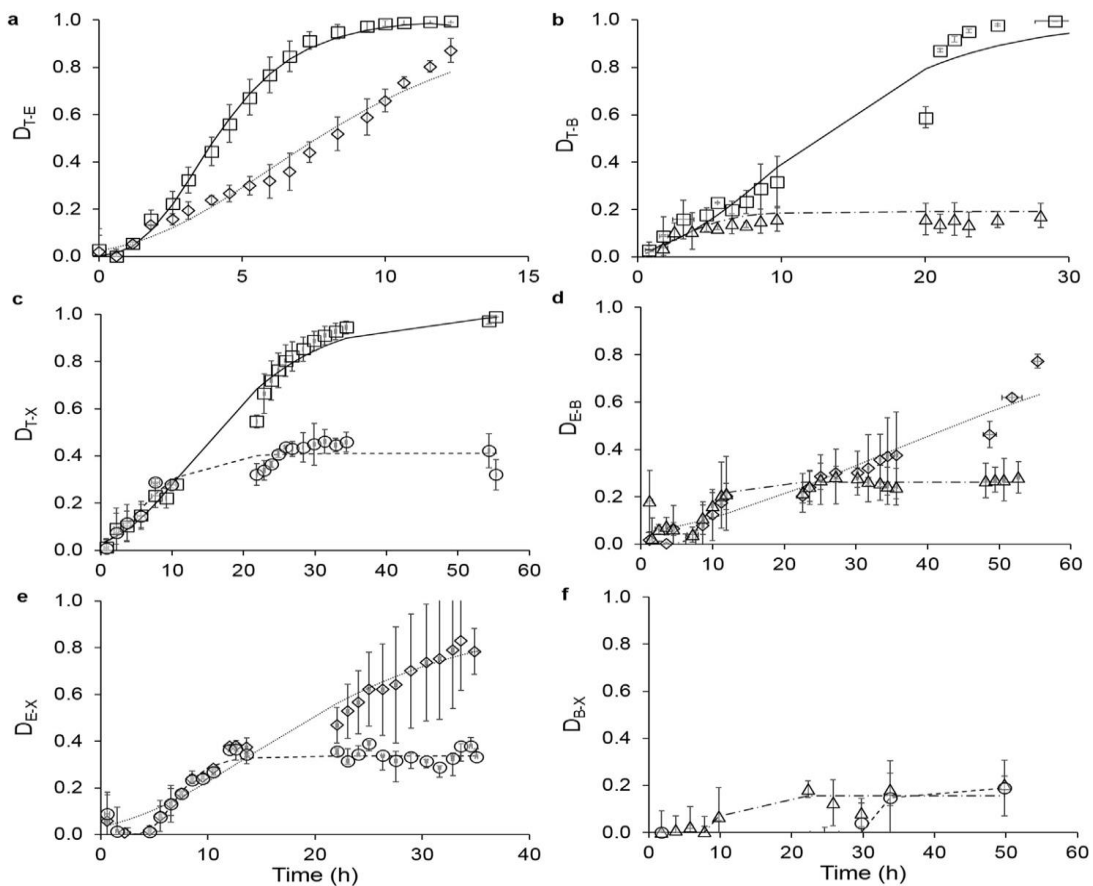


Fig. 5. Time course of the cumulative degradation of (a) T-E, (b) T-B, (c) T-X, (d) E-B, (e) E-X, (f) X-B. Toluene (\square - \rightarrow), (b) Ethylbenzene (\diamond \circ \circ), (c) Xylene (\circ ----) and Benzene (\blacktriangle - \rightarrow \rightarrow) Symbols represent experimental data, while the lines represent the Gompertz Model fitting. Vertical lines represent the standard deviation between duplicates of the same experimental conditions.

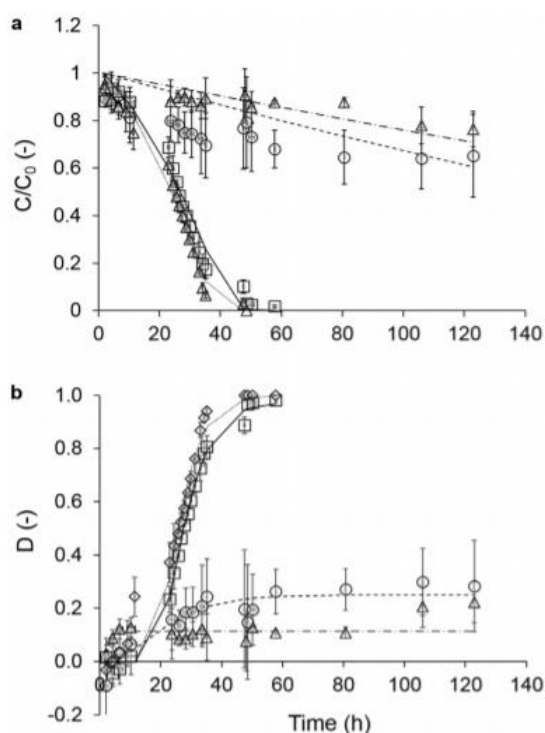


Fig. 6. Time course of (a) the relative concentration (C/C_0) and (b) the cumulative degradation of (a) Toluene (\square), (b) Ethylbenzene (\diamond), (c) Xylene (\circ) and Benzene (\blacktriangle) in the quaternary BTEX mixture. Symbols represent experimental data, while the lines represent the Monod Model (5a) and the Gompertz Model (5b) fitting. Vertical lines represent the standard deviation between duplicates of the same experimental condition.

Table 6

Kinetic parameters of the quaternary BTEX mixture degradation test (T - toluene; E - ethylbenzene; X - xylene; B - benzene; K_s - half velocity parameter; μ_{max} - maximum specific growth rate; Y_{XS} - biomass yield coefficient; D_{max} - maximum degradation potential; R_m - maximum production rate; λ - lag-phase).

	T	E	B	X
Monod Model				
K_s ($mg\ m^{-3}$)	100	100	500	500
μ_{max} (h^{-1})	0.051	0.059	0.001	0.010
Y_{XS} ($mg\ mg^{-1}$)	1.500	1.500	0.075	0.664
R^2	0.970	0.983	0.286	0.737
Gompertz Model				
D_{max} ($mg\ mg^{-1}$)	0.973	1.000	0.114	0.250
R_m ($mg\ mg^{-1}\ h^{-1}$)	0.151	0.179	0.122	0.022
λ (h)	18.490	18.120	1.608	5.718
R^2	0.987	0.967	0.154	0.468

3.4. Molecular analyses

The Shannon-Wiener diversity indexes obtained from the samples studied were significantly different depending on the target compound or mixtures. The data obtained for the community supporting the individual BTEX biodegradation showed a higher diversity for

most recalcitrant compounds, the maximum value being recorded for xylene ($H_B = 3.27$ and $H_X = 3.40$). On the other hand, the indexes calculated for the community growing on the readily biodegradable compounds were lower than expected, the lowest diversity index being recorded for T ($H_E = 2.88$ and $H_T = 2.10$). On the contrary, the diversity indexes obtained for communities treating the dual mixtures ranged from 2.50 for the mixture B-X to 3.29 for the mixture B-E. This indicates that while the individual degradation of B and X mediated a higher diversity in the microbial population, the presence of these recalcitrant compounds in a mixture resulted in low diversity indexes. Finally, the microbial community growing on the quaternary mixture was also characterized by a low index (2.76), probably caused by the antagonistic BTEX interactions in the system. Nevertheless, a relatively high richness was recorded in all the samples. This is in accordance with previous studies reporting that low pollutants concentrations mediate a high biodiversity, which is significantly reduced at higher pollutant concentrations (Estrada et al., 2012; Lebrero et al., 2012).

According to the Pearson's similarity indexes, the community enriched in the B-X mixture showed the lowest similarity with the rest of the samples (for instance, a 29% similarity was obtained with the inoculum and 26 and 36% of similarity was recorded with the B and X communities, respectively) (Figure S1). Overall, the communities enriched in either T or E showed similarities over 90% among them. The analysis of these results, together with those obtained during the biodegradation tests, suggests that the degradation of the most readily biodegradable compounds required both a lower specialization and a lower microbial diversity, as supported by the high degradation rates and similarities and the low diversity values for the community enriched in toluene. On the other hand, the degradation of the mixture B-X also resulted in low diversity values, as above mentioned, while the degradation was rapidly inhibited probably due to metabolites accumulation (with only ~10% of the pollutants degraded). In this particular case, the results were attributed to the selection of a specific group of microorganisms during the acclimation period able to grow on these recalcitrant substrates, which is also in accordance with the low similarity values observed.

From the 27 bands sequenced from the DGGE gel (Fig. 7, Table S5), 14 bands were identified as Proteobacteria, becoming the dominant phylum of this study. In addition, 5 other phyla were identified: Actinobacteria (4 band), Bacteroidetes (2 bands), Firmicutes (1 band), Deinococcus-thermus (1 band) and Verrucomicrobia (1 band). Finally, 3 bands remained as unclassified bacteria.

Species from the Alphaproteobacteria class, retrieved in all samples except in the inoculum, have been described as capable of degrading toluene with nitrate as electron acceptor (Shinoda et al., 2005). Bands 1, 2 and 3 belonged to the Rhodocyclaceae family and Thauera genus, facultative anaerobes, which have been classified as capable of performing autotrophic and heterotrophic denitrification processes, as well as able to degrade petroleum hydrocarbons in hypersaline environments (Evans et al., 1991; Xu et al., 2015). In addition, the genus Schlegelella and the Xanthomonadaceae family recorded in 2 bands

have been associated to denitrification processes (bands 6 and 12), while the genus Zoogloea (bands 4 and 5) has been associated to benzene and BTEX degradation (Weelink et al., 2010; Xu et al., 2015). Finally, the bands classified as Alphaproteobacteria (7, 8 and 9) were also found in a denitrifying process of quinoline removal (Liu et al., 2006). On the other hand, the bands identified into Actinobacteria phylum (15 and 16) have been described in several studies as VOC degraders (Lebrero et al., 2014; Akmirza et al., 2017). Moreover, Actinobacteria and Deinococcus-thermus have been associated to the biodegradation of aliphatic hydrocarbons (Militon et al., 2010). Similarly, the bands identified within the Ignavibacteriae and Firmicutes phyla (bands 23 and 25) were previously identified in samples subjected to anaerobic benzene degradation and anaerobic biodegradation of total petroleum hydrocarbons, respectively (Van der Zaan et al., 2012; Zhang and Lo, 2015).

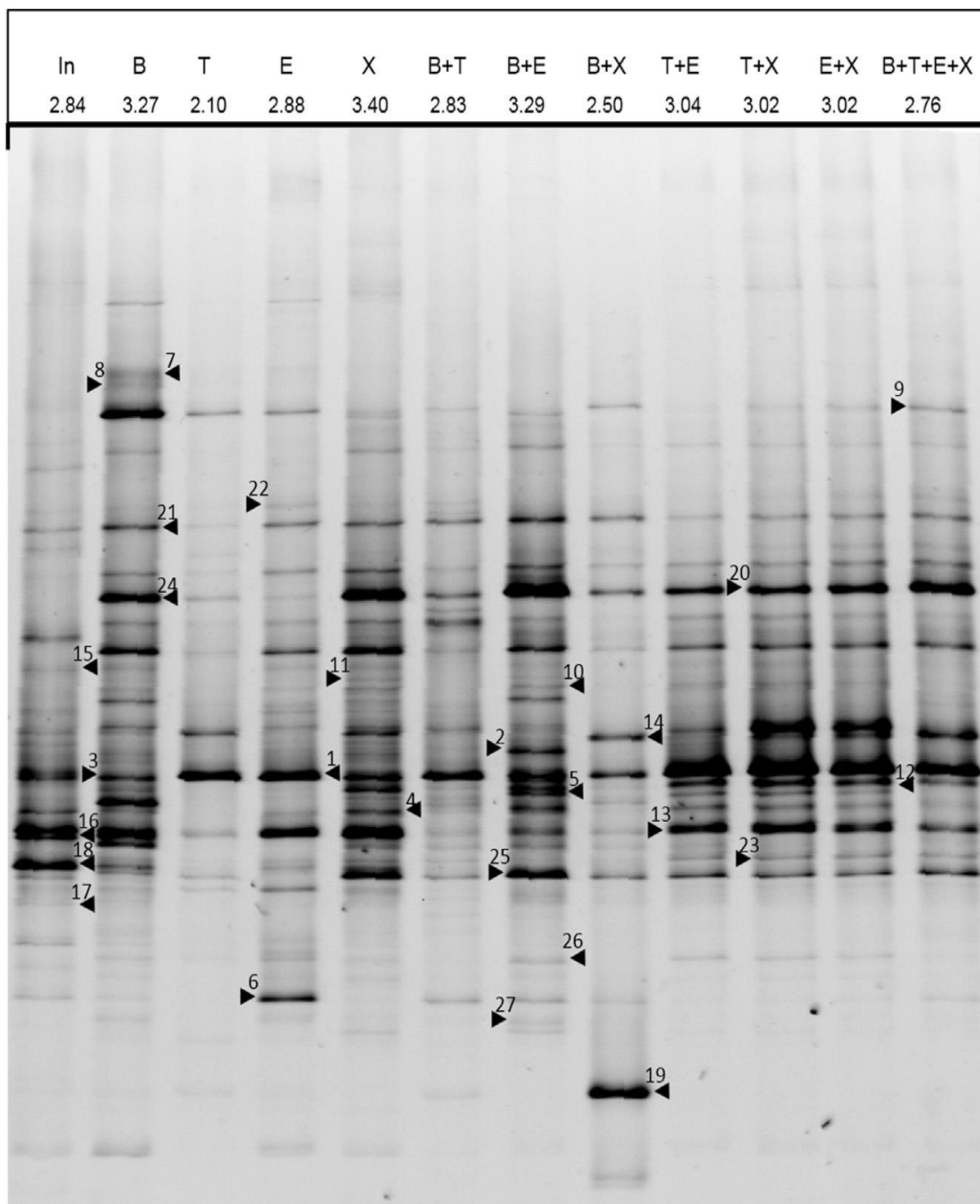


Fig. 7. DGGE profile of the main bacterial communities (In - Inoculum; T - toluene; E - ethylbenzene; X - xylene; B - benzene).

4. Conclusions

This study evaluated for the first time the biodegradation kinetics and the interactions during the anoxic biodegradation of BTEX present as single compounds or in dual or quaternary mixtures, by a previously acclimated

bacterial consortium. A complete set of kinetic parameters and their confidence intervals, calculated with the Monod model and a modified Gompertz model, are provided. Results showed that both T and E are readily biodegradable by the bacterial consortium under anoxic conditions, with maximum

biodegradation rates of 0.318 and 0.473 h⁻¹ being recorded for these pollutants when degraded individually. However, the build-up of inhibitory intermediates in the liquid media resulted in a partial biodegradation of xylene and benzene when feed individually. The co-degradation of an additional BTEX decreased the specific pollutant biodegradation rates regardless of the dual BTEX mixture, which confirmed the occurrence of a competitive inhibition. These interactions had not been previously quantified under anoxic conditions prior to the current study. Whereas Monod model provided an accurate description of the biodegradation of T and E, the Modified Gompertz model supported better fit for B and X degradation. Furthermore, the Gompertz model accurately represented the inhibitory interactions between BTEX mixtures, although it failed in representing the degradation of the recalcitrant compounds when all four BTEX were present simultaneously.

Acknowledgments

This research was supported by the Spanish Ministry of Economy and Competitiveness and the European Union through the FEDER Funding Program (RED NOVEDAR project, CTM2015-70442-R) and the Regional Government of Castilla y León (UIC71).

Appendix A. Supplementary data

Supplementary data related to this article can be found at

<https://doi.org/10.1016/j.jenvman.2018.02.023>.

References

- Abuhamed, T., Bayraktar, E., Mehmetoglu, T., Mehmetoglu, U., 2004. Kinetics model for growth of *Pseudomonas putida* F1 during benzene, toluene and phenol biodegradation. *Process Biochem.* 39, 983e988.
- Akmirza, I., Pascual, C., Carvajal, A., Perez, R., Muñoz, R., Lebrero, R., 2017. Anoxic biodegradation of BTEX in a biotrickling filter. *Sci. Total Environ.* 587e588, 457e465.
- American Water Works Association (AWWA), 2012. Standard Methods for the Examination of Water and Wastewater. Am. Water Work. Assoc. Public Work. Assoc. Environ. Fed., 1469.
- Annesini, M.C., Piemonte, V., Tomei, M.C., Daugulis, A.J., 2014. Analysis of the performance and criteria for rational design of a sequencing batch reactor for xenobiotic removal. *Chem. Eng. J.* 235, 167e175.
- Barona, A., Elias, A., Arias, R., Acha, E., Cano, I., 2007. Desorption and biofiltration for the treatment of residual organic gases evolved in soil decontamination processes. *Chem. Eng. Technol.* 30, 1499e1505.
- Blok, J., 1994. Classification of biodegradability by growth kinetic parameters. *Ecotoxic. Environ. Saf.* 27, 294e305.
- Chen, J., Zhu, R., Yang, W., Zhang, L., 2010. Treatment of a BTo-X-contaminated gas stream with a biotrickling filter inoculated with microbes bound to a wheat bran/red wood powder/diatomaceous earth carrier. *Bioresour. Technol.* 101, 8067e8073.
- Chi-Wen, L., Ya-Wen, C., Shen-Long, T., 2007. Multisubstrate biodegradation kinetics of MTBE and BTEX mixtures by *Pseudomonas aeruginosa*. *Process Biochem.* 42, 1211e1217.
- Corseuil, H.X., Gomez, D.E., Schambeck, C.M., Ramos, D.T., Alvarez, J.J., 2015. Nitrate addition to groundwater impacted by ethanol-blended fuel accelerates ethanol removal and mitigates the associated metabolic flux dilution and inhibition of BTEX biodegradation. *J. Contam. Hydrol.* 174, 1e9.
- Deeb, R.A., Alvarez-Cohen, L., 1999. Temperature effects and substrate interactions during the aerobic biotransformation of BTEX mixtures by toluene-enriched consortia and *Rhodococcus rhodochrous*. *Biotechnol. Bioeng.* 62, 526e533.
- Dette, H., Melas, V.B., Strigul, N., 2005. Application of optimal experimental design in microbiology. In: Wong, W., Berger, M. (Eds.), *Optimal Designs: Their Roles and Applications*. Wiley and Sons Ltd, New York, pp. 137e180.
- Dou, J., Liu, X., Hu, Z., 2008. Substrate interactions during anaerobic degradation of BTEX by the mixed cultures under nitrate reducing conditions. *J. Hazard. Mater.* 158, 264e272.
- El-Naas, M.H., Acio, A.J., El Telib, A.E., 2014. Aerobic biodegradation of BTEX: progresses and prospects. *J. Environ. Chem. Eng.* 2, 1114e1122.
- Ellis, T.G., Barbeau, D.S., Smets, B.F., 1996. Respirometric technique for determination of extant kinetic parameters describing biodegradation. *Water Environ. Res.* 68, 917e926.
- Estrada, J.M., Kraakman, N.J.R.B., Muñoz, R., Lebrero, R., 2011. A comparative analysis of odor treatment technologies in wastewater treatment plants. *Environ. Sci. Technol.* 45, 1100e1106.
- Estrada, J.M., Rodríguez, E., Quijano, G., Muñoz, R., 2012. Influence of gaseous VOC concentration on the diversity and biodegradation performance of microbial communities. *Bioprocess Biosyst. Eng.* 35, 1477e1488.
- Evans, P.J., Mang, D.T., Kim, K.S., Young, L.Y., 1991. Anaerobic degradation of toluene by a

- denitrifying bacterium. *Appl. Environ. Microbiol.* 57, 1139e1114.
- Goldsmith, J.C.D., Balderson, R.K., 1988. Biodegradation and growth kinetics of enrichment isolates on benzene, toluene and xylene. *Water Sci. Technol.* 20, 505e507.
- Hâne, B.G., Jéager, K., Drexler, H.G., 1993. The Pearson product-moment correlation coefficient is better suited for identification of DNA fingerprint profiles than band matching algorithms. *Electrophoresis* 14, 967e972.
- Jiang, B., Zhou, Z., Dong, Y., Tao, W., Wang, B., Jiang, J., Guan, X., 2015. Biodegradation of benzene, toluene, ethylbenzene, and o-, m-, and p-xylenes by the newly isolated bacterium *Comamonas* sp. *JB. Appl. Biochem. Biotechnol.* 176, 1700e1708.
- Khan, A., Szulejko, J.E., Kim, K.H., Brown, R.J.C., 2018. Airborne volatile aromatic hydrocarbons at an urban monitoring station in Korea from 2013 to 2015. *J. Environ. Manag.* 209, 525e538.
- Lebrero, R., Rodríguez, E., Estrada, J.M., García-Encina, P.A., Muñoz, R., 2012. Odor abatement in biotrickling filters: effect of the EBRT on methyl mercaptan and hydrophobic VOCs removal. *Bioresour. Technol.* 109, 38e45.
- Lebrero, R., Gondim, A.C., Pérez, R., García-Encina, P.A., Muñoz, R., 2014. Comparative assessment of a biofilter, a biotrickling filter and a hollow fiber membrane bioreactor for odor treatment in wastewater treatment plants. *Water Res.* 49, 339e350.
- Lebrero, R., Angeles, R., Pérez, R., Muñoz, R., 2016. Toluene biodegradation in an algal-bacterial airlift photobioreactor: influence of the biomass concentration and of the presence of an organic phase. *J. Environ. Manag.* 183, 585e593.
- Leili, M., Farjadfar, S., Sorial, G.A., Ramavandi, B., 2017. Simultaneous biofiltration of BTEX and Hg₂ from a petrochemical waste stream. *J. Environ. Manag.* 204, 531e539.
- Lin, C., Cheng, Y., Tsai, S., 2007. Multi-substrate biodegradation kinetics of MTBE and BTEX mixture by *Pseudomonas aeruginosa*. *Process Biochem.* 42, 1211e1217.
- Littlejohns, J.V., Daugulis, A.J., 2008. Kinetics and interactions of BTEX compounds during degradation by a bacterial consortium. *Process Biochem.* 43, 1068e1076.
- Liu, B., Zhang, G., Feng, X., Liu, Y., Yan, X., Zhang, X., Wang, L., Zhao, L., 2006. *Thauera* and *Azoarcus* as functionally important genera in a denitrifying quinoline removal bioreactor as revealed by microbial community structure comparison. *FEMS Microbiol. Ecol.* 55, 274e286.
- Mathur, A.K., Majumder, C.B., 2010. Kinetics modelling of the biodegradation of benzene, toluene and phenol as single substrate and mixed substrate by using *Pseudomonas putida*. *Chem. Biochem. Eng. Q.* 24, 101e109.
- McDonald, G., 2003. *Biogeography: Space, Time and Life*. Wiley, New York, p. 409.
- McGinnis, S., Madden, T.L., 2004. BLAST: at the core of a powerful and diverse set of sequence analysis tools. *Nucleic Acids Res.* 32, W20eW25.
- Mazzeo, D.E.C., Levy, C.E., Angelis, D.F., Marin-Morales, M.A., 2010. BTEX biodegradation by bacteria from effluents of petroleum refinery. *Sci. Total Environ.* 408, 4334e4340.
- Militon, C., Boucher, D., Vachelard, C., Perchet, G., Barra, V., Troquet, J., Peyretailade, E., Peyret, P., 2010. Bacterial community changes during bioremediation of aliphatic hydrocarbon-contaminated soil. *FEMS Microbiol. Ecol.* 74, 669e681.
- Morlett-Chavez, J.A., Ascacio-Martínez, J.A., Rivas-Estilla, A.M., Velázquez-Vadillo, J.F., Haskins, W.E., Barrera-Saldana, H.A., Acuna-Askar, K., 2010. Kinetics of BTEX biodegradation by a microbial consortium acclimatized to unleaded gasoline and bacterial strains isolated from it. *Int. Biodeterior. Biodegrad.* 64, 581e587.
- Muñoz, R., Souza, T.S.O., Glittmann, L., Pérez, R., Guillermo, G., 2013. Biological anoxic treatment of O₂-free VOC emissions from the petrochemical industry: a proof of concept study. *J. Hazard. Mater.* 260, 442e450.
- Oh, Y.S., Shareefdeen, Z., Baltzis, B.C., Bartha, R., 1994. Interactions between benzene, toluene and p-xylene (BTX) during their biodegradation. *Biotechnol. Bioeng.* 44, 533e538.
- Rahul, A.K., Balomajumder, C., 2013. Biological treatment and modelling aspect of BTEX abatement process in a biofilter. *Bioresour. Technol.* 142, 9e17.
- Robledo-Ortiz, J.R., Ramirez-Arreola, D.E., Perez-Fonseca, A.A., Gomez, C., Gonzalez-Reynoso, O., Ramos-Quirarte, J., Gonzalez-Nunez, R., 2011. Benzene, toluene, and o-xylene degradation by free and immobilized *P. putida* F1 of postconsumer agave-fiber/polymer foamed composites. *Int. Biodeterior. Biodegrad.* 65, 539e546.
- Roest, K., Heilig, H.G., Smidt, H., de Vos, W.M., Stams, A.J.M., Akkermans, A.D.L., 2005. Community analysis of a full-scale anaerobic bioreactor treating paper mill wastewater. *Syst. Appl. Microbiol.* 28, 175e185.
- Shim, H., Yang, S.T., 1999. Biodegradation of benzene, toluene, ethylbenzene, and oxylene by a coculture of *Pseudomonas putida* and *Pseudomonas fluorescens* immobilized in a fibrous-bed bioreactor. *J. Biotechnol.* 67, 99e112.
- Shim, H., Hwang, B., Lee, S., Kong, S., 2005. Kinetics of BTEX biodegradation by a coculture of *Pseudomonas putida* and *Pseudomonas*

fluorescens under hypoxic conditions. *Biodegradation* 16, 319e327.

Singh, K., Singh, R.S., Rai, B.N., Upadhyay, S.N., 2010. Biofiltration of toluene using wood charcoal as the biofilter media. *Bioresour. Technol.* 101, 3947e3951.

Shinoda, Y., Akagi, J., Uchihashi, Y., Hiraishi, A., Yukawa, H., Yurimoto, H., Sakai, Y., Kato, N., 2005. Anaerobic degradation of aromatic compounds by *Magnetospirillum* strains: isolation and degradation genes. *Biosci. Biotechnol. Biochem.* 69, 1483e1491.

Strigul, N., Dette, H., Melas, V.B., 2009. A practical guide for optimal designs of experiments in the Monod model. *Environ. Model. Softw.* 24, 1019e1026.

Trigueros, D.E.G., M_odenés, N.A., Kroumov, D.A., Espinoza-Quiñones, F.R., 2010. Modelling of biodegradation process of BTEX compounds: kinetic parameters estimation by using Particle Swarm Global Optimizer. *Process Biochem.* 45, 1355e1361.

Van der Zaan, B.M., Saia, F.T., Stams, A.J., Plugge, C.M., de Vos, W.M., Smidt, H., Langenhoff, A.A., Gerritse, J., 2012. Anaerobic benzene degradation under denitrifying conditions: Peptococcaceae as dominant benzene degraders and evidence for a syntrophic process. *Environ. Microbiol.* 14, 1171e1181.

Vogt, C., Kleinstüber, S., Richnow, H., 2011. Anaerobic benzene degradation by bacteria. *Microb. Biotechnol.* 4, 710e724.

Wang, Q., Garrity, G.M., Tiedje, J.M., Cole, J.R., 2007. Naive Bayesian classifier for rapid assignment of rRNA sequences into the new bacterial taxonomy. *Appl. Environ. Microbiol.* 73, 5261e5267.

Weelink, S., van Eekert, M., Stams, A., 2010. Degradation of BTEX by anaerobic bacteria: physiology and application. *Rev. Environ. Sci. Biotechnol.* 9, 359e385.

Whiting, R.C., 1995. Microbial modelling in foods. *Crit. Rev. Food Sci.* 35, 467e494.

Xu, G., Peng, J., Feng, C., Fang, F., Chen, S., Xu, Y., Wang, X., 2015. Evaluation of simultaneous autotrophic and heterotrophic denitrification processes and bacterial community structure analysis. *Appl. Microbiol. Biotechnol.* 99, 6527e6536.

Zhang, Z., Lo, I.M.C., 2015. Biostimulation of petroleum-hydrocarbon-contaminated marine sediment with co-substrate: involved metabolic process and microbial community. *Appl. Microbiol. Biotechnol.* 99, 5683e5696.

Zwietering, M.H., Jongenburger, I., Rombouts, F.M., Van't Riet, K., 1990. Modelling of bacterial growth curve. *Appl. Environ. Microbiol.* 56, 1875e1881.



Universidad de Valladolid

CHAPTER 6

Anoxic Biodegradation of BTEX in a Biotrickling Filter

Anoxic biodegradation of BTEX in a biotrickling filter

Ilker Akmirza ^{a,b}, Celia Pascual ^a, Andrea Carvajal ^c, Rebeca Pérez ^a, Raúl Muñoz ^a, Raquel Lebrero ^{a,*}

^a Department of Chemical Engineering and Environmental Technology, University of Valladolid, Dr. Mergelina s/n., Valladolid 47011, Spain

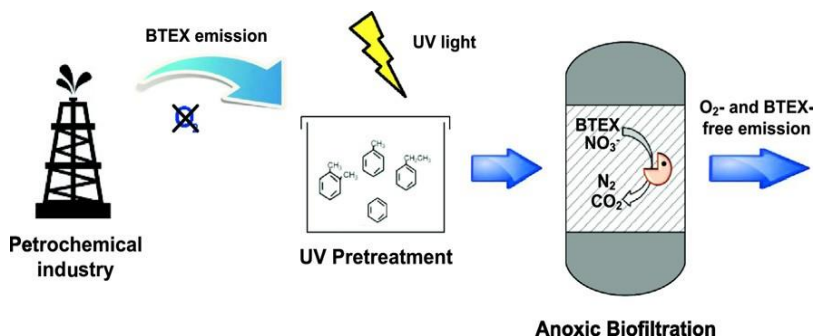
^b Department of Environmental Engineering, Technical University of Istanbul, 34469 Istanbul, Turkey

^c Department of Chemical Engineering and Environmental Technology, Technical University Federico Santa Maria, Chile

HIGHLIGHTS

- Anoxic removals N 90% were achieved for toluene and ethylbenzene ($\sim 1.4 \text{ g m}^{-3} \text{ h}^{-1}$).
- 45% of xylene ($0.6 \text{ g m}^{-3} \text{ h}^{-1}$) was removed at 2 m h^{-1} of liquid recycling velocity.
- The low benzene abatement was attributed to accumulation of toxic metabolites.
- UV oxidation of intermediates present in the liquid phase enhanced benzene removal.
- UV pretreatment of the emission resulted in a deterioration of BTEX biodegradation.

GRAPHICAL ABSTRACT



Abstract

Emissions of BTEX (benzene, toluene, ethylbenzene and xylene) from the petrochemical industry are characterized by a low pollutants concentration and the absence of oxygen. Biodegradation of these pollutants using nitrate as the electron acceptor is of key interest to reuse the residual gas for inertization purposes. However, the biological mineralization of BTEX is often limited by their recalcitrant nature and the toxicity of the secondary metabolites produced. The potential of an anoxic biotrickling filter for the treatment of a model O₂-free BTEX-laden emission at inlet individual concentrations of $\sim 700 \text{ mg m}^{-3}$ was here evaluated. A UV oxidation step was also tested both in the recycling liquid and in the inlet gas emission prior to biofiltration. Removal efficiencies N 90% were achieved for both toluene and ethylbenzene, corresponding to elimination capacities (ECs) of $1.4 \pm 0.2 \text{ g m}^{-3} \text{ h}^{-1}$ and $1.5 \pm 0.3 \text{ g m}^{-3} \text{ h}^{-1}$, respectively, while $\sim 45\%$ of xylene ($\text{EC} = 0.6 \pm 0.1 \text{ g m}^{-3} \text{ h}^{-1}$) was removed at a liquid recycling rate of 2 m h^{-1} . Benzene biodegradation was however limited by the accumulation of toxic metabolites in the liquid phase. The oxidation of these intermediates in the recycling liquid by UV photolysis boosted benzene abatement, achieving an average EC of $0.5 \pm 0.2 \text{ g m}^{-3} \text{ h}^{-1}$ and removals of $\sim 40\%$. However, the implementation of UV oxidation as a pretreatment step in the inlet gas emission resulted in the deterioration of the BTEX biodegradation capacity of the biotrickling filter. Finally, a high bacterial diversity was observed throughout the entire experiment, the predominant phyla being *Proteobacteria* and *Deinococcus-thermus*.

1. Introduction

Benzene, toluene, ethylbenzene and xylene (BTEX) are volatile aromatic hydrocarbons responsible for health problems such as irritation headaches, or even liver and kidney damage and cancer (benzene has been classified as Group A-known human carcinogen by EPA) (Gallastegui et al., 2011; Wang et al., 2013). Moreover, BTEX are included in the Hazardous Air Pollutants List and rank 78 in the CERCLA List from the 275 substances identified to pose most significant potential threat to human health (Rahul and Balomajumder, 2013). Thus, the minimization and abatement of BTEX play an important role in human and environmental health due to their widespread use in many industrial sectors (petrochemistry, pulp and paper or paints and dyes (Lu et al., 2002)) and their highly toxic, corrosive and genotoxic properties (Lu et al., 2002; Rene et al., 2012).

Approximately 20% of all volatile organic compound (VOC)-laden emissions in the USA are released by facilities devoted to oil and gas production, bulk fuel/solvent storage and petroleum refining, while petroleum refining and bulk storage constitute ~ 15% of the total non-methane VOC emissions in Europe (EEA, 2011; EPA, 2008; Muñoz et al., 2013). In this context, BTEX account for up to 59% (w/w) of the gasoline pollutants and represent about 80% of the VOC emissions in petrochemical plants (El-Naas et al., 2014). Therefore, a significant number of BTEX emissions are characterized by their O₂-free nature (since N₂ or CO₂ are used for inertization purposes in the petrochemical industry) and their explosion risk when O₂ is present.

Up to date, several physical-chemical treatment technologies such as incineration, catalytic oxidation, and adsorption have been used for the abatement of BTEX (Chen et al., 2010). However, the high capital and operating costs associated to these technologies, their high energy requirements and non-environmentally friendly nature have boosted the development of new treatment technologies. In this context, the biotreatment of BTEX provides a sustainable and low-cost alternative to physical-chemical technologies. Biological systems such as biofilters, bioscrubbers and biotrickling filters (BTFs) are well-established technologies for abatement of diluted VOC emissions (less than 1000 mg m⁻³) (Balasubramanian et al., 2012; Estrada et al., 2011). In particular, BTFs have several advantages over other biofiltration technologies such as lower

pressure drop across the packed bed due to the high porosity of the inert packing material easier control of the operating parameter (Moussavi and Mohseni, 2007; Yan et al., 2016). However, limited information is still available in literature on this particular topic, and both positive and detrimental effects of this hybrid technology should be investigated.

In this work, the potential of anoxic biofiltration for the removal of BTEX from an O₂-free waste-gas stream was investigated. In addition, the technical feasibility of a photolysis unit based on UV radiation as a pretreatment technology was tested both in the liquid and in the gas phase before biotrickling filtration. Finally, the dynamics of the bacterial population were also assessed by DGGE-sequencing.

2. Materials and Methods

2.1. Inoculum

Activated sludge from the denitrification-nitrification wastewater treatment plant of Valladolid (Spain) was used as inoculum in order to decrease the acclimation period of the microbial community to anoxic pollutant biodegradation. 2 L of the activated sludge were centrifuged for 10 min at 10000 rpm and resuspended in 200 mL of fresh mineral salt medium (MSM) with a final volatile suspended solids (VSS) concentration of 7580 mg L⁻¹. The inoculum was added to the biotrickling filter and recycled through the packed bed for 1 day to promote microbial attachment and biofilm formation.

2.2. Chemicals and mineral salt medium

All chemicals for MSM preparation were purchased from PANREAC (Barcelona, Spain) with a purity of at least 99%. Benzene, toluene, ethylbenzene and o-xylene (99.0% purity) were obtained from Sigma-Aldrich (Madrid, Spain). The MSM was composed of (g·L⁻¹): Na₂HPO₄·12H₂O, 6.15; KH₂PO₄, 1.52; MgSO₄·7H₂O, 0.2; CaCl₂, 0.038; and 10 mL L⁻¹ of a trace element solution containing (g L⁻¹): EDTA, 0.5; FeSO₄·7H₂O, 0.2; ZnSO₄·7H₂O, 0.01; MnCl₂·4H₂O, 0.003; H₃BO₃, 0.03; CoCl₂·6H₂O, 0.02; CuCl₂·2H₂O, 0.001; NiCl₂·6H₂O, 0.002; NaMoO₄·2H₂O, 0.003 (Muñoz et al., 2013). NO₃⁻ (supplemented as NaNO₃ in a 8 g L⁻¹ stock solution) was used as electron acceptor for BTEX oxidation and as nitrogen source for microbial

growth.

2.3 Experimental setup and operating procedure

The laboratory scale biotrickling filter consisted of a cylindrical jacketed PVC column (0.084 m inner diameter, 45 cm height) packed with Kaldnes rings to a working volume of 2 L (Fig. 1). An external 1.2 L jacketed holding tank stirred at 400 rpm (Agimatic-S, Selecta®, Spain) was used as a MSM reservoir. The MSM was continuously recycled from the top of the column by a positive displacement pump (Milton Roy Iberica, G Series, Spain) at 2 m h^{-1} . The BTEX inlet stream was prepared by injecting a liquid mixture containing the four components with a syringe pump (Fusion 100, Chemyx Inc. USA) to a N_2 gas stream (Abello Linde Spain, purity N 99.999%). The polluted gas stream, with a concentration of $742 \pm 95 \text{ mg benzene m}^{-3}$, $712 \pm 84 \text{ mg toluene m}^{-3}$, $702 \pm 96 \text{ mg ethylbenzene m}^{-3}$ and $712 \pm 84 \text{ mg xylene m}^{-3}$, was supplied from the bottom of the column in a counter current mode with the trickling liquid flow. The flow rate was controlled to maintain a gas empty bed residence time of 30 min, resulting in inlet loads of $1.4 \pm 0.2 \text{ g m}^{-3} \text{ h}^{-1}$ for toluene, ethylbenzene and xylene and $1.5 \pm 0.2 \text{ g m}^{-3} \text{ h}^{-1}$ for benzene.

The system was operated for 208 days (Table 1). From day 0 to 34, 200 mL of MSM were daily exchanged with new MSM. The MSM renewal rate was subsequently increased to 600 mL (days 34—208). Between days 85 and 90, the pH was manually controlled at ~ 7 by addition of a 6 M HCl solution to the recycling MSM, terminating afterwards any pH control strategy due to the rapid process performance deterioration observed and in order to avoid any irreversible damage to the microbial community. Once the previous BTEX degradation performance was recovered by day 122, a 600-mL quartz photoreactor containing a UV lamp (Pen-Ray WL254 NM) was installed in the recycling liquid stream interconnecting the 1.2-L

external tank with the packed bed column. The UV lamp provided an irradiation at the inner photoreactor wall of 4.0 mW cm^{-2} . Following performance stabilization, the UV photolysis pretreatment was started by day 139. By day 172, the 600 mL-quartz photoreactor was installed in the inlet gas line, the polluted stream flowing through the tank before entering the packed column. Finally, the UV light was removed by day 191 returning to the initial configuration, and the system was operated without pretreatment until day 208. Inlet and outlet BTEX and CO_2 concentrations in the gas phase were daily measured using a gas-tight syringe (Hamilton, USA) by GC-FID and GC-TCD, respectively. Liquid samples were also daily drawn to determine the pH and the concentrations of total organic carbon (TOC), inorganic carbon (IC) and total nitrogen (TN), while nitrate (NO_3^-) and nitrite (NO_2^-) concentrations in the liquid phase were measured by HPLC-IC. Samples from the inoculum and the biofilm at the end of the operating period were drawn and frozen at -80°C for microbial population analyses.

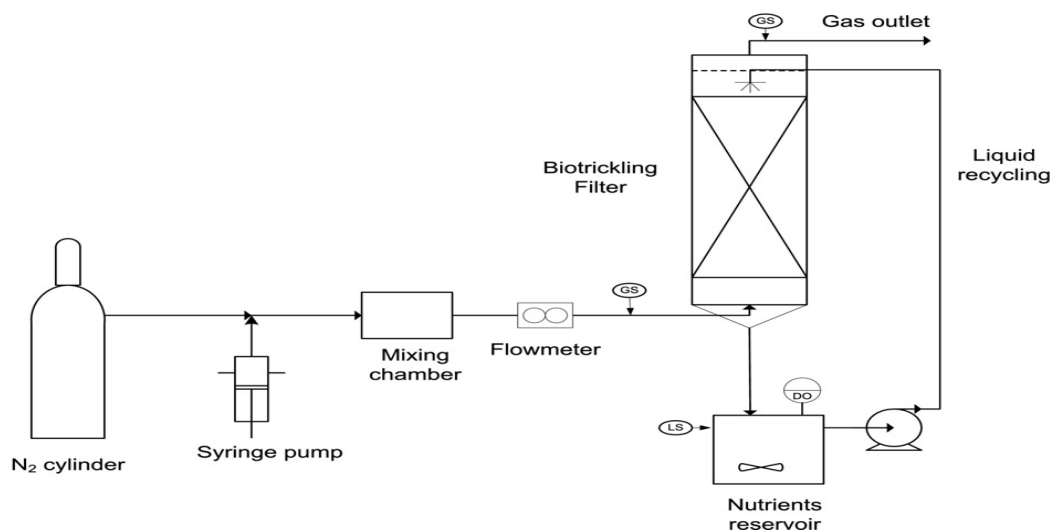


Fig. 1. Schematic representation of the experimental setup

2.4 Analytical procedures

BTEX concentration in the gas phase was analysed in a Bruker 3900 gas chromatograph (Palo Alto, USA) equipped with a flame ionization detector and a Supelco Wax ($15 \text{ m} \times 0.25 \text{ mm} \times 0.25 \text{ }\mu\text{m}$) capillary

Table 1 Experimental conditions established during the eight operational stages.

Stage	Days	Dilution rate (d^{-1})	pH control	UV pretreatment	Total liquid reservoir (L)
I	0-34	0.17	No	No	1.2
II	34-85	0.5	No	No	1.2
III	85-90		Yes	No	1.2
IV	90-122		No	No	1.2
V	122-139		No	No	1.8
VI	139-172		No	Liquid line	1.8
VII	172-191		No	Gas line	1.8
VIII	191-208		No	No	1.2

column. Oven temperature was initially maintained at $50 \text{ }^\circ\text{C}$ for 1 min, increased at $50 \text{ }^\circ\text{C min}^{-1}$ up to $70 \text{ }^\circ\text{C}$ and then at $65 \text{ }^\circ\text{C min}^{-1}$ to a final temperature of $140 \text{ }^\circ\text{C}$. CO_2 concentration in the gas phase was determined in a Bruker 430 gas chromatograph (Palo Alto, USA) coupled with a thermal conductivity detector and equipped with a CP-Molsieve 5A ($15 \text{ m} \times 0.53 \text{ m} \times 15 \text{ m}$)

and a P-PoraBOND Q ($25 \text{ m} \times 0.53 \text{ m} \times 10 \text{ m}$) columns. The oven, injector and detector temperatures were maintained at $40 \text{ }^\circ\text{C}$, $150 \text{ }^\circ\text{C}$ and $175 \text{ }^\circ\text{C}$, respectively. Helium was used as the carrier gas at 13.7 mL min^{-1} . Nitrite and nitrate concentrations in the liquid phase were analysed via HPLC-IC using a Waters 515 HPLC pump coupled with a conductivity detector (Waters432) and equipped with an IC-PAK Anion HC column ($4.6 \times 150 \text{ mm}$) and an IC-Pak Anion Guard-Pak (Waters). Samples were eluted isocratically at 2 mL min^{-1} (at room temperature) with a solution of distilled water/acetonitrile/n-butanol/buffer at 84/12/2/2% v/v (Muñoz et al., 2013). Samples for the determination of the concentration of TOC, IC and TN in the liquid phase were measured using a Shimadzu TOC-VCSH analyzer (Japan) coupled with a TNM-1 chemiluminescence module. Biomass concentration was estimated as VSS according to Standard Methods (American Water Works Association, 2012). More specifically, a 50 mL sample was filtered in a pre-dried and pre-weighted filter ($1 \text{ }\mu\text{m}$ pore size) and evaporated for 24 h at $105 \text{ }^\circ\text{C}$. The corresponding residue was weighted and further dried in a furnace at $550 \text{ }^\circ\text{C}$ for another 24 h. The amount of VSS was determined from the resulting solid after combustion.

Tablo 2: RDP classification of the DGGE bands sequenced and corresponding matches (BLASTN) using the NCBI database with indication of the similarity percentages and sources of origin. The presence/absence of each band in each sample tested together with its intensity are also shown.

Taxonomic placement (50% confidence level)	Band n°	1	2	3	Closest relatives in BlastName (accession number)	Similarity (%)	Source of origin
Phylum <i>Proteobacteria</i>	1	x	xxx	xxx	Uncultured bacterium (GU980094)	96	Activated biomass (sludge samples) of a common effluent treatment plant (CETP) that receives wastewater from industries making chloro- and nitro-containing products
	2	xx			Uncultured bacterium (JX627825)	94	Membrane bioreactor treating acetone, toluene, limonene and hexane
Class <i>Alphaproteobacteria</i>	3	x	xx	xxx	Uncultured bacterium (KM290856) Uncultured bacterium (KP718816)	97 96	Earthworm compost High-rate denitrifying reactor treated with synthetic wastewater
	4	x	xx	xx	Uncultured bacterium (KM290856) Uncultured bacterium (KP718816)	98 97	Earthworm compost High-rate denitrifying reactor treated with synthetic wastewater
	5		xxx	xxx	Uncultured bacterium (KM290856) Uncultured bacterium (KP718816)	99 97	Earthworm compost High-rate denitrifying reactor treated with synthetic wastewater
Class <i>Gammaproteobacteria</i>	6	xx			Uncultured bacterium (KU726385) Uncultured bacterium (HG380574)	95 90	Ann Arbor drinking water treatment plant Wastewater
Order <i>Xanthomonadales</i>	7	xx	x	xx	Uncultured bacterium (KJ707450)	89	Waste water treatment plant's biofilter
Family <i>Xanthomonadaceae</i>							
Genus <i>Dokdonella</i>	8	xxx	xx	xx	Bacterium enrichment culture (KR090645) Uncultured bacterium (KT835604) Uncultured bacterium (KP054220) Uncultured bacterium (KJ783009)	99 99 99 99	Nitrifying microbial culture Activated sludge Nitrification and denitrification reactors Petrochemical wastewater treatment plant sludge
Phylum							
Class <i>Deinococcus-thermus</i>							
Order <i>Deinococcales</i>							
Family <i>Trueperaceae</i>							
Genus <i>Truepera</i>	9		xx	xx	Uncultured bacterium (DQ345944) Uncultured bacterium (KP911210) Uncultured <i>Thermus/Deinococcus</i> group bacterium (HQ727577)	99 99 97	UASB reactor Composting process Petroleum-contaminated soils
	10	xx	xxx	xxx	Uncultured bacterium (DQ345944) Uncultured bacterium (EU083501) Uncultured <i>Thermus/Deinococcus</i> group bacterium (HQ727577)	99 98 97	UASB reactor Hexadecane-degrading denitrifying consortium Petroleum-contaminated soils
	11		xx	xx	Uncultured bacterium (KU648784) Uncultured bacterium (KM294370)	99 97	Anaerobic full-scale reactors Sludge
	12		xx	xx	Uncultured <i>Deinococci</i> bacterium (HQ392846) Uncultured bacterium (KU649843) Uncultured bacterium (FN598011)	98 97 97	HRAPs treating piggyery wastewater Anaerobic full-scale reactors Activated sludge
Phylum <i>Actinobacteria</i>							
Class <i>Actinobacteria</i>							
Subclass <i>Actinobacteridae</i>							
Order <i>Bifidobacteriales</i>							
Family <i>Bifidobacteriaceae</i>							
Genus <i>Bifidobacterium</i>	13	xx			<i>Bifidobacterium longum</i> (CP000605)	94	
Phylum <i>Chloroflexi</i>	14		xxx	xxx	Uncultured bacterium (KP641120)	92	High-rate denitrifying reactor treated with synthetic wastewater

2.5 Microbiological procedure

Genomic DNA was extracted using the protocol described in the Fast® DNA Spin Kit for Soil (MP Biomedicals, LLC) handbook. The V6— V8 region of the bacterial 16S rRNA genes was amplified by polymerase chain reaction (PCR) using the universal bacterial primers 968-F-GC and 1401-R (Sigma-Aldrich, St. Louis, MO, USA). The PCR mixture contained 1 µL of each primer (10 ng µL⁻¹ each primer), 25 µL of BIOMIX ready-to-use 2 reaction mix (Bioline, Ecogen), 2 µL of the extracted DNA, and Milli-Q water up to a final volume of 50 µL. The PCR thermo-cycling pro-

gram consisted of 2 min of pre-denaturation at 95 °C, 35 cycles of denaturation at 95 °C for 30 s, annealing at 56 °C for 45 s, and elongation at 72 °C for 1 min, with a final 5-min elongation at 72 °C.

The DGGE analysis of the amplicons was performed with a D-Code Universal Mutation Detection System (Bio Rad Laboratories) using 8% (w/v) polyacrylamide gels with a urea/formamide denaturing gradient of 45 to 65%. DGGE running conditions were applied according to Roest et al. (2005). The gels were stained with GelRed Nucleic Acid Gel Stain (biotium) for 1 h. The most relevant bands were excised from the DGGE gel in order to identify

the bacteria present in the samples, resuspended in 50 μL of ultrapure water and

DGGE profiles were compared using the GelCompar IITM software (Applied Maths BVBA, Sint-Martens-Latem, Belgium). After image normalization, bands were defined for each sample using the bands search algorithm within the program. The peak heights in the densitometric curves were also used to determine the diversity indices based on the Shannon–Wiener diversity index (H), calculated as follows:

$$H = -\sum [P_i \ln(P_i)]$$

where H is the diversity index and P_i is the importance probability of the bands in a lane ($P_i = n_i/n$, where n_i is the height of an individual peak and n is the sum of all peak heights in the densitometric curves). Therefore, this index reflects both the sample richness (relative number of DGGE bands) and evenness (relative intensity of every band). According to McDonald (2003) it ranges from 1.5 to 3.5 (low and high species evenness and richness, respectively).

Similarity indices were calculated from the densitometric curves of the scanned DGGE profiles by using the Pearson product–moment correlation coefficient (Häne et al., 1993). The taxonomic position of the sequenced DGGE bands was obtained using the RDP classifier tool (50% confidence level) (Wang et al., 2007). The closest cultured and uncultured relatives to each band were obtained using the BLAST search tool at the NCBI (National Centre for Biotechnology Information) (McGinnis and Madden, 2004) (Table 2). Sequences were deposited in GenBank Data Library under accession numbers KY003166–KY003180.

3. Results and Discussion

3.1 Biotrickling filter performance

Following BTF start-up, the removal efficiency of both toluene (T) and ethylbenzene (E) gradually increased and stabilized by day 2 of operation at 78 ± 6 and $91 \pm 5\%$, respectively (Fig. 2A and B), corresponding to

maintained at 60 °C for 1 h to allow DNA extraction from the gel. A volume of 5 μL of the elimination capacities (ECs) of $1.05 \pm 0.18 \text{ g m}^{-3} \text{ h}^{-1}$ for toluene and $1.19 \pm 0.22 \text{ g m}^{-3} \text{ h}^{-1}$ for E-benzene. On the contrary, a highly fluctuating xylene (X) removal was recorded during this first stage, with values as low as 2% increasing sporadically up to 44% (Fig. 2C). Similarly, benzene (B) removal remained low and fluctuating at $10 \pm 11\%$ (Fig. 2D). The biodegradation of BTEX resulted in an average total CO_2 production of $5.8 \pm 2.2 \text{ g m}^{-3} \text{ h}^{-1}$ throughout the first operating period (Fig. 3). The pH value of the collected leachate rapidly increased after BTF start-up from 7 to 8.8 likely due to the denitrification

By the end of stage I, a mass transfer test was performed by increasing ~ 2 times the BTEX inlet concentration in order to determine if the system was limited either by mass transfer or by biological activity. Inlet and outlet gas samples were hourly taken to analyze BTEX and CO_2 concentrations (Fig. 4). The EC increase recorded for T, E and X as a result of the higher inlet load clearly showed that BTF performance was limited by the transport of these target compounds from the gas phase to the biofilm. Although adsorption in the packing material could initially contribute to the higher EC recorded, a stable removal performance was maintained throughout the test and no negative removals due to TEX desorption was subsequently observed. This suggested that all the compounds transferred were biodegraded in the biofilm, confirming the capacity of the microbial community to mineralize higher loads. In the particular case of benzene, the initial increase in EC observed (up to $\times 4.5$) was followed by a removal deterioration (negative EC) when previous inlet concentrations were restored.

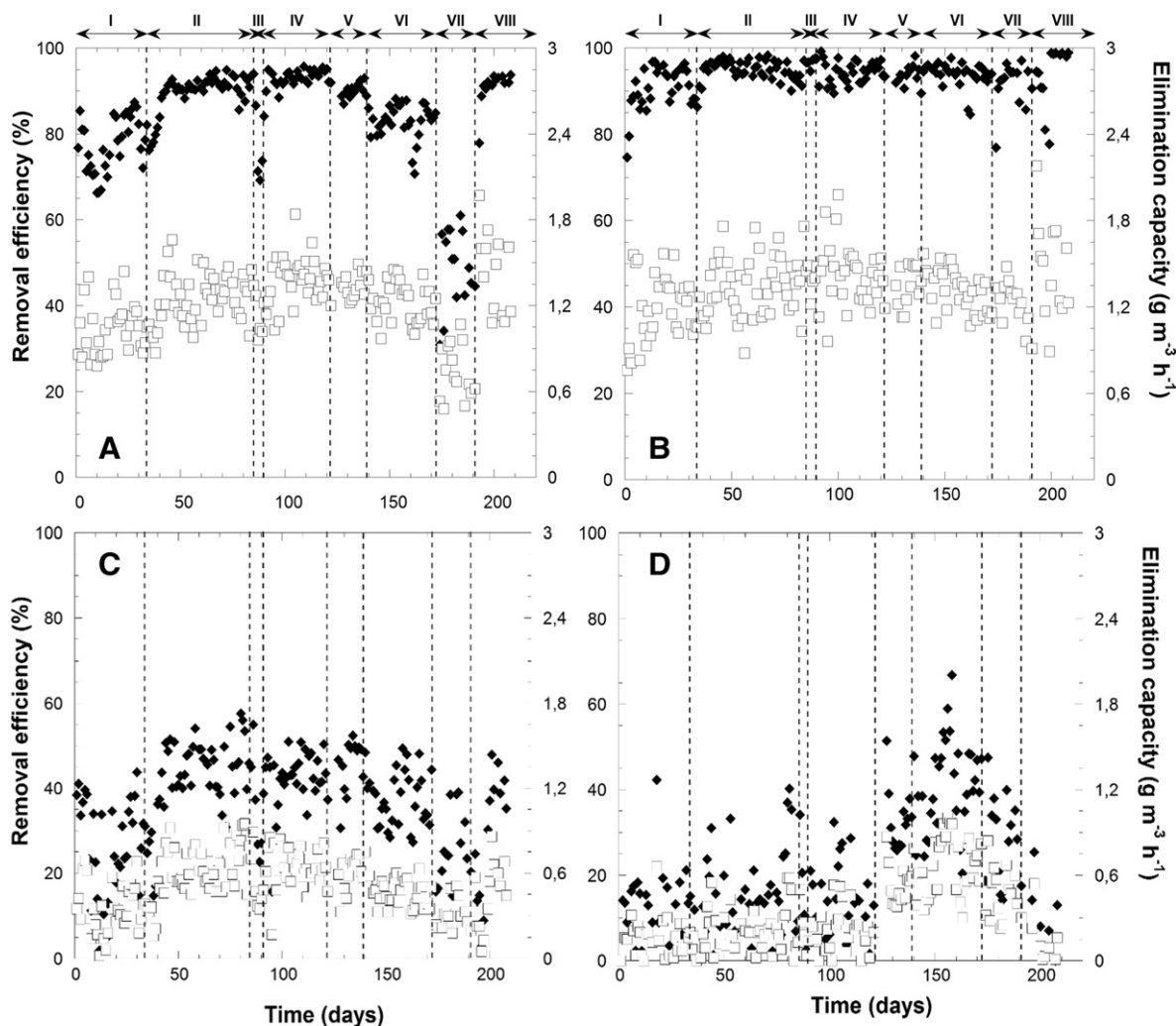


Fig. 2. Time course of toluene (A), ethylbenzene (B), xylene (C) and benzene (D) removal efficiency (◆) and elimination capacity (□). Dashed lines represent different operating stages as indicated in the upper part of the figure

This suggested a temporal benzene accumulation (either by adsorption in the biofilm or in the packing material or absorption in the recycling media) as a result of the higher concentration gradient during the mass transfer test, and a subsequent desorption of this compound before being biodegraded. Therefore, the limited biodegradation observed for B during stage I was in this case attributed to the accumulation of inhibitory intermediate metabolites as previously observed by other authors during the aerobic biodegradation of BTEX (El-Naas et al., 2014; Trigueros et al., 2010). In order to overcome this particular

limitation, the amount of MSM daily exchanged was increased by a factor of 3 from day 34 of operation. The new operating conditions resulted in a significant enhancement of the abatement performance for xylene, while no improvement of benzene removal was observed during stage II. In this sense, toluene RE stabilized by day 42 at $91.4 \pm 1.9\%$, E removal rapidly achieved a steady value of $94.9 \pm 2.2\%$ and xylene RE reached $45.2 \pm 6.9\%$ (~1.9 times higher than that recorded in stage) by day 40, corresponding to ECs of 1.3 ± 0.2 , 1.3 ± 0.2 and 0.7 ± 0.2 g m⁻³ h⁻¹, respectively.

It is worth noticing that, although previous studies have reported similar T and E removal efficiencies than those here recorded (Lu et al., 2002; Rene et al., 2012; Wang et al., 2013), the ECs here achieved are lower than those observed during aerobic biofiltration of BTEX due to the lower inlet loads applied in this study (Balasubramanian et al., 2012; Chen et al., 2010; Gallastegui et al., 2011). In this sense, higher BTEX inlet concentrations are usually tested under aerobic conditions (up to 3 orders or magnitude higher than those found in O₂-free petrochemical emissions, Torretta et al., 2015) and significantly lower EBRTs can be applied due to the faster VOCs biodegradation rates commonly observed when oxygen is used as electron acceptor. The increase in pollutants removal in stage II did not result in a higher CO₂ production, which remained nearly stable at $5.5 \pm 0.7 \text{ g m}^{-3} \text{ h}^{-1}$. The constant PCO₂ was likely mediated by a higher amount of carbon being directed to the anabolic pathway for biomass production, therefore decreasing the mineralization rate. On the contrary, no enhancement in benzene biodegradation was obtained after the increase in dilution rate, with a fluctuating value of $10.2 \pm 11.6\%$. During stage II, the pH remained stable at 8.4 ± 0.1 .

At this point, it is important to highlight that previous studies have reported that neutral pH values promote benzene removal, and most BTEX degrading bacteria present optimum biological activity at a pH between 6 and 8 under aerobic conditions (El-Naas et al., 2014; Hong and Lee, 2006). The effect of pH on BTEX biodegradation under anoxic conditions was then tested by addition of a 6 N HCl into the liquid reservoir in stage III in order to reach a final value of 7.3 ± 0.1 . This decrease in pH negatively affected T and X biodegradation, with steady state REs during this stage of 77.0 ± 7.8 and $33.7 \pm 13.1\%$, respectively. Ethylbenzene removal was not affected by the pH change and remained at $96.0 \pm 1.7\%$, while BTF operation at neutral pH resulted in a limited effect on B biodegradation, with REs of $15.5 \pm 12.2\%$. Due to the detrimental effect of the neutral pH on T and X abatement and the

insignificant enhancement of B biodegradation, pH control was stopped by day 90. During this stage, the CO₂ production experienced a noticeable increase reaching values of $7.8 \pm 1.5 \text{ g m}^{-3} \text{ h}^{-1}$ as a result of the enhanced CO₂ mass transfer from the liquid to the gas phase under more acidic conditions.

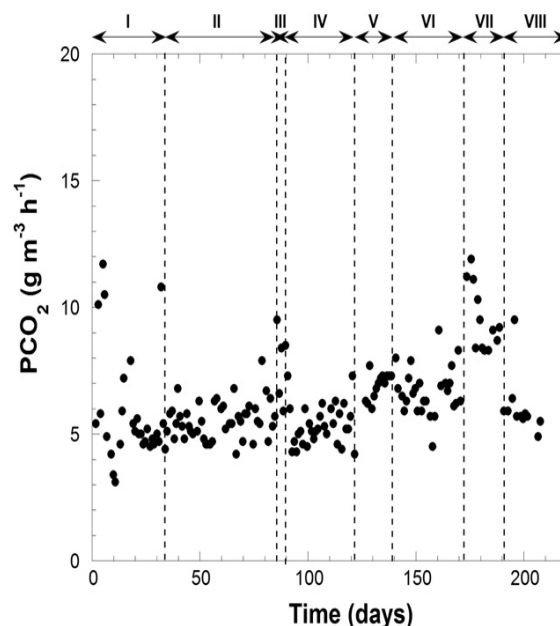


Fig. 3. Time course of CO₂ production. Dashed lines represent different operating stages as indicated in the upper part of the figure.

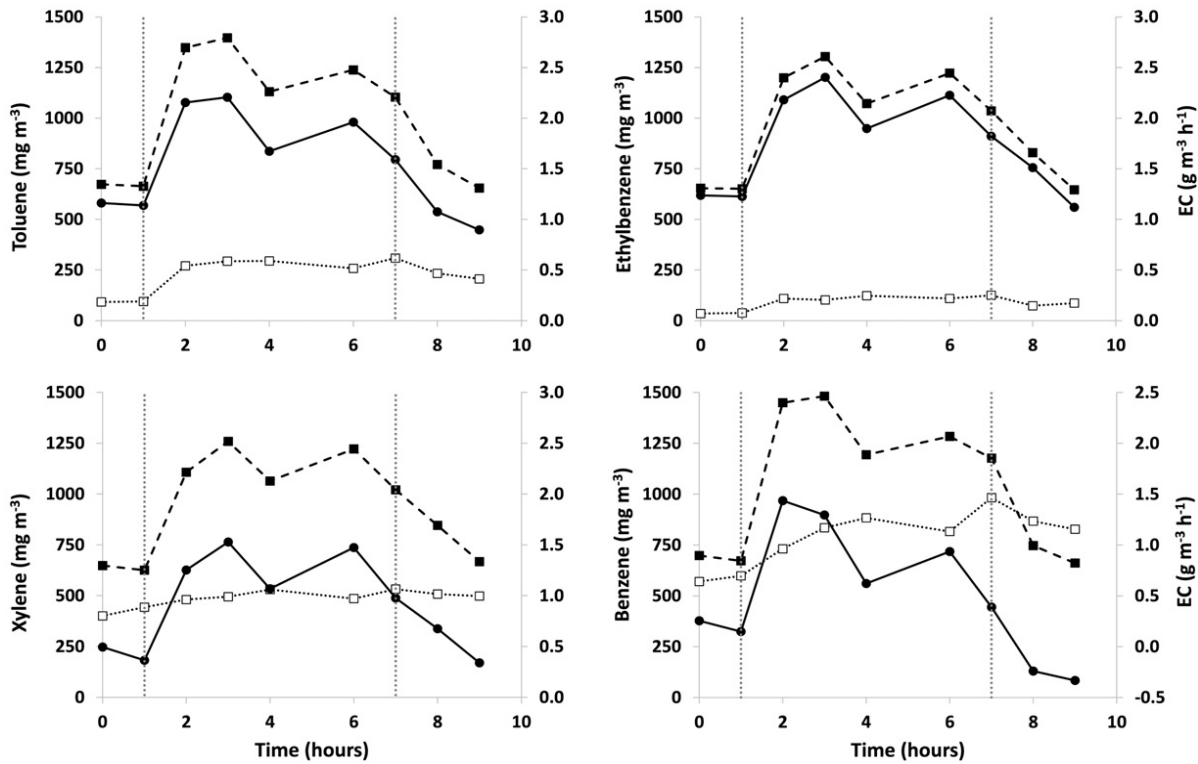


Fig. 4. BTEX inlet concentration (■, dashed line), outlet concentration (□, dotted lined) and elimination capacity (●, continuous line) during the mass transfer test.

The previous T, E, X and B removal efficiencies were rapidly recovered once the pH was restored in stage IV (8.5 ± 0.1), with steady REs of 93.2 ± 1.7 , 93.9 ± 2.4 , 41.9 ± 6.8 and $9.8 \pm 10.8\%$, respectively. CO_2 production also stabilized at comparable values than those recorded during the second stage ($5.3 \pm 0.8 \text{ g m}^{-3} \text{ h}^{-1}$). The BTF was operated under these conditions until day 122, when a 600 mL photoreactor was placed in the liquid recycling line interconnecting the 1.2 L-reservoir and the BTF column. The increase in the MSM volume only affected B removal performance, which significantly increased up to $33.9 \pm 8.6\%$, corresponding to an EC of $0.5 \pm 0.2 \text{ g m}^{-3} \text{ h}^{-1}$. E and X REs remained roughly stable between days 122 and 139 at 93.7 ± 2.2 and $45.2 \pm 6.1\%$, respectively (corresponding to ECs of 1.4 ± 0.1 and $0.6 \pm 0.1 \text{ g m}^{-3} \text{ h}^{-1}$), while a slight decrease in T removal to $89.9 \pm 2.0\%$ was recorded ($1.3 \pm 0.1 \text{ g m}^{-3} \text{ h}^{-1}$). The sustained abatement

of benzene during the 17 days of stage V confirmed that the superior removal here recorded was not associated to a merely benzene absorption in the liquid. The higher MSM volume likely act as a buffer reservoir of toxic metabolites, resulting in an enhanced biodegradation capacity of the microbial community. This also led to a higher PCO_2 during this stage, with an average value of $6.9 \pm 0.5 \text{ g m}^{-3} \text{ h}^{-1}$.

Previous studies on aerobic BTEX removal have already confirmed the inhibitory effect of the secondary metabolites produced during pollutant biodegradation. For instance, toxic inhibitory metabolites such as catechol and methylated catechols have been identified as intermediates in the aerobic biodegradation routes of these pollutants (El-Naas et al., 2014). Moreover, while the metabolites concentration in aerobic biodegradation systems is usually low at low inlet BTEX concentrations, previous observations suggest

a higher accumulation of these intermediates at similar inlet concentrations when working under anoxic conditions (Muñoz et al., 2013; Saucedo-Lucero et al., 2014). Other studies also observed a detrimental effect of feeding BTEX mixtures on the removal of a specific compound. Gallastegui et al. (2011) reported the inhibition of xylene biodegradation when toluene was also fed to the biofilter. In the particular case of both X and B, their recalcitrant nature typically limits their degradation in biological systems. In this context, a pretreatment stage based on UV oxidation might partially oxidize BTEX or their toxic metabolites into more biodegradable and less toxic intermediates such as acetaldehyde or formaldehyde (Moussavi and Mohseni, 2007). By day 139, the UV lamp was installed in the photoreactor to test its oxidation capacity in the liquid phase. While E removal was not affected by this modification, a slight decrease in T and X REs was recorded, reaching steady values of 82.6 ± 4.0 and $37.1 \pm 6.6\%$, respectively. On the contrary, a gradual increase in benzene removal was observed during this stage, achieving a maximum value of 66.8% ($EC_{max} = 1.0 \text{ g m}^{-3} \text{ h}^{-1}$), with average values of $40.5 \pm 10.5\%$ and $0.6 \pm 0.1 \text{ g m}^{-3} \text{ h}^{-1}$. The differences in the chemical structure of these compounds usually led to the formation of by-products with different properties (such as water solubility) or biodegradability after their photolysis (Moussavi and Mohseni, 2007), which might explain the different effect on the biodegradation efficiencies recorded for each BTEX. PCO_2 remained stable at $6.7 \pm 0.9 \text{ g m}^{-3} \text{ h}^{-1}$, and no pH change was either recorded, remaining at 8.5 ± 0.1 . By day 172, the UV system was installed in the inlet gas line to partially breakdown BTEX prior BTF feeding. Surprisingly, a deterioration in the abatement performance was observed for all BTEX compounds under this configuration. T biodegradation was significantly affected and the RE and EC decreased to $48.8 \pm 8.7\%$ and $0.7 \pm 0.2 \text{ g m}^{-3} \text{ h}^{-1}$ respectively.

Similarly, lower E, X and B removals were recorded, decreasing the corresponding REs to 91.7 ± 5.1 , 24.5 ± 9.4 and $28.0 \pm 10.2\%$, respectively. Unexpectedly, CO_2 production significantly increased up to values of $9.3 \pm 1.6 \text{ g m}^{-3} \text{ h}^{-1}$. This result could be attributed to an increase in the mineralization rate due to the biodegradation of the by-products formed after BTEX photolysis, thus a higher amount of carbon was directed to CO_2 production in spite of the lower removal efficiencies recorded. The pH also decreased as a result of UV pretreatment and remained at 8.0 ± 0.1 during stage VII.

Finally, the UV lamp was removed from the gas line by day 191 and the BTF was operated until day 208 as stand-alone treatment unit. Comparable T, E and X abatement efficiencies (REs of 90.8 ± 4.4 , 95.4 ± 3.9 and $33.6 \pm 11.7\%$, respectively) to those recorded during stage II (under similar operating conditions) were immediately recovered. Conversely, almost no B removal was observed during this stage VIII.

3.2 Internal structure and molecular composition of the microbial communities

The Shannon–Wiener diversity indices calculated from the bacterial DGGE gel were high for all the samples (this index often ranges from 1.5 to 3.5 (McDonald, 2003)), although a slight decrease in the diversity was observed in both the attached and suspended biomass at the end of the experiment ($H = 3.01$ and 3.20 , respectively) compared to that of the inoculum ($H = 3.67$) (Fig. 5). Moreover, whereas the similarity coefficient between the attached and the suspended biomass was higher than 94%, nearly no similarity was observed between the inoculum and the attached and suspended microbial communities (lower than 4%). The particular conditions applied in the anoxic BTF likely promoted the development of a marginal percentage of the microbial communities (able to grow in oxygen free environments) present in the inoculum

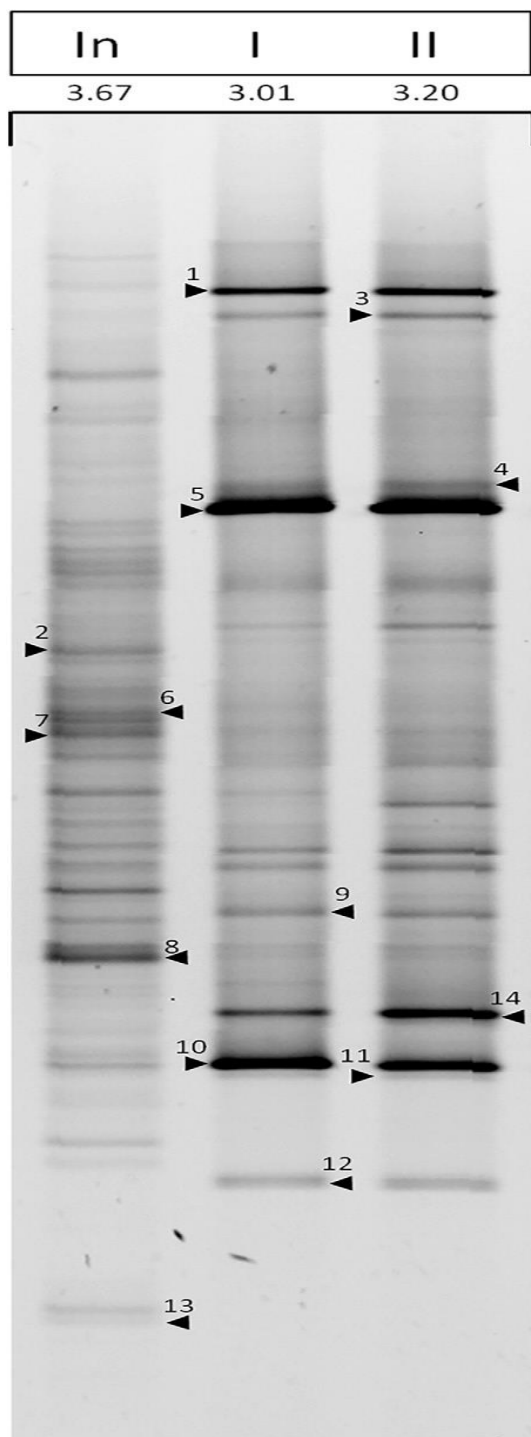


Fig. 5. DGGE profile of the main bacterial communities present in the inoculum (In) and the attached (1) and suspended biomass (2) by the end of the experimentation period. The Shannon-Wiener diversity indexes are indicated in the upper part of the gel. The sequenced bands are indicated by “▶” and the corresponding number of each band

According to the RDP classifier tool, the

14 bands sequenced from the DGGE gel belonged to four different phyla (Fig. 5, Table 2): *Proteobacteria* (8 bands), *Deinococcus-thermus* (4 bands) *Actinobacteria* (1 band) and *Chloroflexi* (1 band). *Proteobacteria* was the predominant phylum, with the genus *Dokdonella* as the main representative (band 8). This genus is commonly isolated from soil or activated sludge, and many members from *Dokdonella* spp. are denitrifying bacteria (Yoo et al., 2009; Yoon et al., 2006). Bands 3, 4 and 5 belonged to the *Alphaproteobacteria* class, which have been previously described as toluene degraders using nitrate as the electron acceptor (Shinoda et al., 2005). Within the *Proteobacteria* phylum, two of the bands present in the inoculum (2 and 6) were not retrieved from the samples at the end of the experiment.

Bands 9 to 12 belonged to the *Deinococcus-thermus* phylum and were present in both the attached and suspended microbial communities. Members of this phylum have been associated to the biodegradation of aliphatic hydrocarbons and identified in air treatment bioreactors (Lebrero et al., 2015; Li et al., 2013; Militon et al., 2010). Blast search tool identified band 13 with the specie *Bifidobacterium Longum*, within the *Actinobacteria* phylum. Genus *Bifidobacterium* has been identified in microbial communities from activated sludge (Estrada et al., 2012), however it was only retrieved in the inoculum sample. Finally, microorganisms classified into the *Chloroflexi* phylum (band 14), which have been related to toluene biodegradation in a wide variety of biological systems (Fowler et al., 2014), were found in both final biomass samples.

4. Conclusions

The continuous biodegradation of BTEX under anoxic denitrifying conditions was tested for the first time in a biotrickling filter as an end-of-pipe technology for the abatement of O₂-free BTEX emissions

commonly found in the petrochemical industry. Toluene and ethylbenzene, the easiest biodegradable compounds, were efficiently removed (> 90%) from the BTF startup, while the biodegradation of xylene was initially limited by the mass transfer of this pollutant from the gas emission to the liquid media. The low and unstable benzene abatement was associated to the accumulation of toxic intermediates. Their oxidation by a UV lamp installed in the recycling liquid line resulted in significantly higher benzene removals (up to 66.8%). Unexpectedly, the sequential coupling of the BTF with a UV-based pretreatment photoreactor did not result in an enhanced BTEX abatement performance but rather in the overall deterioration in the BTEX removal efficiency of the process. Despite the satisfactory REs achieved, the average ECs recorded (1.4, 1.5, 0.6 and 0.5 g m⁻³ h⁻¹ for toluene, ethylbenzene, xylene and benzene, respectively) were lower than those reported for aerobic biofiltration due to the lower BTEX inlet loads here tested. Finally, the particular features of the anoxic BTF here evaluated entailed a low similarity between the inoculum and the final microbial community developed, however a high diversity was always maintained throughout the entire experiment.

Acknowledgements

This work was supported by the Regional Government of Castilla y Leon (UIC 71). The program “Becas Iberoamérica. Jóvenes Profesores e Investigadores. Santander Universidades” from Santander Bank is also gratefully acknowledged for the mobility grant of Andrea Carvajal.

References

- American Water Works Association, 2012. *Standard Methods for the Examination of Water and Wastewater*. American Water Works Association/American Public Works Association/Water Environment Federation.
- Balasubramanian, P., Philip, L., Bhallamudi, S.M., 2012. Biotrickling filtration of VOC emissions from pharmaceutical industries. *Chem. Eng. J.* 209, 102–112.
- Chen, J.M., Zhu, R.Y., Yang, W.B., Zang, L.L., 2010. Treatment of a BTo-X-contaminated gas stream with a biotrickling filter inoculated with microbes bound to a wheat bran/red wood powder/diatomaceous earth carrier. *Bioresour. Technol.* 101, 8067–8073.
- EEA, 2011. *Annual European Union Greenhouse Gas Inventory 1990–2009 and Inventory Report, Technical Report No. 2/2011*.
- El-Naas, M.H., Acio, J.A., El Telib, A.E., 2014. Aerobic biodegradation of BTEX: progresses and prospects. *Journal of Environmental Chemical Engineering* 2, 1114–1122.
- EPA, 2008. *National Summary of VOC Emissions*. United States Environmental Protection Agency.
- Estrada, J., Kraakman, N.J.R., Muñoz, R., Lebrero, R., 2011. A comparative analysis of odour treatment technologies in wastewater treatment plants. *Environ. Sci. Technol.* 45, 1100–1106.
- Estrada, J.M., Rodríguez, E., Quijano, G., Muñoz, R., 2012. Influence of gaseous VOC concentration on the diversity and biodegradation performance of microbial communities. *Bioprocess Biosyst. Eng.* 35, 1477–1488.
- Fowler, S.J., Gutierrez-Zamora, M.L., Manfield, M., Gieg, L.M., 2014. Identification of toluene degraders in a methanogenic enrichment culture. *FEMS Microbiol. Ecol.* 89, 625–636.
- Gallastegui, G., Ramirez, A.A., Elias, A., Jones, J.P., Heitz, M., 2011. Performance and macrokinetic analysis of biofiltration of toluene and p-xylene mixtures in a conventional biofilter packed with inert material. *Bioresour. Technol.* 102, 7657–7665.

- Häne, B.G., Jäger, K., Drexler, H.G., 1993. The Pearson product-moment correlation coefficient is better suited for identification of DNA fingerprint profiles than band matching algorithms. *Electrophoresis* 14, 967—972.
- Lebrero, R., Hernández, L., Pérez, R., Estrada, J.M., Muñoz, R., 2015. Two-liquid phase partitioning biotrickling filters for methane abatement: exploring the potential of hydrophobic methanotrophs. *J. Environ. Manag.* 151, 124—131.
- Li, L., Han, Y., Yan, X., Liu, J., 2013. H₂S removal and bacterial structure along a full-scale biofilter bed packed with polyurethane foam in a landfill site. *Bioresour. Technol.* 147, 52—58.
- Lu, C., Lin, M.R., Chu, C., 2002. Effects of pH, moisture, and flow pattern on trickle-bed air biofilter performance for BTEX removal. *Adv. Environ. Res.* 6, 99—106.
- McDonald, G., 2003. *Biogeography: Space, Time and Life*. Wiley, New York.
- McGinnis, S., Madden, T.L., 2004. BLAST: at the core of a powerful and diverse set of sequence analysis tools. *Nucleic Acids Res.* 32.
- Milton, C., Boucher, D., Vachelard, C., Perchet, G., Barra, V., Troquet, J., Peyretailade, E., Peyret, P., 2010. Bacterial community changes during bioremediation of aliphatic hydrocarbon-contaminated soil. *FEMS Microbiol. Ecol.* 74, 669—681.
- Moussavi, G., Mohseni, M., 2007. Using UV pretreatment to enhance biofiltration of mixtures of aromatic VOCs. *J. Hazard. Mater.* 144, 59—66.
- Mudliar, S., Giri, B., Padoley, K., Satpute, D., Dixit, R., Bhatt, P., Pandey, R., Juwarkar, A., Vaidya, A., 2010. Bioreactors for treatment of VOCs and odours — a review. *J. Environ. Manag.* 91, 1039—1054.
- Muñoz, R., Souza, T.S.O., Glittmann, L., Pérez, R., Guillermo, G., 2013. Biological anoxic treatment of O₂-free VOC emissions from the petrochemical industry: a proof of concept study. *J. Hazard. Mater.* 260, 442—450.
- Rahul, Mathur A.K., Balomajumder, C., 2013. Biological treatment and modelling aspect of BTEX abatement process in a biofilter. *Bioresour. Technol.* 142, 9—17.
- Rene, E.R., Mohammed, B.T., Veiga, M.C., Kennes, C., 2012. Biodegradation of BTEX in a fungal biofilter: influence of operational parameters, effect of shockloads and substrate stratification. *Bioresour. Technol.* 116, 204—213.
- Roest, K., Heilig, H.G., Smidt, H., de Vos, W.M., Stams, A.J.M., Akkermans, A.D.L., 2005. Community analysis of a full-scale anaerobic bioreactor treating paper mill wastewater. *Syst. Appl. Microbiol.* 28, 175—185.
- Saucedo-Lucero, O., Marcos, R., Salvador, M., Arriaga, S., Muñoz, R., Quijano, G., 2014. Treatment of O₂-free toluene emissions by anoxic biotrickling filtration. *Chemosphere* 117, 774—780.
- Shinoda, Y., Akagi, J., Uchihashi, Y., Hiraishi, A., Yukawa, H., Yurimoto, H., Sakai, Y., Kato, N., 2005. Anaerobic degradation of aromatic compounds by magnetospirillum strains: isolation and degradation genes. *Biosci. Biotechnol. Biochem.* 69, 1483—1491.
- Torretta, V., Collivignarelli, M.C., Raboni, M., Viotti, P., 2015. Experimental treatment of a refinery waste air stream, for BTEX removal, by water scrubbing and biotrickling on a bed of *Mitilus edulis* shells. *Environ. Technol.* 36, 2300—2307.
- Trigueros, D.E.G., Módenes, N.A., Kroumov, D.A., Espinoza-Quñones, F.R., 2010. Modeling of biodegradation process of BTEX compounds: kinetic parameters estimation by using particle swarm global

- optimizer. *Process Biochem.* 45, 1355–1361.
- Wang, Q., Garrity, G.M., Tiedje, J.M., Cole, J.R., 2007. Naïve Bayesian classifier for rapid assignment of rRNA sequences into the new bacterial taxonomy. *Appl. Environ. Microbiol.* 73, 5261–5267.
- Wang, X., Lu, B., Zhou, X., Li, W., 2013. Evaluation of o-xylene and other volatile organic compounds removal using a xylene-acclimated biotrickling filter. *Environ. Technol.* 34, 2691–2699.
- Yan, L., Liu, J., Feng, Z., Zhao, P., 2016. Continuous degradation of BTEX in landfill gas by the UV-Fenton reaction. *Royal Society of Chemistry* 6, 1452–1459.
- Yoo, S.H., Weon, H.Y., Anandham, R., Kim, B.Y., Hong, S.B., Jeon, Y.A., Koo, B.S., Kwon, S.W., 2009. *Dokdonella soli* sp. nov., a gammaproteobacterium isolated from soil. *Int. J. Syst. Evol. Microbiol.* 59, 1965–1968.
- Yoon, J.-H., Kang, S.-J., Oh, T.-K., 2006. *Dokdonella koreensis* gen. nov., sp. nov., isolated from soil. *Int. J. Syst. Evol. Microbiol.* 56, 145–150.



Universidad de Valladolid

CHAPTER 7

**Trimethylamine Abatement in Algal-Bacterial
Photobioreactors Coupled with Nitrogen Recovery**

Trimethylamine abatement in algal-bacterial photobioreactors coupled with nitrogen recovery

Celia Pascual¹, Ilker Akmirza^{1,2}, Raúl Muñoz¹, Raquel Lebrero¹

¹Department of Chemical Engineering and Environmental Technology, University of Valladolid, Dr. Mergelina s/n., Valladolid 47011, Spain

²Department of Environmental Engineering, Technical University of Istanbul, 34469 Istanbul, Turkey

Author for correspondence: raquel.lebrero@iq.uva.es

*Unpublished Manuscript

Abstract

Trimethylamine (TMA) is an odorous volatile organic compound emitted by industries such as fish processing plants or wastewater treatment plants. Treatment of these TMA-loaded air emissions can be performed by biodegradation. In this work, the removal of trimethylamine is studied in two different biological processes: a bubble column reactor (BC) inoculated with activated sludge and a bubble column photobioreactor (PBC) with a consortium of algae and bacteria. The results indicated that the PBC reached higher removal efficiencies and removal capabilities than the BC operating at the same conditions. BC reached a removal efficiency and elimination capacity of $78 \pm 5 \%$ and $12.1 \pm 2.2 \text{ g TMA m}^{-3} \text{ h}^{-1}$, respectively, while PBC reached $97 \pm 3 \%$ and $16.0 \pm 2.1 \text{ g TMA m}^{-3} \cdot \text{h}$, at an empty bed resident time (EBRT) of 2 min and a TMA concentration higher than 500 mg m^{-3} . The good performance of the photobioreactor allowed to reduce the operating EBRT to 1.5 and 1 min, maintaining high REs of $98 \pm 2\%$ and $94 \pm 6\%$, and ECs of 21.2 ± 2.3 and $28.1 \pm 2.8 \text{ g m}^{-3} \cdot \text{h}^{-1}$, respectively. In the same way, BCB system improved the quality of the liquid effluent discharged by a decrease of 30 % in TN concentration. Moreover, the algal-biomass produced could be further valorized improving the economic balance of the biological process.

1. Introduction

The widespread release of odorous emissions to the atmosphere has become crucial due to their adverse effects on human health and the environment (Wei et al. 2015; Xue et al. 2013). Among odorous compounds, trimethylamine (TMA, C_3H_9N) has been identified as a potentially toxic and likely carcinogenic malodorous volatile organic compound with a low odor threshold level of $0.2 \mu\text{g m}^{-3}$ (Chang et al. 2004; Wan et al. 2011). TMA is emitted in wastewater treatment and composting facilities, livestock farms and fish meal manufacturing plants; being partially responsible for the unpleasant odor that characterizes these emissions (Chang et al. 2004; Ding et al. 2008). Proper management of TMA emissions according to environmental regulatory limits is crucial not only to avoid safety and health hazards, but also to eliminate environmental impacts (i.e. greenhouse effect, acid rain and eutrophication) (Chang et al. 2004; Perillo and Rodríguez 2016). Moreover, previous studies pointed out that TMA has an inhibitory impact upon the synthesis of macromolecules such as DNA, RNA and proteins, besides inducing teratogenic effects on animal embryos (Ding et al. 2008; Kim et al. 2003; Liffourrena and Lucchesi 2014).

Biotechnologies have been widely proven as cost-effective and environmentally friendly alternatives to physical-chemical technologies for the abatement of odorous and toxic gaseous compounds (Estrada et al. 2011; Ho et al. 2008). Moreover, microorganisms belonging to different genera are capable of using TMA as the only carbon and energy source (i.e. *Paracoccus*, *Hyphomicrobium*, *Methylophilus*, *Arthrobacter*, *Aminobacter*, *Haloanaerobacter* and *Bacillus*). In this context, previous studies have

demonstrated the feasibility of biologically degrading TMA in packed bed bioreactors such as biofilters and biotrickling filters (Aguirre et al. 2018; Ding et al. 2008; Wan et al. 2011). However, even if high TMA removal rates have been achieved, the accumulation of NH_3 (end product of the aerobic oxidation of TMA) leads to alkalization and might limit biological degradation (Ho et al. 2008). In addition to this drawback, the high gas empty bed residence time (EBRT) required represents an important limitation for their implementation at large scale.

In the past decades, algal-bacterial based technologies have been widely studied for their capacity to simultaneously degrading toxic and/or recalcitrant organic materials and depleting nutrients such as ammonium at high removal rates (Borde et al. 2003; Muñoz and Guieysse 2006). In this context, processes based on the symbiotic interaction between microalgae and bacteria may constitute a competitive alternative where TMA is oxidized by bacteria and $N-NH_3$ is fixed as algal biomass. Microalgae also fix part of the CO_2 produced and provide oxygen during the photosynthetic activity, thus reducing both the CO_2 footprint and the aeration and energy input requirements (Kang et al. 2017). Moreover, the biomass generated in these processes can be further valorized as biofuel, for biogas production through digestion or as animal feedstock, among others applications (Munoz and Guieysse, 2006). Nevertheless, the implementation of microalgae-bacteria processes for waste gas treatment has been scarcely studied. In this regard, the configuration of the photobioreactor is of key importance and might ensure efficient light penetration in the algal-bacterial cultivation broth. Bubble column reactors ensure construction and operation simplicity (Chang et al. 2017; Merchuk et al. 2007), provide close gas-

liquid contact and high mass and heat transfer efficiency, and present low operating costs (Vo et al. 2018; Zhang et al. 2018).

This research comparatively studied the TMA removal performance of a bubble column bioreactor (BC) inoculated with activated sludge and a bubble column photobioreactor (PBC) operating with an algal-bacterial consortium. Results from this research will allow to elucidate the TMA abatement capacity of the PBC while demonstrating the potential benefits on the quality of both the treated gaseous stream (in terms of CO₂ reduction) and the liquid effluent (lower concentration of N-containing species). The specialization of the microbial community in the PBC will be also analyzed by pyrosequencing.

2. Materials and Methods

2.1 Inoculum

Activated sludge from Valladolid wastewater treatment plant (Valladolid, Spain) was used to inoculate the BC, while a mixed inoculum containing activated sludge and microalgae was used to inoculate the PBC. Microalgae were obtained from a biogas upgrading high rate algal pond at a total suspended solids (TSS) concentration of 1.62 g L⁻¹ and volatile suspended solids (VSS) of 1.48 g L⁻¹ (Franco-Morgado et al. 2017).

2.2 Chemicals and mineral salt medium

The mineral salt medium (MSM) was composed of (g L⁻¹): Na₂HPO₄ · 12H₂O, 6.15; KH₂PO₄, 1.52; MgSO₄ · 7H₂O, 0.2; CaCl₂, 0.038; and 10 mL L⁻¹ of a SL4 solution containing (g L⁻¹): EDTA, 0.5; FeSO₄ · 7H₂O, 0.2; ZnSO₄ · 7H₂O, 0.01; MnCl₂ · 7H₂O, 0.003. All the chemical used for the preparation of the MSM were purchased in Panreac (Barcelona, Spain). Trimethylamine (45 % purity) was obtained from Sigma Aldrich (San Luis, EEUU).

2.3 Experimental setup and operating procedure

The experimental setup (Fig. 1) consisted of a cylindrical PVC column (height, 0.58 m; inner diameter, 0.094 m) with a working volume of 4 L. The synthetic contaminated stream was prepared by injecting a TMA liquid solution (Sigma-Aldrich, Spain, 45 % w/w) with a syringe pump (Fusion 100, Chemyx Inc. USA) into an air stream of 2 L min⁻¹, resulting in an average inlet concentration of 558.2 ± 78.2 mg m⁻³. The gas stream first entered a mixing chamber in order to ensure complete TMA evaporation and homogenization before being fed to the reactor through a porous diffuser (pore diameter of 10 µm) located at the bottom.

For the inoculation of the BC, 2 L of the aerobic activated sludge were centrifuged for 10 min at 10000 rpm and the pellet resuspended in 1 L of MSM. The inoculum was added to the BC and fresh MSM was supplemented upon filling the 4 L of working volume, resulting in TSS and VSS concentrations of 2.79 and 2.13 g L⁻¹, respectively.

The inoculation of the PBC was performed by centrifugation of 1 L of the aerobic activated sludge and 1 L of the microalgae culture (10 min, 10000 rpm). The pellets were resuspended in 1 L of MSM, added to the PBC and filling up to 4 L with fresh MSM at initial TSS and VSS concentrations of 2.18 and 1.76 g L⁻¹, respectively.

The BC was operated for 78 days at an empty bed residence time (EBRT) of 2 min and daily replacement of 250 mL of the culture broth with fresh MSM. During the first 50 days of operation, all the biomass was recovered from the retrieved cultivation broth by centrifugation and returned to the bioreactor (equivalent to an infinite solid retention time) in order to promote biomass accumulation until reaching ~ 3 g VSS L⁻¹. From day 45

onwards, 75 of the 250 mL of the cultivation broth daily retrieved were discarded (cell retention time = 53.3 days) in order to maintain a constant VSS concentration in the bioreactor.

The PBC was operated for 103 days after inoculation. CO₂ was added to the inlet gas stream at a concentration of 6 % v/v in order to supply inorganic carbon for microalgae. To this end, 1.88 L min⁻¹ of air stream were mixed with 0.12 L min⁻¹ of pure CO₂ (Abelló Linde, Spain). A set of LED lights was installed around the reactor column, providing a photosynthetic active radiation (PAR) of ~ 250 μmol m⁻² s⁻¹. The PBC was operated during the first 54 days at an EBRT of 2 min and a daily MSM exchange rate of 250 mL (equivalent to a dilution rate of 0.0625 d⁻¹). Between days 55 and 79, the EBRT was reduced to 1.5 min and the MSM exchange rate increased up to 375 mL d⁻¹. Finally, from day 80 onwards, the EBRT was further decreased to 1 min and 500 mL of MSM were daily exchanged. During the first 12 days of operation, the biomass was recovered from the withdrawn cultivation broth and returned to the PBC after centrifugation in order to increase VSS concentration in the reactor. From this day on, the amount of biomass returned to the system was adjusted in order to maintain an approximately constant biomass concentration of 3.5 g VSS L⁻¹.

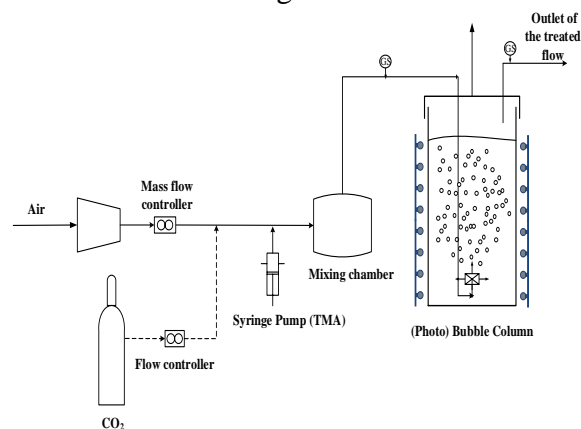


Fig. 1. Schematic representation of the experimental setup. GS: Gas sampling port

2.4 Analytical Procedures

TMA concentration was analyzed in a Bruker 3900 gas chromatograph (Palo Alto, USA) equipped with a flame ionization detector and a Supelco HP-5-MS (30 m × 0.25 μm × 0.25 μm). The oven, detector and injector temperatures were kept constant at 250, 300 and 200 °C, respectively, for 2.5 min.

CO₂ and O₂ concentrations were determined in a Bruker 430 gas chromatograph (Palo Alto, USA) coupled with a thermal conductivity detector and equipped with a CP-Molsieve 5A (15 m × 0.53 m × 15 m) and a P-PoraBOND Q (25 m × 0.53 m × 10 m) columns. Oven, detector and injector temperatures were kept constant at 45, 200 and 150 °C for 5 min, respectively.

The pressure in the inlet stream was daily measured using a differential pressure sensor IFM (Essen, Germany) to check the actual flow of the inlet gas into the reactor. The pH was daily analyzed in the cultivation broth using a glass membrane electrode PH BASIC 20, Crison (Barcelona, Spain). Dissolved oxygen (DO) and temperature were also analyzed in the cultivation broth of the PBC using a Cellox 325 oxygen meter with a temperature sensor, WTW (New York, EEUU). Two times per week, samples of the liquid phase of both bioreactors were drawn for the determination of TSS, total organic carbon (TOC), inorganic carbon (IC), total nitrogen (TN), ammonia (NH₄⁺), nitrite (NO₂⁻) and nitrate (NO₃⁻) concentrations. The TSS concentration was estimated according to standard methods (American Water Works Association, 2012). TOC, IC and TN concentrations were measured using a Shimadzu TOC-VCSH analyzer (Japan) coupled with a TNM-1 chemiluminescence module. NH₄⁺ was analyzed with an Orion Dual Star ammonium electrode (Thermo Scientific, The Netherlands). Finally, 1 mL samples

for nitrite and nitrate determination were filtered with 0.22 μm filters and analyzed by liquid chromatography HPLC-IC using a Waters 515 HPLC pump coupled with a conductivity detector (Waters 432) and equipped with an IC-PAK Anion HC column (4.6 \times 150 mm) and an IC-Pak Anion Guard-Pak (Waters). Samples were eluted isocratically at 2 mL min^{-1} (at room temperature) with a solution of distilled water/acetonitrile/n-butanol/buffer at 84/12/2/2% v/v (Muñoz et al., 2013). The determination of the algal-bacterial biomass carbon (C), hydrogen (H) and nitrogen (N) content, at the end of the experimental period of the PBC, was performed using a conducted in a LECO CHNS-932 analyzer.

2.5 DNA extraction, illumina library preparation and pyrosequencing

Two samples were drawn for biological analysis from the cultivation broth of the PBC: I-PBC (corresponding to the algal-bacterial inoculum) and F-PBC (at the end of the experimental period). Total genomic DNA was extracted from 500 μL of sample using the Fast DNA Spin kit for soil (Biomedical, USA) according to the manufacturer's instructions. DNA concentration was estimated by the Qubit fluorometer from Invitrogen, and the final concentration of the DNA sample was normalized to 5 ng μL^{-1} . The extracted DNA was stored at -20°C prior to pyrosequencing. Amplicon sequencing was carried out targeting the 16S V3 and V4 regions (464bp, *Escherichia coli* based coordinates) with the bacterial primers S-D-Bact-0341-b-S-17 and S-D-Bact-0785-a-A-21, forward and reverse, respectively, which were chosen according to (Klindworth et al., 2013). Illumina adapter overhang nucleotide sequences were added to the gene-specific sequences, thus resulting in the following full-length primers for the analysis: 5'TCGTTCGGCAGCGTCAGATGTGTAT

AAGAGACAGCCTACGGGNGGCWGCAG (16S amplicon PCR forward primer), and 5'GTCTCGTGGGCTCGGAGATGTGTA TAAGAGACAGGACTACHVGGGTATCTAATCC (16S amplicon PCR reverse primer). Indexed paired-end libraries were generated using the Nextera XT DNA Sample Preparation Kit (Illumina, San Diego, CA), with a reduced number of PCR cycles (25) using 55°C as annealing temperature. Libraries were then normalized and pooled prior to sequencing. Non-indexed PhiX library (Illumina, San Diego, CA) was used as performance control. Samples containing indexed amplicons were loaded onto the MiSeq reagent cartridge and onto the instrument along with the flow cell for automated cluster generation and paired-end sequencing with dual s (2 \times 300bp run, MiSeq Reagent Kit v3) (Illumina, San Diego, CA). The pyrosequencing analysis was carried by the Foundation for the Promotion of Health and Biomedical Research of Valencia Region (FISABIO, Spain).

Only reads with quality value scores ≥ 20 in more than 99% of the sequence after demultiplexing were extracted for further analysis. All sequences with ambiguous base calls were discarded. Quality assessment was performed using the PRINSEQ-LITE program (Schmieder and Edwards, 2011). After quality assessment, paired-end reads were joined together with the FASTQ-JOIN program (Aronesty, 2011). The eventual chimeras belonging to PCR artifacts among the sequences were discarded using the USEARCH program (Edgar, 2010), and taxonomic assignments were then carried out using the RDP-Classifer from the Ribosomal Database Project (Cole et al., 2009; Wang et al., 2007), which is available from the RDP website (<http://rdp.cme.msu.edu/classifier/>). Simpson and Shannon indexes

were calculated using the Vegan library version 2.3e1 (Oksanen et al., 2015). The Krona tool was used to represent relative abundances and confidences within the complex hierarchies of metagenomics classifications (Ondov et al., 2011). The nucleotide sequence dataset was deposited in the European Nucleotide Archive (ENA) or NCBI under the study.

2.7 Data analysis

The statistical data analysis was performed using SPSS 20.0 (IBM, USA). The results are given as the average \pm standard deviation. Significant differences were analyzed by ANOVA and post-hoc analysis for multiple group comparisons. Differences were considered to be significant at $p \leq 0.05$.

3. Results and discussion

3.1 Performance of the activated sludge bioreactor (BC).

Immediately after BC start-up, TMA removal efficiency (RE) reached values of $\sim 80\%$, recording an average removal of $78 \pm 5\%$ during the complete experimentation period (Fig. 2, white bars). The maximum RE (88.3%) was observed by day 52 of operation, corresponding to an inlet TMA concentration of 658.7 mg m^{-3} . The average elimination capacity (EC) in the system was $12.1 \pm 2.2 \text{ g TMA m}^{-3} \text{ h}^{-1}$, and the maximum EC value of $16.65 \text{ g TMA m}^{-3} \text{ h}^{-1}$ was achieved by day 64 at an inlet TMA concentration of 637.6 mg m^{-3} . By day 30 of operation, a mass transfer test was performed by increasing ~ 2 times the TMA inlet concentration for 11 hours in order to determine if the system was limited by biological activity or by mass transfer (Fig. S1, supplementary materials).

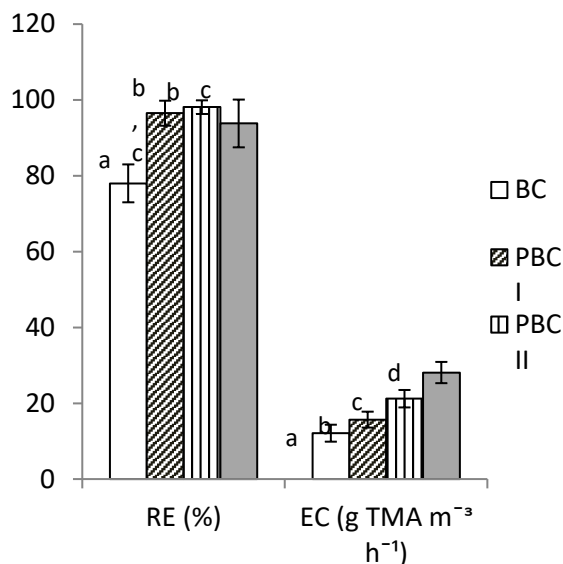


Fig. 2. Average TMA removal efficiencies and elimination capacities in the BC (white bars) and the PBC at the three EBRTs tested: (I) 2 min, (II) 1.5 min and (III) 1 min. Vertical lines represent standard deviation. Columns within each group with different letters were significantly different at $p < 0.05$.

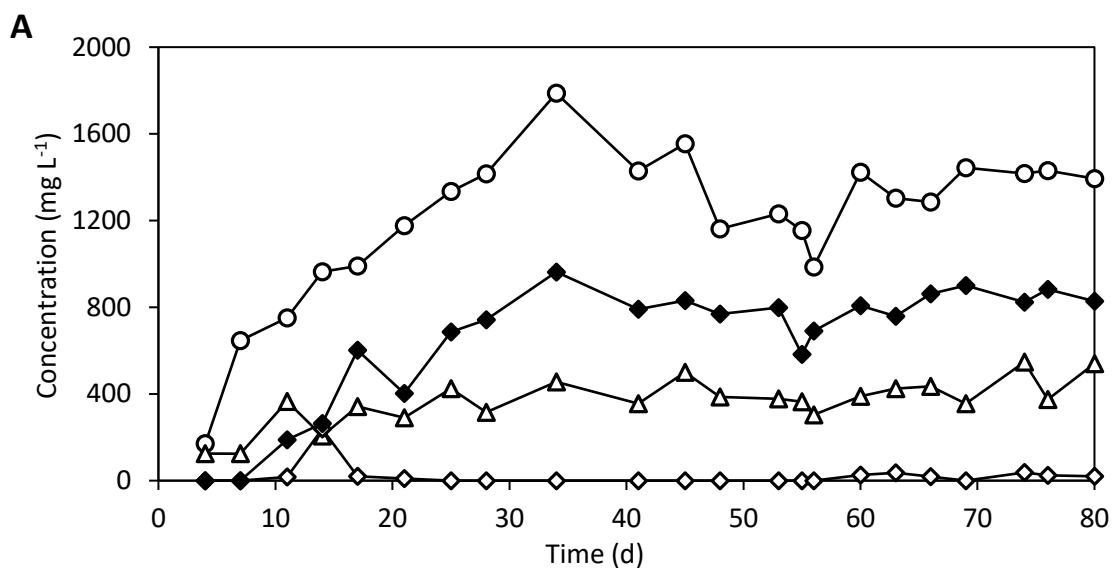
Inlet and outlet gas samples were hourly taken to analyze TMA and CO_2 concentrations. The TMA inlet concentration increased from $\sim 480 \text{ mg m}^{-3}$ up to $1041 \pm 159 \text{ mg m}^{-3}$ during the test. As a result, a concomitant increase in the EC up to $22.3 \text{ g m}^{-3} \text{ h}^{-1}$ was observed compared with previous steady values of $11.4 \text{ g m}^{-3} \text{ h}^{-1}$, corroborating that system was limited by mass transfer.

A high CO_2 production was recorded right after the start-up of the BC, reaching a maximum concentration of 5.79 g m^{-3} by day 3 of operation. This high production rate ($121.9 \text{ g CO}_2 \text{ m}^{-3} \text{ h}^{-1}$) was attributed to the degradation of both TMA and cell debris and death biomass from the inoculum. From this day, CO_2 concentration gradually decreased until stabilizing at 1.61 ± 0.67 from day 27 onwards. The activation of nitrifying bacteria, autotrophic consumers of CO_2 , likely contributed to the reduction of the

emitted CO₂, with final production values of 27.9 g CO₂ m⁻³ h⁻¹.

As previously mentioned, ammonia is produced from the aerobic degradation of TMA, and its accumulation in the cultivation broth might result in inhibitory effects in the microbial community. Thus, the analysis of the variation of the pH and the nitrogen species in the liquid phase is of key importance in biological reactors devoted to TMA removal. From day 0 to 10, the pH fluctuated between 7 and 8, this neutral value being likely associated with NH₄⁺ accumulation (NH₄⁺ concentration in the cultivation broth increased up to 365 mg N-NH₄⁺ L⁻¹ by day 10). This behavior has been previously reported in biofilters treating TMA (Ho et al. 2008). During these days, neither NO₂⁻ nor NO₃⁻ accumulation were observed (Fig.3 A). Between days 11 and 50, a gradual decrease in the pH was recorded, reaching a minimum value of 4.21 on day 49 (Fig. S2A). This pH decrease was attributed to the activation of nitrifying bacteria, which began to oxidize NH₄⁺ to NO₃⁻ up to a maximum value of 830 mg N-NO₃⁻ L⁻¹ by day 45 and triggered the acidification of the medium.

Similarly, Ho et al. (2008) observed an increase in nitrite and nitrate concentration and a decrease in NH₄⁺ concentration when species of nitrifying bacteria were inoculated in their biotrickling filter. In our particular case, NO₂⁻ accumulation was negligible compared to NO₃⁻ accumulation. After this period, the concentration of nitrogen species in the culture medium stabilized, reaching steady values of 411.3 ± 78.6 mg N-NH₄⁺ L⁻¹ and 793.3 ± 96.1 mg N-NO₃⁻ L⁻¹ and an average pH of 5.4 ± 0.4. Despite the high concentrations of NH₄⁺ and NO₃⁻, no toxic effect on the microbial community was observed, which was able to maintain constant TMA degradation regardless of the pH of the culture broth. An initial decrease in the VSS concentration was observed due to cell lysis, reaching a minimum value of 1.07 g L⁻¹ by day 4 (Fig. S3.A). From day 4 onwards, the VSS concentration began to increase up to a maximum value of 3.74 g L⁻¹ on day 45. Finally, a steady concentration of 3.0 ± 0.1 g L⁻¹ was maintained by setting a constant solids retention time.



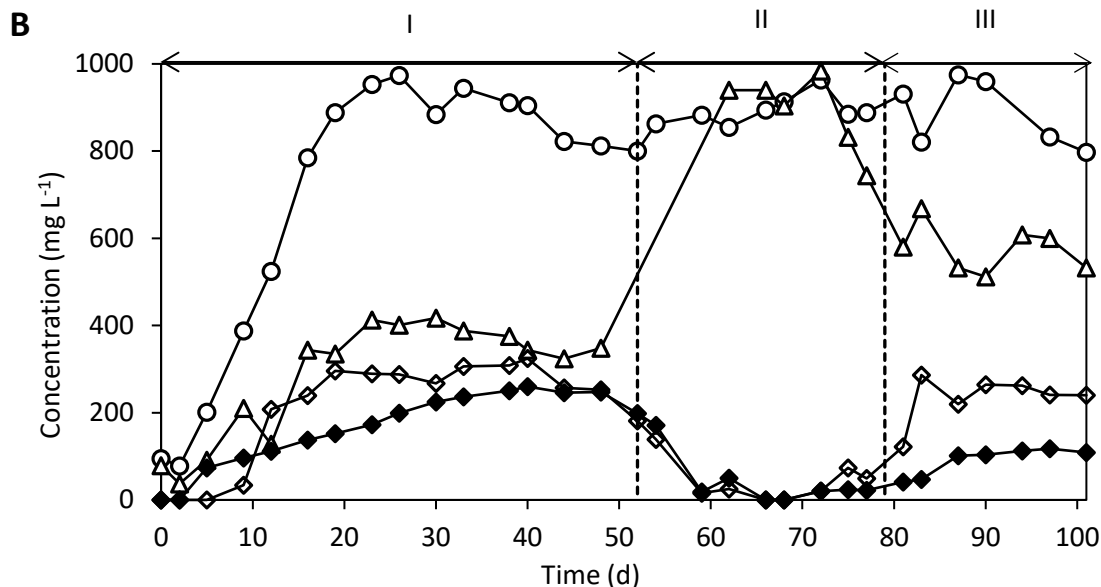


Fig. 3. Time course of the nitrogen species in the BC (A) and the PBC (B): TN (\circ), N-NH_4^+ (Δ), N-NO_3^- (\blacklozenge) and N-NO_2^- (\diamond).

3.2 Performance of the algae-bacteria photobioreactor (PBC)

Following PBC start-up, a high removal performance was immediately recorded, maintaining average REs of $97 \pm 3\%$ and ECs of $16.0 \pm 2.1 \text{ g m}^{-3} \text{ h}$ during the first operating stage at an EBRT of 2 min (Fig. 2). TMA outlet concentrations were significantly lower compared to those observed in the BC, with average values of $22.1 \pm 18.5 \text{ mg m}^{-3}$. This outlet TMA concentration was even below the detection limit on certain days of operation. A maximum EC of $18.5 \text{ g m}^{-3} \text{ h}^{-1}$ was recorded on day 4 corresponding to a TMA inlet concentration of 654.8 g m^{-3} . The good performance of the photobioreactor allowed to further reducing the operating EBRT to 1.5 min (stage II) and 1 min (stage III), maintaining high REs of $98 \pm 2\%$ and $94 \pm 6\%$, respectively. The increase in TMA load resulted in ECs considerably higher under these operating conditions, reaching stationary values of 21.2 ± 2.3 and 28.1 ± 2.8

$\text{g m}^{-3} \cdot \text{h}^{-1}$, respectively (Fig. 2, PBC stages II and III). These results were considerably better than those obtained in previous biodegradation studies. For instance, Wan et al. (2011) recorded a RE of $\sim 79\%$ in a biotrickling filter that treated a contaminated stream with 420 mg m^{-3} of TMA, corresponding to a maximum EC of $13.95 \text{ g TMA m}^{-3} \text{ h}^{-1}$ at an EBRT of 60 s.

A net CO_2 consumption (taking into account CO_2 supplemented and CO_2 produced by heterotrophic bacteria) of $\sim 9\%$ was recorded throughout the experimental period as a result of inorganic carbon assimilation by microalgae and nitrifying bacteria. An average CO_2 concentration value of $151.8 \pm 21.0 \text{ g m}^{-3}$ was obtained regardless of the operating conditions. On the other hand, the outlet O_2 concentration exceeded the inlet concentration value throughout the complete experimentation period.

In terms of nitrogen species, NH_4^+ concentration steadily increased after PBC start-up at an EBRT of 2 min, reaching a

steady value of $368.9 \pm 34.2 \text{ mg N-NH}_4^+ \text{ L}^{-1}$ from day 16 onwards. However, nitrifying bacteria were activated much earlier compared to the BC, resulting in the accumulation of NO_3^- and NO_2^- from days 5 and 9, respectively. In addition, NO_2^- concentration increased above NO_3^- concentration by day 12. From day 33 onwards, these nitrogen species stabilized at $289.6 \pm 32.7 \text{ mg N-NO}_2^- \text{ L}^{-1}$ and $248.1 \pm 8.4 \text{ mg N-NO}_3^- \text{ L}^{-1}$ (Fig. 3B I). When the EBRT was reduced to 1.5 min (stage II), a sharp decrease in the concentration of both nitrite and nitrate was observed, maintaining steady values of $47.9 \pm 26.6 \text{ mg N-NO}_2^- \text{ L}^{-1}$ and $22.1 \pm 1.8 \text{ mg N-NO}_3^- \text{ L}^{-1}$ during this stage. On the contrary, ammonia concentration increased up to $853.3 \pm 121.4 \text{ mg N-NH}_4^+ \text{ L}^{-1}$, which suggested a inhibition of the nitrifying bacteria, highly sensitive to ammonia loading (Awolusi et al. 2016). A slight recovery of the nitrifying activity was observed during stage III, decreasing ammonia concentration to $592.7 \pm 60.1 \text{ mg N-NH}_4^+ \text{ L}^{-1}$ while increasing nitrate and nitrite concentrations to steady values of 252.2 ± 23.4 and $110.8 \pm 5.9 \text{ mg N L}^{-1}$, respectively (Fig. 3B).

An average temperature of $30.7 \pm 1.0 \text{ }^\circ\text{C}$ was recorded in the PBC cultivation broth, slightly higher than the controlled room temperature ($25 \text{ }^\circ\text{C}$) due to the illumination of the reactor with LED lights. The DO in the medium remained at 5.7 ± 0.8 , 6.7 ± 0.4 and $7.2 \pm 0.2 \text{ mg L}^{-1}$ in stages I, II and II, respectively, always below the saturation value of the water at the operating temperature (7.6 mg L^{-1}), due to aerobic degradation. However, the increase in the DO when increasing the EBRT can be attributed to the higher nitrogen load and thus a higher growth of microalgal biomass and photosynthetic activity. As well as the concentration of O_2 in the treated gas stream, this value confirmed that the system was not limited by oxygen

availability. The pH remained roughly constant throughout the complete experimentation period, with average values of 6.7 ± 0.3 , 7.7 ± 0.2 and 7.4 ± 0.2 at stages I, II and III, respectively (Fig. S2B).

After inoculation, TSS and VSS concentrations of 2.18 and 1.76 g L^{-1} , respectively, were recorded. A decrease in VSS concentration was observed during the first operating days, reaching a minimum value of 1.15 g L^{-1} . From day 5, biomass concentration recovered increasing up to $3.84 \text{ g VSS L}^{-1}$ on day 12 (Fig. S3B). A daily purge of biomass was then implemented in order to keep an almost constant VSS concentration of 3.13 ± 1.04 , 4.41 ± 0.39 and $3.65 \pm 0.61 \text{ g L}^{-1}$, in stages I, II and III, respectively. It is important to remark that a higher biomass growth was recorded in the PBC compared to the BC due to the contribution of the algal biomass.

3.3 Comparative analysis between BC and PBC

Overall, the PBC showed a better TMA removal performance than the conventional BC at an EBRT of 2 min, with $\text{EC} \times 1.3$ times higher compared to those obtained in the BC at this EBRT. This improved behavior was attributed to the pH, which was maintained close to optimum values (6-8) for enzymatic activity of TMA-degrading bacteria (Chang 2004). In this sense, during BC operation, the pH was below this optimal interval likely due to nitrification, while an average value of 6.7 ± 0.3 was recorded in the PCB due to N assimilation by microalgae. This enhanced behavior allowed reducing the EBRT in the PCB to 1 min, resulting in statistically similar REs and considerably higher ECs (up to $\times 2.3$).

Likewise, an improvement in the quality of the liquid effluent in terms of N content was observed in the PBC. A total nitrogen mass balance showed that 30 % less nitrogen is discharged in the exchanged PBC cultivation broth compared to that of the BC,

even for EBRTs of 1.5 and 1 min where TMA load was 1.5 and 2 times higher, respectively (Fig. 4). TN concentration decreased significantly from a value of $1306.7 \pm 148.7 \text{ mg L}^{-1}$ in the BC to 878.8 ± 58.4 , 893.1 ± 33.8 and 886.1 ± 77.9 in the PBC at stages I, II and III, respectively, this decrease being associated to nitrogen assimilation by algal biomass. In this context, nitrogen is the second most abundant element of algal biomass, with a content ranging between 5 and 10 % of its dry weight, as the analysis of algal-bacterial biomass CHN content showed (42.3 ± 4.2 % C, 6.0 ± 0.6 % H and 6.2 ± 1.3 % N). It can be assimilated in the forms of NO_3^- , NO_2^- , NO or NH_4^+ , although assimilation of the smaller forms of nitrogen is preferred by microalgae, thus hindering nitrite and nitrate uptake when ammonia is present (Markou et al. 2014). Surprisingly, even though NH_4^+ and NO_2^- would be the preferred forms for algae assimilation, their concentrations increased in the PBC during stages I and II, respectively. This was likely due to the inhibition of different stages of the nitrification process, where ammonia oxidizing bacteria (AOB) oxidize NH_4^+ to NO_2^- , which is subsequently oxidized to NO_3^- by nitrite-oxidizing bacteria (NOB). In this regard, the accumulation of nitrite in stage I was attributed to the partial nitrification of NH_4^+ as a result of the high temperature in the reactor (~ 31 °C), which could hinder the activity of NOB bacteria such as *Nitrobacter* (optimum temperature range ~ 24 – 25 °C) (Awolusi et al. 2016; Huang, Gedalanga, and Olson 2010). Thus, an incomplete nitrification would trigger the accumulation of NO_2^- in the medium. On the other hand, NH_4^+ concentration increased in stage II. The higher TMA load applied at this lower EBRT might inhibit nitrifying bacteria activity due to their greater sensitivity to changes in NH_4^+ loading rates (Awolusi et al. 2016; Hu et al. 2009), ceasing the nitrification process. In stage III,

NO_2^- concentration increased significantly up to close values to those of stage I, probably due to the adaptation of nitrifying bacteria to the operating temperature and NH_4^+ loading rates.

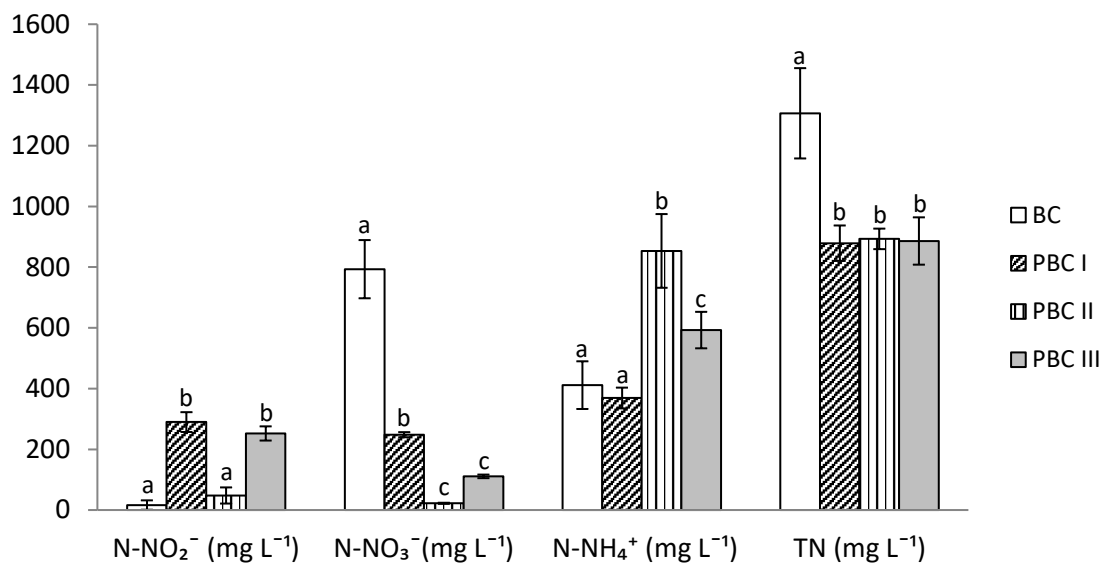


Fig. 4. Concentration profiles of nitrogen-containing species in the BC (white columns) and PBC at the three EBRTs tested: (I) 2 min, (II) 1.5 min and (III) 1 min. Vertical lines represent standard deviation. Columns within each group with different letters were significantly different at $p < 0.05$.

Finally, a biomass production of ~ 0.23 and $0.70 \text{ g biomass d}^{-1}$ was recorded in the BC and the PBC, respectively. This excess biomass harvested from the PBC might be further valorized and thus increase the profitability of the TMA degradation process.

4. Conclusion

This study proved the feasibility of biologically abating TMA from waste gas streams in bacterial and algal-bacterial bubble column reactors. The reactor inoculated with activate sludge achieved REs of 78 % and ECs of $12 \text{ g TMA m}^{-3} \text{ h}^{-1}$ for an inlet TMA concentration of $\sim 500 \text{ mg m}^{-3}$ and an EBRT of 2 min. Conversely, the photobioreactor operated with an algal-bacterial consortium increased the REs by $> 10 \%$ and reached ECs of $16 \text{ g TMA m}^{-3} \cdot \text{h}^{-1}$ under similar conditions. This improved performance allowed for further reducing the EBRT to 1.5 and 1 min, maintaining satisfactory stationary REs of $98 \pm 2 \%$ and $94 \pm 6 \%$, respectively. The

ECs recorded at these EBRTs were considerably higher as a result of the higher TMA loads, with steady state values of 21.2 ± 2.3 y $28.1 \pm 2.8 \text{ g m}^{-3} \text{ h}^{-1}$ at 1.5 and 1 min, respectively. Algal activity in the PBC also resulted in an improvement of the quality of the withdrawn cultivation broth by decreasing the TN concentration by $\sim 30 \%$, as well enhancing the economic viability of the biological process through a subsequent algal biomass revalorization.

References

- Aguirre, Alberto et al. 2018. "Biofiltration of Trimethylamine in Biotrickling Filter Inoculated with *Aminobacter Aminovorans*." *Electronic Journal of Biotechnology* 33:63–67.
- American Water Works Association, 2012
American Water Works Association
- Standard Methods for the Examination of Water and Wastewater
American Water Works Association/American Public Works Association/Water Environment Federation (2012)
- Awolusi, Oluyemi Olatunji, Mahmoud Nasr, Sheena Kumari, and Faizal Bux. 2016. "Artificial Intelligence for the Evaluation of Operational Parameters Influencing Nitrification and Nitrifiers in an Activated Sludge Process." *Microbial Ecology* 72(1):49–63.
- Borde, Xavier et al. 2003. "Synergistic Relationships in Algal-Bacterial Microcosms for the Treatment of Aromatic Pollutants." *Bioresource Technology* 86(3):293–300.
- Cantera, Sara, José M. Estrada, Raquel Lebrero, Pedro a. García-Encina, and Raúl Muñoz. 2016. "Comparative Performance Evaluation of Conventional and Two-Phase Hydrophobic Stirred Tank Reactors for Methane Abatement: Mass Transfer and Biological Considerations." *Biotechnology and Bioengineering* 113(6):1203–12.
- Chang, Chang-tang. 2004. "Biofiltration of Trimethylamine-Containing Waste Gas by Entrapped Mixed Microbial Cells." 55:751–56.
- Chang, Chang Tang, Bor Yann Chen, I. Shing Shiu, and Fu Teng Jeng. 2004. "Biofiltration of Trimethylamine-Containing Waste Gas by Entrapped Mixed Microbial Cells." *Chemosphere* 55(5):751–56.
- Chang, J. S. et al. 2017. *Photobioreactors*.
- Ding, Ying, Weixiang Wu, Zhiying Han, and Yingxu Chen. 2008. "Correlation of Reactor Performance and Bacterial Community Composition during the Removal of Trimethylamine in Three-Stage Biofilters." *Biochemical Engineering Journal* 38(2):248–58.
- Estrada, José M., N. J. R. Bart Kraakman, Raúl Muñoz, and Raquel Lebrero. 2011. "A Comparative Analysis of Odor Treatment Technologies in Wastewater Treatment Plants." *Environmental Science & Technology* 45(3):1100–1106.
- Franco-Morgado, Mariana, Cynthia Alcántara, Adalberto Noyola, Raúl Muñoz, and Armando González-Sánchez. 2017. "A Study of Photosynthetic Biogas Upgrading Based on a High Rate Algal Pond under Alkaline Conditions: Influence of the Illumination Regime." *Science of the Total Environment* 592:419–25.
- Ho, Kuo Ling, Ying Chien Chung, Yueh Hsien Lin, and Ching Ping Tseng. 2008. "Biofiltration of Trimethylamine, Dimethylamine, and Methylamine by Immobilized *Paracoccus* Sp. CP2 and *Arthrobacter* Sp. CP1." *Chemosphere* 72(2):250–56.
- Hu, J. et al. 2009. "Effect of Organic Carbon on Nitrification Efficiency and Community Composition of Nitrifying Biofilms." *Journal of Environmental Sciences-China* 21(3):387–94.
- Huang, Zhonghua, Phillip B. Gedalanga, and Betty H. Olson. 2010. "Distribution of *Nitrobacter* and *Nitrospira* Communities in an Aerobic Activated Sludge Bioreactor and Their Contributions to Nitrite Oxidation." *Proceedings of the Water Environment Federation* 2010(15):2390–2403.
- Kang, Du, Qichao Zhao, Yonghong Wu, Chenxi Wu, and Wu Xiang. 2017. "Removal of Nutrients and Pharmaceuticals and Personal Care Products from Wastewater Using Periphyton Photobioreactors Removal of Nutrients and Pharmaceuticals and Personal Care Products from Wastewater Using Periphyton Photobioreactors Removal of Nutrient." *Bioresource Technology*.

- Kim, Song Gun, Hee Sung Bae, Hee Mock Oh, and Sung Taik Lee. 2003. "Isolation and Characterization of Novel Halotolerant and/or Halophilic Denitrifying Bacteria with Versatile Metabolic Pathways for the Degradation of Trimethylamine." *FEMS Microbiology Letters* 225(2):263–69.
- Liffourrena, Andrés S. and Gloria I. Lucchesi. 2014. "Degradation of Trimethylamine by Immobilized Cells of *Pseudomonas Putida* A (ATCC 12633)." *International Biodeterioration and Biodegradation* 90:88–92.
- Markou, Giorgos, Dries Vandamme, and Koenraad Muylaert. 2014. "Microalgal and Cyanobacterial Cultivation: The Supply of Nutrients." *Water Research* 65:186–202.
- Merchuk, J. C., F. Garcia-Camacho, and E. Molina-Grima. 2007. "Photobioreactor Design and Fluid Dynamics." *Chemical and Biochemical Engineering Quarterly* 21(4):345–55.
- Munoz, Raul and Benoit Guieysse. 2006. "Algal-Bacterial Processes for the Treatment of Hazardous Contaminants: A Review." *Water Research* 40(15):2799–2815.
- Perillo, P. M. and D. F. Rodríguez. 2016. "Low Temperature Trimethylamine Flexible Gas Sensor Based on TiO₂ Membrane Nanotubes." *Journal of Alloys and Compounds* 657:765–69.
- Vergara, C., R. Munoz, J. L. Campos, M. Seeger, and D. Jeison. 2016. "Influence of Light Intensity on Bacterial Nitrifying Activity in Algal-Bacterial Photobioreactors and Its Implications for Microalgae-Based Wastewater Treatment." *International Biodeterioration and Biodegradation* 114:116–21.
- Vo, Hoang Nhat Phong et al. 2018. "Effects of Nutrient Ratios and Carbon Dioxide Bio-Sequestration on Biomass Growth of *Chlorella* Sp. in Bubble Column Photobioreactor." *Journal of Environmental Management* 219:1–8. 9).
- Wan, Shungang, Guiying Li, Lei Zu, and Taicheng An. 2011. "Bioresource Technology Purification of Waste Gas Containing High Concentration Trimethylamine in Biotrickling Filter Inoculated with B350 Mixed Microorganisms." *Bioresource Technology* 102(12):6757–60. Retrieved (<http://dx.doi.org/10.1016/j.biortech.2011.03.059>).
- Wei, Zaishan et al. 2015. "Thermophilic Biotrickling Filtration of Gas-Phase Trimethylamine." *Atmospheric Pollution Research* 6(3):428–33.
- Xue, Niantao, Qunhui Wang, Juan Wang, Jianhua Wang, and Xiaohong Sun. 2013. "Odorous Composting Gas Abatement and Microbial Community Diversity in a Biotrickling Filter." *International Biodeterioration and Biodegradation* 82:73–80.
- Zhang, Chao, Xigang Yuan, Yiqing Luo, and Guocong Yu. 2018. "Prediction of Species Concentration Distribution Using a Rigorous Turbulent Mass Diffusivity Model for Bubble Column Reactor Simulation Part I: Application to Chemisorption Process of CO₂ into NaOH Solution." *Chemical Engineering Science* 184:161–71.



Universidad de Valladolid

CHAPTER 8

Conclusion

Conclusion

In this thesis work, odorous emissions from food and petrochemical industry were investigated in order to obtain an adequate characterization and ultimately enhance the cost-effectiveness and environmental friendliness of their abatement. The studies were carried out in two universities (Istanbul Technical University, Turkey and Valladolid University, Spain).

Chapter 3 presents a complete characterization of a waste-gas emission from a real bakery yeast fermentation process. The chemical composition and the sensorial properties of this gas stream from bakery yeast process were determined for the first time in terms of both objective and subjective parameters. Instrumental analyses identified ethanol, acetaldehyde and acetone as the major malodorous VOCs in the emission, which reached a maximum concentration of 1181 mg m^{-3} during the first hours of the fermentation cycle. The odor concentration of the waste gas analysed via dynamic olfactometry resulted in an odor concentration of 39725 OUE m^{-3} that exceeded by a factor of 40 the odor legal limits and made compulsory the proper management of fermentation process emissions. With this purpose, the study also identified the need to implement effective treatment technologies to abate these high concentrations of VOCs and odor prior discharge into the atmosphere. In this context, since biotechnologies represent the most sustainable alternative for the abatement of malodorous VOC at concentrations $<2000 \text{ mg m}^{-3}$, a semi-pilot scale operation was successfully implemented to treat ethanol, the dominant odorous VOC in bakery yeast fermentation emissions. The biofilter showed an almost complete biodegradation of ethanol even at concentrations higher than those found during peak emissions hour (RE of $97 \pm 1\%$ and EC of $31.7 \pm 1.2 \text{ g m}^{-3} \text{ h}^{-1}$), thus complying with legal regulations. Biofilter feeding with a waste gas containing ethanol, acetaldehyde and acetone resulted in a lower abatement performance compared to the treatment of individual VOCs likely due to substrate interactions, where ethanol and acetaldehyde abatement were balanced at $\sim 90\%$ and acetone was partially removed (70 %).

Within the work conducted in **Chapter 4** it was demonstrated that a lab-scale bio-scrubber offered a promising alternative to remove the sulphurous odor of ET from waste gas stream under anoxic conditions. Prior to anoxic bioscrubber operation, batch experiments were carried out to verify the biodegradability of ET under anoxic conditions. The Monod model was used to estimate the values for μ_{\max} , K_s , Y_{XS} and q_{\max} , which were obtained as 0.14 h^{-1} , 1.17 mg L^{-1} ,

0.52 g_x/g_s and 0.26 g_s/g_x h, respectively. The bioscubber operating conditions (EBRT, irrigation rate and inlet concentration) were optimized, the best ET degradation being achieved at an inlet concentration of 150 mg m⁻³, irrigation rate of 0.23 m³ m⁻² h⁻¹ and EBRT of 90s. S^o rather than SO₄²⁻ was obtained as the main end product at an average experimental yield value close to the theoretical value (Y_{ET/NO₃⁻}) of 0.74.

Chapter 5 evaluated for the first time the biodegradation kinetics and the interactions during the anoxic biodegradation of BTEX present as single compounds or in dual or quaternary mixtures, by a previously acclimated bacterial consortium. A complete set of kinetic parameters and their confidence intervals, calculated with the Monod model and a modified Gompertz model, were provided. Results showed that both toluene and ethylbenzene were readily biodegradable by the bacterial consortium under anoxic conditions, with maximum biodegradation rates of 0.318 and 0.473 h⁻¹ being recorded for these pollutants when degraded individually. However, the build-up of inhibitory intermediates in the liquid media resulted in a partial biodegradation of xylene and benzene when fed individually after long lag phase of 7 and 4.3 h⁻¹ respectively, compared with toluene and ethylbenzene with a lag phase less than 1 h. The co-degradation of an additional BTEX decreased the specific pollutant biodegradation rates regardless of the dual BTEX mixture, which confirmed the occurrence of a competitive inhibition. These interactions had not been previously quantified under anoxic conditions prior to the current study. Whereas Monod model provided an accurate description of the biodegradation of toluene and ethylbenzene (R² ~0.97), the Modified Gompertz model supported better fit for benzene and xylene degradation (R² ~0.91). Furthermore, the Gompertz model accurately represented the inhibitory interactions between BTEX mixtures, although it failed in representing the degradation of the recalcitrant compounds when all four BTEX were present simultaneously.

The continuous biodegradation of BTEX under anoxic denitrifying conditions was tested in **Chapter 6** for the first time in a biotrickling filter as an end-of-pipe technology for the abatement of O₂-free BTEX emissions commonly found in the petrochemical industry. Toluene and ethylbenzene, the easiest biodegradable compounds, were efficiently removed (>90%) from the BTF startup, while the biodegradation of xylene was initially limited by the mass transfer of this pollutant from the gas emission to the liquid media. The low and unstable benzene abatement was associated to the accumulation of toxic intermediates. Their oxidation by a UV

lamp installed in the recycling liquid line resulted in significantly higher benzene removals (up to 66.8%). Unexpectedly, the sequential coupling of the BTF with a UV-based pretreatment photoreactor did not result in an enhanced BTEX abatement performance but rather in the overall deterioration in the BTEX removal efficiency of the process. Despite the satisfactory REs achieved, the average ECs recorded (1.4, 1.5, 0.6 and 0.5 g m⁻³ h⁻¹ for toluene, ethylbenzene, xylene and benzene, respectively) were lower than those reported for aerobic biofiltration due to the lower BTEX inlet loads here tested. Finally, the particular features of the anoxic BTF here evaluated entailed a low similarity between the inoculum and the final microbial community developed, however a high diversity was always maintained throughout the entire experiment.

Chapter 7 illustrated the superior performance of algal-bacterial photobioreactors compared to conventional bacterial bioreactors as a result of the microalgae-mediated N fixation and enhanced nitrification induced by photosynthetic oxygen production. This resulted in superior trimethylamine (TMA) removal efficiencies and supported process operation at short gas residence times. While conventional bioreactor inoculated with activate sludge achieved REs of 78 % and ECs of 12 g TMA m⁻³ h⁻¹ for an inlet TMA concentration of ~ 500 mg m⁻³ and an EBRT of 2 min, the photobioreactor operated with an algae-bacterial consortium increased the REs by > 10 % and reached ECs of 16 g TMA m⁻³ h⁻¹ under similar conditions. This improved performance allowed for further reducing the EBRT to 1.5 and 1 min, maintaining satisfactory stationary REs of 98 ± 2 % and 94 ± 6 %, respectively. ECs recorded at these EBRTs were considerably higher because of the higher TMA loads, with steady state values of 21.2 ± 2.3 and 28.1 ± 2.8 g m⁻³ h⁻¹ at 1.5 and 1 min, respectively. Algal activity also resulted in an improvement of the quality of the withdrawn cultivation broth by decreasing the TN concentration by ~ 30 %, as well enhancing the economic viability of the biological process through a subsequent algal biomass revalorization.

Based on the outcomes and limitations encountered throughout this thesis, further research in the characterization and abatement of emissions from food and chemical/petrochemical industries should focus on:

- Development of innovative air pollution treatment technologies to overcome mass transfer limitation and the detrimental effects of substrate interactions during the biodegradation of complex VOC mixtures.
- Scale-up the biological processes to pilot and full-scale applications.
- Improvement and optimization of dynamic olfactometry and instrumental analysis.
- Integration and optimization of the abatement of ET-laden waste gas emissions within use of nitrification phase wastewater (as electron acceptor source) in WWTPs to achieve mutual benefits.
- Determination of potential inhibitory by-products during the anoxic biodegradation of BTEX emissions.
- Development of innovative microbiological strategies to enhance the biodegradation of recalcitrant compounds (benzene and xylene).
- New microbiological or technological approaches should be explored in order to improve mass transfer in biotrickling filters treating moderately (like BTEX) and highly hydrophobic pollutants.
- Optimization of operation parameters of algal –bacterial photobioreactors to treat amine group VOCs



Universidad de Valladolid

CHAPTER 9

About the Author

Bio

Ilker AKMIRZA (İzmit, Turkey 1986) graduated in 2009 from Yildiz Technical University, Turkey as Environmental Engineer. He started his Master studies at the same year at the Environmental Engineering Department of Istanbul Technical University, Turkey, where he is working as teaching and research assistant since 2011. He finished his master studies under the supervision of Prof.Dr. Kadir ALP on atmospheric dispersion modelling of industrial waste gases. İlker Akmirza graduated in June 2012 from his master and started the following month to PhD studies at the same department. Within the collaboration in October 2014 between İstanbul Technical University and Valladolid University, he joined Department of Chemical Engineering and Environmental Technology- University of Valladolid the VOCs and Odors Treatment Group as Joint- PhD student under the supervision of Prof.Dr Kadir Alp, Prof. Dr. Raúl Muñoz and Assis. Prof. Dr. Raquel Lebrero.

EDUCATION

September 2012 – to date Joint PhD Student at Dept of Environmental Engineering Istanbul Technical University, Istanbul, Turkey and Dept of Chemical Engineering and Environmental Technology Valladolid University, Valladolid, Spain. *“Removal Of Odor Emissions From Food Fermentation And Petrochemical Production Processes With Using Biological Treatment Methods”*

September 2009 – June 2012 Master in Environmental Science and Engineering: Istanbul Technical University, Istanbul Turkey. *“Development of Control Strategies for Food Industry Sourced Odor Emissions”*

September 2005 – June 2009 Bachelor in Environmental Engineering: Yildiz Technical University, Istanbul (Turkey).

September 1997 – June 2005 I Istanbul Erkek Gymnasium (Education Language was German)

LANGUAGES

Turkish: Mother Tongue

English: Fluent (TOEFL)

German: Fluent (Sprachdiplom Stufe 2)

Spanish: Intermediate

JOB EXPERIENCE

- 2015-to date Department of Chemical Engineering and Environmental Technology, Valladolid University (Valladolid, Spain): Researcher
- 2011-to date Department of Environmental Engineering Istanbul Technical University (Istanbul, Turkey): Research and Teaching Assistant
- 2016- to date Researcher, Executive, The Scientific and Research Council of Turkey Turkish-German Joint Project. Improvement of Anaerobic Biodegradation Efficiency of Petroleum Derivatives Waste - ZERO WASTE
- 2013 – 2018 Researcher, the Scientific and Research Council of Turkey Project: Removal of Odor Emissions from Food Fermentation and Petrochemical Production Sectors via Using Bioscrubber and Biofilter
- 2015 - 2017 Researcher, Investigation of Ammonia Removal by Anammox Process after Anaerobic Treatment of Chicken Wastes
- 2011 – 2012 Researcher, the Scientific and Research Council of Turkey Project Project: Compatible Hazardous Waste Management with EU Legislation
- 2010 – 2014 Scholarship Student. The Scientific and Research Council of Turkey Project Project: Management of Domestic and Municipal Treatment Sludge in Turkey
- 2009 – 2011 Scholarship Student. The Scientific and Research Council of Turkey Project: Acute and Chronic Effects of Estrogenic Hormones in Wastewater

SCHOLARSHIP

Graduate Scholarship Program, The Scientific and Technological Research Council of Turkey (TUBITAK)

STUDY FIELDS

- Air Pollution
- Air Pollution Modelling
- Odor Pollution Monitoring and Measuring
- Environmental Biotechnologies
- Microalgae
- Aerobic/Anaerobic Treatment Technologies

TEACHING (ASSISTED LECTURES)

- **Odor and VOC Control in Environmental Systems** (2011-2017). Istanbul Technical University Environmental Engineering Department (Master)
- **Air Pollution** (2011-2017) Istanbul Technical University Environmental Engineering Department (Bachelor)
- **Graduation Design Project** (2013- 2017) Istanbul Technical University Environmental Engineering Department (Bachelor)
- **Anaerobic Treatment Processes** (2013-2017) Istanbul Technical University Environmental Engineering Department (Bachelor)
- **Fundamentals of Anaerobic Treatment** (2013-2016) Istanbul Technical University Environmental Engineering Department (Bachelor)
- **Atmospheric Chemistry** (2016). Istanbul Technical University Environmental Engineering Department (Master)
- **Environmental Modelling Principles** (2016) Istanbul Technical University Environmental Engineering Department (Bachelor)
- **Water Supply and Environmental Sanitation** (2013-2016). Istanbul Technical University Civil Engineering Department (Bachelor)
- **Water Supply and Wastewater Disposal** (2012-2015). Istanbul Technical University Environmental Engineering Department (Bachelor)
- **Microbiology** (2011-2013). Istanbul Technical University Environmental Engineering Department (Bachelor)
- **Environmental Microbiology** (2011-2013). Istanbul Technical University Environmental Engineering Department (Bachelor)

CONFERENCE ORGANIZATION

Istanbul Technical University XIII. Industrial Pollution Control Conference, Istanbul, Turkey.

Istanbul Technical University XII. Industrial Pollution Control Conference, Istanbul, Turkey.

PUBLICATION LIST

International JCR publications

1. Mhemid, R.K.S., **Akmirza, I.**, Shihab, M.S., Turker, M., Alp, K., 2019. Ethanethiol gas removal in an anoxic bio-scrubber. *J. Environ. Manage.* 233, 612–625. <https://doi.org/10.1016/j.jenvman.2018.12.017>
2. Mhemid, R.K.S., Alp, K., Turker, M., **Akmirza, I.**, Shihab, M.S., (2018). Removal of Dimethyl Sulfide via a Bio-Scrubber under Anoxic Conditions. *Environ. Technol.* 0, 1–48. <https://doi.org/10.1080/09593330.2018.1545801>
3. Shihab, M.S., Alp, K., Türker, M., **Akmirza, I.**, Mhemid, R.K., (2018). Removal of Ethanethiol using a Biotrickling Filter with Nitrate as an Electron Acceptor. *Environ. Technol.* 0, 1–44. <https://doi.org/10.1080/09593330.2018.1545804>
4. **Akmirza, I.**, Turker, M., Alp, K. (2018). Characterization And Treatment Of Yeast Production Process Emissions In A Biofilter. *Fresenius Environmental Bulletin* Volume 27 No:10/2018 P: 7099-7107
5. Carvajal, A., **Akmirza, I.**, Navia, D., Pérez, R., Muñoz, R., Lebrero, R., (2018). Anoxic denitrification of BTEX: Biodegradation kinetics and pollutant interactions. *J. Environ. Manage.* 214, 125–136. <https://doi.org/10.1016/j.jenvman.2018.02.023>
6. **Akmirza, I.**, Pascual, C., Carvajal, A., Perez, R., Munoz, R., Lebrero, R. (2017). Anoxic Biodegradation of BTEX in a biotrickling filter. *Science of Total Environment* 587-588 :457-465.

International JCR publications in process

1. Pascual, C., R., Munoz, **Akmirza, I.**, Lebrero, R. Trimethylamine abatement in algal-bacterial photobioreactors coupled with nitrogen recovery
2. **Akmirza, I.**, R., Munoz, Lebrero, R. Toluene and Ethylbenzene Removal Performance in BCB under N-Limiting Conditions

International non-JCR publications

1. **Akmirza, I.**, Carvajal, A., Muñoz, R, Lebrero, R. (2016) Interactions between BTEX compounds during their anoxic degradation. Chemical Engineering Transactions. Vol 54.

CONFERENCES

Oral presentation (International)

1. **Akmirza, I.**, Alp, K., Turker, M., Etlı, S., Yılmaz, M. (2017). Characterization And Treatment Of Odorous Food Fermentation Process Emissions Via Pilot-Scale Biofilter. The 25th International Conference on Modelling, Monitoring and Management of Air Pollution 25 - 27 April 2017, Cadiz, Spain (**Oral presentation**).
2. **Akmirza, I.**, Carvajal, A., Muñoz, R, Lebrero, R. (2016) Interactions between BTEX compounds during their anoxic degradation 5th International Conference on Environmental Odor Monitoring and Control , 28-30 September, 2016 Ischia, Italy (**Oral presentation**).
3. Alp, K., Turker, M. Guler U., Yılmaz, M., **Akmirza, I.**, Etlı, S. (2016). Characterization Of Odor Emissions at Food Fermentation Process. The 24th International Conference on Modelling, Monitoring and Management of Air Pollution 20 - 22 June 2016, Creete, Greece (**Oral presentation**).
4. Avsar, E., Kaya, E., Cubukcu, A., **Akmirza, I.** Evaluation Of The Regional Air Quality Effects Of Istanbul Cebeci Quarry And Crushing-Sifting Facilities In Terms of PM10 and SO2 Concentrations, 14th International Multidisciplinary Scientific Geo Conferences SGEM, June 2014 Bulgaria (**Oral presentation**).
5. Alp, K., Toroz, I., Avsar, E., Erdogan, E., Ozlem, B., **Akmirza, I.** Effects Of Quarry Operation Processes To Air Quality In Istanbul Cebeci Zone According To PM10 Emissions The Seventh International Conference On Environmental Science And Technology June 2014, Houston, USA (**Oral presentation**)
6. Avsar, E., Kaya, E., Cubukcu, A., **Akmirza, I.** Environmental Impact Of Aggregate Quarries In The Cebeci District On The Air Quality Of The Region 13th International Multidisciplinary Scientific Geo Conferences SGEM, June 2013 Bulgaria (**Oral presentation**).
7. Avsar, E., Toroz, I., Hanedar, A., **Akmirza, I.**, Yılmaz, M. Physical Characterization Of Natural Organic Matter And Determination Of Disinfection By Product Formation Potentials

İn İstanbul Surface Waters. IWA 5TH Eastern European Young And Senior Water Professionals Conference, 26-28 June 2013, Kiev, UKRAINE. (**Oral Presentation**).

8. **Akmirza, I.**, Alp, K., Avsar, E. “Determination Of Odor Emissions From Food Fermentation Process With Aermod Dispersion Model In Ambient Air”, 2013, 5th IWA Conference on Odors and Air Emissions, San Francisco/ United States of America, 4-7 March 2013 (**Oral Presentation**).

Oral presentation (National)

1. Alp, K., Turker, M., **Akmirza, I.**, Etili, S., Yilmaz, M. “Kokuya Sebep Olan Gıda Fermantasyon Prosesi Atıkgaz Akımı Karakterizasyonu ve Biyolojik Aritimi”, 2017, VII. Ulusal Hava Kirliliği ve Kontrolü Sempozyumu, 1-3 Kasım 2017, Antalya , Türkiye (**Oral Presentation**).

POSTERS

1. Pascual, C., R., Munoz, **Akmirza, I.**, Lebrero, R. Trimethylamine abatement in algal-bacterial photobioreactors coupled with nitrogen recovery 7th International Conference on Biotechniques for Air Pollution Control and Bioenergy 19 – 21 July 2017. La Coruña. Spain

Thanks...

I would like to express my deep appreciation and thanks for my dear supervisors, Dr. Raul Munoz and Dra. Raquel Lebrero for their encouragement and guidance during not only this thesis work but in every step of my life in Spain and made me feel in my home during my stay in Valladolid. I will always appreciate to them for having me chance on the academic life and giving a life-time experience and it was great honour to work under their supervisions. They have always motivated and supported me both in the academic and personal life and become true friends for my rest of life.

I would also like to thank my co-supervisor, Dr. Kadir ALP who has supported and encourage me during this study. He has shared with me his all deep experience and my vision has expanded with his valuable approaches. I appreciate his many useful comments on this work, but even more so, I appreciate his advice and willingness to discuss any questions or ideas that I have had.

I would also like to to thank to the all my lovely friends Alma, Oswaldo, Dimas, Sara, Jarrett, Juan Carlos, David, Celia, Chari, Roxi, Yadira, Victor, Zaineb, Ambu, Zane, Ana, Judith, Esther, Rebecca, Andrea in Gas Treatment and Microalgae Research Group of Valladolid University.

Many thanks go the technicians of IQ of Valladolid University Araceli, Monica, Enrique Marcos, Enrique Munoz

The most special thanks to my mom Sule Akmirza and my dad Ahmet Akmirza for their support, personal sacrifice and their extraordinary patience during my life.

I would also thanks to my lovely dear wife Zehra Akmirza for her never-ending love, support and patient during my long PhD journey.

And I especially want to thank my cousins Volkan Can and Kaan Utku Can for their support and motivation.